ISSN 2313–5891 (Online)
ISSN 2304–974X (Print)

Ukrainian Food Journal

Volume 9, Issue 2
2020

Kyiv **Київ**

2020

Ukrainian Food Journal is an international scientific journal that publishes innovative papers of the experts in the fields of food science, engineering and technology, chemistry, economics and management.

Ukrainian Food Journal – міжнародне наукове періодичне видання для публікації результатів досліджень фахівців у галузі харчової науки, техніки та технології, хімії, економіки і управління.

Ukrainian Food Journal is abstracted and indexed by scientometric databases:

Ukrainian Food Journal індексується наукометричними базами:

Index Copernicus (2012)
EBSCO (2013)
Google Scholar (2013)
UlrichsWeb (2013)
CABI full text (2014)
Online Library of University of Southern Denmark (2014)
Directory of Research Journals Indexing (DRJI) (2014)
Directory of Open Access scholarly Resources (ROAD) (2014)
European Reference Index for the Humanities and the Social Sciences (ERIH PLUS) (2014)
Directory of Open Access Journals (DOAJ) (2015)
InfoBase Index (2015)
Chemical Abstracts Service Source Index (CASSI) (2016)
FSTA (Food Science and Technology Abstracts) (2018)
Emerging Sourses Citaton Index (2018)

Ukrainian Food Journal включено у перелік наукових фахових видань України з технічних наук, категорія А (Наказ Міністерства освіти і науки України № 358 від 15.03.2019)

Editorial office address:

National University
of Food Technologies
68 Volodymyrska str.
Kyiv 01601, **Ukraine**

Адреса редакції:

Національний університет
харчових технологій
вул. Володимирська, 68
Київ 01601

e-mail: **ufj_nuft@meta.ua**

Scientific Council of the National University of Food Technologies approved this issue for publication. Protocol № 11, 25.06.2020

Рекомендовано вченою радою Національного університету харчових технологій. Протокол № № 11, 25.06.2020

Ukrainian Food Journal publishes original research articles, short communications, scientific news in the related fields and also literature reviews.

Topics coverage:

Food engineering	Food nanotechnologies
Food chemistry	Food processing
Food microbiology	Economics and management in food industry
Physical property of food	Automation of food processes
Food quality and safety	Food packaging

Periodicity of the journal – 4 issues per year.

Reviewing a Manuscript for Publication. All scientific articles submitted for publication in "Ukrainian Food Journal" are double-blind peer-reviewed by at least two reviewers appointed by the Editorial Board: one from the Editorial Board and one reviewer that is not affiliated to the Board and/or the Publisher.

Copyright. Authors submitting articles for publication are expected to provide an electronic statement confirming that their work is not an infringement of any existing copyright and will not indemnify the publisher against any breach of legislation and/or international standards in academic publishing. For the ease of dissemination, all papers and other contributions become the legal copyright of the publisher unless agreed otherwise.

Academic ethics policy. The Editorial Board of "Ukrainian Food Journal" strictly follows all internationally acknowledged rules and regulations on academic publishing and academic ethics. For more details on this see: Miguel Roig (2003, 2006) "Avoiding plagiarism, self-plagiarism, and other questionable writing practices. A guide to ethical writing". The Editorial Board suggests that all potential contributors of the journal, reviewers and readers follow this guidance in order to avoid misconceptions.

For a **Complete Guide for Authors** please visit our website:

http://ufj.ho.ua

International Editorial Board

Contents

Effect of clary sage (*Salvia sclarea* L.) essential oil on paper packaging materials

Iliana Kostova[1], Veska Lasheva[2], Hafize Fidan[3], Darina Georgieva[1], Stanka Damyanova[1], Albena Stoyanova[3]

1 – Angel Kanchev" University of Ruse, Razgrad Branch, Razgrad, Bulgaria
2 – University of Chemical Technology and Metallurgy, Sofia, Bulgaria
3 – University of Food Technologies, Plovdiv, Bulgaria

Keywords:

Packaging
Paper
Clary sage
Salvia *sclarea*
Essential oil
Antimicrobial

Article history:

Received 14.07.2019
Received in revised form 26.10.2019
Accepted 30.06.2020

Corresponding author:

Hafize Fidan
E-mail:
hfidan@abv.bg

DOI: 10.24263/2304-974X-2020-9-2-3

Abstract

Introduction. The aim of research – to determine the effect of clary sage (*Salvia sclarea* L.) essential oil on paper packaging materials.

Materials and methods. Three packaging materials have been studied based on paper coated with clary sage essential oil. The chemical composition of the clary sage essential oil is determined chromatographically. Antimicrobial effect of essential oil was determined against Gram-positive, Gram-negative bacteria, yeasts, and fungi using the agar diffusion method.

Results and discussion. The chemical composition of the clary sage essential oil showed a predominant amount of oxygenated monoterpenes (83.43%), followed by monoterpene hydrocarbons (7.86%), and sesquiterpene hydrocarbons (5.16%). The major components of the clary sage essential oil were linalyl acetate, β-linalool, α-terpineol, limonene, and geranyl acetate that determined the antimicrobial action of the oil.

The essential oil exhibited a fungicidal action against the tested molds and yeasts. Its high antimicrobial properties could be probably due to the high content of linalyl acetate (40.31%) and *β*-linalool (22.72%).

Our results showed high fungicidal efficacy for the three types of packaging materials. The suppressive action against *C. albicans* during the investigated shelf life period was about 100%. It was found a high efficiency of the recycled paper against *A. brasiliensis* (99.2% - 81.9%). It was determined that the bactericidal effect of the tested packaging materials was lower than the Gram-negative bacterium *S. abony*.

Conclusions. Clary sage essential oil could be used as an antimicrobial agent in the food industry due to its antimicrobial properties, in order to improve the quality of the products and extend their shelf life.

Introduction

Clary sage essential oil is obtained by steam distillation of flowering inflorescences of the plant. The main constituents in the essential oil are linalyl acetate (45– 65%) and β-linalool (15–25%). It has a musky, bittersweet smell [1]. It has an antibacterial and antiseptic action [2,3]. It is mainly used in the perfumery, cosmetics, aromatherapy, and phytotherapy. The leaves and inflorescences are used also for flavoring of some foods - meat, dairy, vegetables, *etc*. [1].

The usage of plant extracts and essential oils is preferred in the development of novel active packings due to the ability of the antimicrobial substance to contact the product or to penetrate food [4,5].The interest in the usage of essential oils in packing systems has increased in recent years due to their high antimicrobial activity. An antimicrobial active packaging developed based on packing paper and essential oils has been used successfully in the storage of strawberries [6].

The aim of the present study is to develop a wrapping paper with the clary sage essential oil and to study its antimicrobial efficacy.

Materials and methods

Materials

Packaging papers. Three types of wrapping papers were used - 100% recycled paper weighing 70 g/m^2, 100% bleached pulp 40 g/m^2 and 100% unbleached pulp 40 g/m^2.

Essential oil. The clary sage essential oil was provided by a manufacturer in Bulgaria.

Methods

Paper analysis. Microscopic analysis was performed to demonstrate the composition of the fibrous material from which the packaging papers were obtained.

From the physico-mechanical properties, the length of tear of the test paper samples was determined. The samples used have been analyzed before and after treatment with clary sage essential oil [7].

Oil analysis. The physical and chemical parameters (appearance, color, odor, relative density, refraction, and acid number) of the clary sage essential oil were determined [8].

The GC-MS analysis was carried out with an Agilent 5975C MSD system coupled to an Agilent 7890A gas chromatograph (Agilent Technologies Inc., Santa Clara, CA). Agilent J&W HP-5MS column (0.25 μm, 30 m x 0.25 mm) was used with helium as a carrier gas (1.0 mL min^{-1}). The operational conditions were: oven temperature 35 °C/3 min, 5 °C/min to 250 °C for 3 min, total run time 49 min; injector temperature 260 °C; ionization voltage 70 eV; ion source temperature 230 °C; transfer line temperature 280 °C; solvent delay 4.25 min and mass range 50 - 550 Da. The MS was operated in scan mode. One μL of the sample was injected into the GC/MS system at a split ratio of 30:1. The GC analysis was carried out using an Agilent 7890A GC system; FID temperature 270 °C. In order to obtain the same elution order with GC/MS, simultaneous triplicate injections were done by using the same column and the same operational conditions.

The identification of compounds was made by comparing their mass spectra with those from mass spectra libraries and by comparing the literature and estimated Kovat's (retention) indices that were determined using mixtures of homologous series of normal alkanes from C_8 to C_{40} in hexane, under the conditions described above [9]. The percentage ratio of volatile components was computed using the normalization method of the GC/FID peak areas.

Determination of antimicrobial activity. The antimicrobial activity of clary sage essential oil was tested against test microorganisms provided by the National Bank for Industrial Microorganisms and Cell Cultures in Sofia, Bulgaria: Gram-positive bacteria: *Staphylococcus aureus* ATCC 6538, *Bacillus subtilis* ATCC 6633; Gram-negative bacteria: *Escherichia coli* ATCC 8739, *Pseudomonas aeruginosa* ATCC 9027, *Salmonella abony* NTCC 6017; yeast: *Saccharomyces cerevisiae* ATCC 2601, *Candida albicans* ATCC 10231; and fungal strain: *Aspergillus brasiliensis* ATCC 16404.

The antimicrobial activity was determined by the agar well diffusion method with a well size of 8 mm. The growth media were Tryptic soy agar (Merck) for the tested bacterial strains and Sabouraud-Dextrose-Agar (Merck) for the yeast and fungi. The media were inoculated with a 24-h suspension of the bacterial species with a density of approximately 10^7 CFU mL (turbidity: 0.5 McFarland standards). Media melted and cooled to 50 °C were inoculated with the tested microorganisms and then equally dispensed into Petry dishes. Next, a hole with a diameter of 8 mm was punched aseptically with a sterile cork borer, and a volume (50 μL) of the antimicrobial agent was placed into the well. After that, the agar plates were incubated at 37 °C or 28 °C for 24 or 72 h according to the microbial species. After cultivation, the distinct zone of growth inhibition around the wells was measured using a digital caliper. The diameter of the zones, including the diameter of the well, was recorded in mm, for instance, up to 15 mm the microbial culture was poorly sensitive, from 15 to 25 mm it was considered sensitive, and over 25 mm it was considered as very sensitive. The tests were performed in parallel with solvent controls [10].

Determination of the antimicrobial properties of paper coated with clary sage essential oil. The clary sage essential oil was applied with a pump dispenser on both sides of each paper square (5/5 cm squares) and dried. The antimicrobial activity of coated papers was examined after 2 h, 24 h, and 5 days. A 24 h-culture was prepared from each bacterial test microorganism. With a wire loop, vegetative material was taken and suspended in 10 mL of saline. The suspensions prepared were with a cell concentration of about 10^3 CFU/mL. Yeast and mold suspensions were prepared in the same manner, but the cultures used were at the age of 48 h for yeast and 120 h for mold. In aseptic conditions with sterile tweezers, each square coated with essential oil was placed in a sterile petri dish. With sterile pipette on each square was dropped 0.1 mL of the prepared cell suspensions and carefully spread over the surface of the paper and then they were placed in a thermostat at 30–35 °C for 2 h. Aseptically with a sterile pipette, in every petri dish were dropped 20 mL of Tryptic soy agar for bacteria or Sabouraud-dextrose agar for yeast and molds. The following control samples were also prepared: clary sage essential oil and microorganism free paper and essential oil free paper with suspension from the current microorganism were obtained. Samples were cultivated in a thermostat at 30–35° C for 24–48 h for bacterial species and at 20–25 °C for 48–72 h for yeast and 120 h for mold. The colonies grown in the petri dishes were encountered [10].

Results and discussion

The clary sage essential oil is a light yellow liquid with musky and bitter-sweet odor.

Indicators as appearance, color, odor, relative density refractive index, and an acid number of lary sage essential oil were presented in Table 1. The results are in agreement with the data found in the literature [1].

Table 1

Indicators of clary sage essential oil

Indicators	Clary sage essential oil
Appearance	Liquid
Color	Light yellow
Odor	Musky, bitter-sweet
Relative density (d_{20}^{20})	0.9034 ± 0.00
Refractive index (n_D^{20})	1.4602 ± 0.05
Acid number (mg KOH/g clary sage essential oil)	1.52 ± 0.02

Chemical composition of clary sage essential oil

The chemical composition of the clary sage essential oil was shown in Table 2.

In the clary sage essential oil were identified 30 constituents representing 98.97% of the total content of the oil as 5 of them were in concentrations above 1% and the rest 25 constituents were in concentrations under 1%. The main constituents in the clary sage essential oil (above 3%) were: linalyl acetate (40.31%), β-linalool (22.72%), α-terpineol (7.74%), limonene (5.40%), and geranyl acetate (4.63%). These constituents determined the antimicrobial properties of the clary sage essential oil [2,3].

The differences between the essential oil yield in this study and that from other studies, reported in the literature [1,11,12] are probably due to the climatic conditions in the respective locality where the plants were grown, and also to the plant parts processed and extracted.

The distribution of major groups of aroma substances in the clary sage essential oil was also shown in Table 2. Oxygenated monoterpenes and monoterpene hydrocarbons dominated in the clary sage essential oil.

The physico-mechanical parameters (length of the tear in the longitudinal direction and relative longitudinal extension) of three different types of papers were presented (Table 3).

The results showed that the paper coatings with clary sage essential oil affected their properties as the length of the tear in the longitudinal direction and relative longitudinal extension. A decrease in the physico-mechanical parameters (breaking length by about 200 m) was indicated. The results showed that the loosening of the hydrogen bonds occurred when the clary sage essential oil has penetrated. These changes were not significant and the papers could be used for their intended purpose.

Table 2

Chemical composition of the clary sage essential oil

Name	RT[1]	RI[2]	Content, % of TIC[3]
α-Pinene	9.69	932	0.22
β-Pinene	11.08	975	0.31
β-Myrcene	11.51	988	1.49
p-Cymene	12.64	1020	0.21
Limonene	12.81	1025	5.40
cis-Linalyl oxide	14.11	1067	0.37
Terpinolene	14.56	1084	0.36
β-Linalool	15.08	1090	22.72
α-Terpineol	17.94	1188	7.74
Linalyl formate	18.40	1215	0.38
β-Citronellol	18.81	1224	0.94
Nerol	19.53	1230	0.41
Linalyl acetate	19.75	1254	40.31
α-Citral	20.04	1268	0.43
Neryl formate	20.25	1280	0.11
Geranyl formate	20.82	1297	0.24
Linalyl propanoate	21.76	1334	0.65
α-Cubebene	22.05	1345	0.88
Citronellyl acetate	22.14	1350	0.85
Neryl acetate	22.46	1361	2.78
Geranyl acetate	23.01	1380	4.63
β-Cubebene	23.19	1386	0.37
β-Bourbonene	23.27	1389	0.23
β-Caryophyllene	24.12	1420	1.54
β-Selinene	25.63	1487	0.28
α-Selinene	25.80	1496	1.81
Spathulenol	28.09	1577	1.92
Caryophyllene oxide	28.58	1582	0.12
(2-Z,6-E)-Farnesyl acetate	34.66	1821	0.20
n-Docosane	40.53	2200	1.07
Total, %			98.97
Aliphatic hydrocarbons, %			1.08
Monoterpene hydrocarbons, %			7.86
Oxygenated monoterpenes, %			83.43
Sesquiterpene hydrocarbons, %			5.16
Oxygenated sesquiterpenes, %			2.26
Phenyl propanoids, %			0.21

1 - retention time, min;
2 - retention (Kovat's) index;
3 - identified at > 0.05% of TIC

Table 3

Length of packing paper cuts

Paper kind	Bleached cellulose				Unbleached cellulose				Recycled paper			
	Length of tear in the longitudinal direction	Relative longitudinal extension	Length of transverse rupture	Relative extension in the transverse direction	Length of tear in the longitudinal direction	Relative longitudinal extension	Length of transverse rupture	Relative extension in the transverse direction	Length of tear in the longitudinal direction	Relative longitudinal extension	Length of transverse rupture	Relative extension in the transverse direction
	m	%	m	%	m	%	m	%	m	%	m	%
Untreated with clary sage essential oil	2500	1.4	2200	1.6	5800	1.0	1800	1.5	2800	0.8	1900	2.0
Treated with clary sage essential oil	2200	1.2	2000	1.4	5600	0.8	1600	1.2	2600	0.6	1600	1.8

Antimicrobial activity of clary sage essential oil

The clary sage essential oil exhibited a fungicidal action against the tested strains of mold and yeast, with an inhibition zone diameter between 16.5 and 23.1 mm (Fig. 1). It was determined a bactericidal effect of clary sage essential oil on Gram-positive bacteria *S. aureus* (18.6 mm) and *B. subtilis* (17.9 mm) as the antimicrobial activity was determined to be lower against Gram-negative bacteria *S. abony* (16.7 mm)), *E. coli* (15.8 mm) and *P. aeruginosa* (14.6 mm). The antimicrobial properties of clary sage essential oil have been studied by other researchers [2,3]. We consider that there is a correlation between the antimicrobial activity of clary sage essential oil and its chemical composition [3, 13]. Its high antimicrobial properties against the investigated test-microorganisms could be probably due to the high content of linalyl acetate (40.31%) and *β*-linalool (22.72%).

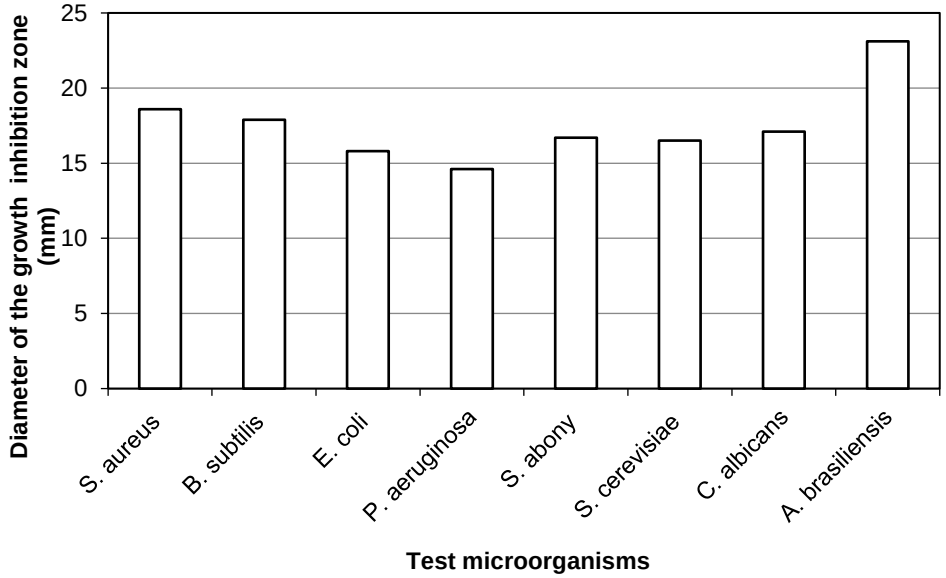

Figure 1. Antimicrobial activity of clary sage essential oil

Antimicrobial properties of paper coated with clary sage essential oil

The antimicrobial activity of different papers coated with clary sage essential oil was presented (Figure 2, 3 and 4).

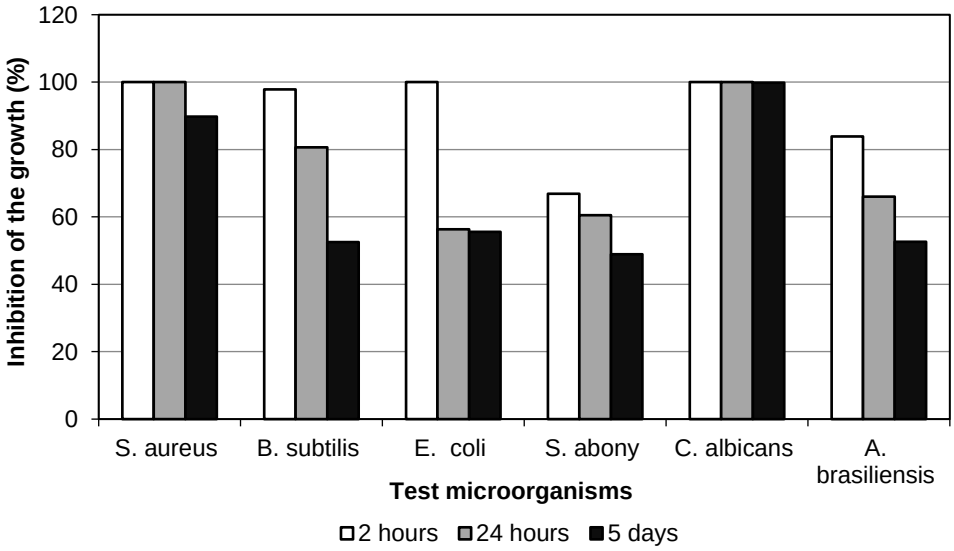

Figure 2. The antimicrobial effectiveness of bleached cellulose wrapping paper coated with clary sage essential oil

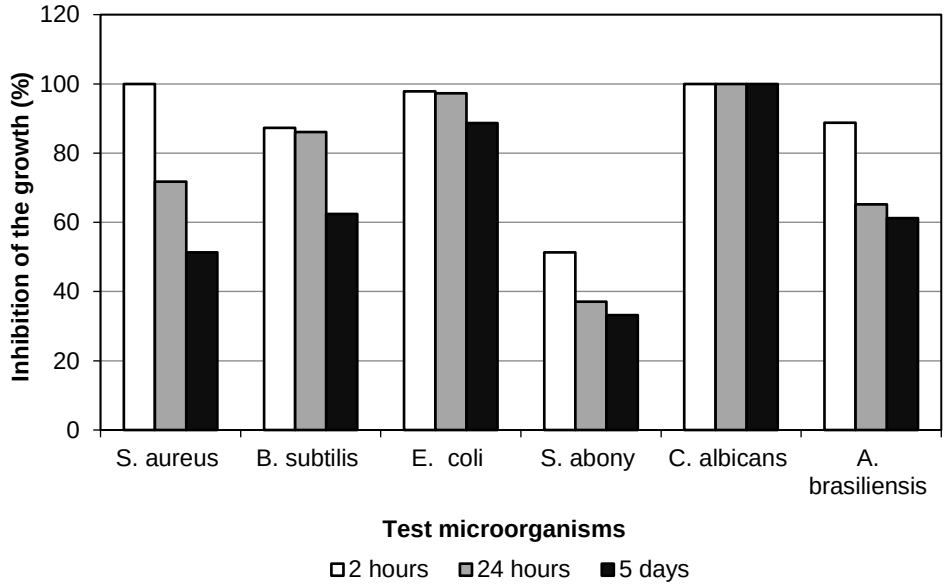

Figure 3. The antimicrobial effectiveness of unbleached cellulose wrapping paper coated with clary sage essential oil

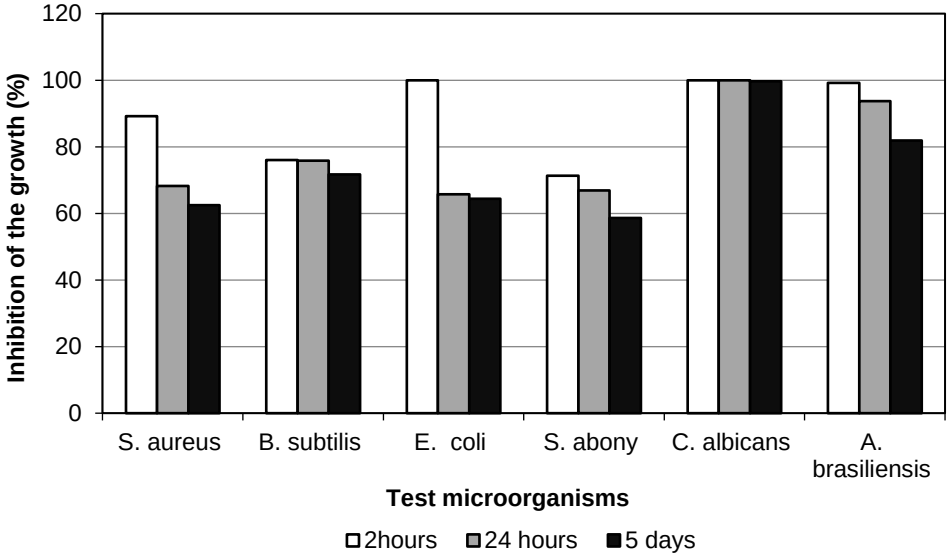

Figure 4. The antimicrobial effectiveness of recycled paper coated with clary sage essential oil

The results obtained two hours after application of the clary sage essential oil to bleached cellulose wrapping paper (Figure 2) showed inhibitory action of *S. aureus* growth (100% efficiency) and *B. subtilis* (97.8%). Keeping the paper for 24 h did not affect its antimicrobial action against *S. aureus*, but it was decreased against *B. subtilis* (80.6%). After 5 days of storage, antimicrobial effect decreased to 89.8% for *S. aureus* and 52.5% for *B. subtilis*.

Packaging paper had a full inhibitory effect on *E. coli* (100%) two hours after clary sage essential oil application and weaker activity for *S. abony*, where viable cells decreased to 66.9%. After 24 h-storage, the antimicrobial action against *E. coli* and *S. abony* was found to be 56.3% and 60.5%, respectively. The five-day storage period reduced the antimicrobial effectiveness to 48.9% for *S. abony*.

Full inhibition of *C. albicans* yeast growth and 83.9% in the *A. brasiliensis* mold growth was observed 2 h after the clary sage essential oil application. After 24 h, the antimicrobial activity remained 100% in *C. albicans* and decreased to 66% in *A. brasiliensis*. After 5 days, this efficiency was 99.8% for *C. albicans* and 52.6% for *A. brasiliensis.*

Our results for the unbleached cellulose wrapping paper (Figure 3) showed an inhibition of the growth of Gram-positive test organisms *S. aureus* (100%) and *B. subtilis* (87.3%) two hours after the addition of clary sage essential oil. Keeping the paper for 24 h reduced the antibacterial action to 71.8 and 86.1%, respectively. After a five-day storage period, it was determined that the antimicrobial effectiveness was 51.3% against *S. aureus* and 62.4% against *B. subtilis.*

Among the Gram-negative bacteria, *S. abony* was less affected than *E. coli* by unbleached cellulose paper. After 2 h of storage, the growth of *E. coli* was reduced to 97.8%, while the growth of *S. abony* was found to be 51.3%. After 24 h of paper storage, the effectiveness of the antimicrobial action against *E. coli* did not change significantly and was 97.3%, while it was determined to be decreased to 37.1% for *S. abony*. Our results showed that the antimicrobial action was decreased to 88.7% for *E. coli* and 33.2% for *S. abony* after five-day storage.

Full inhibition of viable cells was detected in *C. albicans* 2 h after treatment of the wrapping paper with clary sage essential oil.

Unbleached cellulose wrapping paper started to inhibits the growth of *A. brasiliensis* (88.8%) 2 h after the addition of the clary sage essential oil.

The usage of recycled paper (Figure 4), 2 h after the addition of clary sage essential oil, led to the suppression of the *S. aureus* (100%) and *B. subtilis* (76%) growth. After 24 h-storage, its antibacterial action against *S. aureus* decreased to 89.2%. After five days, the effectiveness of *S. aureus* was 68.2%, while it was 71.7% against *B. subtilis.*

Recycled paper inhibited the growth of *E. coli* and *S. abony* bacteria by 100% and 71.3%, respectively, two hours after the treatment with clary sage essential oil. After 24 h-storage and 5 day-storage, its antimicrobial activity against *E. coli* decreased to 64.4%.

Treatment of recycled paper led to 100% inhibition of *C. albicans* yeast growth and 99.2% of *A. brasiliensis* mold. After 24 h, the effectiveness of the antimicrobial activity remained at the same level as both test microorganisms. After 5 days of storage, the antimicrobial effect was 99.7% for *C. albicans* and 81.9% for *A. brasiliensis.*

Previous studies showed that terpene essential oil components are effective on the biological activities on the common prominent pathogenic and spoilage food-related bacteria [14]. Our results for antimicrobial potential of clary sage essential oil are in agreement with the data found in the literature. Its high antimicrobial action could be probably due to the high content of oxygenated monoterpenes linalyl acetate and β-linalool.

Conclusion

1. The results obtained showed high fungicidal efficacy for the three types of packaging materials. The suppressive action against *C. albicans* during the investigated shelf life varied about 100%. A high antimicrobial efficiency against *A. brasiliensis* was found in the recycled paper (99.2% - 81.9%). The antimicrobial effectiveness in the bleached paper was found to be 83.9% and reduced to 52.6%, while the antimicrobial activity of unbleached paper reduces from 88.8% at the beginning of the experiment to 61.2% at the end of the storage period.
2. The bactericidal efficacy of the three types of packaging papers, coated with clary sage essential oil against the Gram-positive test microorganisms tested was found to be among 100% and 76% and reduced to 89.8% - 52.5% at the end of the five-day storage period. It was determined that the bactericidal effect of the tested packaging materials was lower than the Gram-negative bacterium *S. abony*.
3. Clary sage essential oil may be used in food packing as an antimicrobial agent in order to improve its quality and extend its shelf life.

Acknowledgments: The authors acknowledge the support of the Science Fund of the University of Ruse, Bulgaria (project 2019/BRz-01).

References

1. Georgiev E., Stoyanova A. (2006), *Directory of specialization of aromatic and cosmetic industries*, UFT Publ. House, Plovdiv.
2. Hristova Y., Gochev V., Wanner J., Jirovetz L., Schmidt E., Girova T., Kuzmanov A. (2013), Chemical composition and antifungal activity of essential oil of *Salvia sclarea* L. from Bulgaria against clinical isolates of *Candida* species, *Journal of BioScience and Biotechnology*, 2(1), pp. 39–44.
3. Cui H., Zhang X., Zhou H., Zhao C., Lin L. (2015), Antimicrobial activity and mechanisms of *Salvia sclarea* essential oil, *Botanical Studies*, 56 (16), pp. 1–8.
4. Wyrwa J., Barska A. (2017), Innovations in the food packaging market: active packaging, *European Food Research Technology*, 243, pp.1681–1692.
5. Yildirim S., Röcker B., Pettersen M. K., Nilsen-Nygaard J., Ayhan Z., Rutkaite R., Radusin T., Suminska P., Marcos B., Coma V. (2018), Active packaging *Applications for Food, Comprehensive Reviews in Food Science and Food Safety*, 17, pp. 165–199.
6. Rodríguez A., Batlle R., Nerín C. (2007), The use of natural essential oils as antimicrobial solutions in paper packaging. Part II, *Progress in Organic Coatings* 60, pp. 33–38.
7. Ivanova N., Bencheva S. Todorova D. (2009), *A guide to exercises in the chemistry, technology and properties of paper*, UCTM, Sofia.
8. Stoyanova A., Georgiev E., Atanasova T. (2007), *A handbook for laboratory practice in essential oils*, Acad. Publ. House of the University of Food Technologies, Plovdiv.
9. Adams R. P. (2001), *Identification of essential oil components by gas chromatography/quadrupole mass spectroscopy. (R. P. Adams, Ed.)*, Carol Stream, USA: Allured Publishing Corporation

10. Zaika L. L. (1988), Spices and herbs: Their antimicrobial activity and its determination *Journal of Food Safety*, 2, pp. 97–118, DOI: 10.1111/j.1745-4565.1988.tb00511.x
11. Cai J., Ping L., Xiaolan Z., Qingde S. (2006), Comparative analysis of clary sage (*S. sclarea* L.) oil volatiles by GC–FTIR and GC–MS, *Food Chemistry*, 99 (2), pp. 401–407.
12. Carruba A., Torre R., Piccaglia R., Marotti M. (2002), Characterization of an Italian biotype of clary sage (*Salvia sclarea* L.) grown in a semi-arid Mediterranean environment, *Flavour and Fragrance Journal*, 17 (3) pp. 191–194.
13. Yousefzadi, M., Sonboli, A., Karimic, F., Ebrahimi, S. N., Asghari, B., A. Zeinalia (2007), Antimicrobial activity of some *Salvia* species essential oils from Iran, *Z. Naturforsch.* Pt C 62, (7-8), pp. 514–518.
14. Friedman M., Henika P.R., Mandrell R.E. (2002), Bactericidal activities of plant essential oils and some of their isolated constituents against *Campylobacter jejuni*, *Escherichia coli*, *Listeria monocytogenes*, and *Salmonella enterica*, *Journal of Food Protectio*, 65, pp. 1545–1560.

Mechanism of water-binding and water-retention of food additives nanoparticles based on double oxide of two- and trivalent iron

Iryna Tsykhanovska[1], Victoria Evlash[2], Olga Blahyi[1]

1 – Ukrainian Engineering-Pedagogics Academy, Kharkiv, Ukraine
2 – Kharkiv State University of Nutrition and Trade, Kharkiv, Ukraine

Keywords:

Water
Binding
Retention,
Nanoparticle
Iron oxide
Clusterophilicity

Article history:

Received
25.05.2019
Received in revised
form 19.11.2019
Accepted
30.06.2020

Corresponding author:

Iryna Tsykhanovska
E-mail:
cikhanovskaja@
gmail.com

DOI:
10.24263/2304-974X-2020-9-2-4

Abstract

Introduction. The mechanism of water-binding and water-retention health additives based on double oxide of two- and trivalent iron "Magnetofood"(Fe_3O_4).

Materials and methods. A model system based on nanoparticles of the "Magnetofood" (Fe_3O_4) additive is added to water, starch, egg white, fat, linoleic acid, wheaten wheat. water-retaining capacity (WRC) was achieved by energy dispersive x-ray (EDX) and IR-Fourier spectroscopy (FTIR), the Shokh method, the indicator method (IM), the differential thermal analysis (DTA), the coefficient of water absorption (cm^3/g) was determined on the Dogadkina device, the swelling properties of powder raw materials, effective viscous flow at the Reotest-2 rotational viscometer.

Results and discussion. The mechanism of interaction of food additive nanoparticles based on double oxide of two- and trivalent iron "Magnetofood" (FAM) by self-organization of nanoparticles of the additive (NP Fe_3O_4) in electrostatic complexes with proteins, polysaccharides and fats such as "clusters", "cavitates", "clathrates". It was found that in food systems that contain proteins, polysaccharides, water, their university is adjusted due to the "clusterophilicity" of FAM and the ability of NP Fe_3O_4 to polarize, electrostatic coordination, the formation of aqua associates.

A shift in the maximum absorption of the Fe–O bond was detected in the high-frequency region by (57±2) cm^{-1} compared with the experimental sample of pure FAM indicates the chemical interaction of iron cations with FAM molecules of macromolecular compounds (starch, egg white, fat).

The chemical composition is determined of model systems of macromolecular compounds with FAM: for particles of pure FAM – Fe particles 75,5%; O 24,5%; for additive particles coated with egg white – Fe 44,7%; O 26, 9%; C 21,4%; N 5,9%; S 1,1%; for additive particles coated with starch – Fe 41,7%; O 35,7%; C 22,6%; for additive particles coated with linoleic acid – Fe 45,6%; O 34,7%; C 19,7%; for additive particles coated with sunflower oil – Fe 39,7%; O 36,7%; C 23,67%.

The ratio established of bound and free moisture in solvated FAM: the amount of bound water: physico-chemical 68,9–69,4%, physico-mechanical 21,5–22,3% and free 8,8–9,1%.

Conclusions. For the first time, models of the interaction of NP Fe_3O_4 with water, proteins, fats, and carbohydrates have been proposed to substantiate the mechanism of water-retention of food additive nanoparticles based of double oxide of two- and trivalent iron.

Introduction

One of the most important functional and technological properties of food raw materials and food systems, which determines the course of technological processes, output, quality and timing of preserving the freshness of finished products, is the water-retaining capacity (WRC), that is, the ability to bind and retain water. The study of the mechanisms of binding and retention of water by food ingredients will allow rational use of new types of food raw materials and predict the behavior of components in food systems during cooking and storage of finished products.

To improve water-retaining capacity of raw materials and food systems, used food additives of different origin: chemical compound (ammonium salt ortofosfornoj acids; meta-, ortho-, poly-, pyrophosphates of sodium, potassium; lactates, citrates, etc) [1]; the special composition of enzymes DSM [2, 3]; biologically active substance of vegetable, fruit and herbal additives [4–7]; a variety of polysaccharides: citrus fibre; hydrocolloid vegetable (banana and Apple powder; coconut meal; guar and xanthan gums), Polydextrose, cellulose ethers [5-11]; natural powdery substance on the basis of dairy and egg products [12–15]; functional ingredients derived from industrial by-products (skin, hooves, feathers, offal, seeds, bran, whey, etc.) [16, 17]; supplements of different chemical composition: based on wheat, soybean, chickpea, enzymes, microalgae, and others [18–22]; nanoparticles of metal oxides (especially ZnO deposited on a film of carboxyme-thylcellulose) [23–25]; micro- and nano-sized meat, fish, avian powders [23, 24].

The main disadvantages of known additives are narrow focus and lack of comprehensive action. At the same time, the performance of nano-additives in innovative food products is determined by a wide range of functional and technological properties, due to their high dispersion, shape, structure and physical and chemical parameters.

Modern achievements and experience of domestic and foreign specialists in the field of innovative food technologies [1–25] allow us to apply their results for further research and use of nanomaterials, in particular metal oxides with stable physical and chemical indicators for correcting the functional and technological properties of food raw materials and improving consumer characteristics of food products [24, 25].

Interaction of nanoparticles with biopolymers of food systems (proteins, carbohydrates, lipids) is a complex of complex chemical reactions. An important role is played by the supramolecular organization of nanoparticles and the structure of the organic matrix, which results in the formation of spatial nanostructures that significantly affect the functional and technological properties of raw materials and food systems [26–35].

Therefore, the work on creating new functional and technological properties of food systems using nano-powders food additives of complex action is relevant. It is important to understand the mechanisms of water-binding and water-retention.

Since there is insufficient data on the study and justification of the mechanism of water-permeation capacity of food additives in the nanometer range, in this paper we present research related to the determination of the nature of interaction of food nanoparticles based on double oxide of two- and trivalent iron “Magnetofood” (FAM) with water, proteins, fats, polysaccharides – the main components of the technological environment. FAM has stable physical and chemical parameters, a wide range of functional and technological properties (structure-forming, stabilizing, water- and fat- retention, sorption, etc.) and promising technological applications [30–42].

The aim of the research is to study the mechanism of water-binding and water-retention by nanoparticles of a food additive based on double oxide of two- and trivalent iron “Magnetofood” (FAM).

To achieve this goal, the following tasks were set:

- To study the mechanism of interaction of high-molecular compounds (starch, egg protein, higher fatty acid, fat) with FAM nanoparticles using IR spectroscopy;

- To establish the chemical composition of experimental samples of FAM pure and coated with starch, egg white, linoleic acid, sunflower oil using energy-dispersive x-ray spectroscopy;
- To study the water-binding and water-retention of FAM by determining the coefficient of water absorption in various media, the degree of swelling, the water absorption capacity of the food additive;
- Determine the indicator method and differential thermal analysis of the ratio of bound and free moisture in solvated FAM;
- To study the effect of FAM nanoparticles on water-retention, swelling and effective viscosity of model systems of rye-wheat flour and starch.

Materials and methods

Materials

Research object: water-retaining capacity of powdered ingredients of food raw materials, in particular nanoparticles of a food additive based on double oxide of two-and trivalent iron "Magnetofood" (FAM).

Research subjects:

- Food additive based on double oxide of two-and trivalent iron "Magnetofud" (FAM) [Patent UA. 126502; TC U 10.8-2023017824-001:2018] – a highly dispersed brown or black powder with a particle size of 70–80 nm. The chemical composition of FAM is double iron oxide ($FeO \cdot Fe_2O_3$ or Fe_3O_4), which was obtained by chemical coprecipitation from aqueous solutions of ferrous and trivalent salts in an alkaline medium [36];
- Model system: suspension of FAM in water – obtained by dispersing the calculated amount of FAM in drinking water deaerated and demineralized at a temperature of 18–20 °C for (5–7)×60 s, followed by holding for (10–12)×60 s [33]; "starch+magnetofood", "egg white+magnetofood", "linoleic acid+magnetofood", "sunflower oil+magnetofood", "rye-wheat flour (60:40) (RWF)+magnetofood": suspension of FAM in 1% (13%) starch (flour) solution was obtained by introducing the calculated amount of FAM in 1% (13%) starch (flour) solution) at a temperature of (20–23) °C due to constant mixing n=(2,0–2,2) s^{-1} for (5–7)×60 s [37]. Suspension of FAM in 3% egg white solution was obtained by introducing the calculated amount of FAM in 3% egg white solution at a temperature of (18–20) °C by constant stirring n=(2,0–2,2) s^{-1} for (3–5)×60 s, followed by holding for (5–7)×60 s [38]. Fat suspensions of FAM were obtained by peptising the calculated amount of FAM into oil (linoleic acid) at a temperature of (45–50) °C (rational ratio of components –FAM: fat (wt.%)=50:50; that is, 2.5 g of suspension contains 1.25 g of FAM) with careful mixing (n=2.0–2.2 s^{-1}) for (3–4)×60 s, followed by cooling the mixture to a temperature (18–20) °C due to constant mixing n=(2.0–2.2) s^{-1} [34, 35, 39–42].

Research methods

Fourier-infrared spectroscopy (FTIR)

Vibrational spectra of experimental samples were obtained using the method of IR-Fourier spectroscopy [50] on a Tensor 37 Fourier spectrometer manufactured by Bruker (Germany), controlled by the OPUS software package with standard calibration capabilities

in the frequency range (4000–400) sm^{-1} in the absorption format (IR-Fourier spectra of samples were taken in KBr tablets) [26, 29, 34].

Energy-dispersive x-ray spectroscopy (EDX)

To establish the chemical composition of the test samples, a scanning electron microscope JSM-820 (JEOL) with an EDX prefix was used. X-ray spectra were obtained by bombarding experimental samples with electrons using a voltage of 20 kV (corresponding to the lines of characteristic spectra of Iron, Carbon, Sulfur, Nitrogen and Oxygen). The determination of the elemental composition of the experimental samples was performed by analyzing the obtained spectra of characteristic x-ray radiation [26, 28, 34, 35].

Indicator refractometric method

It consists in determining the difference in dry matter between sugar solutions-"indicator" and FAM, solvated in sugar solution [43].

The bound moisture was determined by the formula (1):

$$X = \frac{B \times (b_2 - b_1)}{P \times b_2}, \quad (1)$$

where X – the amount of bound water, g per 1 g of dry matter;

b_1 and b_2 – the initial and final concentration of sucrose solution,%;

B – the mass of 20 cm^3 10% sucrose solution, g;

P – the weight of dry matter, g.

Free moisture was determined by the formula (2):

$$Y = \frac{(C_0 - C_1) \times m \times 100}{C_1 \times g \times W}, \quad (2)$$

where Y– free water content, % of the total content;

C_0, C_1 – initial and final concentrations of sucrose solution,%;

m – mass of the initial sucrose solution, g;

g – weight, g;

W – total water content in 1 g of the sample, g.

Differential thermal analysis (DTA)

Thermographic determination was performed on the derivatograph system Q-1500D of the company MOM (Hungary) for the weight of samples 0.5 g for the following modes of removal of derivatograms: sensitivity of the DTA – 250 galvanometer, DTG – 500 galvanometer, TG – 500 galvanometer, the rate of change of the heating temperature – 4 °C/60 sec [44]. Based on the *TG* curve, which corresponds to the process of dehydration, the temperature curve T was built according to the degree of change of the mass α to the temperature T. On the *TG* curve at 5 °C was found to change the mass of the sample, which corresponds to the mass fraction of moisture at a temperature T, and total mass fraction of moisture, determined in *TG* curve at the end of the process of dehydration. The degree of change in mass a was calculated using the formula (3):

$$\alpha = \frac{\Delta m_T}{m}, \quad (3)$$

where α is the degree of mass change,

Δm_T is the change in the mass of the sample at temperature (T), 10^{-3} g;

m is the total mass fraction of moisture contained in the sample, 10^{-3} g.

Coefficient of water absorption (degree of swelling) of food additive "Magnetofood"

The degree of swelling (Q,%) was determined on the Dogadkina device at two temperatures: (20±1) °C and (50±1) °C in media traditionally used in food technologies [45] according to the formula (4):

$$Q = \frac{M_H}{M_O} \times 100 = \frac{\rho V}{M_O} \times 100 , \quad (4)$$

where M_O – weight of the suspension before swelling, g;

M_H – weight of the suspension after swelling, g;

ρ – density of the absorbed liquid, g/cm^3;

V – volume of the absorbed liquid, cm^3 ($V=2\times Dh\times K_n$);

h – height of the column of the absorbed liquid, cm;

D – diameter of the tube, cm;

K_n – coefficient of the device.

Water absorptive capacity (WAC) of food additive "Magnetofood"

The method is based on bound moisture at T=293K by various hydromodule of FAM followed by centrifugation and determination of WAC (α_m,%) by standard weight method [46, 47] according to the formula (5):

$$\alpha_m = \frac{m - m_o}{m_o} , \quad (5)$$

where m_o and m are the mass of the FAM hitch before and after solvation.

The swelling properties of powder raw materials

It was determined by infusing 1% of the water suspension of the experimental sample during the day. Swell (N_b, cm^3/g) was estimated as the maximum amount of water that an object can absorb and hold until dynamic equilibrium occurs, related to the weight of the suspension [12, 42].

Water retaining capacity (WRC) of powder raw materials

WRC (%) was determined by the Schoch method as the amount of water that was adsorbed and retained by the raw component during the process of infusing and centrifuging the water suspension [12,48, 49].

Effective viscosity

It was determined on a rotary viscometer "Reotest-2" in 13% aqueous suspensions of model systems of starch and flour. The choice of concentration is determined by obtaining solutions with the optimal viscosity for the study on this device. The viscosity of the samples was measured for 30 minutes every 10×60 s at temperatures of (23±2) °C and (40±2) °C [12,48, 49].

Results and discussion

Scientific justification of the interaction of FAM with the main components of food systems – proteins, fats, polysaccharides, water

The chemical activity of "Magnetofood" nanoparticles (NPM) is determined mainly by electrostatic – dipole-dipole (vandervaals) and ion-dipole interactions. Donor-acceptor (coordination) interactions, such as hydrogen bonds, are also involved in the adsorption of proteins, fats, carbohydrates, and water on the surface of the NPM [26, 28-35].

Figure 1 shows the schemes of NPM solvation, which explains the regularities of the formation of the properties of food systems, in particular the bound water capacity. On the surface of the NPM are variously polarized areas ($^{+\delta}$Fe) and ($^{-\delta}$O). The Fe^{2+} and Fe^{3+} NPM cations are structure-forming [26, 28, 30]. High tension electric field created by cations of iron magnetic nanoparticles additives, enhances the polarization of the molecules that are next and this contributes to a further ordering of the dipoles (e.g., peptide bonds, HO^--groups, COO^--groups, H_2O and others) outside the particle surface and chemisorption [26, 28– 31].

In a neutral environment (pH=6,8–7,0), polarized NPM are formed (Figure 1, a), which then pass into solvated particles and solvated aquacomplexes [30]. In an acidic environment (pH<6,8) (Figure 1, b), protonated, then solvated-protonovani NPM, which then form solvated aquaasociati [30]. In an alkaline environment (pH>7,0) (Figure 1, c), hydroxylating NPM are first formed, then solvated-hydroxylating NPM arise, which then form solvatocomplexes [30].

For a more detailed explanation of the mechanism of interaction of proteins, polysaccharides, and fats with NPM, consider the electrostatic coordination interactions that occur between NPM and the ionogenic groups of these compounds. As a result, electrostatic complexes are formed: "clathrates" (Figure 2) and "cavitati" (Figure 3) [30–32].

In an internal molecular complex – "clathrate" (Figure 2, a) of the "complex-cell" type (Figure2, b), the donor is a Nitrogen atom of the heterocyclic systems Histidine (His) and Tryptophan (Trp), which has a free electron pair on the outer shell. NPM ferum cations (Fe^{2+}, Fe^{3+}), which have vacant 3d-orbitals, act as a complex-forming acceptor. As a result, three intramolecular coordination ligaments are formed that strengthen the electrostatic complex [30].

Complex associates of polyheterocyclic ligands of protein molecules with NPM, combining fragments of two polypeptide chains of histidine and tryptophan with iron cations (Fe^{2+}, Fe^{3+}) due to intermolecular complexation, are the mizmolecular complex "cavitat" – "NPM+protein".

In addition to the fact that the iron cations (Fe^{2+}, Fe^{3+}) of the NPM are coordinated in a linear ligand (Figure 3, a), they also firmly hold a similar ligand located perpendicular (Figure 3, b). Such a complex structure is strong due to the multiplicity of formed coordination links [30–32].

Under the influence of "Magnetofood" nanoparticles ($NPFe_3O_4$) high-molecular compounds (proteins, polysaccharides, higher fatty acids, fats) undergo structural changes, forming fairly stable structures with $NPFe_3O_4$. Figure 4 shows the process of self-organization of $NPFe_3O_4$ into electrostatic complexes with proteins, polysaccharides and fats. The $NPFe_3O_4$ complex with gliadin (Figure 4, a) is stabilized by coordination (donor-acceptor) bonds of Fe atoms with Oxygen and Nitrogen atoms of Glutamine and Tryptophan residues, as well as by electrostatic hydrophobic interactions of aliphatic side chains of leucine residues and π-π–stacking interactions of aromatic fragments of tryptophan residues.

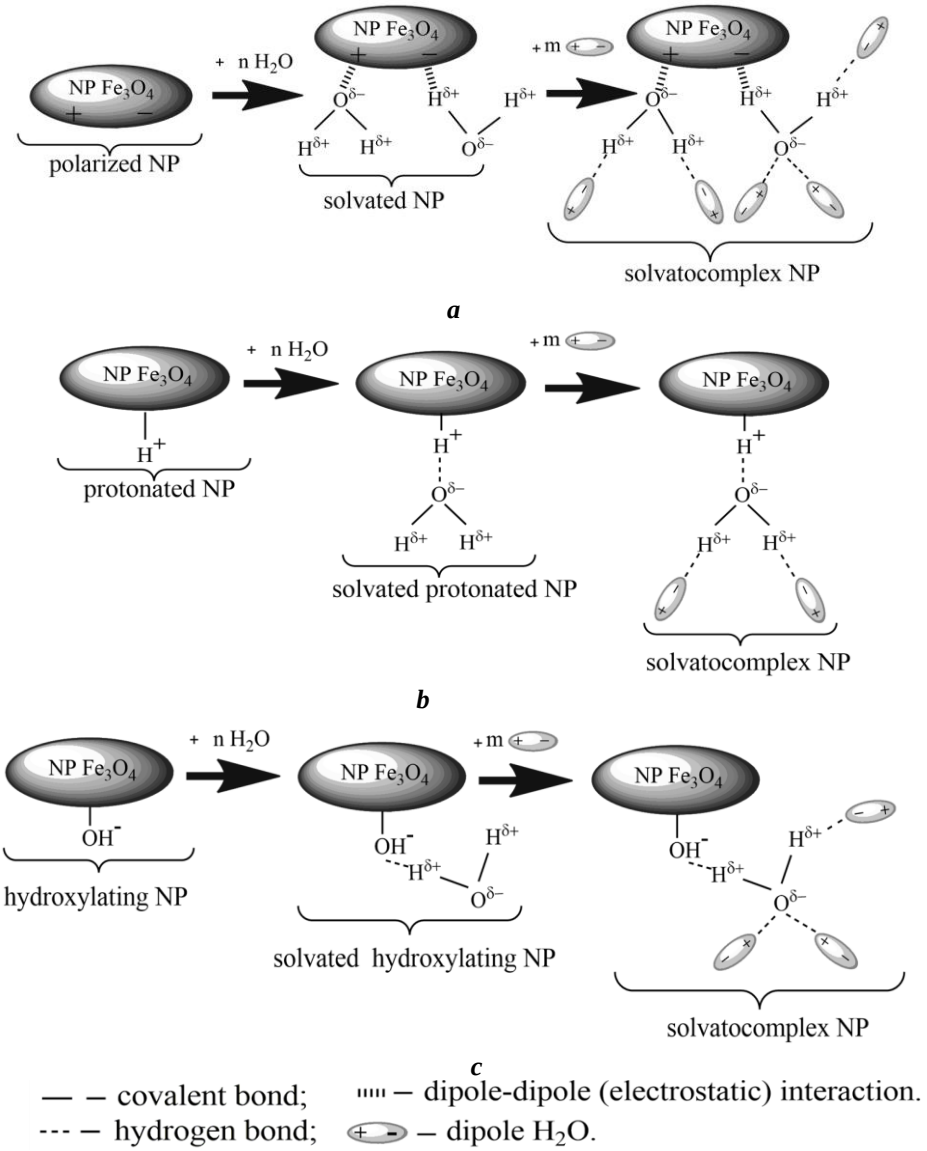

Figure 1. Mechanisms of FAM solvation at different pH levels in aquatic environments: a – neutral (pH~7.0); b – acidic (pH<7, 0); c – alkaline (pH>7, 0)

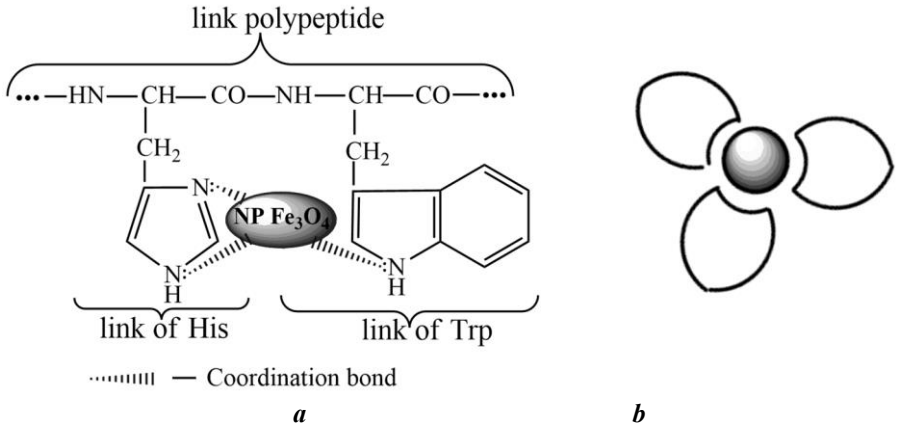

Figure 2. Intramolecular complex – "clathrate" type "complex-cell", formed by NPM and a link in the Gliadin polypeptide chain:
***a* – "clathrate" – "NPM+protein"; *b* – "complex-cell" – "NPM+protein"**

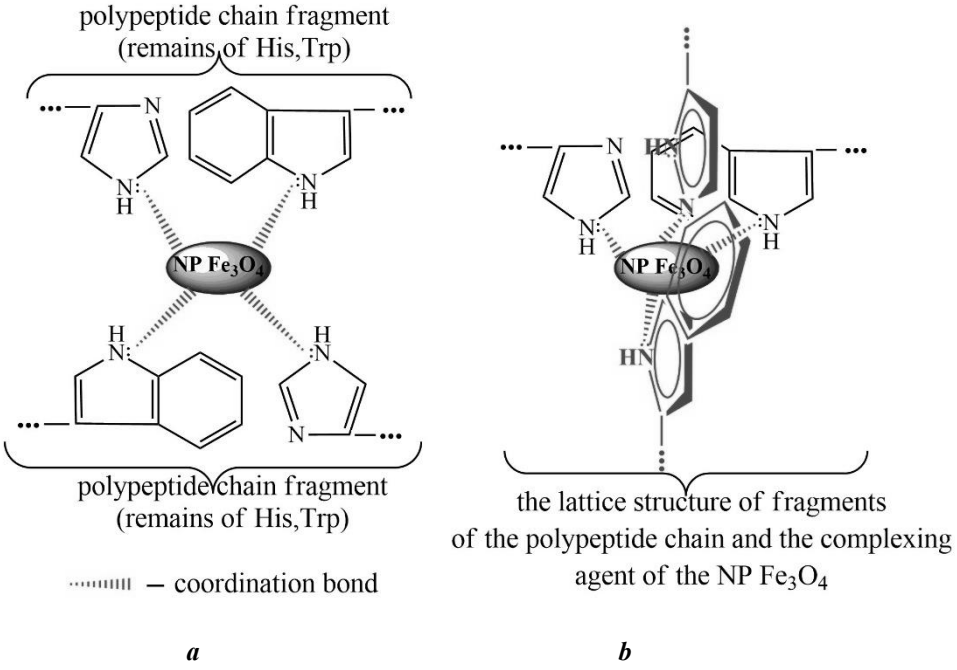

Figure 3. Intermolecular complex of NPM with links of two polypeptide chains:
***a* – "cavitate" – "NPM+protein";**
***b* – spatial structure "cavitate" – "NPM+protein"**

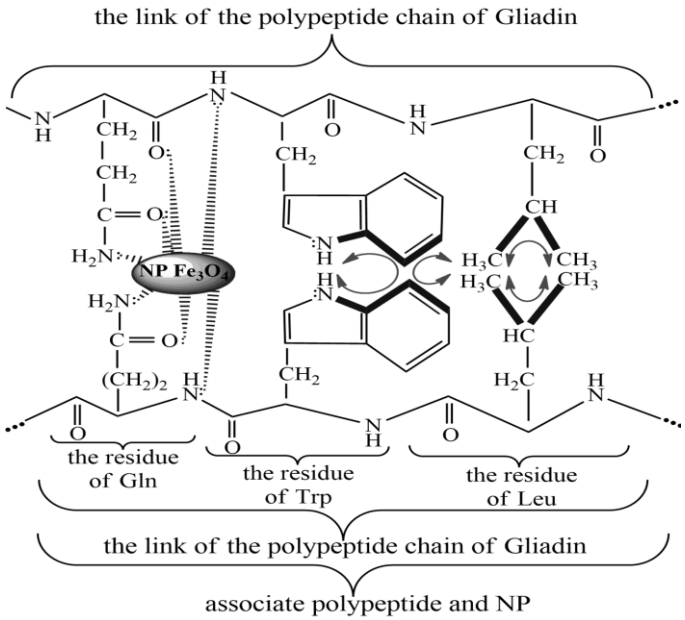

a

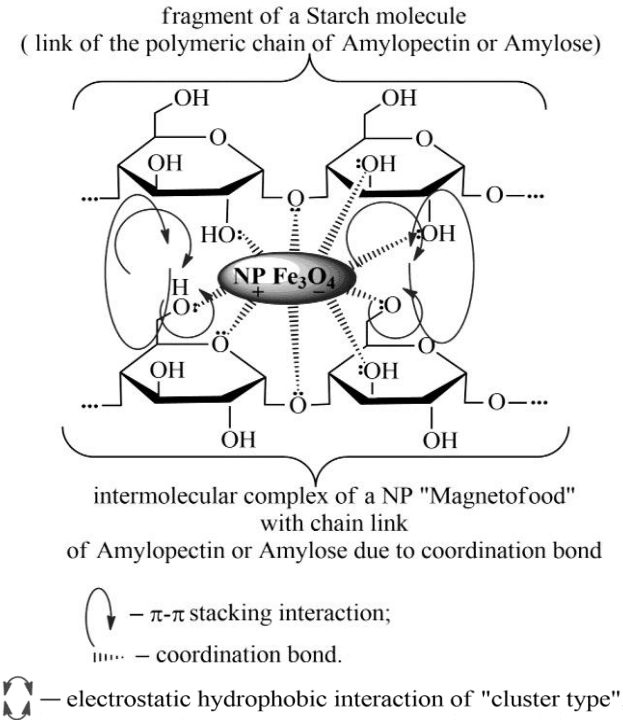

b

Figure 4. Electrostatic complexes of $NPFe_3O_4$ with:
***a* – protein (gliadin); *b* – polysaccharide (amylopectin); *c* – fat (triglyceride)**

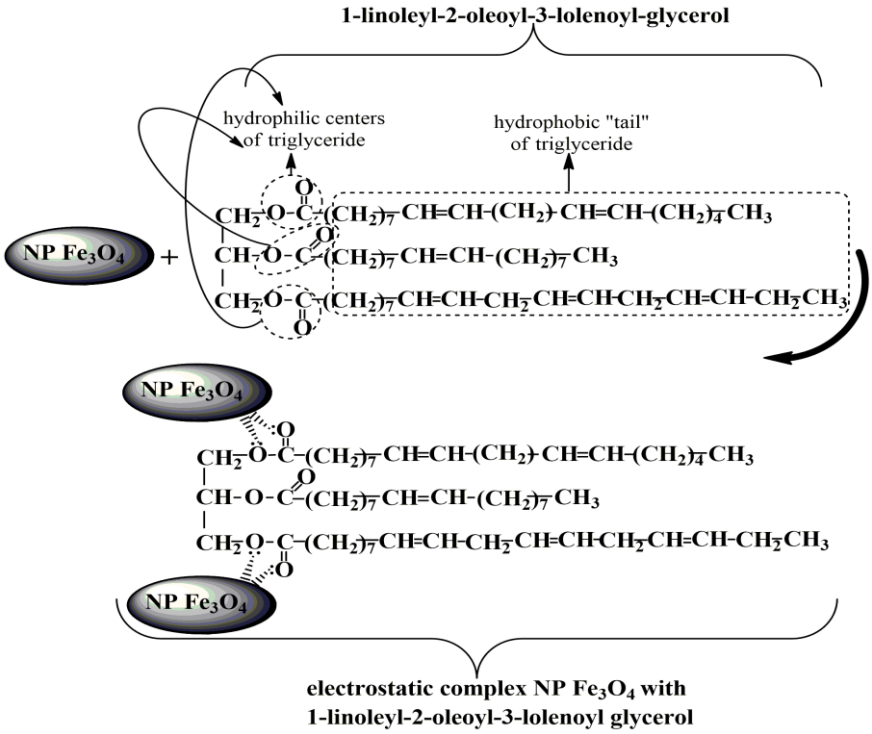

c

Figure 4 (*Continue*). Electrostatic complexes of $NPFe_3O_4$ with: *a* – protein (gliadin); *b* – polysaccharide (amylopectin); *c* – fat (triglyceride)

All this causes a more branched structure and intertwining of protein macromolecules. As a result, there are formations such as "clusters", "clathrates", "cavitates" and "loops" [30–32, 34, 35].

Intermolecular complexes of $NPFe_3O_4$ with links of two main chains of amylopectin (Figure 4, b) are formed due to coordination bonds of Fe atoms with Oxygens (etheric, pyranose and hydroxyl) of D-glucopyranose residues, amplifying the π-π stacking interaction of pyranose cycles in the "plane-to-plane" type. In the amylopectin molecule, the π-π stacking interaction is due to electrostatic forces: hydrophobic and dispersive london forces between the glucopyranose residues. All this contributes, first, to an increase in the degree of branching of the main chain of the polysaccharide, in particular amylopectin, and second, to the appearance of "cluster" – type formations [30, 32].

Under the influence of $NPFe_3O_4$, fats undergo structural changes, forming supramolecular associations from $NPFe_3O_4$ – electrostatic complexes (Figure 4, c) due to the coordination bonds of Fe atoms with Oxygen atoms of the natural group of triglycerides, which causes their chemosorption on the reactively active surface of polar $NPFe_3O_4$ [34, 35]. Figure 5 shows the bound water of $NPFe_3O_4$ in food systems containing proteins and polysaccharides.

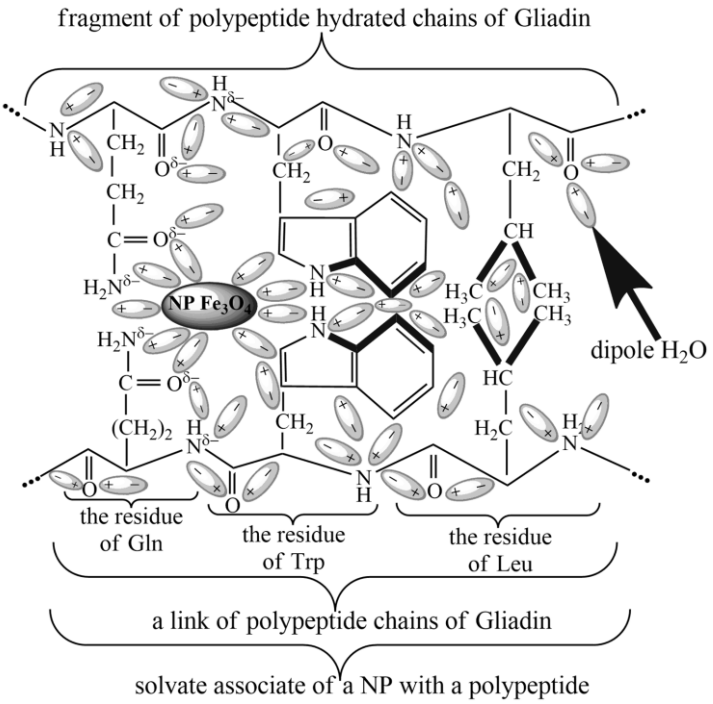

a

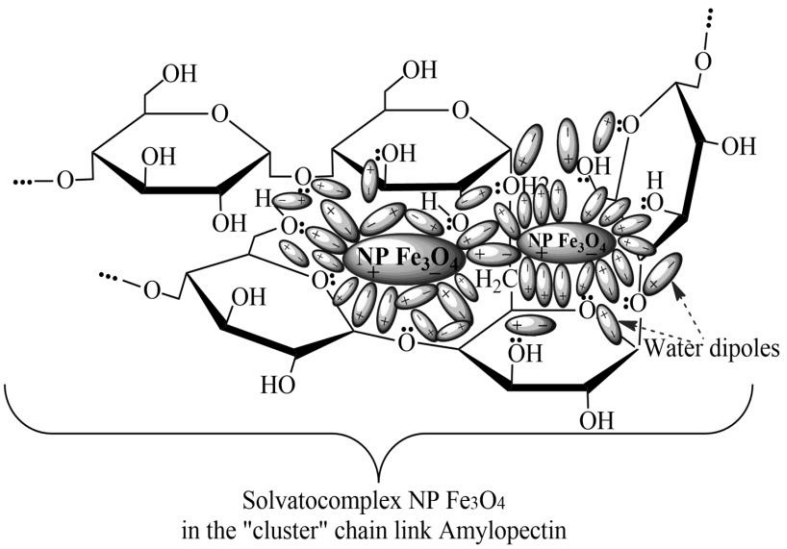

b

Figure 5. Distribution of water dipoles in "clusters" of links of solvated polymer chains structured by NPFe_3O_4:
***a* – gliadin; *b* – amylopectin; *c* – cellulose**

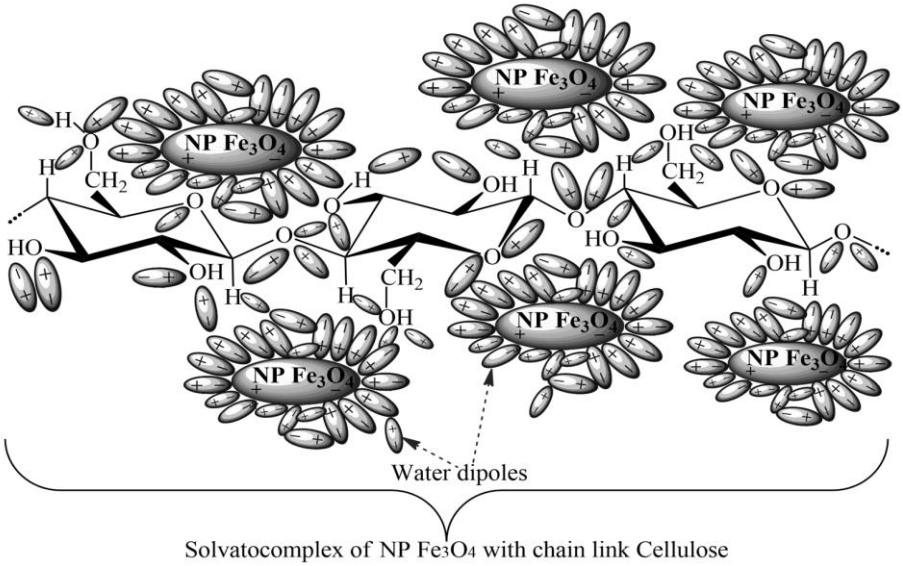

c

Figure 5. (Continue). Distribution of water dipoles in "clusters" of links of solvated polymer chains structured by $NPFe_3O_4$:
***a* – gliadin; *b* – amylopectin; *c* – cellulose**

Water accumulation is observed around the polar $NPFe_3O_4$ and in "clusters" and "loops" between two Gliadin chains (Figure 5, a), where both intermicellar and intramicellar water can be retained (due to hydrogen, dipole-ion and dipole-dipole bonds with $NPFe_3O_4$ and hydrophilic groups of amino acid residues) [30, 32]. H_2O dipoles also form hydrogen bonds without breaking the strength. Side branches that appear in the protein macrostructure contribute to the extension of the main chains, without breaking the "cross-linking". This facilitates the interaction of protein macromolecules with H_2O dipoles and improves the hydration of protein fragments. The result is an increase the WRC of food systems and finished products.

When FAM is introduced into food products (in particular, gel-like type), polysaccharide molecules are exposed to polar $NPFe_3O_4$ (Figure 5, b). That is, when polysaccharides are hydrated in the presence of $NPFe_3O_4$, a system of hydrogen, hydrophobic, electrostatic, and coordination bonds is formed, which contributes to the stability of the carbohydrate structure [31, 32]. Water molecules, forming hydrogen bonds, penetrate deeper polysaccharides (in particular starch) in the least organized parts of the chain macromolecules of carbohydrate and form of education "$NPFe_3O_4$+polysaccharide+H_2O" on type "cluster" (Figure 5, b). $NPFe_3O_4$ form aquacomplex, and in "clusters" occur solvatatsii. This pushes the polymer chains apart and improves water penetration into the starch. This water absorption weakens the micromolecular bonds in dense layers and promotes the penetration of moisture into the most crystalline layers. This process goes through the gelation stage, when the starch grains swell and increase in volume. As a result, the WRC of the carbohydrate-containing system increases.

Due to the open (linear unbranched) structure of cellulose (Figure 5, c), the availability of hydrophilicity centers ($NPFe_3O_4$, OH^--groups, etc.), the high reactivity and complex-opening ability of polar $NPFe_3O_4$ increases the energy potential of hydrophilic components of cellulose and color: adsorption of H_2O dipoles in microcapillars (which are built in a three-dimensional mesh structure); penetration of H_2O dipoles inside the cellulose (due to expansion of polymer chains and weakening of micro-macromolecular bonds in dense layers). As a result, solvatoassociates are formed and the water-retaining capacity of the structural polysaccharide (cellulose) increases [31, 32].

Experimental confirmation of interaction of a food additive based on double oxide of two- and trivalent iron "Magnetofood" with proteins, fats, polysaccharides, water

Fourier-infrared spectroscopy. The results of Fourier-IR spectroscopic studies of model systems of egg protein, starch, linoleic acid and sunflower oil with FAM are shown in table 1 and table 2.

The intensive wide band with the maximum absorption (3341±4) cm^{-1} is shifted in the complex asociati to the low-frequency region in comparison with the frequency of free OH^--groups and Amide A (N–H) (3406±4) cm^{-1} (Table 1). This indicates the participation of hydroxyl Oxygens and amide Nitrogens in the formation of coordination bonds with Fe atoms of FAM [26, 27].

Table 1

Comparison of wave numbers of individual peaks in the IR-spectra of the complex associate "egg white+magnetofood" and the starting substances

(egg white, food additive "Magnetofood" – FAM)

Communication fluctuations	Position of maxima (wave numbers), cm^{-1}			Offset, $см^{-1}$
	Egg white	FAM	«egg white+magnetofood»	
ν(O–H), ν(N–H)–Amide A	3406±5	–	3341±5	-65
ν_{as} (C–H)	2927±4	–	2927±4	0
ν_s(C–H)	–	–	2360±4; 2342±3	–
ν (C=O)–Amide I	1653±3	–	1642±3	-11
$\delta_{pl.}$(N–H)–Amide II	1539±3	–	1527±3	-12
$\delta_{pl.}$(C–H)	1451±3	–	1442±3	-9
$\delta_{pl.}$(C–C)	1239±2	–	1239±2	–
$\delta_{ext.pl.}$ (C–C)	–	–	1155±2	–
$\delta_{ext.pl.}$ (C–C)	1079±2	–	1027±2	-52
ν (Fe–O)	–	532±2	588±2	+56

There are also intense bands with maxima at (2360±4) cm^{-1} and (2342±3) cm^{-1}, which are absent in the egg protein spectrum. These peaks can be attributed to the symmetric valence (ν_s) oscillations of the C–H bond, which is confirmed by the electrostatic hydrophobic interactions of aliphatic side chains of amino acid residues in "clathrates" and "cavitates", which occur under the action of $NPFe_3O_4$ [27]. During the adsorption of egg white on the surface of the $NPFe_3O_4$, the absorption bands of valence vibrations of Amide I ν(C=O) and plane deformation vibrations of Amide II $\delta_{pl.}$(N–H) are shifted to a lower

frequency in the region: ν(C=O)=(1642±3) cm^{-1}; $\delta_{pl.}$(N–H)=(1527±3) cm^{-1}, respectively [27, 34].

The absorption bands of plane and out-of-plane deformation vibrations $\delta_{pl.}$(C–H) and $\delta_{ext.pl.}$(C–C) are shifted to a lower frequency – in the region: $\delta_{pl.}$(C–H)=(1442±3) cm^{-1} and $\delta_{ext.pl.}$(C–C)=(1027±2) cm^{-1} respectively, a new absorption band of plane deformation vibrations $\delta_{pl.}$(C–C)=(1155±2) cm^{-1} is also observed. This is confirmed by the electrostatic hydrophobic interactions of aliphatic and cyclic amino acid residues in complex associate [27, 34].

In the spectrum of pure FAM (Table 1), there is an absorption line of the Fe–O bond with a maximum value of ~532 cm^{-1}, which is in good agreement with the data from literature sources of ~530 cm^{-1} [26, 28, 35]. The shift of the maximum of the corresponding absorption band of the Fe–O bond valence vibrations in the "egg protein+magnetofood" complex to the region of ~ 588 cm^{-1} is due to the influence of surface egg protein molecules, their interference in the near-surface layer of Fe_3O_4 nanoparticles and chemical interaction with ferum cations. Thus, the research results confirm the formation of a complex between egg protein and $NPFe_3O_4$.

Comparison of IR-spectra (Table 2) shows that the wave numbers of peaks differ in the spectra of the initial substances (starch, FAM) and the "starch+magnetofood" complex, indicating the chemical interaction in the carbohydrate-magnetofood model system. In the spectrum of the "starch+magnetofood" complex, there is a shift of the intense band of free OH^-– groups (3443±5) cm^{-1} to the low-frequency region – (3415±5) cm^{-1}, which indicates the participation of hydroxyls in the topic of hydrogen bonds and electrostatic coordination interactions with Fe atoms of FAM [26, 27].

Table 2

Comparison of wave numbers of individual peaks in the IR-spectra of the complex associate "starch+magnetofood" and initial substances (starch, FAM)

Communication fluctuations	Position of maxima (wave numbers), cm^{-1}			Offset, $см^{-1}$
	Starch	FAM	«starch+magnetofood»	
ν(O–H)	3443±5	–	3415±5	-28
ν_{as} (C–H)	2927±4	–	2917±4	-10
ν_s(C–H)	–	–	2360±4; 2342±3	–
ν (C–O–C)	1653±3	–	1640±3	-13
$\delta_{pl.}$(C–O–C)	1457±3	–	1441±3	-16
$\delta_{pl.}$(C–C)	1162±2	–	1152±2	-10
$\delta_{пл.}$(C–C)	–	–	1081±2; 1021±2	–
$\delta_{ext.pl.}$ (C–C)	982±2		922±2	-60
$\delta_{ext.pl.}$ (C–C)	857±2		847±2	-10
$\delta_{ext.pl.}$ (C–C)	763±2		753±2	-10
ν (Fe–O)	–	532±2	589±2	+57

Displacement of the peak of valence ν (C–O–C) by (13±3) cm^{-1} and plane deformation vibrations DPL.(C–O–C) at (16±3) cm^{-1} in the low-frequency region in comparison with the experimental starch sample indicates the presence of coulomb and coordination interactions between Fe atoms of FAM and Oxygens (ether, pyranose and hydroxyl) of D-glucopyranose residues [27].

The appearance of new absorption bands in the region (700–1200) cm^{-1}, which characterize the fluctuations of the carbon skeleton, and the shift to the lower frequency region of some characteristic absorption bands (C–C) bonds indicates the presence of hydrophobic and dispersive london interactions between the residues of glucopiranose [26, 27]. The shift of the maximum absorption of the Fe–O bond to the high-frequency region (57±2) cm^{-1} in comparison with the experimental sample of pure FAM indicates the chemical interaction of FAM ferum cations with starch molecules. All this confirms the presence of chemical interaction in the complex asociati "starch+magnetofood" [27, 34].

The study of chemosorption of linoleic acid and 1-linoleyl-2-oleoyl-3-linolenoylglycerol on the surface of FAM nanoparticles is given in previous studies [34, 35, 42], which indicates the chemical interaction of higher fatty acid and fat with Fe_3O_4 nanoparticles.

Energy-dispersive spectroscopy (EDX)

The chemical composition of model systems was determined using EDX-spectra: "magnetofood–Fe_3O_4" (sample 1), "starch+magnetofood" (sample 2), "egg protein+magnetofood" (sample 3), "linoleic acid+magnetofood" (sample 4), "sunflower oil+magnetofood" (sample 5) (Table 3).

Table 3

Chemical composition of experimental samples of compositions "protein (or fat or polysaccharide)+magnetofood" based on the results of EDX-spectra

Samples	Elemental composition					
	Fe		O		C	
	Mass%	Atomic%	Mass%	Atomic%	Mass%	Atomic%
1	75,5±3,7	42,9±2,1	24,5±1,2	57,1±2,8	–	–
2	41,7±2,1	36,7±1,8	35,7±1,6	27,4±1,4	22,6±1,1	32,6±1,6
3*	44,7±2,2	37,0±1,7	26,9±1,3	22,8±1,1	21,4±1,0	31,2±1,5
4	45,6±2,3	37,5±1,7	34,7±1,5	26,6±1,3	19,7±0,9	30,9±1,4
5	39,7±1,9	35,5±1,6	36,7±1,8	29,6±1,5	23,6±1,2	34,9±1,7

** Note: Sample 3 – mass %: N(5,9±0,3); S(1,1±0,05); atomic %: N(2,1±0,1); S(0,7±0,03).*

On the EDX spectra of all experimental samples, peaks of about 0.8; 6,3 and 6,8 keV are associated with the absorption of kinetic energy of electrons by the Fe atom [27, 28]. The spectra of NP Fe_3O_4 covered with egg white, linoleic acid, oil and starch contain two more peaks: about 0,27 keV and 0,47 keV. These absorption bands belong to the C and O atoms [27, 28, 34, 35]. Moreover, the peak at 0,47 keV, characteristic of the O atom, is also present in the spectrum of pure FAM; and the peaks of about 0,3 and 1,2 keV are associated with the absorption of kinetic energy by the electrons of the N and S atoms, respectively [27, 28, 34]. Fe, O, and C (H cannot be investigated) and N and S (for sample 3) are the main components in the system "protein (fat, polysaccharide) of magnetofood" (Table 3).

Thus, systems with $NPFe_3O_4$ have a chemical composition: *sample 1* (FAM) – Fe 75,5%; O 24,5%; *sample 2* ($NPFe_3O_4$ covered with starch) – Fe 41,7%; O 35,7%; C 22,6%; *sample 3* ($NPFe_3O_4$ covered egg white) – Fe 44,7%; O 26, 9%; C 21.4%; N 5,9%; S 1,1%; *sample 4* ($NPFe_3O_4$ covered with rich linoleic acid) – Fe 45,6%; O 34, 7%; C 19,7%; *sample 5* ($NPFe_3O_4$ coated with sunflower oil) – Fe 39,7%; O 36,7%; C 23,6%.

So, in the experimental *samples (2–5)* a new chemical element (C) appears, and in the experimental *sample 2* two more elements (N and S), which are absent in pure FAM (*sample 1*). The result indicates that FAM nanoparticles were successfully obtained (*sample 1*) and the main substances of food systems: proteins, fats, polysaccharides (*samples 2–5*) chemosorbated on FAM particles.

Determination of FAM bound moisture forms

Depending on the heterogeneity of multicomponent systems, FAM can behave as a functional additive with a high hydration capacity with a wide range of actions in food production technologies, especially during the formation of various colloidal systems. Table 4 shows the coefficients of water absorption of FAM in media traditionally used in food technologies [45].

Table 4

Coefficient of water absorption of FAM in various environments

Polar environment	The coefficients of water absorption of FAM, rel.un.	
	t=20±2˚C	t=50±2˚C
Sodium bicarbonate, pH=6,0	12,4±0,4	12,8±0,4
Ethanoic acid solution, pH=4,5	12,8±0,4	13,0±0,4
Sodium chloride solution, 0,5 %	13,1±0,5	13,4±0,5
Sodium chloride solution, 1,7 %	13,4±0,5	13,5±0,5
Solution of sucrose, 1,1 %	13,6±0,5	13,7±0,5
Solution of sucrose, 5,0 %	13,8±0,6	14,0±0,6
Milk	12,6 ± 0,4	12,9±0,4

Increase in the temperature of the environment to (50±2) °C (Table4) promotes hydration ability of FAM, which are caused, firstly, nano size particles Fe_3O_4 with a developed active surface area and a significant interaction of FAM particles with the aqueous phase [30, 33]; second, the presence of polarized sections, and structure-forming cations of iron on the surface, exhibit pronounced hydrophilic properties and childist to education aquacomplex [31, 32, 37].

The clusterofilnosty NP "Magnetofood" (NPM) [30] and the presence of a defective near-surface layer [33, 35, 39] significantly affect the intensity of hydration – (degree of swelling, K_{sw}) and water absorptive capacity (WAC) of the food additive (Figure 6).

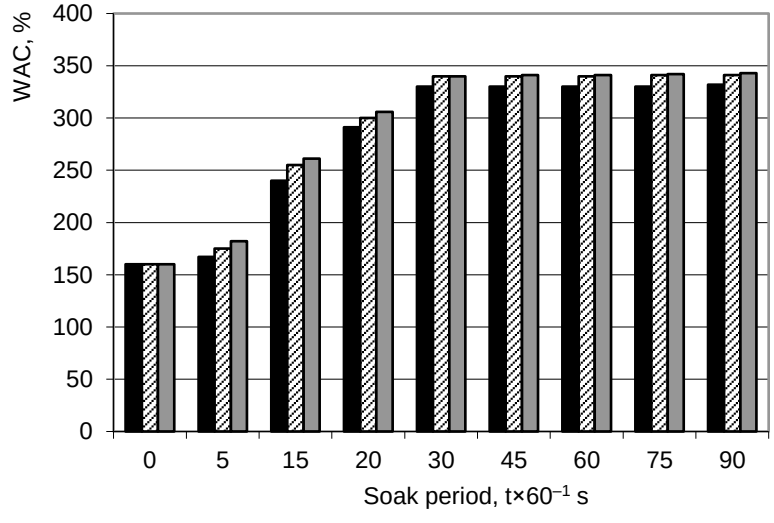

a

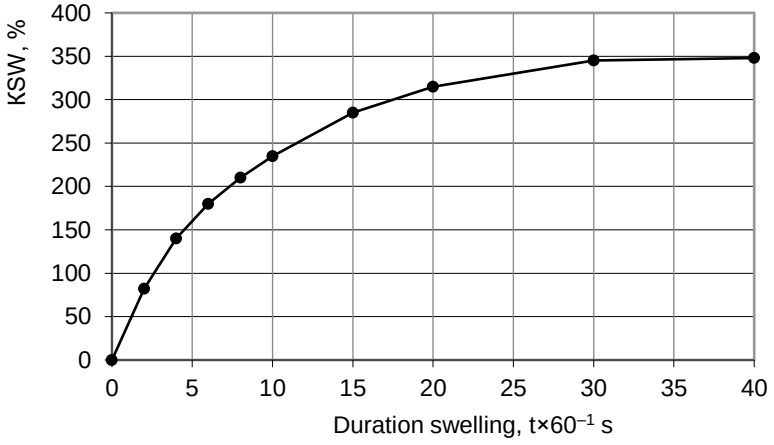

b

Figure 6. Intensity of FAM hydration:
a – WAC of "magnetofood+water" systems in the ratio of FAM:H_2O
–1:3; –1:5; –1:10;
b – swelling kinetics.

The weight of all systems "magnetofood+water" (Figure 6, a) is maximized by 2,0–2,2 times in 30×60 s. Thus, the greatest WAC is observed for these systems with a ratio of 1:5 and 1:10, and the minimum is 1:3. Region at $\tau<10\times60^{-1}$s(Figure 6, b) is characterized by high speed of swelling due to the filling of microdefects of the surface layer additives and water adsorption on the developed surface of NPM water molecules with their electrostatic forces as individual molecules or in the form of a film of a thickness of several molecules. Next, an aquacomplex is formed, since the following aquashares (polimolecular adsorption layers) appear on top of the formed aquaplive (monomolecular adsorption layer), which are attracted

by molecular forces (including hydrogen bonds) [30, 32]. After (25±5)×60 s the swelling process ends and reaches a maximum value of K_{sw}=340–350%.

Based on the analysis of the forms of water bond in FAM after swelling (indicator and thermogravimetric methods) the amount of bound water was determined: physical-chemical 68,9–69,4%, physical-mechanical 21,5–22,3% and free 8,8–9,1% (Figure 7). This fact confirms the bound water capacity of FAM.

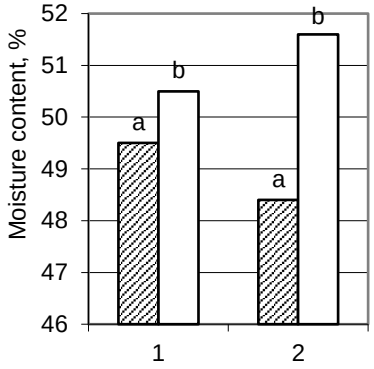

Figure 7. Distribution of water on the forms in the FAM after swelling, the specific methods: 1 – differential thermal analysis; 2 – indicator; a – free, osmotic and physical-mechanical moisture; b – the amount of bound moisture

The ability of FAM to bound and retain water confirmed experimentally in model systems "rye-wheat flour (RWF)+magnetofood" and "starch+magnetofood" increase (compared to control): *swelling* (S_w) of 1,15–1,2 times for starch and 1,1–1,3 times for flour and the *water-retaining capacity* (*WRC*) – 1,15–1,3 times for starch and–1,15–1,27 times for flour (Figure 8).

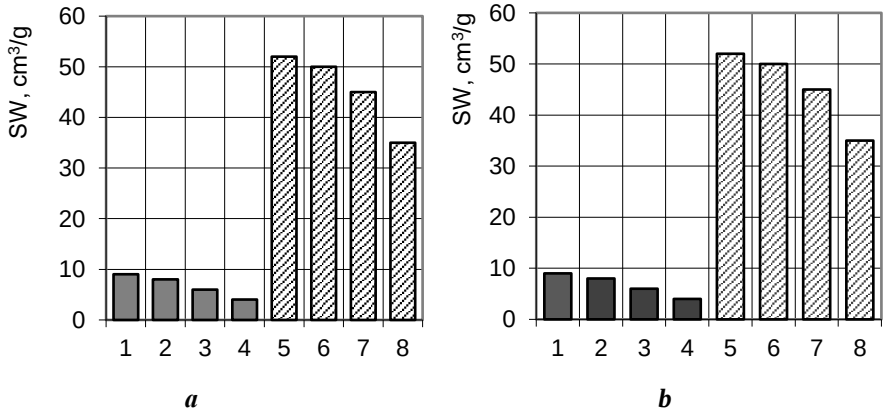

Figure 8. Swelling (*Sw*) (a) and *WRC* (b) systems "RWF+magnetofood" and "starch+magnetofood" with different amounts of FAM, mas.%: 1, 5 – RWF, starch 0, 2%; 2, 6 – RWF, starch 0, 15%; 3, 7 – RWF, starch 0, 1%; 4, 8 – RWF, starch 0%

This is due to the ability NPM branching of the polymer chain of the macromolecules due to the "cavitativ", "clathrativ" and the side chains, extending the main chain of macromolecules of proteins and polysaccharides [30–32].

Also, the nanoparticles form a hydrophilic additive of solvatation with protein-carbohydrate complexes food systems, increasing haratio the ability of the feed components, in particular proteins and polysaccharides [30–32].

Under the influence of the applied shear stress, the formed aggregates are gradually destroyed, and in samples with FAM more slowly. This explains the high pseudoplasticity of water suspensions of experimental starch and flour samples. As a result, their viscosity decreases (Figure 9).

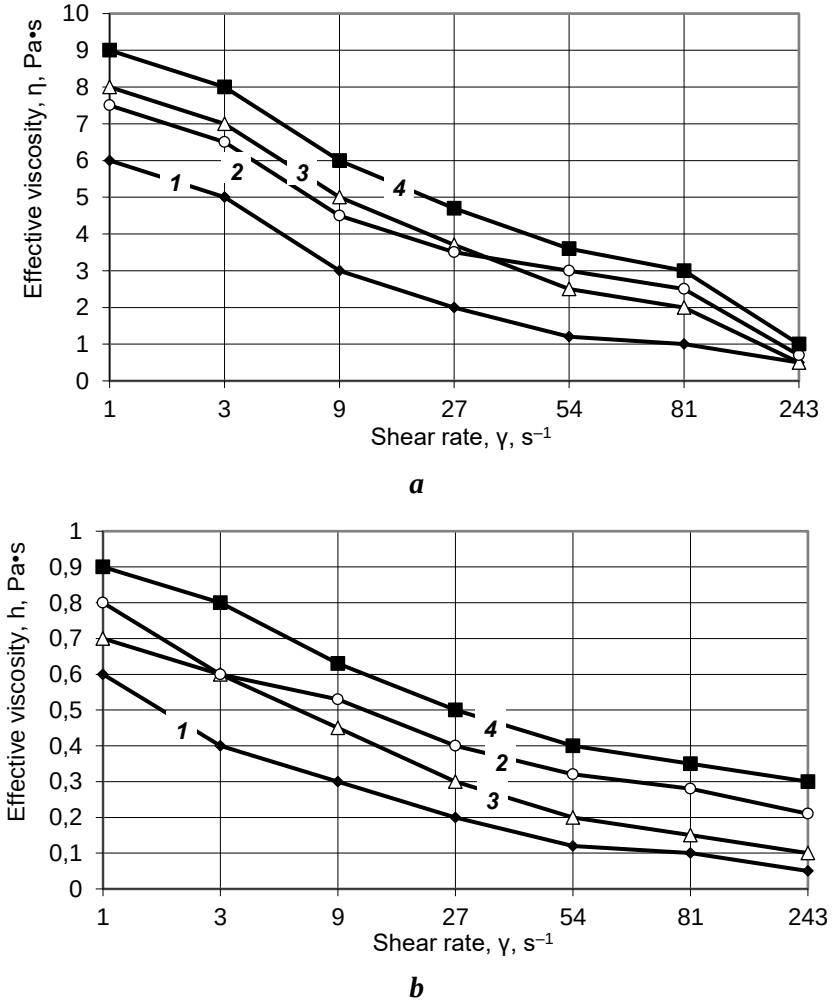

Figure 9. Effective viscosity of 13% of water suspensions at different temperatures and mass fraction of FAM, mas.%: a – "starch (St)+magnetofood"; b – "RWF+magnetofood" (1 – control and 2 – 0,15% FAM at 23 °C; 3 – control and 4 – 0,15% FAM at 40 °C)

The use of FAM increases the viscosity of aqueous suspensions of starch and flour at both temperatures (compared to the control) by an average of 27–31% for starch and 20–24 % for flour at 21–25 °C and 15,0–17% for starch and 9–11% for flour at 38–42 °C. That is, the process of destruction of the internal structures of the dispersed system is slowed down when adding FAM to the system (due to the structure-forming and stability-forming ability of this additive) [30–32]. Moreover, the introduction of FAM into the system accelerates and strengthens the processes of hydration and dissolution of starch and flour [30, 37, 38].

Increase in the viscosity of 13% of water suspensions of starch and flour during proofing (shear rate γ=9 s^{-1}) – 30×60^{-1} s (Figure 10) by 1,15–1,35 times at temperature of 21–25 °C and 1,13–1,26 times at a temperature of 38–42 °C for starch and 1,1–1,27 times at a temperature of 21–25 °C and 1,1–1,22 times at a temperature of 38–42 °C for flour (compared to the control) is associated with the continuation of the processes of hydration and dissolution (due to the clusterofilnosti and amphifilnosti FAM) [30, 33].

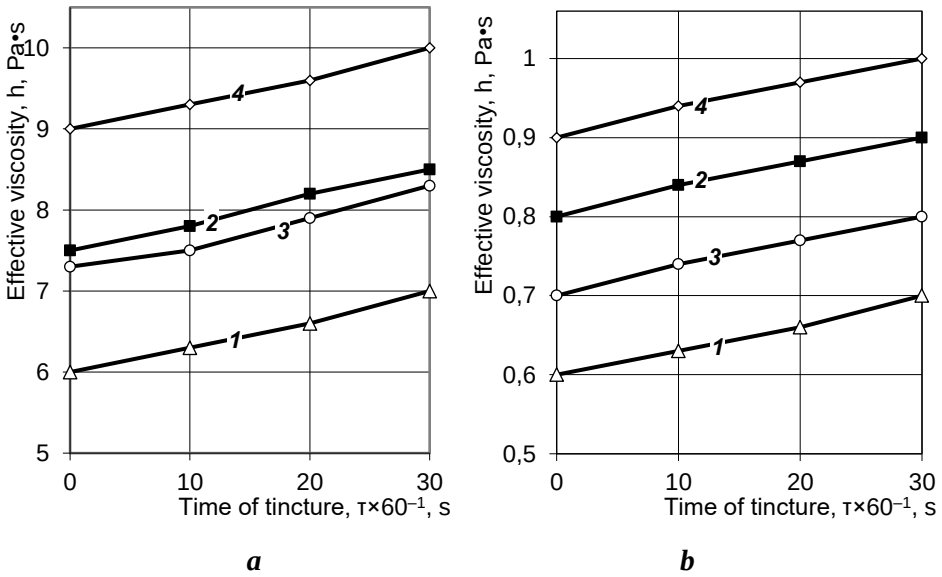

Figure 10. Dependence of the effective viscosity of 13% water suspensions on the time of tincture at different amounts of FAM, mas.%: a – "starch (St)+magnetofood"; b – "RWF+ magnetofood" (1 – control and 2 – 0,15% FAM at 23 °C; 3 – control and 4 – 0,15% FAM at 40 °C)

Adding a food additive based on double oxide of two- and trivalent iron "Magnetofood" (FAM) to the system accelerates and strengthens the processes of hydration and dissolution of starch and flour. The thickening properties of the food additive and its ability to bind and retain water have been experimentally confirmed. These properties are important in hal- and foam-like, emulsified and emulsified-suspension systems.

Conclusions

Proved the mechanism of water retention nanoparticles of food additives, based of double oxide of two- and trivalent iron "Magnetofood" (Fe_3O_4) due to clusterophilicity and amphiphilicity food supplements and the ability of $NPFe_3O_4$ polarization, electrostatic coordination, formation of aqua associates. The introduction of a food additive based on double oxide of two- and trivalent iron "Magnetofood" into the poliphase system increases the water-retaining capacity of its components (in particular, proteins, polysaccharides), which contributes to improving the quality indicators and shelf life of finished products in comparison with the control.

The conducted research shows the high hydration capacity of a food additive based on double oxide of two- and trivalent iron "Magnetofood" (FAM), which in food production technologies can improve the functional and technological properties of heterogeneous dispersed systems and improve the timing of preserving the freshness of finished products.

References

1. Trokhymenko V., Kalchuk L., Didukh M., Kovalchuk T., Zakharin V. (2018), Vykorystannia kharchovykh dobavok u kovbasnomu vyrobnytstvi ta yikh vplyv na orhanizm liudyny, *Visnyk Sumskoho natsionalnoho ahrarnoho universytetu, Seriia «Tvarynnytstvo»*, 2(34), pp.233–237.
2. Maforimbo E., Skurray G., Nguyen M. (2007), Evaluation of l–ascorbic acid oxidation on SH concentration in soy–wheat composite dough during resting period, *Food Sci. and Technol.*, 40(2), pp. 338–343.
3. Rosell C., Aja S., Bean S., Lookhart G. (2003), Wheat flour proteins as affected by transglutaminase and glucose oxidase, *Cereal Chem.*, 80(1), pp. 52–55.
4. Chugunova O., Pastushkova E. (2015). Modelirovaniye organolepticheskikh pokazateley khleba s rastitelnymi dobavkami. *Vestnik YuUrG,. Seriya «Pishchevyye i biotekhnologii»*, 3(4), pp. 80–87.
5. Tamazova S., Lisovoi V., Pershakova T., Kazimirova M. (2016), Pishchevye dobavki na osnove rastitelnogo syria, primeniaemye v proizvodstve khlebobulochnykh i muchnikh konditerskikh izdelii, *Politematicheskii setevoi elektronnyi nauchnyi zhurnal KubGAU*, 122(8), pp. 1–8.
6. Rosliakov Iu.F., Vershinina O.L., Gonchar V.V. (2016), Nauchnye razrabotki dlia khlebopekarnoi i konditerskoi otraslei, *Tekhnologii pishchevoi i pererabatyvaiushchei promyshlennosti, APK-produkty zdorovogo pitaniia*, 6, pp. 1–6.
7. Rosliakov Ju., Vershinina O., Gonchar V. (2010), Perspektivnye issledovaniia tekhnologii khlebobulochnykh izdelii funktsionalnogo naznacheniia, *Izvestiia vuzov, Pishchevaia tekhnologiia*, 1, pp.123–125.
8. Gorshunova K., Semenova P., Bessonov V. (2012), Vzaimodeistvie gidrokolloidov i vodorastvorimykh vitaminov pri konstruirovanii obogashchennykh pishchevykh produktov, *Pishchevaia promyshlennost*, 11, pp. 46–49.
9. Filips G. O, Viliams P. A. (2006), *Spravochnik po gidrokolloidam, Per. s angl. pod red. Kochetkovoi A. A. i Sarafanovoi L. A.*, GIORD, Sankt–Peterburg.
10. (2013), *Tsitrusovye volokna Herbacel AQ Plus – tip N: spetsifikatsii dlia pishchevykh dobavok i retseptury*, Available at: http://specin.ru.

11. Domoroshchenkova M., Demianenko T., Kamysheva I. (2007), Issledovanie funktsionalno–tekhnologicheskikh svoistv izoliatov soevykh belkov, *Maslozhirovaia promyshlennost*, 4, pp. 24–28.
12. Renziaeva T., Pozniakovskii V. (2009), Vodouderzhivaiushchaia sposobnost syria i pishchevykh dobavok v proizvodstve muchnykh konditerskikh izdelii, *Khranenie i pererabotka selkhozsyria,* 8, pp. 35–38.
13. Renziaeva T., Tuboltseva A., Ponkratova E., Lugovaia A., Kazantseva, A. (2014), Funktsionalno–tekhnologicheskie svoistva poroshkoobraznogo syria i pishchevykh dobavok v proizvodstve konditerskikh izdelii, *Tekhnika i tekhnologiia pishchevykh proizvodstv*, 4, pp. 43–49.
14. Anup S., Atanu H., Shrikant C. (2012), Comprehensive Reviews in Food Science and Food Safety, *Institute of Food Technologists,* 11, pp. 518–528.
15. Bae S., Cho M., Jeong J. (2017), Effects of Various Calcium Powders as Replacers for Synthetic Phosphate on the Quality Properties of Ground Pork Meat Products, *Korean J. Food Sci Anim Resour*, 37(3), pp. 456–463.
16. Martins Z., Pinho O., Ferreira, I. (2017). Food industry by–products used as functional ingredients of bakery products, *Trends in Food Science & Technology*,67, pp. 106–128.
17. Lai W., Khong N., Lim S., Hee Y., Sim B., Lau K., Lai O. (2017), A review: Modified agricultural by–products for the development and fortification of food products and nutraceuticals, *Trends in Food Science & Technology*, 59, pp. 148.
18. Bharath K., Prabhasankar P. (2014), Low glycemic index ingredients and modified starches in wheat based food processing: A review, *Trends in Food Science & Technology,* 35(1), pp. 32–41.
19. Ngemakwe P., Le Roes-Hill M., Jideani V. (2014), Advances in gluten–free bread technology, *Food Science and Technology International,* 21(4), pp. 256–276.
20. Bird L., Pilkington C., Saputra A., Serventi L. (2017), Products of chickpea processing as texture improvers in gluten–free bread, *Food Science and Technology International*, 23(8), pp. 690–698.
21. García–Segovia P., Pagán–Moreno M., Lara I., Martínez-Monzó J. (2017), Effect of microalgae incorporation on physicochemical and textural properties in wheat bread formulation, *Food Science and Technology International,* 23(5), pp. 437–447.
22. Boubaker M., Omri A., Blecker C., Bouzouita N. (2016), Fibre concentrate from artichoke (Cynara scolymus L.) stem by-products: Characterization and application as a bakery product ingredient, *Food Science and Technology International,* 22(8), pp. 759–768.
23. Ramachandraiah K., Choi M.-J., Hong G.-P. (2018), Micro– and nanoscaled materials for strategy–based applications in innovative livestock products: A review, *Trends in Food Science & Technology*, 71, pp. 25–35.
24. Hansen S., Heggelund L., Besora P., Mackevica A., Boldrin A., Baun A. (2016), Nanoproducts – what is actually available to European consumers?, *Environmental Science: Nano*, 1, pp. 1–8.
25. Thiruvengadam M., Rajakumar G., Chung M. (2018), Nanotechnology: current uses and future applications in the food industry, *3 Biotech,* 8(1), pp. 74–83.
26. Drmota A., Kosak A., Znidarsik A. (2008), A mechanism for the adsorption of carboxylic acids onto the surface of magnetic nanoparticles, *Materials and technology,* 42, pp. 79–83.
27. Mahdavi M., Ahmad M. B., Haron M., Namvar F., Nadi B., Ab Rahman M., Amin J. (2013), Synthesis, Surface Modification and Characterisation of Biocompatible Magnetic Iron Oxide Nanoparticles for Biomedical Applications, *Molecules,* 18, pp. 7533–7548.

28. Zhang L., He R., Gu H.-C. (2006), Oleic acid coating on the monodisperse magnetite nanoparticles, *Applied Surface Science, APSUSC–14301*, 7, pp. 1–7.
29. Chernyshova I., Ponnurangam S., Somasundaran P. (2011), Adsorption of Fatty Acids on Iron (Hydr)oxides from Aqueous Solutions, *Langmuir*, 27(16), pp. 10007–10018.
30. Tsykhanovska I., Evlash V., Alexandrov A., Lazareva T., Svidlo K., Gontar T., Yurchenko L., Pavlotska L. (2018), Substantiation of the mechanism of interaction between biopolymers of rye-and-wheat flour and the nanoparticles of the «Magnetofood» food additive in order to improve moisture–retaining capacity of Dough, *Eastern-European Journal of Enterprise Technologies*, 2/11(92), pp. 70–80.
31. Tsykhanovska I., Evlash V., Alexandrov A., Lazareva T., Bryzytska O. (2018), Substantiation of the interaction between the lipo- and glucoproteids of rye-wheat flour and nanoparticles of the food additive «Magnetofood», *Eastern–European Journal of Enterprise Technologies*, 4/11(94), pp. 61–68.
32. Tsykhanovska I., Evlash V., Alexandrov A., Lazareva T., Yevlash T. (2018), Substantiation of the mechanism of interaction of between the carbohydrates of rye–wheat flour and nanoparticles of the polyfunctional food additive «Magnetofood», *Eastern-European Journal of Enterprise Technologies*, 3/11(93), pp. 59–68.
33. Levitin E. Ia., Vedernikova I. A., Tsikhanovskaia I. V. (2007), Issledovanie elektropoverkhnostnykh svoistv magnetitovykh dispersnykh sistem na vodnoi osnove, *Eastern–European Journal of Enterprise Technologies*, 3/4 (27), pp. 16–18.
34. Tsykhanovska I., Evlash V., Alexandrov A., Gontar T. (2018), Mechanism of fat-binding and fat-contenting of the nanoparticles of a food supplement on the basis of double oxide of two- and trivalent iron, *Ukrainian Food Journal*, 7(4), pp. 702–715.
35. Tsykhanovska I., Evlash V., Alexandrov A., Gontar T., Shmatkov D. (2019), The study of the interaction mechanism of linoleic acid and 1–linoleyl–2–oleoyl–3–linolenoyl–glycerol with Fe_3O_4 nanoparticles, *Chemistry & chemical technology Chemistry*, 13(3), pp. 303–316.
36. Iliukha N., Barsova Z., Kovalenko V., Tsikhanovskaia I. (2010), Tekhnologiia proizvodstva i pokazateli kachestva pishchevoi dobavki na osnove magnetita, *Eastern-European Journal of Enterprise Technologies*, 6/10(48), pp. 32–35.
37. Tsykhanovska I., Evlash V., Alexandrov A., Lazareva T., Yevlash T. (2018), Investigation of the water-retaining capacity of the carbohydrate complex of rye-wheat dough with addition of polyfunctional food supplement «Magnetofood», *Eureka: Life Sciences*, 3/15(3), pp. 56–64.
38. Tsykhanovska I., Yevlash V., Lazarieva T., Shynhisov A. (2019), Doslidzhennia strukturno–mekhanichnykh pokaznykiv ta pinoutvorennia zefirnykh mas z riznymy strukturoutvoriuvachamy pry vvedenni v retsepturu kharchovoi dobavky «Mahnetofud», *Pratsi TDAU, Tekhnichni nauky*, 2(19), pp. 168–189.
39. Aleksandrov O.V., Tsykhanovska I.V., Barsova Z.V., Dudenko N.V., Pavlotska L.F., Skurikhina L.A. (2015), *Kolektyvna monohrafiia, Povnotsenne kharchuvannia: innovatsiini aspekty tekhnolohii, enerhoefektyvnoho vyrobnytstva, zberihannia ta marketynhu, Oderzhannia ta doslidzhennia vlastyvostei biolohichno–aktyvnykh dobavok na osnovi lipido–mahnetytovykh suspenzii*, KhDUKhT, Kharkiv, pp. 138–167.
40. Tsykhanovska I., Aleksandrov O., Lazarieva T., Hontar T., Pavlotska L. (2016), *Kolektyvna monohrafiia, Povnotsenne kharchuvannia: innovatsiini aspekty tekhnolohii, enerhoefektyvnoho vyrobnytstva, zberihannia ta marketynhu, Vykorystannia zhyro–mahnetytovoi suspenzii dlia pidvyshchennia kharchovoi tsinnosti tsukerok «Sukhofrukty v shokoladi», zbahachenykh zalizovmisnoiu kharchovoiu dobavkoiu*, KhDUKhT, Kharkiv, pp. 143–170.

41. Tarasiuk N., Barsova Z., Tsykhanovska I. (2012), Tekhnolohiia otrymannia oliino–mahnetytovыkh suspenzii, *Khimichni Karazinski chytannia – 2012 (KhKCh12): tezy IKh Vseukr. nauk. konf., 23–26 kvitnia 2012 roku, Kharkivskyi natsionalnyi un–t im. V. N. Karazina.* pp. 326–327.
42. Tsykhanovska I., Alexandrov A., Gontar T., Kokodiy N., Dotsenko N. (2016), Stability and morphological characteristics of lipid–magnetite suspensions, *Eureka: Life Sciences,* 3(3), pp. 14 – 25.
43. Iurchak V., Berzina N., Shmarovoz V., Prishchepa M. (1989), Opredelenie sviazannoi vody indikatornym metodom v khlebopekarnom proizvodstve, *Izvestiia vuzov, Pishchevaia tekhnologiia,* 4, pp. 78–80.
44. Nilova L., Kalinina I., Naumenko N. (2013), Metod differentsialno–termicheskogo analiza v otsenke kachestva pishchevykh produktov, *Vestnik IuUrGU, Pishchevye i biotekhnologii,* 1(1), pp. 43–49.
45. Krainiuk L., Savgira Iu., Pozdniakova E., Iancheva M. (2000), K voprosu o sovershenstvovanii metodiki opredeleniia vodosviazyvaiushchei sposobnosti miasa i miasoproduktov, *Progresivni tekhnologiï ta udoskonalennia protsesiv kharchovikh virobnitstv: zb. nauk. prats,* 1, pp. 119–123.
46. Svidlo K., Peresichnyi M. (2011), Technology of functional public catering foods with dietary additives, *Proceedings of 11th International Congress on Engineering and Food «Food Process in Changing World», 22–26 May 2011, National Technical University of Athens, School of Chemical Engineering,* pp. 2035–2037.
47. Diakov A., Torianik A., Svidlo K., Lipovoi D. (2013), Issledovanie vlagosoderzhaniia shrota i kletchatki ovsa i proektirovanie na ikh osnove tekhnologii smuzi gerodieticheskogo naznacheniia, *Protsessy i apparaty pishchevykh proizvodstv, Sankt–Peterburg: SPBGUNiPT,* 1, pp. 10.
48. Rikhter M., Augustat Z., Shirbaum F. (1975), *Izbrannye metody issledovaniia krakhmala,* Pishchevaia promyshlennost, Moscow.
49. Renziaeva T., Pozniakovskii V. (2009), Vodouderzhivaiushchaia sposobnost syria i pishchevykh dobavok v proizvodstve muchnykh konditerskikh izdelii, *Khranenie i pererabotka selkhozsyria,* 8, pp. 35–42.
50. Posudin Y.I., Peiris K.S., Kays S.J. (2015), Non–destructive detection of food adulteration to guarantee human health and safety, *Ukrainian Food Journal*, 4(2), pp. 207–260.

Effect of some unconventional ingredients on the production of black beer

Marius Ciocan, Adriana Dabija, Georgiana Gabriela Codină

Stefan cel Mare University of Suceava, Suceava, Romania

Keywords:

Black beer
Acorn
Topinambur
Molasses

Article history:

Received
02.09.2019
Received in revised
form 16.01.2020
Accepted
30.06.2020

Corresponding author:

Adriana Dabija
E-mail:
adriana.dabija@
fia.usv.ro

DOI:
10.24263/2304-
974X-2020-9-2-5

Abstract

Introduction. The aim of this research is to determine the effect of some unconventional ingredients such as the acorn flour, topinambur flour and molasses in order to develop a beverage similar to black beer.

Materials and methods. Black beer was obtained according to a conventional method of obtaining beer in a pilot scale brewery. In the manufacturing recipe, brown malt has been replaced with acorn flour, topinambur flour and molasses with 50% sucrose in the following variants: variant 1 – 0.5:1.5:1; variant 2 – 1:1:1; variant 3- 1:1.5:0.5; variant 4 – 1.25:1.25:0.5. For fermentation of bottom-fermenting yeast was used. The extract content, alcohol content and apparent fermentation for the black beer samples were analysed with the Anton Paar device.

Results and discussion. The CO_2 content, foam height, foam stability, total acidity of beer, for all the analyzed samples are within the admitted limits for the black beers. The sensory characteristics of the black beer samples evaluated, namely appearance, colour, odour, taste, gas release and foam stability indicates the fact that the variant 1 of the black beer received the lowest score whereas the variant 4 received the highest one. The sensory analysis results were unexpected ones, the non gluten beers obtained being very well appreciated, the panellists preferring them over commercial black beers made from traditional ingredients. The black beer obtained in all four experimental versions are beers with an alcoholic concentration which ranged between 7.06% and 8.16%, with a high degree of final fermentation, which ranged between 73.26% for variant 2 and 85.85% for variant 4. The data obtained with the unconventional raw materials as the acorn flour, topinambur flour and molasses were comparable to commercial black beer, which acted as the control sample. The best result regarding the final fermentation degree (85.85%) was obtained for the variant 4, even higher than those obtained for the commercial beer (80.20%). Also, the variant 4 was the best appreciated from the sensory point of view. This variant can be proposed to obtain black beer on an industrial scale because it has good physico-chemical properties comparable to a black beer on the market.

Conclusions. Black beer, obtained on the basis of an innovative manufacturing recipe, presented good sensorial characteristics, a freshly roasted coffee flavour, a fruity taste and bittersweet.

Introduction

Nowadays, the beer production from other raw materials than barley or wheat malt is an increasing one in the beer industry field. The new innovative products meet consumers demand especially those suffering from celiac disease. The gluten content in commercial beers is below the limits of Codex Alimentarius Standard (20 ppm), but even so may create healthy problems to the consumers due to their different clinical sensitivity to the beer gluten content [1].

Over the last years, different strategies can be applied to produce gluten-free beers [2]. Some approaches for the biological or chemical elimination of barley gluten (hordein) or wheat gluten (gliadin) have been proposed [3]. For example, Fanari et al. (2018) proposed two different deglutinization treatments: an enzymatic process based on *Aspergillus niger* prolyl endopeptidase and a precipitation process by silica gel [4].

Many studies has been carried out into the use of other cereals in the brewing of beer such as maize, rice, sorghum, teff, millet, and triticale, pseudocereals (buckwheat, amaranth, quinoa), and another ingredients such as cassava, chestnut, honey, sugar, molasses etc. [5-15].

The future studies should be performed to improve the quality of innovative beer assortments from new unconventional raw materials in order to satisfy the consumers demand.

This current study proposes the use of three ingredients as malt substitutes for obtaining black beer: acorn flour, topinambur flour and molasses.

Acorn flour is obtained from *Quercus* sp. fruits from ancient times through drying, maturation, milling, detanization processes and it is used in the manufacture of various bakery products, beverages, pastry-confectionery, pasta, biscuits, as a coffee substitute etc.[16,17,18]. Acorn flour is an important source of antioxidant substances, has a high fat content (of which over 80% unsaturated fat), protein and a considerable amount of calcium, magnesium, potassium, phosphorus, iron, copper and zinc, vitamins from the B complex (B_1, B_2, B_3 and B_6) [19,20]. Acorn flour has anti-inflammatory, mineralizing, antianemic, antirash, antitumor, antioxidant, diuretic, energizing favouring insulin secretion properties. This flour is recommended for the treatment of gastritis, ulcer, enteritis, anaemia, mental disorders, fatigue, mental exhaustion, overuse and headaches [21,22].

Topinambur tubers have been brought to the attention of specialists and consumers due to their properties, being recommended by many nutritionists for consumption. Topinambur is currently recognized as a culture used for the production of long-standing ethyl alcohol, including beer production [23,24]. The topinambur tubers were also used to produce brandy in France and Germany or for sake in Japan. The topinambur flour is a valuable, easy-to-use product, and its addition to bakery, pastry and pasta-making recipes improves their nutritional value [25,26]. The topinambur flour is rich in fiber (36.4% on average), mineral substances (calcium, iron, selenium, potassium, phosphorus) and vitamins (B vitamins, vitamin C, β-carotene) [27]. Topinambur is also rich in inulin (over 50% of the dry substance), which can be easily hydrolysed and then converted into ethyl alcohol. The yield in ethyl alcohol is equivalent to that of sugar cane and twice as high as that of ethyl alcohol obtained from corn. Other uses of topinambur flour are: extruded products, confectionery products, gelatine products, sugary products, functional granules, culinary products etc. [28,29,30].

Molasses is the last by-product from the manufacture of sugar following repeated crystallization of sucrose and from which can still be obtained by crystallization. Nowadays, in the US, Europe, Australia, as well as in our country, molasses is the main raw material used in the production of bakery yeast and a valuable raw material for the production of ethyl

alcohol (containing an average of 50% sucrose). The chemical composition of molasses varies depending on the raw material used in the manufacture of sugar (beet or sugar cane) and the technological process applied in the sugar factories. The benefits of molasses cover a wide range of health problems: acne and other skin diseases, headaches, anaemia, stress, obesity, diabetes, constipation, prostate disorders, premenstrual symptoms, or cancer [31,32].

The main objective of this research was to use these unconventional raw materials that have been previously developed to obtain brew, a beverage similar in aroma, taste and mouth feel to black beer. To our acknowledgments no other studies has been made for non-gluten black beer production with the ingredients used in this research. This fact will lead to a diversification of black beer assortments which may satisfy the consumers.

Materials and methods

Materials

In our research the following ingredients were used: acorn flour and topinambur flour obtained from Bio Boom Company Romania, molasses from Agrana Romania Company, a bottom fermentation yeast from Grama Trading Company under the trade name Saflager W 34/70 (Fermentis, Belgium), and hop pellets from Agrosiro Serv Impex Company (Sighisoara, Romania). All the raw materials used in the process came from trustworthy suppliers with technical quality specifications, in compliance with the current food safety legislation.

In order to obtain the black beer, several experimental variants were elaborated in which the three basic ingredients – acorn flour, topinambur flour and molasses – replaced the barley malt from the classic beer recipe. Thus, the ratio between acorn flour, topinambur flour and molasses was: variant 1 – 0.5:1.5:1; variant 2 – 1:1:1; variant 3- 1:1.5:0.5; variant 4 – 1.25:1.25:0.5.

Beer production

Brewing was carried out in a pilot scale brewery (30 L, Braumeister, Speidel, Germany). The technological process of obtaining the beer respected the classical technology through the decoction process with two mashes [33]. Thus, acorn flour and topinambur flour were mashing separately, until boiling for gelatinization of the starch. Then, those 2 mash were inserted into the main mash to obtain the wort using the following mashing programme: mashing in at 45 °C; rest for 30 min; ramp heating within 15 min to 63 °C; rest for 30 min; ramp heating within 5 min to 65 °C; rest for 30 min; ramp heating within 5 min to 72 °C and rest for 60 min. At this temperature saccharification was monitored every 10 min, until the reaction with iodine did not took place anymore. Mashing off temperature was 78 °C, and then the mash was filtered to obtain the wort.

The wort was boiled with hops for 60 min under atmospheric pressure, cooled to 12 °C and fermented for 5 to 7 days at 12 °C using a bottom fermentation yeast. The fermentation trials were performed simultaneously under the same conditions. Fermentation was followed by a maturation period of 21 days at 4 °C. Filtration was carried out using a plate filter, and then the filtered beer was bottled using a manual bottling unit.

Bottled black beer was stored to the dark at 4 °C until analysis.

Beer analyses

The final beer was analyzed for its physical-chemical and sensorial properties. The extract content, alcohol content and apparent fermentation were determinated by Anton Paar (Anton Paar GmbH, Austria) using an automated beer analyzer. The CO_2 content, foam height, foam stability, total acidity of beer, was measured [34, 35].

A sensory evaluation of the beers was carried out by a trained, 25-member tasting panel (10 women and 15 men, 24-60 years old), following the 20 points method. The points ranged from 0 to 5 for each attributes: appearance, colour, odour, taste, gas release and foam stability. A point of 0 meant that the attribute was absent whereas a point of 5 indicated that the attribute was extremely strong [36].

Statistical analysis

Data were expressed as means ± standard deviations for triplicate determination. Statistical analysis was performed using XLSTAT statistical package (free trial version, Addinsoft, Inc. Brooklyn, NY, USA) at a significance level of $p < 0.05$.

Results and discussion

Physicochemical characteristics of black beer samples

The beer samples obtained were analyzed from the physicochemical point of view, and the results obtained were compared with an assortment of commercial black beer. The results obtained were shown in Table 1 and Table 2. Beer constituents were provided from the raw materials (acorn flour, topinambur flour, molasses, carbohydrate sources), bitter and flavour substances from wort production, as well as from fermentation and maturation.

Foam, foaming capacity and foam stability distinguish beer from other beverages. A good, white and stable foam stability is a key parameter which reflects the fact that it was handled correctly during the brewing process. The characteristics of the foam are: volume, density and persistence. The volume of the foam depends on the carbon dioxide content and the amount of surfactants. The slow release of carbon dioxide, in small, uniform bubbles, is explained by its bounding to colloids from the extract: dextrin, proteins, bitter resins from hops etc. [37].

The persistence of the foam depends on the degree of dispersion of the colloidal substances in the beer, which forms a resistant film around the carbon dioxide bubbles. The persistence of the foam is favoured by the bitter resins of the hops and by the nitrogenous substances, complex, but it is diminished by the presence of fats and the amount of alcohols content. The beer must have long and persistent foam, must be clear and shiny and must maintain these characteristics for the longest period of time possible [7].

Considering Table 1 one can observe that the samples with the highest foam stability are samples 2 and 4, followed by samples 3 and 1.

CO_2 content is crucial for the ability to foam and other beer sensory properties. In the beer samples analyzed, the CO_2 content is within the limit of min. 0.4 g/100 mL drink [34]. The highest value of this parameter was recorded for the sample 4, namely 4.8 g CO_2 /100 g beer. This value was higher even than those obtained for the market beer sample, whose value was only 4.06 g CO_2 /100 g beer.

Table 1

Physicochemical properties for black beers by standard methods

Beer samples – mean (SD)	CO_2 [g/100 mL]	FH [mm]	FS [min]	TA [mL NaOH 1N /100 mL]
Beer 1 (B1)	4.1±0.1^{ab}	28.0±1.0^{a}	4.00±1.0^{ab}	2.80±0.20^{ab}
Beer 2 (B2)	4.0±0.1^{ab}	48.0±2.0^{a}	8.00±1.0^{a}	2.90±0.05^{ab}
Beer 3 (B3)	3.9±0.2^{ab}	42.0±2.0^{a}	5.00±0.0^{ab}	2.95±0.05^{ab}
Beer 4 (B4)	4.8±0.1^{a}	58.0±2.0^{a}	7.00±1.0^{ab}	3.50±0.10^{a}
Commercial beer sample (BC)	4.06±0.11^{b}	59.33±4.16^{a}	7.00±1.0^{b}	3.26±0.11^{b}
F-ratio	9.862	5.617	7.194	8.069
P-value	0.002	0.012	0.005	0.004

Physicochemical properties: CO, colour, FH, foam height, FS, foam stability, TA, total acidity
The values are means±standard deviations of three replicates.
Means in the same column followed by different letters are significantly different ($p < 0.05$).

Table 2

Physicochemical properties for black beers by Anton-Paar device

Beer samples – mean (SD)	OE [°P]	ALC [% v/v]	pH	GFF [%]
Beer 1 (B1)	17.85±0.08^{a}	8.16±0.04^{a}	4.60±0.02^{ab}	77.04±0.50^{ab}
Beer 2 (B2)	17.05±0.05^{a}	7.60±0.03^{a}	4.53±0.01^{ab}	73.26±0.33^{ab}
Beer 3 (B3)	16.87±0.03^{a}	7.06±0.04^{a}	4.56±0.03^{ab}	79.87±0.23^{ab}
Beer 4 (B4)	16.92±0.02^{a}	7.40±0.04^{a}	5.02±0.02^{a}	85.85±0.15^{a}
Commercial beer sample (BC)	14.85±0.08^{a}	7.20±0.20^{a}	4.60±0.03^{b}	80.20±0.20^{b}
F-ratio	12.178	9.972	9.500	8.965
P-value	0.001	0.002	0.002	0.002

Physicochemical properties: OE, original extract, ALC, alcohol concentration, GFF, final fermentation degree
The values are means±standard deviations of three replicates.
Means in the same column followed by different letters are significantly different ($p < 0.05$).

The extract of the primitive must and the alcohol concentration of the beer are the most important determinations, at least from the financial point of view [38]. The black beer obtained in all 4 experimental versions is a beer with an alcoholic concentration between 7.06% and 8.16%, with a high degree of final fermentation, with values between 73.26% for variant 2 and 85.85 % for variant 4 (Table 2). It can be observed that beer samples 4, recorded the best results regarding the final fermentation degree (85.85%), even higher than the beer from (80.20%).

Sensorial characteristics of black beer samples

Sensory analysis is of essential importance in assessing the quality of beer. The taste, the smell, the colour, the clarity, the foaming, the release of the carbon dioxide bubbles, are the best recommendation and are, at the same time, the result of all the technological operations [10, 39]. To perform the sensory analysis of the 4 experimental variants, the 20 points sensory method was used. The results of the sensory analysis are shown in Table 3.

Table 3

Sensorial properties for the dark beers samples

Beer samples – mean (SD)	AP	CO_S	OD	TA	GR	FS_S	PT
Beer 1 (B1)	2.00± 0.34^{a}	2.66± 0.46^{a}	0.66± 0.11^{a}	5.60± 0.10^{a}	1.80± 0.60^{a}	1.06± 0.23^{a}	13.80± 0.20^{a}
Beer 2 (B2)	2.20± 0.34^{a}	3.73± 0.46^{a}	0.80± 0.20^{b}	5.60± 0.10^{a}	2.20± 0.34^{a}	1.46± 0.23^{a}	16.00± 0.20^{a}
Beer 3 (B3)	2.20± 0.34^{ab}	2.94± 0.46^{ab}	0.60± 0.10^{ab}	6.06± 0.80^{a}	2.00± 0.34^{ab}	1.46± 0.23^{ab}	15.26± 0.61^{ab}
Beer 4 (B4)	2.60± 0.34^{a}	4.00± 0.10^{a}	1.00± 0.10^{a}	6.53± 0.80^{ab}	2.40± 0.10^{a}	1.86± 0.23^{a}	18.40± 0.40^{a}
Commercial beer (BC)	3.00± 0.10^{b}	4.00± 0.10^{b}	0.86± 0.11^{b}	6.53± 0.80^{b}	2.60± 0.34^{b}	1.86± 0.20^{b}	18.86± 0.41^{b}
F-ratio	7.228	9.088	11.933	10.294	7.865	8.695	9.221
P-value	0.009	0.004	0.001	0.002	0.007	0.005	0.004

Sensorial properties: AP, appearance, CO_S, colour, OD, odour, TA, taste, GR, gas release, FS_S, foam stability

Means in the same column followed by different letters are significantly different ($p < 0.05$).

From the sensory point of view, the most appreciated by tasters was beer sample 4, followed by beer sample 2 and beer sample 3.

Relationship between characteristics of the beer samples obtained

Table 4 shown the Pearson correlation between the sensorial and physico-chemical data of the black beer analyzed samples. It may be seen that all the sensorial values for total points (PT) are significant correlated with the physico-chemical data of the analyzed beer samples and with each sensory characteristics analyzed. Therefore the highest significant direct influence according to the correlation obtained ($p<0.01$) on PT for the analyzed samples presented the beer's physico-chemical characteristics foam stability (FH), r=0.925 and total acidity (TA), r= 0.823. A significant negative influence on PT presented the physico-chemical characteristics original extract (OE) r = -0.776 at a significant level of $p = 0.01$ and alcohol concentration (ALC), r = – 0.584 at a significant level of $p = 0.05$. It may be also noticed that between physico-chemical data ALC and OE it is a direct significant correlation (r=0.648) at a level $p = 0.01$, a similar one been also obtained by Codină *et al.* (2011)[40]. From the sensorial characteristics point of view, it seems that all of the analyzed sensorial parameters presented a highly significant ($p<0.01$) influence on PT except gas release (GR) which presented a lower significant influence one ($p<0.05$), between these characteristics (PR and GR) being the lowest correlation value of r = 0.636.

Table 4

Pearson correlation of physicochemical and sensorial properties for the black beers samples

	CO	FH	FS	TA	OE	ALC	pH	GFF	AP	CO_S	OD	TA	GR	FS_S	PT
CO	**1**	0.386	0.214	**0.661****	0.077	0.008	**0.939****	**0.721****	0.216	0.359	**0.595***	0.475	0.273	0.412	**0.514***
FH		**1**	**0.762****	**0.789****	**-0.731****	**-0.654****	0.455	0.483	**0.697****	**0.845****	**0.636***	0.396	**0.689****	**0.834****	**0.925****
FS			**1**	0.337	-0.413	-0.307	0.201	-0.016	0.334	**0.721**	0.485	0.000	**0.639***	**0.615***	**0.603***
TA				**1**	-0.475	-0.485	**0.758****	**0.783****	**0.708****	**0.665****	**0.671****	0.502	0.401	**0.711****	**0.823****
OE					**1**	**0.648****	0.054	-0.235	**-0.743****	**-0.571***	-0.316	-0.456	**-0.562***	**-0.645****	**-0.776****
ALC						**1**	-0.083	-0.401	-0.486	-0.384	-0.072	-0.426	-0.373	**-0.644****	**-0.584***
pH							**1**	**0.845****	0.278	0.395	**0.635***	0.403	0.236	0.460	**0.520***
GFF								**1**	0.410	0.302	0.455	**0.535***	0.281	**0.536***	**0.572***
AP									**1**	0.463	**0.535***	0.387	**0.522***	**0.516***	**0.763****
CO_S										**1**	**0.627***	0.239	**0.443***	**0.733****	**0.796****
OD											**1**	0.387	0.298	0.430	**0.687****
TA												**1**	0.135	0.426	**0.647****
GR													**1**	0.467	**0.636***
FS_S														**1**	**0.822****
PT															**1**

Significant at $p < 0.01^{**}$, at $p < 0.05^{*}$.

Physico-chemical properties: CO, colour, FH, foam height, FS, foam stability, TA, total acidity, OE, original extract, ALC, alcohol concentration, GFF, final fermentation degree.

Sensorial properties: AP, appearance, CO_S, colour, OD, odour, TA, taste, GR, gas release, FS_S, foam stability

Principal component analysis (PCA) shown in Figure 1 carried out on black beer samples explain all the data variation. The first two principal components explain 71.44% of the total variance (PC1=54.83% and PC2=16.61%). The both PCA components, PC1 and PC2 underline a very good correlation between physico-chemical characteristics CO and GFF and between OE and ALC. Also it may be noticed a very good correlation between all the sensorial characteristics analyzed, most of them being placed at the left part of the graph, characteristics which reflect highly significant correlation coefficients. The closed association between sensory and physico-chemical characteristics of the beer analyzed samples it may be noticed between CO_S, FS_S and FS at a level of $p = 0.01$ which may be clearly seen in the left part of the graph.

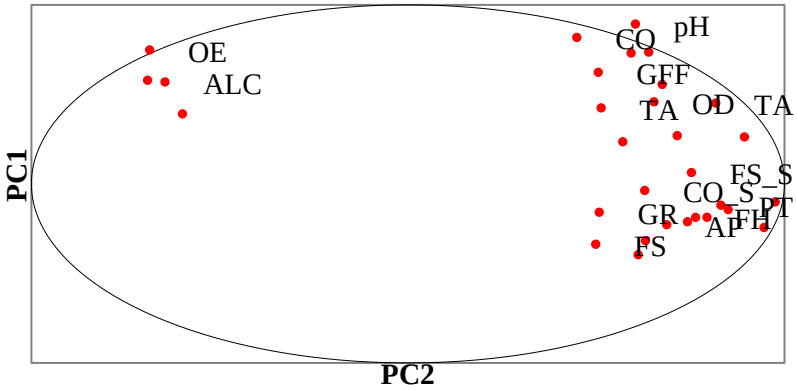

Figure 1. PCA loadings of black beer properties

Conclusion

These researches proposed to obtain a new assortment of black beer, having as basic ingredients unconventional raw materials, respecting the classical technological process of obtaining beer. The new product is part of the category of undistilled black beer alcoholic beverages, whose composition includes only natural ingredients: water, acorn flour, topinambur flour, molasses, hops and yeast, without the addition of food additives. The uniqueness of the product is mostly due to the ingredients used in the manufacturing recipe of the finished product: the use of acorn and topinambur flour as raw materials and the capitalization of molasses, as a by-product of sugar production.

The product has been conceived as a product that can be easily reproduced on an industrial scale, from micro-factories to high-capacity production companies, through a simple process, in accordance with the regulations in force, respecting food safety.

References

1. Deželak, M., Gebremariam, M. M., Zarnkow, M., Becker, T., Košir, I. J. (2015), Part I: the influence of serial repitching of Saccharomyces pastorianus on the uptake dynamics of metal ions and fermentable carbohydrates during the fermentation of barley and gluten-free buckwheat and quinoa wort, *J. Inst. Brew.*, 121(3), pp. 356–369.

2. Watson, H. G., Vanderputten, D., Van Landschoot, A., Decloedt, A. I. (2019), Applicability of different brewhouse technologies and gluten-minimization treatments for the production of gluten-free (barley) malt beers: Pilot-to industrial-scale, *J. Food Eng.*, 245, pp. 33–42.
3. Kerpes, R., Fischer, S., Becker, T. (2017), The production of gluten-free beer: Degradation of hordeins during malting and brewing and the application of modern process technology focusing on endogenous malt peptidases, *Trends Food Sci Technol.*, 67, pp. 129–138.
4. Fanari, M., Forteschi, M., Sanna, M., Zinellu, M., Porcu, M. C., Pretti, L. (2018), Comparison of enzymatic and precipitation treatments for gluten-free craft beers production, *Innov Food Sci Emerg Technol.*, 49, pp. 76–81.
5. Ceccaroni, D., Sileoni, V., Marconi, O., De Francesco, G., Lee, E. G., Perretti, G. (2019), Specialty rice malt optimization and improvement of rice malt beer aspect and aroma, *LWT–Food Sci Technol*, 99, pp. 299–305.
6. Phiarais, B. P. N., Mauch, A., Schehl, B. D., Zarnkow, M., Gastl, M., Herrmann, M., Arendt, E. K. (2010), Processing of a top fermented beer brewed from 100% buckwheat malt with sensory and analytical characterisation, *J. Inst. Brew.*, 116(3), pp. 265–274.
7. Mayer, H., Ceccaroni, D., Marconi, O., Sileoni, V., Perretti, G., Fantozzi, P. (2016), Development of an all rice malt beer: A gluten free alternative, *LWT-Food Sci Technol*, 67, pp. 67–73.
8. Di Ghionno, L., Sileoni, V., Marconi, O., De Francesco, G., Perretti, G. (2017), Comparative study on quality attributes of gluten-free beer from malted and unmalted teff [*Eragrostis tef* (zucc.) trotter], *LWT-Food Sci Technol* , 84, pp. 746–752.
9. Adiamo, O. Q., Fawale, O. S., Olawoye, B. (2018), Recent Trends in the Formulation of Gluten-Free Sorghum Products, *J. Culin. Sci. Technol.*, 16(4), pp. 311–325.
10. Gebremariam, M. M., Zarnkow, M., Becker, T. (2014), Teff (*Eragrostis tef*) as a raw material for malting, brewing and manufacturing of Gluten-Free foods and beverages: a review, *J. Food Sci. Technol*, 51(11), pp. 2881–2895.
11. De Meo, B., Freeman, G., Marconi, O., Booer, C., Perretti, G., Fantozzi, P. (2011), Behaviour of malted cereals and pseudo-cereals for gluten-free beer production, *J. Inst. Brew.*, 117(4), pp. 541–546.
12. Bogdan, P., Kordialik–Bogacka, E. (2017), Alternatives to malt in brewing, *Trends Food Sci Tech*, 65, pp. 1–9.
13. Van Landschoot, A. (2011), Gluten-Free barley malt beers,*Cerevisia*, 36, pp. 93–97.
14. Hager, A.S., Taylor, J.P., Waters, D.M., Arendt, E.K. (2014), Gluten free beer–A review, *Trends Food Sci Technol.*, 36(1), pp. 44–54.
15. Rubio–Flores, M., Serna–Saldivar, S. (2016), Technological and engineering trends for production of Gluten-Free beers, *Food Eng. Rev.*, 8 (4), pp. 468–482.
16. Korus, J., Witczak, M., Ziobro, R., Juszczak, L. (2015), The influence of acorn flour on rheological properties of Gluten-Free dough and physical characteristics of the bread, *Eur Food Res Technol*, 240(6), pp. 1135–1143.
17. Ajo, R.Y. (2018), Effect of acorn flour substitution on arabic bread properties, *Pakistan Journal of Agricultural Sciences*, 55(4), pp. 913–919.
18. Parsaei, M., Goli, M., Abbasi, H. (2017), Oak flour as a replacement of wheat and corn flour to improve biscuit antioxidant activity, Food Sci Nutr, 6, pp. 253–258.
19. Al–Rousan, W.M., Ajo, R.Y., Al-Ismail, K.M., Attlee, A., Shaker, R.R., Osaili, T.M. (2013), Characterization of acorn fruit oils extracted from selected mediterranean *Quercus* species, *Grasas Aceites*, 64 (5), pp. 554–560.
20. Correia, P., Leitão, A., Beirão-da-Costa, M. (2009), Effect of drying temperatures on chemical and morphological properties of acorn flours, *Int. J. Food Sci. Technol*., 44, pp. 1729–1736.
21. Ferraz de Oliveira M.I., Machado M., Cancela d'Abreu M. (2012), Acorn chemical compos ition depending on s hedding date and *Quercus* species, *Options Méditerr.*, 101, pp. 229–234.

22. Rakić, S., Kukić-Marković, J., Petrović, S., Tešević, V., Janković, S., Povrenović, D. (2018), Oak kernels–volatile constituents and coffee-like beverages, *J. Agric. Sci.*, 10(5), pp. 117–124.
23. Matías, J., González, J., Royano, L., Barrena, R. A. (2011), Analysis of sugars by liquid chromatography–mass spectrometry in *Jerusalem artichoke* tubers for bioethanol production optimization, *Biomass Bioenerg*, 35(5), pp. 2006–2012.
24. Lim, S.H., Ryu, J.M., Lee, H., Jeon, J.H., Sok, D.E., Choi, E.S. (2011), Ethanol fermentation from *Jerusalem artichoke* powder using *Saccharomyces cerevisiae* KCCM50549 without pretreatment for inulin hydrolysis, *Bioresour. Technol.*, 102(2), pp 2109–2111.
25. Goranova, Z., Baeva, M., Vrancheva, R., Petrova, T., Stefanov, S. (2019), Antioxidant properties and color characteristics of sponge cakes containing functional components, *Ukr. Food J.*, 8 (2), pp. 260–270.
26. Dabija, A., Codină, G. G., Ropciuc, S., Stroe, S. G. (2019), Studies regarding the production of a novel yogurt using some local plant raw materials, *J. Food Process. Pres.*, 43(6), e13826.
27. Yang, L., He, Q.S., Corscadden, K., & Udenigwe, C.C. (2015), The prospects of *Jerusalem artichoke* in functional food ingredients and bioenergy production, *Biotechnol. Rep.*, 5, pp. 77–88.
28. Munim, A., Rod, M.R., Tavakoli, H., & Hosseinian, F. (2017), An analysis of the composition, health benefits, and future market potential of the *Jerusalem artichoke* in Canada, *J.Food Res.*, 6(5), pp. 69–69.
29. Radovanovic, A., Stojceska, V., Plunkett, A., Jankovic, S., Milovanovic, D., Cupara, S. (2015), The use of dry *Jerusalem artichoke* as a functional nutrient in developing extruded food with low glycaemic index, *Food Chem.*, 177, pp. 81–88.
30. Zhang, T., Chi, Z., Zhao, C.H., Chi, Z.M., Gong, F. (2010), Bioethanol production from hydrolysates of inulin and the tuber meal of *Jerusalem artichoke* by *Saccharomyces* sp. W0, *Bioresour. Technol.*, 101(21), pp. 8166–8170.
31. Arshad, M., Hussain, T., Iqbal, M., Abbas, M. (2017), Enhanced ethanol production at commercial scale from molasses using high gravity technology by mutant *S. cerevisiae*, *Braz. J. Microbiol.*, 48(3), pp. 403–409.
32. Fadl, K.S.H., Abbashar, O., Musa, A. (2018), Utilization of mash treatment unit for sterilization and clarification of final molasses in ethanol plant, *Intern.J. Photochem. Photobiol.*, *2*(2), 49.
33. Dabija, A. (2019), *Biotechnologies in the food industry*, Iasi, Performantica Press
34. SR 4230:2004, Beer, Standardization Association of Romania (ASRO), Bucharest, Romania.
35. SR 13355–6:2000, *Beer. Analysis methods. Determination of total acidity, Standardization Association of Romania*, Bucharest, Romania
36. SR 13355–1:1997, *Beer. Analysis Methods. Sensorial Analysis, Standardization Association of Romania (ASRO)*, Bucharest, Romania.
37. Ceppi, E.L.M., Brenna, O.V. (2010), Brewing with rice malt – a Gluten-Free alternative, *J. Inst. Brew.*, 116, pp. 275–279.
38. Guerdrum, L.J., Bamforth, C.W. (2011), Levels of gliadin in commercial beers, *Food Chem.*, 129, pp. 1783–1784.
39. Owheruo, J., Ifesan,B., Kolawole, A. (2019), Physico-chemical properties of malted finger millet (*Eleusine coracana*) and pearl millet (*Pennisetum glaucum*), *Food Sci Nutr*, 7(2), pp. 476–482.
40. Codină, G.G., Mironeasa, S., Leahu, A. (2011), Predicting the sensory quality of some Romanian beers from physical–chemical data using multivariate analysis, *Food and Environment Safety*, 10(1), pp. 36–42.

Influence of wheat food fiber on the structure formation process of whey-creamy cheeses

Olena Grek[1], Kira Ovsiienko[1], Alla Tymchuk[1], Olena Onopriichuk[1], Amit Kumar[2]

1 – National University of Food Technologies, Kyiv, Ukraine
2 – Integral University, Lucknow, India

Keywords:

Fiber
Cheese
Whey
Creamy
Water activity
Rheology

Article history:

Received 29.08.2019
Received in revised form 14.11.2019
Accepted 30.06.2020

Corresponding author:

Olena Onopriichuk
E-mail: olena.onopriychuk@gmail.com

DOI: 10.24263/2304-974X-2020-9-2-6

Abstract

Introduction. Influence research of wheat food fiber (Vitacel WF400) have been carried out in order to rationalize the structure formation process of whey-creamy cheeses.

Materials and Methods. Cheese whey, cream and Vitacel WF400 were the raw materials for the production of whey-creamy cheese. The technological properties of food fiber were determined by the amount of retained fat and adsorbed water, respectively, in the infusion process and suspension centrifugation. The yield value and the water activity in model samples of whey-creamy cheeses, the optimal addition amount of Vitacel WF400 the temperature and the mixing duration of the condensed whey have been determined.

Results and discussion. The water-retainaing capacity in cheese whey and fat holding capacity in cream with mass fat fraction 33 were 104.2±1.0 and 82.0±0.5, respectively. With an increase in the addition amount of Vitacel WF400 (from 1.0 to 4.0) and an increase in the temperature of structure formation (from 62 to 74 °C), the index of yield value increases from 350±1.1 Pa to 430±1.3 Pa. Increasing the temperature to 68 °C, increasing the amount of Vitacel WF400 to 2.5 and reducing the mixing duration to 70 min leads to a decrease in the amount of dispersion medium and the structure coagulation of the samples of whey-creamy cheeses is dehydrated. Model samples of the above products with different amounts of Vitacel WF400 (from 2 to 3) are characterized by a decrease in water activity compared with the control sample. a_w is 0.898 for the control sample.

Upon reaching a dry solids content of 66 and a corresponding decrease in the content of the liquid phase, the index of yield value reaches 427 Pa. The consistency of whey-creamy cheeses samples turns into a plastic pastes state, in which the structure restoration is possible only under the load action, that causes irreversible deformation, which acts on the entire surface area of the phase separation.

With a further temperature increase to 74 °C and a mixing time to 70 min, a further structure compaction occurs – the layers' thickness of the liquid medium decreases, thixotropy and plasticity disappear.

Conclusions. The optimum values of the Vitacel WF400 amount have been justified at the level of 2.5±0.5, temperature – 68±1 °C and mixing time during structure formation – 70±2 min. Whey-creamy cheeses with the rational addition amounts of food fiber are characterized by a decrease in water activity values from 0.885 to 0.823.

Introduction

One way to process whey by concentrating proteins is to produce whey cheese. In addition to the most famous ricotta cheese, whey can be used to produce brown cheese, characteristic and famous especially in the Scandinavian countries [1-3].

For example, Brunost is made from a mixture of whey and cream or sour cream (Rømme), Gjetost – from goat whey and Mysost – from a mixture of milk and/or goat whey [4-6].

The production of brown cheese is based on the moisture evaporation from whey or milk mixture at a temperature of 65±1 °C and a pressure of 0.8 MPa to a dry solids weight ratio of 60±2. After the fat component addition, mass formation occurs up to 73±2% of dry matter under certain conditions in order to avoid uncontrolled growth of lactose crystals and, as a result, granularity of finished products [2]. The physical-chemical indicators of this product are in the following ranges: moisture mass fraction – 17.4–28.2; fat – 1.9–28.7; ashes – 4.0–4.8; pH – 5.1–5.7 [7, 8]. The above processes correspond to the parameters for obtaining a similar product – whey-creamy cheese [7, 9]. The structure formation process is complex and takes place for 90 minutes under an elevated temperature and a mixing speed of 3–4 r/min and requires additional research. Next, the mixture is sent to cooling, with the simultaneous lactose crystallization, packaging and after-cooling.

The consistency of whey-creamy cheeses is characterized by rheological indicators, of which the yield value of the product is the most sensitive to technological changes.

An indicator of water activity (a_w) is one of the important parameters for determining the storage conditions of whey-creamy cheeses. Whey-creamy cheeses are food products with average moisture, a_w values are from 0.60 to 0.91 [10]. Scientific interest has minimal a_w values that are critical for certain types of microorganisms and limit their growth.

It is relevant to improve the technology of whey cheese using modern ingredients to rationalization processes. Probably, that the addition of such components as food fiber with multifunctional properties in functionally significant amount will contribute to the process of structure formation in the finished product [11, 12].

It is expedient to study Vitacel WF400 with a high moisture and fat-holding capacity for use in the technology of whey-creamy cheeses. The stage of preparation and addition into the milk base of the above food fiber, depending on their expected technological effect, requires clarification. As a result, a change in quality indicators, including rheological ones. The real problem is the lack of an integrated approach to solving the problems identified as part of the review.

The aim of this work is to determine the influence of wheat food fiber on the structure formation process of whey-creamy cheeses.

Materials and methods

Materials

The object of research was the technology of whey-creamy cheese with food fiber – Vitacel.

Cheese whey (CW) had the following physical-chemical indicators: mass fat fraction – (0.2±0.1), dry solids – (6.30±0.02), titrated acidity – (18.0±0.1) ºT, pH – 5.32±0.02.

The **cream** had the following physical-chemical indicators: mass fat fraction – (33.0±0.1), dry solids – (38.00±0.01), titrated acidity – (17.0±0.1) ºT, pH 6.57±0.02.

Cream is a compound of whey-creamy cheese, added to condensed whey during structure formation, followed by concentration to 70–80 dry solids.

The **control sample** was whey-creamy cheese obtained according to the above technology without food fiber, which had the following sensory parameters: consistency – homogeneous, plastically, soft, slightly fragile; flavor and aroma – pure milk with a pronounced caramelization flavor, salty; color – light brown, uniform throughout the mass. Physical-chemical indicators: mass solids fraction – 73±2, mass lactose fraction – 48.0±1.5, pH – 5.1±0.1.

For research, model samples of whey-creamy cheese were made with the Vitacel addition in an amount of 1.0 to 4.0 [11].

Food fiber Vitacel WF400 (manufactured by J. Rettenmaier Sohne GmbH, Germany) has the following technological properties: water-holding capacity and fat absorption (per 1 g of product) – 11 g and 6 g, respectively. Water activity is fixed at 0.44, and pH is (6.5±1.5). The bulk mass of Vitacel is 40±2.5 g/dm^3. Average sizes of 90 fiber particles <300 μm. The total amount of food fiber is (98.0±0.5), including cellulose – (72.0±2.0), hemicellulose – (25.5±1.5), lignin – 0.5±0.1. For food fiber, the indicated chemical indicators are follows: mass fat fraction – (0.2±0.02), protein – (0.4±0.06), moisture, not more than 8, ash, not more than 3. According to the manufacturer, Vitacel WF400 has the following microbiological indicators: QMAFAnM (CFO in 0.1 g) – 5×10^4, mold (CFO in 0.1 g) – not more than 50, pesticides and fungicides – < 0.002 mg/kg. Pathogenic microorganisms (salmonella), in 25 g of FF, aflatoxins, Coliform bacterias in 0.1 g were not found. The energy value in 100 g of Vitacel WF400 is 0.09 kcal [13].

Methods

Fat-holding and water-retaining capacities of Vitacel WF400. At the first stage of experimental reseach, the water-retaining (WRC) and the fat-holding (FHC) capacities of food fiber have been investigated.

Fat-holding and water-retaining capacities of Vitacel WF400 were determined by the amount of retained fat and adsorbed water, respectively, in the infusion process and suspension centrifugation. The process was carried out at a temperature of 20 °C in cream and whey.

Fat-holding capacity was calculated by the formula, in:

$$FHC= (c – a)\cdot 100 / m \quad (1)$$

where a – is the supernatant mass, g

c – is the mass of added liquid, g

m – is the sample mass, g [14].

The method for determining WRC of food fiber is similar to FHC, but the process takes place in cheese whey.

Obtaining process of whey-creamy cheeses. The condensation process of whey was carried out to a mass solids fraction in the mixture – (60±2), in a laboratory setup in which the vacuum evaporation conditions in circulating-type apparatuses were simulated.

The structure formation process was carried out at a temperature of 65.0–70.0 °C in a container with mechanical mixing of condensed whey and cream with mass fat fraction (33±1) in the amount of (10±0.3). The mixing speed was 3–4 r/min, hold time – 90±1 min. Whey-creamy cheese was cooled at a rate of 14–16 °C/h to a temperature of 20 °C for 3–4

hours and packaged in hermetic container.

Then the whey-creamy cheese was kept for 12 hours at a temperature of 14–16 °C. In this case, the structure formation process occurs due to the growth of lactose crystals, fat and the swelling of whey proteins. Next, the finished product was stored at a temperature of 2–6 °C and changes in quality indicators were analyzed.

Yield value of model whey-creamy cheese samples. The yield value of model whey-creamy cheese samples was determined on Ulab 3-31 M penetrometer (5 s exposure time, in identical containers using measuring cone with apex angle of 2a = 60º).

The principle of the penetrometer operation is based on measuring the depth of the needle (cone) immersion in the sample at a certain test temperature and load for a certain time. The value is fixed in penetration units.

Sample preparation is carried out as follows: container filling with a pallet; prepressing for 180 s; thermostat control by temperature control device to the set temperature; device preparation for measurements: put a predetermined indenter and install an additional load; taking penetration measurements using a conical indenter with an angle of 60 ° at the apex.

Data experimental computing was carried out as follows:

1. Calculate the average value of the maximum immersion depth of the indenter in the product according to the formula:

$$h_{cp} = (h_1 + h_2 + h_3)/3, \text{ m} \quad (2)$$

2. Determine the error in investigation the value of h:

$$\Delta_h = [(h_{cp} - h_i)/h_{cp}] \cdot 100,\% \quad (3)$$

3. Calculate the yield value taking into account the proportionality coefficients:

$$\theta = k_\alpha \frac{F}{h_{cp}^2} \quad (4)$$

Determine the optimal amount of Vitacel WF400 food fiber. To determine the optimal amount of Vitacel WF400 food fiber, modeling method based on Wilson-Box plan was used [9].

The temperature and the mixing duration of the condensed whey with dry solids weight ratio 60±2 during structure formation in the technology of whey-creamy cheese, the mathematical modeling method was applied using the Wilson-Box plan on a cube. The method is specific samples from a complete factorial experiment of type 3k, where k – is the factors number, 3 – is the levels number at which each variable varies. These plans do not have simple generators and have a complex interrelationship. However, they allow to carry out research with the least of time and resources expenditure.

Experiment planning matrix. In the preparation of the test samples, the amount of Vitacel food fiber (X_3), the temperature of structure formation (X_2), and the mixing duration (X_1) during structure formation were varied according to experiment plan presented in Table 1. Factor variation levels are given in Table 2.

Table 1

Experiment planning matrix by the Wilson-Box method on the cube

N	Independent variables (coded values)						Yield value, Pa (Y_1)
	Mixing duration, min (X_1)		Temperature of structure formation, ºC (X_2)		Vitacel amount, (X_3)		
1	+	90	+	74	+	4	430,00
2	-	50	+	74	+	4	410,00
3	+	90	-	62	+	4	420,00
4	-	50	-	62	+	4	390,00
5	+	90	+	74	-	1	400,00
6	-	50	+	74	-	1	390,00
7	+	90	-	62	-	1	380,00
8	-	50	-	62	-	1	370,00
9	+	90	0	68	0	2,5	400,75
10	-	50	0	68	0	2,5	390,00
11	0	70	+	74	0	2,5	400,75
12	0	70	-	62	0	2,5	390,00
13	0	70	0	68	+	4	400,00
14	0	70	0	68	-	1	350,00
15	0	70	0	68	0	2,5	370,50

Table 2

Factor variation levels

Factor	Designation	Units measure	Factor variation levels		
			upper	zero	lower
			+	0	–
Mixing duration (τ)	X_1	хв	90	70	50
Temperature of structure formation (t)	X_2	ºC	74	68	62
Vitacel WF400 amount (ν)	X_3	%	4	2,5	1

According to the research results, the regression equation coefficients were calculated, the significance analysis of which was determined by the Fisher criterion (Fp). The criterion essence is the decomposition of total dispersion of statistical complex into its constituent elements. Their next assessment makes it possible to determine the change proportion of the effective sign from the factor signs action, that is, to narrow the research scope. This confirms the adequacy of the obtained equations. To determine the functional dependence, which most accurately reproduces the change in indicators, an approximation confidence coefficient (R2) of each function was found [9]. The results accuracy is ensured by three-five times repeatability of the experiments.

Water activity of model whey-creamy cheese samples

Determination of water activity of model whey-creamy cheese samples (control sample) and with food fiber was carried out on a Rotronic instrument modified by Hygro Palm AW (manufacturer Rotronic AG (Switzerland). The measurement range is as follows: 0–1 a_w, sample temperature 5–50 °C, accuracy ±0.01a_w, ±0.1 °C. The water activity analyzer consists of an instrument unit, HC2-AW station, a case for transportation and storage, calibration solutions, plastic cups for samples. The operation principle of the analyzer is to use a dielectric moisture sensor to determine the water activity. Between the two porous electrodes of sealed chamber, a porous polymer is placed. The electrical properties of the polymer vary with the relative moisture in the chamber. The electrodes give a signal based on relative moisture in a closed chamber. This signal is converted by software and displayed on the screen as a value of water activity. The measurement cycle lasts from 3 to 5 minutes. In balanced state the relative moisture in the chamber is equal to the water activity in the test sample. The value of water activity is determined to the third decimal place [13].

Results and discussion

Rational addition amount of Vitacel WF400 to whey-creamy cheeses

Water-retainaing capacity of Vitacel WF400 in cheese whey and fat holding capacity in cream with mass fat fraction 33% have been determined, which were 104.2±1.0 and 82.0±0.5, respectively.

In order to reduce the technological cycle (process) duration of structure formation according to the classical technology, it is 90 min, and obtaining whey-creamy cheese of appropriate quality with FF, experimental data were processed. In addition, it is necessary to prevent the dissolution of the formed lactose crystals in the finished product, to ensure the required quality.

The process of lactose crystallization in the whey-creamy cheese production is carried out during the operation of structure formation. In this case, the crystals size and number can be regulated using several technological methods [15]: supersaturation degree of the aqueous lactose solution, cooling rate, mechanical mixing, seed addition [2, 16].

The optimal addition amount of Vitacel WF400 in whey-creamy cheeses has been found, which ensures the maximum realization of the technological potential of food fiber to obtain a product with quality indicators as closely to control sample as possible.

The determinatoin of yield value at the penetrometer confirms the effect of Vitacel WF400 on the rheological parameters of whey-creamy cheeses with FF. The restrictive factor for adding the maximum amount of wheat fiber is the over-compaction of finished product.

The graphs (response surfaces) illustrating the influence of the Vitacel WF400 amount, the temperature of structure formation and the mixing duration on the index of yield value of the product are presented in Figure 1.

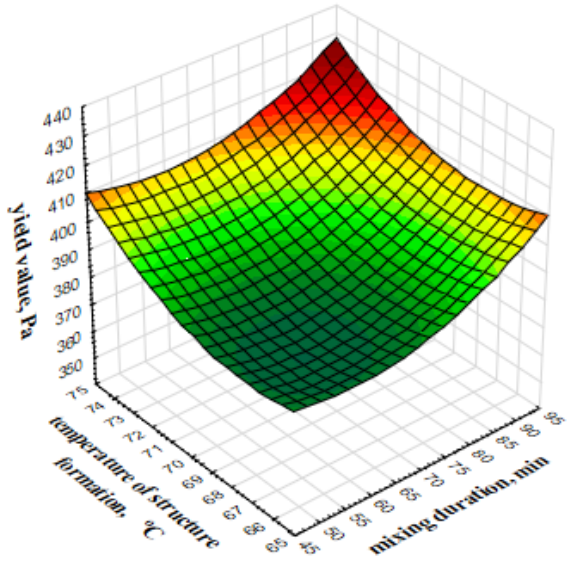

$\Theta = 434{,}97 - 1{,}01\tau - 60{,}33t + 0{,}08\tau^2 - 0{,}06\tau t + 0{,}45t^2;$
$R^2 = 0{,}98$
$90 \le \tau \le 50$
$74 \le t \le 62$

> 420
< 420
< 410
< 400
< 390
< 380

a

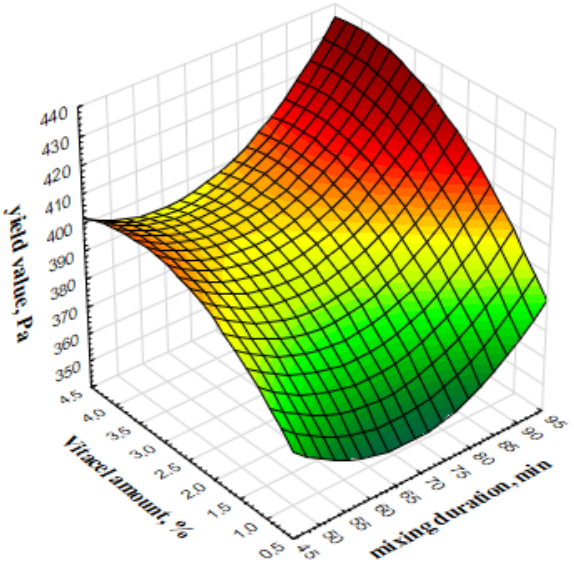

$\Theta = 432{,}29 - 4{,}79\tau + 23{,}45\nu + 0{,}13\tau^2 + 0{,}12\tau\nu_3 - 4{,}31\nu^2$
$R^2 = 0{,}97$
$90 \le \tau \le 50$
$4 \le \nu \le 1$

> 430
< 424
< 414
< 404
< 394
< 384
< 374
< 364
< 354

b

Figure 1. Response surfaces and mathematical models of the influence on the index of yield value of whey-creamy cheeses from:
***a* – the mixing duration and the temperature of structure formation;**
***b* – the Vitacel WF400 amount and the mixing duration;**
***c* – the Vitacel WF400 amount and the temperature of structure formation**

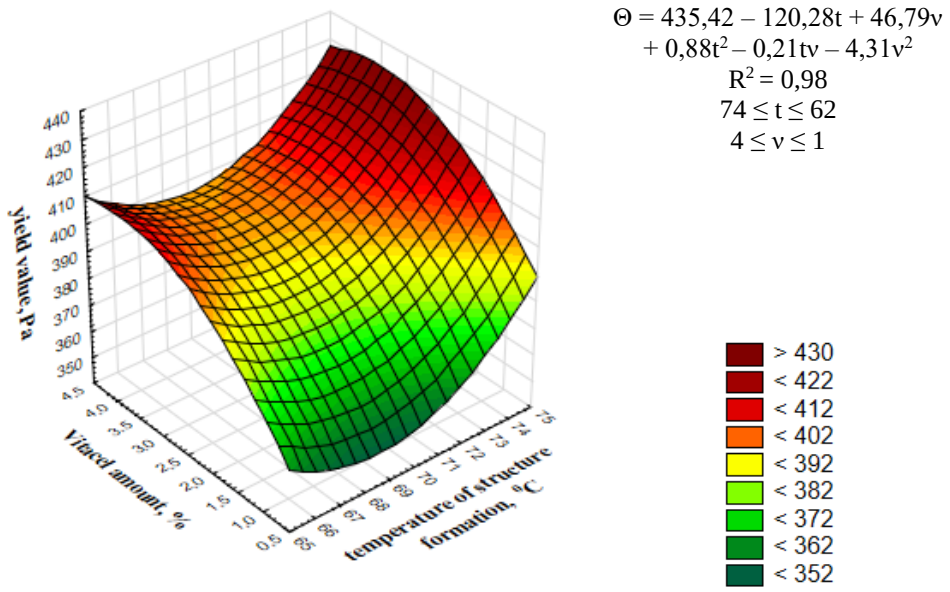

c

Figure 1 (*Continue*). Response surfaces and mathematical models of the influence on the index of yield value of whey-creamy cheeses from:
***a* – the mixing duration and the temperature of structure formation;**
***b* – the Vitacel WF400 amount and the mixing duration;**
***c* – the Vitacel WF400 amount and the temperature of structure formation**

According to the visualized data, with an increase in the addition amount of Vitacel WF400 (from 1.0 to 4.0) and an increase in the temperature of structure formation (from 62 to 74 °C), the index of yield value increases from 350±1.1 Pa to 430±1.3 Pa. The experimental data correlate with the corresponding quality indicators for whey-cream cheeses without food fiber, obtained by the classical technology [2, 7].

The Vitacel WF400 addition promotes the new bonds formation in the structure of whey-creamy cheese. It is a multicomponent system, the basis of which consists of interwoven chains of unfolded denatured whey protein molecules. This net covers and deprives the fluidity system and holds the lactose crystals in a suspended state, which prevents their sedimentation [17]. Water molecules and other components of the concentrate are somehow connected with the skeleton [18].

The dependence of the yield value from the addition amount of Vitacel WF400 in whey-creamy cheeses obtained at a formation temperature of 62, 68 and 74 °C and the mixing duration for 50, 70 and 90 minutes has been established. It has proved that the above indicator increases to 430±1.3 Pa with an increase all variable factors and is inversely related to the

penetration degree. An increase in the FF amount from 3.5 to 4.0 almost does not change the yield value, but leads to a deterioration in the sensory characteristics of the finished product.

Influence of temperature and duration of structure formation process on the consistency of whey-creamy cheeses

At the beginning of structure formation, the coagulation structure prevails in all samples due to the Van-der-waals adhesive power between colloidal particles and dispersed phase molecules – dry solids (proteins, fats, carbohydrates) of whey-creamy cheeses through moisture layers of the dispersion medium – whey [19]. In this case, the mat thickness corresponds to the minimum free energy of the system. This cheese structure keeps stable as long as the the molecules fragments are firmly bound to the particles surface of the dispersed phase and are able to dissolving without bond loss with them in the dispersion medium [20]. At this stage of the process, the coagulation structure of whey-creamy cheeses is able to thixotropy [21]. The Vitacel WF400 addition change the structural and mechanical characteristics of whey-creamy cheeses.

The temperature raising to 68 °C, increasing the Vitacel WF400 amount to 2.5 and reducing the mixing time to 70 min leads to a decrease in the amount of dispersion medium (free moisture in whey). The coagulation structure of cheese samples is dehydrated – their strength increases, and after a certain limit they stop to be reverse-thixotropic. Samples in this state acquire a visco-plastic structure. Independent structure reconstruction in them is preserved, while the spatial skeleton is destroyed without violating the integrity [22].

Upon reaching a dry solids content of 66 and a corresponding decrease in the content of the liquid phase, the index of yield value reaches 427 Pa. The consistency of whey-creamy cheeses samples turns into a plastic pastes state, in which the structure restoration is possible only under the load action, that causes irreversible deformation, which acts on the entire surface area of the phase separation [2].

With a further temperature increase to 74 °C and a mixing time to 70 min, a further structure compaction occurs – the layers' thickness of the liquid medium decreases, thixotropy and plasticity disappear [20, 21].

Further process continuation of structure formation to 90 min leads to biochemical phase transformations of dry solids in whey-creamy cheeses by agglomeration or growing together. The samples' structure acquires a relatively high strength, elasticity and fragility, which is not characteristic for the consistency of such products [22].

So, whey-creamy cheeses are among systems with a viscous-plastic consistency with a controlled yield value. Probably, the indicator change is associated with the technological abilities of wheat fiber for water retention and fat absorption.

Regression analysis of the experimental data carried out in the Statistica 10.0 program made it possible to obtain analytical dependences which reflect the factors influence on the response function in the form of a polynomial equation of the second degree.

Coefficient values of the polynomial equations are presented in Figure 1. Coefficients in which $p < 0.05$ are significant, namely are not equal to zero with a probability of more than 95%. High values of the determination coefficients (R^2) confirm the adequacy of models with experimental data.

It has been established that it is possible to obtain whey-creamy cheeses with the same value of yield value at different temperatures and mixing duration. However, the process prolongation to 90 min at a lower temperature of 62 °C is irrational and energy-consuming. The Vitacel WF400 addition in an amount of 2-3 sufficiently intensifies the process of structure formation. The obtained mathematical model allows to control the structure

rheological parameters depending on the temperature of structure formation and the mixing duration.

Analysis of the obtained dependencies allows to justify the optimal values of Vitacel WF400 amount (X_1) – 2–3, the temperature (X_2) at 68±1 °C, and the mixing duration (X_3) during structure formation – 70±2 min.

The obtained regression equations (mathematical models) can be used in practical purposes for the operational management of the structure formation process by combination of condensed milk whey, cream and food fiber with further concentration.

Determination of water activity in whey-creamy cheeses with Vitacel WF400

The determining results of the water activity in whey-creamy cheeses with different Vitacel WF400 amounts are presented in Figure 2.

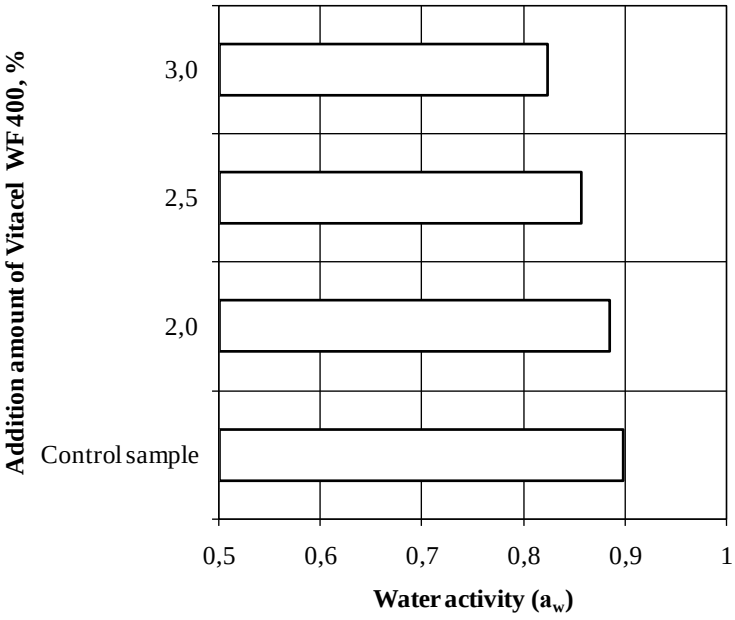

Figure 2. Water activity of whey-creamy cheeses with different Vitacel WF400

Data analysis (Figure 2) showed that whey-creamy cheeses with different amounts (from 2 to 3) of Vitacel WF400 are characterized by a decrease in water activity compared with the control sample. This is due to the technology ability of the water-retainaing capacity and fat absorption by food fiber. The index a_w ranged from 0.885 to 0.823 in all samples of whey-creamy cheeses with FF. For the control sample, a_w is 0.898. Microorganism growth and hydrolytic chemical reactions will be somewhat slowed down at such values.

An analysis of priori information [23, 24] and the obtained results allow to suggest that food fiber addition in the above amounts in the structure formation process leads to decrease of water activity rate in whey-creamy cheeses. This confirms its transition from free to bound state.

By determining the water activity (a_w) it is possible to confirm the Vitacel WF400 effect on the storage parameters of whey-creamy cheeses with food fiber at standard temperatures 2–6 °C.

A limitation for the practical realization of research results is the reconcilability of food fiber with a milk base at the sensory level.

The prospects for further research are related to the selection of other vegetable components with similar properties for solving technological problems in the whey-creamy cheese production.

Conclusions

1. Vitacel WF400 effect, which has a complex of technological properties, on the rationalization of structure formation process in whey-cream cheeses with food fiber has been confirmed. The optimum values of the Vitacel WF400 amount have been justified at the level of 2.5±0.5, temperature – 68±1 °C and mixing time during structure formation – 70±2 min.
2. Data reduction process allows to obtain analytical correspondence in the form of regression equations to calculate the amount effect of the Vitafel WF400, the temperature of structure formation, and the mixing duration on the yield value.
3. Whey-creamy cheeses with the Vitacel WF400 addition 2.5±0.5% are characterized by a_w (from 0.885 to 0.823), which provides growth inhibition of vegetative bacteria forms, partly yeast and creates unfavorable conditions for the development of spore forms of bacteria and mold fungi.

References

1. Zadow J.G. (2012), *Whey and Lactose Processing*, Springer Science & Business Media, DOI: 10.1002/9781118810279.ch15.
2. Hramcov A.G. (2011), *Fenomen molochnoj syvorotki*, Professija, Sankt-Peterburg.
3. Hramcov A.G. (2012), Ispolzovanie molochnoj syvorotki v produktah funkcionalnogo pitanija, *Pererabotka moloka*, 7 (153), pp. 50–53.
4. Fox P.F., Guinee T.P., Cogan T.M., McSweeney P.L.H. (2017), *Fundamentals of Cheese Science*, Boston Springer, Boston.
5. Karpova D.A. (2017), Proizvodstvo gruppy norvezhskih syvorotochnyh syrov tipa Brjunost kak sposob pererabotki molochnoj syvorotki, *Aktualnye voprosy sovershenstvovanija tehnologii proizvodstva i pererabotki produkcii sel'skogo hozjajstva*, 19, pp. 165–166.
6. Honcharenko I.V., Ahii V.M (2019), Bazova tekhnolohiia vyhotovlennia deiakykh vydiv albuminovykh syriv, *Tavriiskyi naukovyi visnyk*, 107, pp. 205–208, DOI: 10.32851/2226-0099.2019.107.28.
7. Skeie S, Abrahamsen R. (2017), Brown Whey Cheese, *Cheese,* 2, pp.1117-1132, DOI: 10.1016/B978-0-12-417012-4.00045-4.
8. Hramcov A.G., Kubanskaja D.M., Sujunchev O.A. (2006), Kompleksnye sistemy syvorotochnogo syra «Laktochiz», *Syrodelie i maslodelie*, 6, pp. 20–21.
9. Grek O., Onopriychuk O., Tymchuk A. (2015), Optimization of the composition of the mixture by simplex method, *Ukrainian Food Journal*, 4 (1), pp. 15–25.

10. Barbosa-Cánovas V.G., Fontana J.A., Schmidt J.S., Labuza P.T. (2007), *Water Activity in Foods: Fundamentals and Applications*, Blackwell and the Institute of Food Technologists, Oxford, DOI:10.1002/9780470376454.
11. Grek O., Tymchuk A., Tsygankov S., Savchenko O., Ovsiienko K., Ochkolyas O. (2019), Study of dietary fiber properties in dairy mixes containing modified fat compositions, *Eastern-European Journal of Enterprise Technologies*, 4, pp. 6-13, DOI: 10.15587/1729-4061.2019.174302.
12. Pryanishnikov, V.V. (2006). «Pischevyie volokna «Vitacel» v myasnoy otrasli, *Myasnaya industriya*, 9, pp. 43–45.
13. Grek O., Tsygankov S., Tymchuk A., Onopriichuk O., Savchenko O., Ochkolyas O. (2019), Research of recipe components influence on the properties of dairy-protein mashes for semi-finished products, *Eastern-European Journal of Enterprise Technologies*, 6/11 (102), pp. 41–48, DOI: 10.15587/1729-4061.2019.183549.
14. Dubrovskaja N.O., Nilova L.P. (2010*), Sovremennye problemy pishhevoj cennosti i kachestva hlebobulochnyh izdelij i vozmozhnye puti ih reshenija*, Michurinskij agrouniversitet, Michurinsk.
15. Hramcov A.G., Pavlov V.A., Nesterenko P.G., Holodov G.I., Evdokimov I.A., Lodygin D.N. (1989), *Pererabotka i ispol'zovanie molochnoj syvorotki*, Rosagropromizdat, Moscow.
16. Zolotoreva M.S., Evdokimov I.A., Volodin D.N., Somov V.S. (2013), Analiz pererabotki molochnoj syvorotki i sozdanie perspektivnyh resursosberegajushhih tehnologij, *Nauka. Innovacii. Tehnologii*, 1, pp. 37–44.
17. McSweeney P., O'Mahony J. (2016), *Advanced Dairy Chemistry. Volume 1B, Proteins : applied aspects*, Springer, New York, DOI: 10.1007/978-1-4939-2800-2.
18. Evdokimov N.S., Petrova L.V. (2012), Fiziko-himicheskie processy pri strukturirovanii koncentrata molochnoj syvorotki, *Dinamika sistem, mehanizmov i mashin*, 5, pp. 111–114.
19. Hiroyuki O. (2016), Van Der Waals Interaction Between Colloidal Particles, *Encyclopedia of Biocolloid and Biointerface Science*, 2, pp. 1087–1094, DOI: 10.1002/9781119075691.ch88.
20. Lamichhane P., Kelly A., Sheehan J. (2018), Structure-function relationships in cheese, *Journal of Dairy Science*, 101 (3), pp. 2692–2709, DOI: 10.3168/jds.2017-13386.
21. Fox P.F., Guinee T.P., Cogan T.M., McSweeney P.L.H. (2017), *Fundamentals of Cheese Science*, Springer, Boston, DOI: 10.1007/978-1-4899-7681-9_14.
22. Everett D., Auty M. (2008), Cheese structure and current methods of analysis, *International Dairy Journal*, 18(7), 759–773.
23. Sukmanov V. A., Sklyarenko E. V. (2012*), Issledovanie aktivnosti vodyi v svezhih myagkih syirah*, Naukovi pratsi Odeskoi natsionalnoi akademii kharchovykh tekhnolohii, 41(1), 18–22.
24. Barbosa-Cánovas G., Fontana Jr. A., Schmidt S., Labuza T. (2007), *Water Activity in Foods: Fundamentals and Applications*, Blackwell Publishing and the Institute of Food Technologists, Iowa, DOI:10.1002/9780470376454.

Time temperature indicator film based on alginate and red beetroot (Beta vulgaris L.) extract: in vitro characterization

Esra Tekin, Işıl Barutçu Mazı, Hasan Türe

Ordu University, Ordu, Turkey

Keywords:

Time temperature indicator
Red beetroot
Betalain
Alginate
PVA

Article history:

Received 28.10.2019
Received in revised form 16.12.2019
Accepted 30.06.2020

Corresponding author:

Işıl Barutçu Mazı
E-mail: ibarutcu@odu.edu.tr

DOI: 10.24263/2304-974X-2020-9-2-7

Abstract

Introduction. This study was aimed to develop and characterize a biodegradable time temperature indicator (TTI) film by incorporating red beetroot (*Beta vulgaris* L.) extract, which is rich in betalain pigments, into alginate (A) / polyvinyl alcohol (PVA) blend film.

Materials and methods. The alginate-PVA blends (APVA) were prepared by mixing the 1% PVA and 3% A solutions at different A:PVA (v/v) ratios (2:3, 1:1, 3:2). TTI films were obtained by addition of ascorbic acid and red beetroot extract to APVA blends and adjusting the pH to 9.5 by adding 2M NaOH. The films were produced by casting technique. The pure A, pure PVA, APVA and TTI films were characterized by using Fourier transform infrared (FT-IR) spectroscopy, thermogravimetric analysis (TGA), and scanning electron microscopy (SEM).The mechanical properties of the films were established through stress/strain tests. The CIE L*a*b* color parameters of TTI film were obtained during seven days of storage at 4, 25, 40 and 60 °C.

Results and discussion. Increasing the concentration of A provided an increase in elastic modulus, tensile strength and elongation at break (%) of APVA and TTI films. TTI(3:2) film had better film flexibility compared to A, APVA, TTI(1:1) and TTI(2:3) films. The ratio of A to PVA in blend films did not create a significant effect on TGA thermograms. Higher A proportion in TTI films decreased the phase separation observed in SEM images. The intensity of O–H stretching band clearly increased in TTI films compared to other films. TTI (3:2) film stored at 4 °C did not undergo color change for 7 days, whereas the color of TTI stored at higher temperatures changed gradually during storage depending on the storage temperature. The changes in b* parameters and hue angle values were more pronounced; and generally b* and hue angle values of the samples stored above 4 °C started to increase significantly beginning of the first day.

Conclusions. The developed TTI film has a potential to monitor the quality changes of the foods, which are improperly stored but normally must be refrigerated, through color changes.

Abbreviations

A: Alginate
APVA: Alginate-PVA blend
E: Elasticity Modulus
EB: Elongation at Break
FT-IR: Fourier Transform Infrared Spectroscopy
G: Glycerol
PVA: Polyvinyl Alcohol
SEM: Scanning Electron Microscopy
TGA: Thermogravimetric Analysis
TS: Tensile Strength
TTI: Time Temperature Indicator

Introduction

Traditional food packaging materials provide protection from environmental influences, contribute to the extended shelf-life, encourage consumers to purchase the product and have convenience attributes such as ease of access, handling [1]. Extensive research has been carried out for the development of food packaging materials and many successful innovations have been implemented for meeting and exceeding customers' demands and expectations [2, 3]. Intelligent packaging which carries information by sensing environment is one of the most popular innovative packaging systems [4]. Intelligent packaging is a system which enhances food safety by informing consumer about quality of the packed food and has extra characteristics such as detection, sensation, recording, tracing and communication [5]. It is known that the shelf life of the food depends on the internal structure of food and outside factors including temperature, relative humidity and outside gas composition [6]. Temperature which designates kinetics of physical, chemical and microbial deterioration is an important environmental factor. Time temperature indicators (TTIs) that record and observe temperature effect on food quality from production to consumption, are an easy to use and an impressive intelligent packaging system [7]. TTIs that confirm consumers with color indicators representing food quality are generally part of the food package [8]. Commercial TTIs have variable working mechanisms based on some mechanical, chemical, enzymatic or microbiological processes [4, 7]. Pennanen et al. [9] stated that much work is still needed to enable TTIs to gain a wider acceptance by the consumers.

Natural pigments that assist tracking food quality with color change can be used in active or intelligent packaging systems as an indicator of food deterioration [10-13]. The employment of natural pigments in indicators is advantageous, since such indicators do not have chemical effect on the packaged food. A couple of studies showed that some natural pigments derived from plants have significant potential as being time temperature indicators in intelligent packaging systems [14-16]. Nofrida et al. [14] used natural dyes of erpa leaves (*Aerva sanguinolenta*) in the development of a TTI film and recorded that the color of film changed from red to yellow at less than one day at room temperature and in 2 hours at 40 °C. Maciel et al. [16] developed a TTI system by coating a cardpaper with chitosan suspension containing anthocyanin pigment as color indicator. The color of this TTI system changed irreversibly from violet to yellow when exposed to temperatures ranging from 40 to 70 °C for 72 hours due to thermal degradation of anthocyanins. Betalains are also an important group of plant derived natural pigments. The color of betalains may change depending on temperature, pH, oxygen, enzyme and light [17]. Red beetroot (*Beta vulgaris* L.) is the most important betalain source used to colorize foods [18]. As a result of thermal degradation, red color of pigment decreases, and finally brown pigment is formed [19].

Natural biopolymers have been used for the development of indicator films in intelligent packaging applications. In the literature there are several reports on polymer-based time temperature indicator films. Nofrida et al. [14] obtained a TTI film using chitosan-PVA

blend. Maciel et al. [15] designed temperature indicator cardpaper films coated with chitosan polymer incorporated with anthocyanins. Pereira et al. [20] developed a time temperature indicator film based on PVA/chitosan. Although several natural polymers have been used to prepare smart packaging with several types of pigments, to date betanin containing alginate-PVA films have not been studied. Alginate and PVA are interesting polymers for the development of intelligent packaging since the film formed by blending them has greater mechanical properties and better cost performance, besides allows the incorporation of substances with specific properties [21, 22].

The aim of this study was to develop a time temperature indicator film based on alginate, PVA and natural betalain pigments extracted from red beetroot. The films were evaluated for chemical structure, and their morphological, mechanical and thermal properties using FT-IR, SEM and TGA. Evaluation of TTI film as a color indicator was performed during seven days of storage at 4, 25, 40 and 60 °C.

Materials and methods

Materials

The fresh red beet (*Beta vulgaris* L.) plants were obtained from the local market (Ordu, Turkey) and stored at 4 °C until extraction. Sodium alginate and polyvinyl alcohol (PVA, M_W =89,000-98,000, 99+% hydrolyzed), L-ascorbic acid and glycerol were purchased from Sigma-Aldrich (St. Louis, MO, USA), and other reagents were of analytical grade.

Preparation of red beetroot extract

Red beetroots (*Beta vulgaris* L.) were washed, hand-peeled and cut into small pieces. 100 g of the grinded beet root was homogenized in 900 ml of distilled water at room temperature using a homogenizer. Then, it was filtered and centrifuged at 4000 rpm for 10 minutes. The obtained solution was diluted with distilled water to obtain a solution volume of 1L. The preparation of indicator film solution was performed immediately after obtaining red beetroot extract.

Preparation of the films

1% PVA solution was obtained by completely dissolving 1.01 g of PVA powder in 100 ml of distilled water on a magnetic stirrer at 80-85 °C. To prepare the 3% alginate (A) film solution, 3.1 g of alginate was dissolved in 100 ml of distilled water under magnetic stirring at 70-75 °C [23]. The alginate-PVA blends (APVA) were prepared by mixing the 1% PVA and 3% A solutions in the proportions given in Table 1. PVA, a non-toxic and biodegradable synthetic polymer, was added in order to improve the mechanical features of the alginate film. To see the effect of glycerol as plasticizer, 1 ml of glycerol was added to 100 ml of each film forming solution as presented in Table 1. All film forming solutions were kept under stirring at 300rpm at room temperature for 24 hours to obtain homogenized solution. Time temperature indicator (TTI) film forming solutions were prepared with the addition of 1 ml glycerol, 0.5 g ascorbic acid and 10 ml of red beetroot extract to 100 ml of the homogenized APVA solutions (Table 1). Then, the final pH of the TTI solutions were adjusted to 9.5 using 2 M NaOH. The casting technique was used for the preparation of films. The solutions (12 g) were spread evenly over Petri dishes (60 mm diameter) and dried in vacuum oven (50mbar, Memmert VO 500, Germany) at 50 °C for 3 hours. The dry films were peeled off from the surface of plate and used for the further analyses.

Table 1

Composition of the film forming solutions

Films	A (3%) / PVA(1%) ratio (v/v)	Glycerol	Ascorbic acid and red beet root extract
A	1/0	-	-
PVA	0/1	-	-
A-G	1/0	+	-
PVA-G	0/1	+	-
APVA(1:1)	1/1	-	-
APVA(3:2)	3/2	-	-
APVA(2:3)	2/3	-	-
APVA(1:1)-G	1/1	+	-
APVA(3:2)-G	3/2	+	-
APVA(2:3)-G	2/3	+	-
TTI(1:1)	1/1	+	+
TTI(3:2)	3/2	+	+
TTI(2:3)	2/3	+	+

Determination of mechanical properties

The dried films were cut into strips (10mm x 50 mm) and conditioned for 48 hours at 25 °C in a desiccator containing over-saturated solution of magnesium nitrate (50% relative humidity) prior to measurement of mechanical properties [24]. The thickness of the film strips was measured at five random positions using a digital caliper (Alpha-tools, Mannheim, Germany; 0.001 mm sensitivity) and the average thickness was used for the tensile tests. The tensile test was performed using a texture analyzing instrument (Texture Analyzer TA.XT.plus (Stable Micro System, England) equipped with miniature tensile grips probe at room temperature. Test method ASTM D1708-10 was used to measure the tensile properties of the films [25]. The crosshead speed was 1 mm/s. Tensile strength (MPa) was calculated by dividing the maximum load at break by the cross-sectional area of the film. Percent elongation at break was determined by dividing the length extended at the moment of rupture by the initial length of the film strip and multiplying by 100. Elasticity modulus (N/mm^2) was also calculated from the slope of the initial linear region of the stress-strain curve. At least 6 specimens for each film type were tested.

Thermogravimetric analysis (TGA)

Thermogravimetric analyses (Labsys Evo, Setaram Instrumentation, Caluire, France) were carried out in nitrogen atmosphere with a sample mass of approximately 9 mg at heating rate of 10 °C min^{-1} in a temperature range of 20-800 °C.

Fourier transform infrared spectroscopy (FT-IR)

Fourier-transform infrared (FT-IR) spectroscopy [51] was conducted by using IR Affinity-1 Spectrometer (Shimadzu Corporation, Kyoto, Japan) in the wave number range from 4000 to 600 cm^{-1} at 4.0 cm^{-1} resolution with 64 scans. Data analysis of each film was performed with Peak Fit (Version 4.12) program. For each replicate two measurements were taken.

Scanning electron microscopy (SEM)

SEM analysis was performed to examine the microstructure of films. SEM analysis was carried out using JSM-6400 Electron Microscope (JEOL Ltd, Tokyo, Japan) equipped with NORAN System 6 X-ray Microanalysis System. Prior to examination, samples were sputter coated with gold–palladium to render them electrically conductive by using Sputter Coater Device (Polaron Range, East Sussex, England).

Colorimetric characterization of TTI film

The TTI (3:2) film was used in the color analysis since it had higher percent elongation at break compared to other TTI films. The TTI (3:2) films were conditioned at different temperatures (4, 25, 40 and 60 °C) for seven days. The CIE L*a*b* color parameters of TTI (3:2) films were measured (Minolta Chromameter CR-400, Osaka, Japan) immediately after being dried and on each day during seven days of storage. Five readings at different locations of the films were measured to obtain a mean value. The hue angle values were calculated by using the following equations [26].

$$Hue = arctan\,(b*/a*), \qquad for\ [+a*, +b*]$$
$$Hue = arctan\,(b*/a*) + 360\,, \qquad for\ \ [+a*, -b*]$$

Statistical analysis

Data were expressed as means ± standard deviations. Statistical analysis was performed using Minitab 17. Differences were considered to be significant at validity of α=0.95.

Results and discussion

Mechanical properties

Elasticity modulus (E), tensile strength (TS) and the elongation at break (EB) of the films were determined from the typical curves obtained through the tensile tests and summarized in Table 2.

Alginate film had E of 3376.0, TS of 49.63 MPa and EB of 4.72%. High E and low EB values mean that pure alginate film tends to be brittle. These results are consistent with the findings of Çaykara and Demirci [21] and Russo et al. [23]. Çaykara and Demirci [21] determined the elongation at break value of pure alginate (1% w/v) as 6.5%. The addition of PVA to the alginate increased the E by 0.2-13.6% and TS by 1.5-10.6. It can be seen that the stretch ability of the alginate film did not develop with the addition of PVA at 1:1 and 3:2 alginate/ PVA ratios. However, addition of PVA at the highest level (APVA (2:3)) provided 23.9% increase in EB of alginate (A) film. Similarly, Russo et al. [23] reported that the addition of PVA to alginate in a ratio of 1:1 did not provide a noticeable increase in strain at break. Compared to pure PVA film, the APVA blend films had higher E, TS and lower EB values as expected. The addition of glycerol to A, PVA and APVA blend films provided remarkable effects on the mechanical properties of films. TS and E of the films decreased significantly while EB values increased. With addition of glycerol, EB values of A, PVA and APVA films increased 9.3, 2.1 and 8.1-11.4 times, respectively. The E and TS of APVA blend films decreased from 2918.20-3370.0 to 26.42-40.26 and from 50.39-54.91 to 1.94-3.08, respectively while the EB values increased from 4.32-5.85% to 47.27-50.25%. This indicates that addition of glycerol made films more ductile. The PVA-G film was the most stretchable film with EB of 223.35%. Increase in the stretch ability of films with higher EB

and lower TS values with the addition of plasticizers has been reported in previous studies evaluating the effect of plasticizers on mechanical properties of films [23, 27, 28]. Plasticizers promote the formation of hydrogen bonds between plasticizers and the polymeric material and weaken the intermolecular forces of attraction in polymer which reduces the tensile strength and improves the flexibility of film by increasing molecular mobility of polymers [22, 27, 28].

Table 2

Elasticity modulus (E), tensile strength (TS) and the elongation at break (EB) for the films

Films	Elasticity modulus ($N/mm^{2)}$	Tensile strength (MPa)	Elongation at break (%)
A	3376.00±332.00	49.63±2.92	4.72±1.31
PVA	466.40±67.70	22.97±3.00	105.64±16.80
A-G	126.43±26.90	12.55±1.51	43.91±4.45
PVA-G	4.43±0.58	4.31±0.50	223.35±48.50
APVA(2:3)	2918.20±314.10	50.39±4.93	5.85±0.99
APVA(1:1)	3201.00±536.00	54.91±0.28	4.32±2.67
APVA(3:2)	3370.00±399.00	53.93±10.53	4.74±0.91
APVA(2:3)-G	26.42±4.45	1.94±0.12	47.27±3.22
APVA(1:1)-G	31.23±5.59	2.24±0.28	49.44±2.67
APVA(3:2)-G	40.26±6.42	3.08±0.42	50.25±2.52
TTI(2:3)	4.41±0.44	0.71±0.01	24.38±1.07
TTI(1:1)	6.45±0.33	1.36±0.11	30.32±3.10
TTI(3:2)	6.32±1.98	1.57±0.10	51.71±3.17

TTI films contain also ascorbic acid and red beet root extract unlike APVA-G films. With the addition of these components, the E of APVA-G films reduced by 79-86%. In addition, when compared to APVA-G films, the tensile strength values of TTI films have also decreased. This suggests the emergence of some intermolecular interactions with the addition of ascorbic acid and beetroot extract. The EB values of APVA (2:3)-G and APVA(1:1)-G films decreased by 48.4% and 38.7% whereas the EB of APVA (2:3)-G film stayed nearly constant. For both APVA and TTI blend films, increasing concentration of alginate provided an increase in E, TS and EB values of the films. TTI (1:1) and TTI(3:2) films had 22.7-30.2%, 50.0-54.8% and 19.6-52.9% higher E, TS and EB values compared to TTI(2:3) film. This means that the higher alginate proportion improved the handling properties of TTI film. The TTI(3:2) film had better film flexibility compared to all other films except PVA film with or without glycerol.

Thermogravimetric analysis

The TGA curves of pure A and PVA and the blends were shown in Figures 1 and 2. The initial, final degradation temperatures and mass loss (%) were determined from TGA and DTG (differential gravimetric analysis) curves. The recorded thermogravimetric plots for all samples showed three mass loss regions. The first mass loss which begin around 26-28 °C was 13 and 26% for PVA and A, respectively. The first loss is ascribed to the removal of

adsorbed water from the polymer matrix [29, 30]. Some authors also stated that the initial mass loss of PVA may also be associated with the splitting or volatilization of small molecules [31, 32]. Higher percent of mass loss of A may be related with the alginate's ability to retain high amounts of water. Comparing to pure A and PVA, initial decomposition temperature of APVA and TTI blends started at higher temperatures (41-45 °C) and the mass loss of blends ranged between 22-25% which were close to that of pure A. There was no clear difference between the blend films.

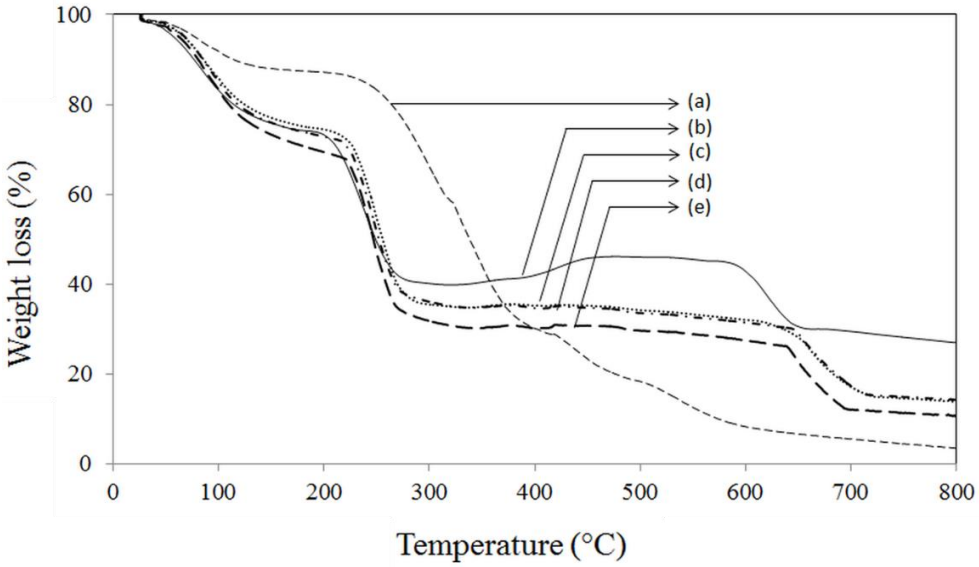

Figure 1. The TGA thermograms of PVA (a), A (b), APVA(1:1) (c), APVA(2:3) (d) and APVA(3:2)(e) samples

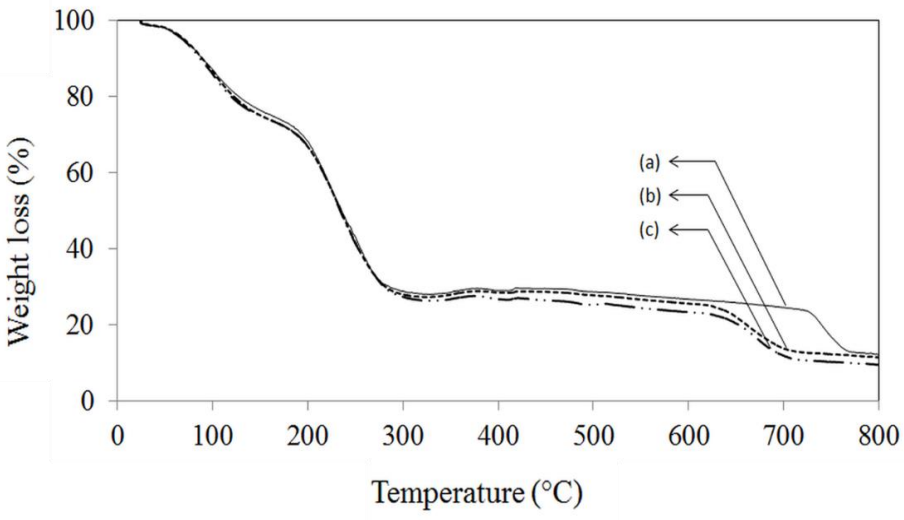

Figure 2. The TGA thermograms of TTI(3:2) (a), TTI(1:1) (b) and TTI(2:3)(c) samples

All the samples showed a more significant mass loss in the second decomposition step. In this stage, the mass loss of pure A and PVA started at similar temperatures (about 185 °C) implying that the thermal stability of pure PVA and A are almost the same [21]. PVA showed a high mass loss (57%) occurring at a temperature region of 185 to 402 °C. This result is in coincidence with literature [29-31]. Ahad et al. [29] reported that the mass loss of PVA occurring in the range of 178 to 368 °C was about 45%. The reason of the higher mass loss of PVA in second stage was attributed to the degradation of the side chain (O-H) and the bond scission in the polymeric backbone by some authors [29, 31-33]. Pure A and APVA blends showed similar mass loss values (34-39%) which were lower than the mass loss (45-46%) of TTI blends. In this step, the start of mass loss raised to higher temperatures (193-197 °C) for APVA blends when compared to pure A or PVA which reveals that the APVA blends have higher thermal stability. Çaykara and Demirci [21] recorded that the mass loss of pure PVA and sodium alginate started at around 230 °C while that of PVA/sodium alginate blends started at higher temperatures due to some specific intermolecular interactions between them. For the TTI blends, however, the initial degradation temperature in the second step decreased below those of pure A and PVA. The mass loss which corresponds to this stage was also higher (about 45–46%) than pure A and APVA blends. This reveals that the addition of glycerol, ascorbic acid and beet root extract to APVA blends reduced the thermal stability. The ratio of A to PVA in blend films did not create a significant effect on TGA thermograms. PVA showed approximately 11% mass loss between 410 and 497 °C which is associated with the decomposition of the main polymer chain [29, 33]. In this stage thermal decomposition of alginate started at higher temperature (568.4 °C) compared to PVA. APVA and TTI blends exhibited enhancement in thermal stability. For TTI blends, the thermal degradation temperature was shifted toward higher temperatures with increasing A content. However, the percent mass loss of APVA or TTI blends did not affected by the ratio of A to PVA.

FT-IR analysis

FT-IR spectra of A, PVA, APVA and TTI blend polymer matrix studied in the range 4000-600 cm^{-1} were presented in Figure 3. For all films, the large bands observed in the range of 3000-3700 cm^{-1} are attributed stretching vibrations of O–H from the intramolecular and intermolecular hydrogen bonds [34-36]. The FT-IR spectra of PVA shows a band between 2900-2940 cm^{-1} indicating the stretching C–H from alkyl groups [34, 37], a band between 1327 - 1421 cm^{-1} indicating bending and wagging of CH_2 vibrations [35], a band at 1083 cm^{-1}' indicating C-O stretching [35, 38]. According to literature, the 1141 cm^{-1} band is sensitive to crystalline parts of the PVA chain [39]. In the FT-IR spectrum of alginate, the peaks at 2926, 1597, 1409 and 1300 cm^{-1} were assigned to aliphatic C–H stretching, antisymmetric COO^- stretching, symmetric COO^- stretching and skeletal vibrations, respectively [36, 40, 41]. The sodium alginate spectrum also shows a band at 1029 cm^{-1} related to stretching vibration of the C-O-C bond [36, 42]. APVA blend films display an FT-IR spectrum that is very similar to alginate. Compared to pure PVA, the O–H stretching band of APVA blend films became wider and shifted to lower frequency which may be related with the formation of intermolecular hydrogen bonding between PVA and alginate. The intensity of O–H stretching band clearly increased in TTI films compared to other films. In addition, the aliphatic C–H stretching, the antisymmetric and symmetric COO^- stretching and the C-O-C stretching vibration band intensities were also clearly higher in TTI films compared to alginate film. In TTI films, a band is appeared at 1716 cm^{-1} probably originated from stretching vibrations of C=C bonds of ascorbic acid [43].

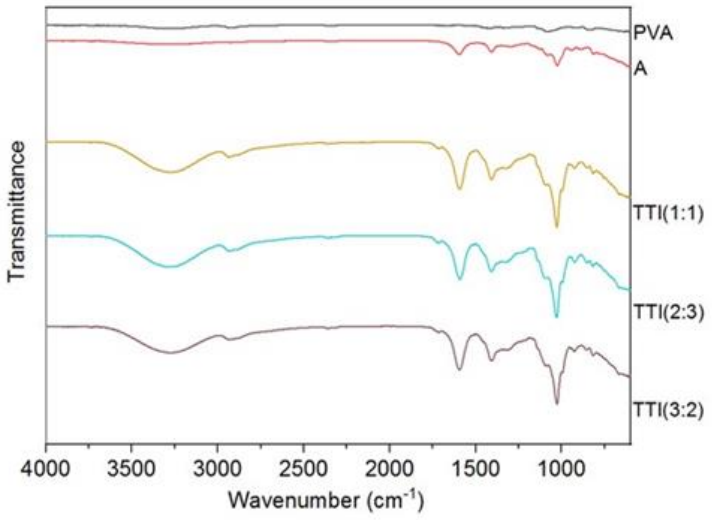

a

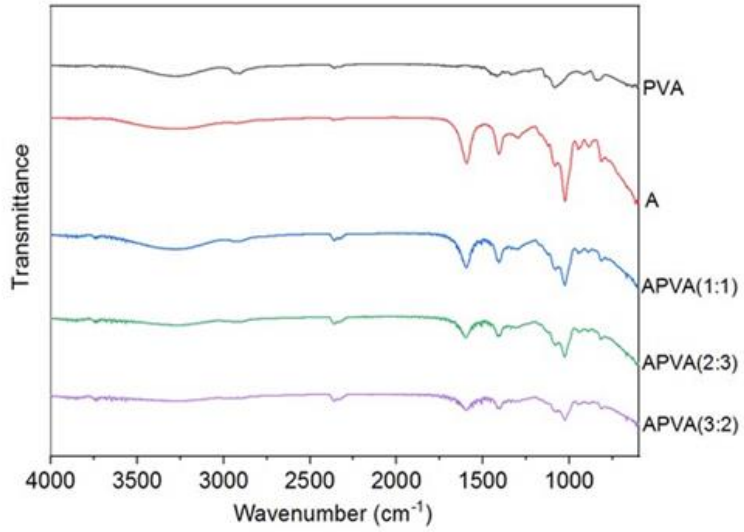

b

Figure 3. FTIR spectra of films

SEM analysis

The SEM micrographs of the surface and cross section of pure PVA and A films were shown in Figure 4.

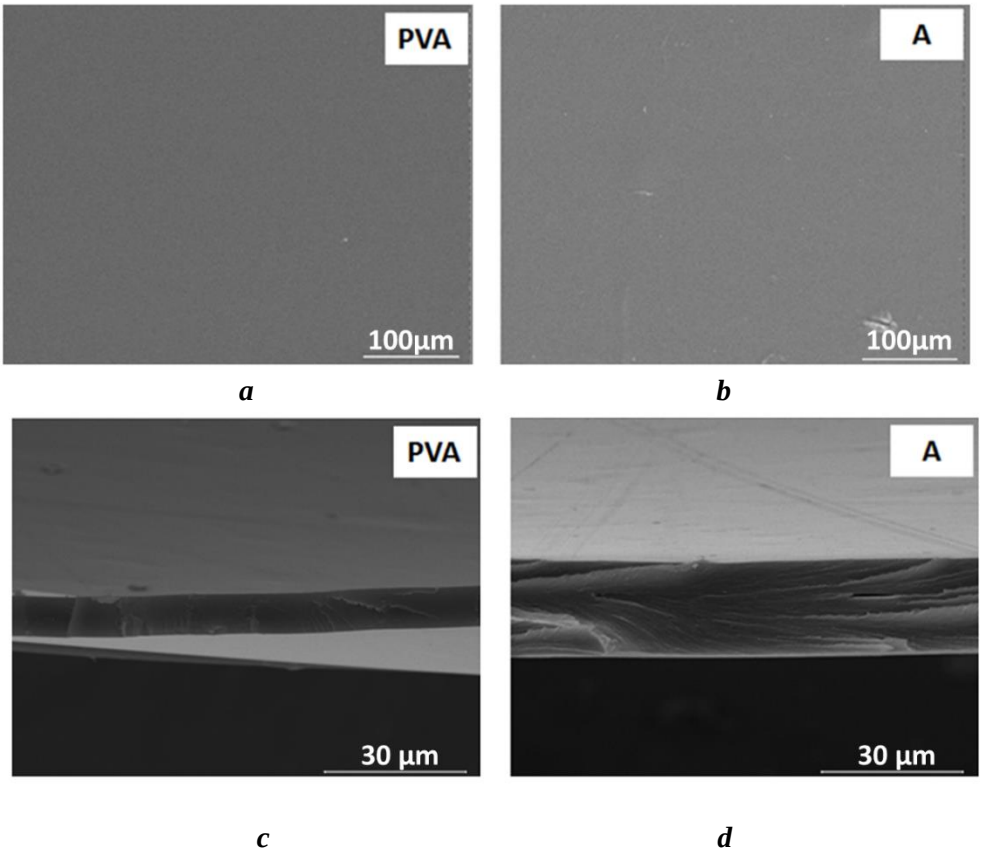

Figure 4. The surface (250x) (a ,b) and the cross section (3000x) (c, d) SEM images of A and PVA films

PVA and A films had smooth, homogeneous and continuous structures as seen from the figure. However, there was a uniform surface roughness observed for APVA (3:2)-G blend film (Figure 5). The surface of the film had no visible crack but had some bulges. The possible reason is that the blend film exhibited phase separation. This is also consistent with several previous studies involving PVA and alginate. Phase separation was observed in sodium alginate/PVA blend membranes by Yeom and Lee [44] and PVA-alginate ester based membranes by Amri et al. [45].

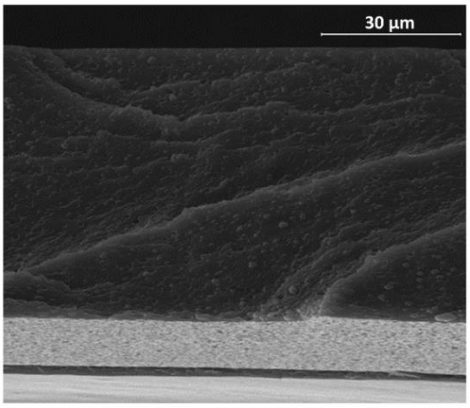

Figure 5. The SEM image of APVA(3:2)-G film (3000x)

Figure 6 presents the SEM micrographs of the surface and cross section of TTI blend films. The appearance of the TTI films were similar to that of APVA(3:2)-G blend film. The surface of the TTI films were flat without any crack but had many small or large sized bulges. It may be observed from the figure that the phase separation is more significant in the TTI(2:3) film which contains higher amount of PVA in its formulation. Yeom and Lee [44] stated that the continuous matrix in sodium alginate/PVA blend membranes was composed mainly of sodium alginate while PVA formed the separated domains. This explains the larger size of separated domains in TTI(2:3) films. The mechanical properties of the film are affected by the uniform distribution of the polymers in the matrix. This result is consistent with the results of mechanical properties of the films. This means that the higher alginate proportion in TTI blend films decreased the phase separation and improved the handling properties of TTI film.

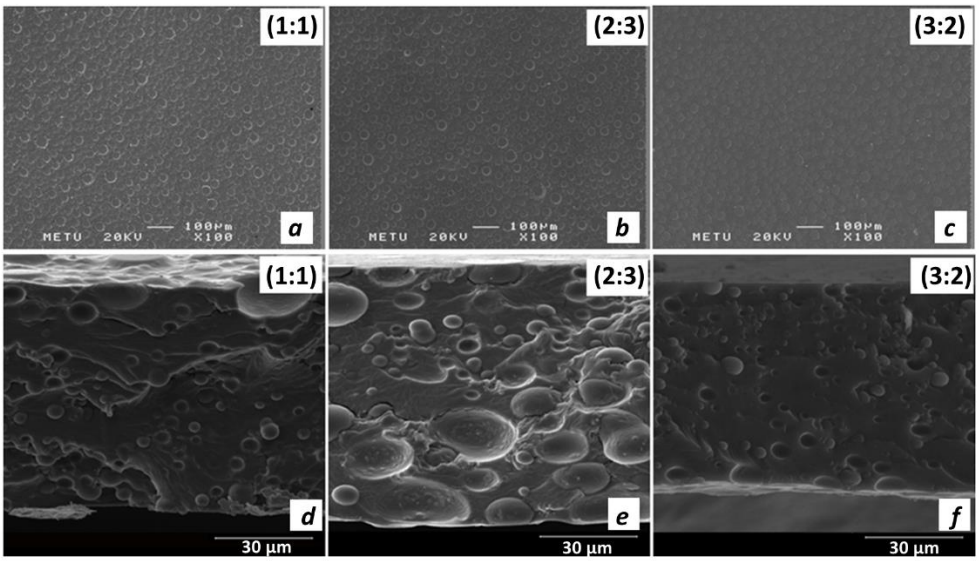

Figure 6. The surface (100x) (a, b, c) and the cross section (3000x) (d, e, f) SEM images of TTI(1:1), TTI(2:3) and TTI(3:2) films

Colourimetric characterization of TTI film

TTI film developed in this study contains water extract of red beetroot as color indicator. Red beet root extract contains a group of water-soluble pigments called betalains [18]. Betalains are classified into two major structural groups of pigments: betacyanins (red-violet) and betaxanthins (yellow-orange) [46]. The pH affects the colorimetric parameters of betalains and the stability of betalain pigments during storage [47]. The pH of TTI film forming solution was adjusted to 9.5 in order to be able to obtain the desired color change at the studied temperatures. The average values of the initial CIE L* a*, b* color parameters of the TTI film were recorded as 76.83±1.70, 29.2 ±1.97 and -9.43±0.28, respectively. The L*, a* and b* color parameters of TTI (3:2) film exposed to different temperatures were recorded each day for 7 days. Table 3 presents the change in L*, a* and b* color parameter of the TTI film. It was found that temperature, time and temperature x time interaction were all important factors affecting the color parameters of the TTI film (Table 4). The L* values of TTI films subjected to 4, 25 and 40 ºC temperatures did not undergo significant changes,

while the L* value of the TTI film exposed to 60 °C decreased significantly on the first day and fluctuated between 58.00±3.69 and 69.24±1.61 throughout following days. Similar to L*, the parameter a* (green-red axis) of TTI film remained nearly constant during seven days of storage at refrigerator temperature (4 °C). At other temperatures, there was a significant reduction in a* value of TTI film at the end of seven days. The reduction in a* value was significant on the third and sixth days of storage at 25 and 40 °C, respectively. At 60 °C, however, significant decrease in a* value was detected on the initial day, and then statistically insignificant reduction in consecutive days was observed until end of storage.

Table 3

Change of the L*, a* and b* color parameter of TTI film exposed to different temperatures

Color Parameter	Day	Temperature			
		4 °C	25 °C	40 °C	60 °C
L*	0	$77.4^{a*A**}\pm0.91$	$78.99^{aA}\pm0.74$	$75.40^{aA}\pm2.88$	$75.55^{aA}\pm2.05$
	1	$76.76^{aA}\pm1.25$	$78.66^{aA}\pm0.77$	$74.52^{aA}\pm2.61$	$58.00^{dB}\pm3.69$
	2	$78.47^{aA}\pm1.77$	$79.26^{aA}\pm1.04$	$75.70^{aA}\pm2.33$	$56.93^{dB}\pm3.70$
	3	$76.53^{aA}\pm0.48$	$78.36^{aA}\pm0.52$	$73.37^{aA}\pm4.70$	$61.84^{cdB}\pm2.61$
	4	$76.46^{aA}\pm0.33$	$78.49^{aA}\pm1.31$	$68.18^{aB}\pm4.61$	$66.45^{bcB}\pm0.22$
	5	$76.83^{aA}\pm1.60$	$79.94^{aA}\pm0.58$	$75.10^{aA}\pm2.27$	$66.53^{bcB}\pm0.18$
	6	$77.17^{aAB}\pm0.29$	$79.47^{aA}\pm0.29$	$73.34^{aB}\pm3.86$	$64.34^{bcC}\pm1.70$
	7	$76.60^{aA}\pm0.53$	$79.17^{aA}\pm0.31$	$73.57^{aB}\pm2.16$	$69.24^{bC}\pm1.60$
a*	0	$28.77^{aA}\pm0.11$	$26.76^{aA}\pm0.48$	$30.67^{aA}\pm3.80$	$30.71^{aA}\pm2.82$
	1	$29.02^{aA}\pm1.08$	$26.94^{aA}\pm0.85$	$29.98^{abA}\pm3.26$	$21.92^{bB}\pm0.90$
	2	$28.31^{aA}\pm1.39$	$26.28^{abA}\pm0.82$	$28.10^{abcA}\pm2.42$	$20.97^{bB}\pm0.89$
	3	$28.81^{aA}\pm0.49$	$24.82^{bcA}\pm0.56$	$26.30^{abcA}\pm4.00$	$19.81^{bcB}\pm0.28$
	4	$28.88^{aA}\pm0.55$	$24.08^{cdB}\pm0.87$	$25.83^{abcB}\pm1.67$	$20.30^{bcC}\pm0.93$
	5	$28.89^{aA}\pm0.80$	$23.11^{deB}\pm0.69$	$24.36^{abcB}\pm2.00$	$20.23^{bcC}\pm0.27$
	6	$28.66^{aA}\pm0.36$	$22.27^{deB}\pm0.20$	$23.90^{bcB}\pm2.93$	$18.78^{bcC}\pm0.53$
	7	$28.20^{aA}\pm0.42$	$22.26^{eB}\pm0.25$	$22.61^{cB}\pm0.25$	$16.09^{cC}\pm0.53$
b*	0	$-9.72^{aA}\pm0.18$	$-9.64^{aA}\pm0.05$	$-9.23^{aA}\pm0.17$	$-9.14^{aA}\pm0.12$
	1	$-9.703^{aA}\pm0.20$	$-8.49^{bB}\pm0.25$	$-5.02^{cC}\pm0.40$	$0.06^{bD}\pm0.01$
	2	$-9.66^{abA}\pm0.10$	$-6.71^{cB}\pm0.44$	$-0.86^{cC}\pm0.68$	$3.84^{cD}\pm0.39$
	3	$-9.57^{bcA}\pm0.10$	$-4.52^{dB}\pm0.25$	$3.10^{dC}\pm2.20$	$6.15^{cdD}\pm0.14$
	4	$-9.47^{bcA}\pm0.03$	$-3.85^{dB}\pm0.21$	$4.10^{dC}\pm1.21$	$7.06^{dD}\pm0.06$
	5	$-9.19^{cA}\pm0.24$	$-2.12^{eB}\pm0.13$	$5.38^{dC}\pm1.75$	$8.00^{eD}\pm0.22$
	6	$-9.03^{cA}\pm0.29$	$0.29^{fB}\pm0.11$	$6.16^{dC}\pm2.65$	$9.73^{fD}\pm1.16$
	7	$-9.00^{cA}\pm0.03$	$1.28^{gB}\pm0.58$	$6.77^{dC}\pm2.28$	$12.59^{gD}\pm0.72$
Hue angle	0	$341.32^{abA}\pm0.32$	$340.18^{gA}\pm0.39$	$343.93^{fA}\pm0.78$	$343.048^{gA}\pm1.16$
	1	$341.49^{abC}\pm0.93$	$342.49^{fC}\pm0.78$	$351.23^{eB}\pm0.35$	$359.011^{fA}\pm1.47$
	2	$341.11^{bD}\pm1.01$	$345.64^{eC}\pm1.26$	$358.15^{dB}\pm1.63$	$10.36^{eA}\pm0.63$
	3	$341.61^{abD}\pm0.29$	$349.65^{dC}\pm0.79$	$8.08^{cB}\pm1.97$	$17.25^{dA}\pm0.61$
	4	$341.84^{abD}\pm0.37$	$350.89^{dC}\pm0.83$	$8.04^{cB}\pm1.28$	$19.22^{cdA}\pm0.72$
	5	$342.34^{abD}\pm0.55$	$354.74^{cC}\pm0.47$	$13.51^{bB}\pm2.07$	$21.59^{cA}\pm0.53$
	6	$342.50^{aD}\pm0.46$	$0.75^{bC}\pm0.20$	$18.130^{abB}\pm2.90$	$27.35^{bA}\pm2.69$
	7	$342.28^{abD}\pm0.31$	$1.30^{aC}\pm0.28$	$21.28^{aB}\pm0.17$	$35.27^{aA}\pm1.55$

*Data are expressed as mean ± standard deviation. For each color parameter, means with different lower case letters (a, b, c) in the same column are significantly different at $p \leq 0.05$.

** For each color parameter, means with different capital letters (A, B, C) in the same row are significantly different at $p \leq 0.05$

The parameter b*(blue-yellow axis) underwent more distinct changes compared to parameters a* and L*. At refrigerator temperature, b* value of TTI film increased from the initial value of -9.72 to -9.57 after three days. This increase was found to be statistically significant. The b* value remained statistically stable in consecutive days and reached to -9.00 at the end of seventh day. At the other temperatures, significant increases in b* values of TTI films were detected on the initial day. At the end of seventh day, the b* values of the samples subjected to temperatures of 25, 40 and 60 °C were 1.28, 6.77 and 12.59, respectively. The effect of temperature on the b* values of the TTI film was statistically significant from the first day. The highest change in the b* value occurred in the film kept at 60 °C. The hue angle is expressed in positive degrees ranging from 0 to 360. The angle of 0° or 360° indicates red color while the angles of 90°, 180° and 270° represent yellow, green and blue colors, respectively. Initially, the TTI film had an average hue value of 342.12. The change in hue value was not significant during 7 days at 4 °C, while significant change was observed from the first day at other temperatures. The hue angle changed in the counterclockwise direction and rapidly passed the red color axis (0°) at 40 and 60 °C.

Table 4

ANOVA showing the effects of temperature (T), storage time (t), and interaction term (T x t) on color values

Source	L*(R^2_{adj}=0.89)		a*(R^2_{adj}=0.82)		b*(R^2_{adj}=0.98)		Hue(R^2_{adj}=0.98)	
	Adj MS	Pvalue	Adj MS	Pvalue	Adj MS	Pvalue	Adj MS	Pvalue
t	41.04	0.00	74.49	0.00	275.16	0.00	1399.73	0.00
T	1268.51	0.00	330.15	0.00	1242.57	0.00	6653.93	0.00
T x t	42.01	0.00	15.38	0.00	37.08	0.00	212.85	0.00
Error	4.56		3.03		0.83		5.50	

MS- mean squares, df- degrees of freedom, R^2_{adj}-adjusted coefficient of determination, P-value < 0.05 denotes significant effect

Higher temperatures accelerated the color change of TTI film as seen in Figure 7. The color of the film exposed to 60°C changed considerably on the first day. The color change at temperatures 40 and 60 °C was visually appreciable by human eyes on the first day. Maciel et al. [15] developed a colourimetric temperature indicator by covering the surface of a card paper with chitosan matrix film containing anthocyanin. The indicator was exposed to temperatures of 20, 40 and 60 °C with or without luminosity (0 or 1000 lx) for 72 hours. They recorded no significant change in a* value irrespective of temperature and luminosity. Similar to our findings, they observed the most significant change in b* parameter and the highest change in b* value was obtained at 60 °C. They stated that the color of the indicator changed from light purple to slightly yellow which is associated with the alteration in anthocyanin structure. It is known that the pigment structure and concentration, temperature, pH, oxygen, light, water activity, metal cations, antioxidants and enzymes are among the factors affecting the stability of betalain pigments [18, 48]. Herbach et al. [49] stated that the degradation rate of betalains increases with increasing temperature which results chromatic changes depending on several degradation and transformation reactions. Herbach et al. [50] reported that thermal treatment of betacyanin solution caused increasing hue angle values.

The yellow compounds formed as a result of degradation reactions like hydrolysis or dehydrogenation may be responsible for the increased b* value of the films [49].

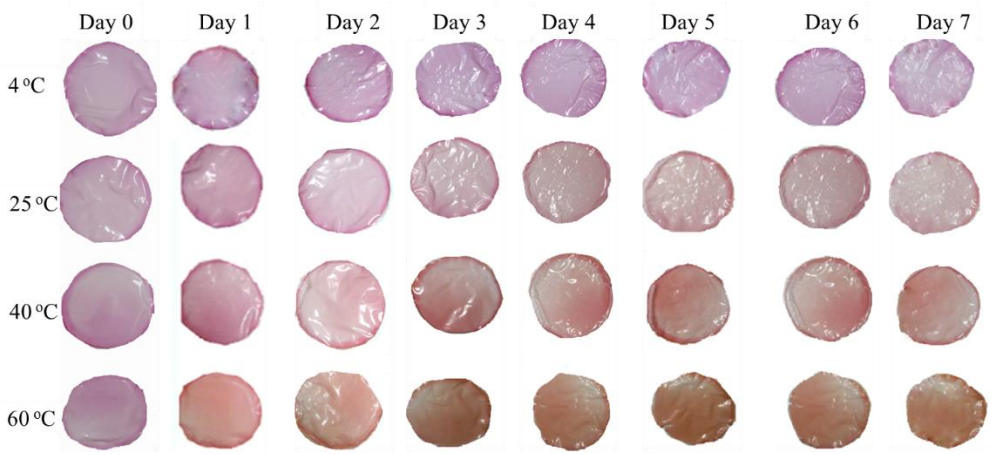

Figure 7. Color images of the TTI films stored at 4, 25, 40 and 60 °C during 7 days

Conclusion

Time temperature indicators applied to intelligent packaging are low-cost and user-friendly systems informing consumers about quality and safety of food. In this study, TTI films were prepared by adding red beet root extract to blend films with different ratio of alginate and PVA. The analysis showed that TTI film made up of A and PVA with a ratio of (3:2) provided enhancement of the mechanical properties and reduction of the phase separation observed in SEM images. The color change of this film was investigated at different temperatures. A visual color change was observed in the film upon exposure to temperatures of 25, 40 and 60 °C while it maintained its color for 7 days at refrigerator temperature. Results indicated that, this indicator may have potential applications to monitor food products requiring refrigeration.

Acknowledgements. This work was supported by a grant from Ordu University (TF 1528)

References

1. Marsh K., Bugusu B. (2007), Food packaging–roles, materials, and environmental issues, *Journal of Food Science*, 72(3), pp. R39–R55.
2. Wyrwa J., Barska A. (2017), Innovations in the food packaging market: active packaging, *European Food Research and Technology*, 243, pp. 1681–1692.
3. Biji K.B., Ravishankar C.N., Mohan C.O., Srinivasa Gopal T.K. (2015), Smart packaging systems for food applications: a review, *Journal of Food Science and Technology*, 52(10), pp. 6125–6135.

4. Janjarasskul T., Suppakul P. (2018), Active and intelligent packaging: The indication of quality and safety, *Critical Reviews in Food Science and Nutrition*, 58 (5), pp. 808–831.
5. Yam K.L., Takhistov P.T., Miltz J. (2005), Intelligent packaging: concepts and applications, *Journal of Food Science*, 70(1), pp. R1–R10.
6. Day B.P.E. (2008), In: Kerry J., Butler P. (eds*), Smart packaging technologies for fast moving consumer goods*, John Wiley, Chichester.
7. Wang S.D., Liu X.H., Yang M., Zhang Y., Xiang K.Y., Tang R. (2015), Review of time temperature indicators as quality monitors in food packaging, *Packaging Technology and Science*, 28(10), pp. 839–867.
8. Kim M.J., Jung S.W., Park H.R., Lee S.J. (2012), Selection of an optimum pH indicator for developing lactic acid bacteria–based time temperature integrators (TTI), *Journal of Food Engineering*, 113(3), pp. 471–478.
9. Pennanen K., Focas C., Kumpusalo–Sanna V., Keskitalo–Vuokko K., Matullat I., et al. (2016), European consumers' perceptions of time–temperature indicators in food packaging. *Packaging Technology and Science*, 29(4), pp. 610–610.
10. Shukla V., Kandeepan G., Vishnuraj M.R., Soni A. (2016), Anthocyanins based indicator sensor for intelligent packaging application, *Agricultural Research*, 5, pp. 205–209.
11. Musso Y.S., Salgado P.R., Mauri A.N. (2019), Smart gelatin films prepared using red cabbage (*Brassica oleracea* L.) extracts as solvent, *Food Hydrocolloids*, 89, pp. 674–681.
12. Silva–Pereira M.C., Teixeira J.A., Pereira-Junior V.A., Stefani R. (2015), Chitosan/corn starch blend films with extract from Brassica oleraceae (red cabbage) as a visual indicator of fish deterioration, *LWT Food Science and Technology*, 61(1), pp. 258–262.
13. Mohebi E., Marquez L. (2015), Intelligent packaging in meat industry: An overview of existing solutions, *Journal of Food Science and Technology*, 52(7), pp. 3947–3964.
14. Nofrida R., Warsiki E., Yuliasih I. (2013), The effect of storage temperature on the erpa leaf (*Aerva sanguinolenta*) color indicator smart label, *Jurnal Teknologi Industri Pertanian*, 23 (3), pp. 232–241.
15. Maciel V.B.V., Yoshida C.M.P., Franco T.T. (2012), Development of a prototype of a colourimetric temperature indicator for monitoring food quality, *Journal of Food Engineering*, 111(1), pp. 21–27.
16. Maciel V.B.V., Yoshida C.M.P., Franco T.T. (2014), Development of temperature indicator prototype: Cardpaper coated with chitosan intelligent films, *Journal of Agricultural Chemistry and Environment*, 3(1), pp. 5–10.
17. Pedreno M.A., Escribano J. (2001), Correlation between antiradical activity and stability of betanine from *Beta vulgaris* L roots under different pH, temperature and light conditions, *Journal of the Science of Food and Agriculture*, 81(7), pp. 627–631.
18. Azeredo H.M.C. (2009), Betalains: properties, sources, applications and stability – a review, *International Journal of Food Science and Technology*, 44(12), pp. 2365–2376.
19. Drdak K.M., Vallova M. (1990), Kinetics of the thermal degradation of betanine, *Die Nahrung*, 34(4), pp. 307–310.
20. Pereira V.A., de Arruda I.N.Q., Stefani R. (2015), Active chitosan/PVA films with anthocyanins from Brassica oleraceae (red cabbage) as time temperature indicators for application in intelligent food packaging, *Food Hydrocolloids*, 43, pp. 180–188.
21. Çaykara T., Demirci S. (2006), Preparation and characterization of blend films of poly(vinylalcohol) and sodium alginate, *Journal of Macromolecular Science Part A Pure and Applied Chemistry*, 43(7), pp. 1113–1121.

22. Senturk Parreidt T., Muller K., Schmid M. (2018), Alginate–based edible films and coatings for food packaging applications, *Foods*, 7(10), pp. 170.
23. Russo R.A., Giuliani B., Immirzi M., Malinconico M., Romano G. (2004), Alginate/polyvinylalcohol blends for agricultural applications: structure–properties correlation, mechanical properties and greenhouse effect evaluation, *Macromolecular Symposia*, 218, pp. 241–250.
24. ASTM D618–61 (1993) Standard practice for conditioning plastics and electrical insulating materials for testing.
25. ASTM D1708–10 (2010) Standard test method for tensile properties of plastics by use of microtensile specimen.
26. McLellan M.R., Lind L.R., Kime R.W. (1995), Hue angle determinations and statistical analysis for multiquadrant hunter L,a,b data, *Journal of Food Quality*, 18(3), pp. 235–240.
27. Kadhim M.M., Shakheer A.I., Fahim A.H., A kadhim M.M.H. (2018), Effect of type and concentration of plasticizer on mechanical properties of protein edible films, *International Journal of Mechanical Engineering and Technology*, 9(10), pp. 1493–1503.
28. Sanyang M.L., Sapuan S.M., Jawaid M., Ishak M.R., Sahari J. (2015), Effect of plasticizer type and concentration on tensile, thermal and barrier properties of biodegradable films based on sugar palm (*Arenga pinnata*) starch, *Polymers*, 7(6), pp. 1106–1124.
29. Ahad N., Saion E., Gharibshahi E. (2012), Structural, thermal, and electrical properties of PVA–sodium salicylate solid composite polymer electrolyte, *Journal of Nanomaterials*, DOI: 10.1155/2012/857569.
30. Anbarasan R., Pandiarajaguru R., Prabhu R., Dhanalakshmi V., Jayalakshmi A., Dhanalakshmi B., Nisha S.U., Gandhi S., Jayalakshmi T. (2010), Synthesis, characterizations, and mechanical properties of structurally modified poly(vinyl alcohol), *Journal of Applied Polymer Science*, 117(4), pp. 2059–2068.
31. Guirguis O.W., Moselhey M.T.H. (2012), Thermal and structural studies of poly(vinyl alcohol) and hydroxypropyl cellulose blends, *Natural Science*, 4(1), pp. 57–67.
32. Pawar R.P. (2015), Study of thermal decomposition and instrumental analysis of synthesised polyvinyl alcohol polymer, *Journal of Ultra Chemistry*, 11(1), pp. 1–6.
33. Pirzada T., Shah S.S. (2014), Water–resistant poly(vinyl alcohol)–silica hybrids through sol–gel processing, *Chemical Engineering Technology*, 37(4), pp. 620–626.
34. Mansur H.S., Sadahira C.M., Souza A.N., Mansur A.A.P. (2008), FTIR spectroscopy characterization of poly(vinyl alcohol) hydrogel with different hydrolysis degree and chemically crosslinked with glutaraldehyde, *Materials Science and Engineering*, 28(4), pp. 539–548.
35. Kumar K.N., Padma R., Rao J.L., Kang M. (2016), Dazzling green emission from graphene oxide nanosheet-embedded co–doped Ce3+ and Tb3+:PVA polymer nanocomposites for photonic applications, *The Royal Society of Chemistry Advances*, 6(59), pp. 54525– 54538.
36. Lawrie G., Keen I., Drew B., Chandler–Temple A., Rintoul L., Fredericks P., Grøndahl L. (2007), Interactions between alginate and chitosan biopolymers characterized using FTIR and XPS, *Biomacromolecules*, 8, pp. 2533–2541.
37. Awada H., Daneault C. (2015), Chemical modification of poly(vinyl alcohol) in water, *Applied Science*, 5, pp. 840–850.

38. Pawde S.M., Deshmukh K. (2008), Characterization of polyvinyl alcohol/gelatin blend hydrogel films for biomedical applications, *Journal of Applied Polymer Science*, 109, pp. 3431–3437.
39. Peppas N.A. (1977), Infrared spectroscopy of semicrystalline poly(viny1 alcohol) networks, *Macromolecular Chemistry and Physics*, 178(2), pp. 595–601. ,
40. Çaykara T., Demirci S., Eroğlu M., Güven O. (2005), Poly (ethylene oxide) and its blends with sodium alginate, *Polymer*, 46(24), pp. 10750–10757.
41. Xiao Q., Gu X., Tan S. (2014), Drying process of sodium alginate films studied by two–dimensional correlation ATR–FTIR spectroscopy, *Food Chemistry*, 164, pp.179–184.
42. Gao C., Pollet E., Averous L. (2017), Properties of glycerol–plasticized alginate films obtained by thermomechanical mixing, *Food Hydrocolloids*, 63, pp. 414–420.
43. Zhang Z.H., Zeng X.A., Brennan C., Brennan M., Han Z., Xiong X.Y. (2015), Effects of pulsed electric fields (PEF) on vitamin C and its antioxidant properties, *International Journal of Molecular Sciences*, 16(10), pp. 24159–24173.
44. Yeom C.K., Lee K.H. (1998), Characterization of sodium alginate and poly(vinyl alcohol) blend membranes in pervaporation separation, *Journal of Applied Polymer Science*, 67(5), pp. 949–959.
45. Amri C., Mudasir M., Siswanta D., Roto R. (2016), In vitro hemocompatibility of PVA–alginate ester as a candidate for hemodialysis membrane, *International Journal of Biological Macromolecules*, 82, pp. 48–53.
46. Delgado–Vargas F., Jimenez A.R., Paredes–Lopez O. (2000), Natural pigments: Carotenoids, anthocyanins, and betalains – characteristics, biosynthesis, processing, and stability, *Critical Reviews in Food Science and Nutrition*, 40(3), pp. 173–289.
47. Cejudo–Bastante M.J., Hurtado N., Delgado A., Heredia F.J. (2016), Impact of pH and temperature on the colour and betalain content of Colombian yellow pitaya peel (*Selenicereus megalanthus*), *Journal of Food Science and Technology*, 53(5), pp. 2405–2413.
48. Belhadj Slimen I., Najar T., Abderrabba M. (2017), Chemical and antioxidant properties of betalains, *Journal of Agricultural and Food Chemistry*, 65(4), pp. 675–689.
49. Herbach K.M., Stintzing, F.C., Carle R. (2006), Betalain stability and degradation-structural and chromatic aspects, *Journal of Food Science*, 71 (4), pp.41–50.
50. Herbach K.M., Stintzing F.C., Carle R. (2006), Stability and color changes of thermally treated betanin, phyllocactin, and hylocerenin solutions, *Journal Agricultural and Food Chemistry*, 54(2), pp. 390–8.
51. Posudin Y.I., Peiris K.S., Kays S.J. (2015), Non-destructive detection of food adulteration to guarantee human health and safety, *Ukrainian Food Journal*, 4(2), pp. 207–260.

Efficiency of apple juice clarification with using of nano-sized mineral oxides

Anastasiia Sachko, Igor Kobasa, Olesya Moysyura, Mariia Vorobets

Yuriy Fedkovych Chernivtsi National University, Chernivtsi, Ukraine

Keywords:

Clarification
Apple juice
Titanium dioxide
Silicon dioxide
Bentonite

Article history:

Received 20.06.2019
Received in revised form 21.11.2019
Accepted 30.06.2020

Corresponding author:

Anastasiia Sachko
E-mail: an.sachko@chnu.edu.ua

DOI:
10.24263/2304-974X-2020-9-2-8

Abstract

Introduction. The aim of presented work was the investigation of the efficiency of clarification of direct pressing apple juice with utilization of nano-sized powders of both silicon dioxide and titanium dioxide, modified silicon dioxide powder in comparison with bentonite clay.

Materials and methods. The juice used for laboratory testing was squeezed from "Glory to the Winners" apples. Modified silicon dioxide powder (AMD-2, specific surface area 280 m^2/g) and nano-dispersed powders of both silicon dioxide (specific surface area 300 m^2/g) and titanium dioxide (specific surface area 50 m^2/g) were selected as clarifiers. For comparison, we used bentonite clay (specific surface area 160 m^2/g). The optical density was measured with spectrophotometr, the content of dry substances was evaluated refractometrically, pH and titratable acidity was determined according to known methods.

Results and discussion. Prospects of mineral oxides of titanium and silicon utilization for clarification of apple juice have been shown. It was established that the most effective clarifiers were SiO_2 powder and suspension. Optimal weight of SiO_2 is 2.5 g per 1 liter of juice; steep time is not more than 24 hours. The form (in powder or suspension) has no significant effect on the result of clarification.

The worst clarification ability bentonite clay demonstrated. It was confirmed that utilization bentonite in suspension form increases the clarification efficiency. Growth a mass of bentonite from 0.1 to 2.5 g per l of juice impairs its optical properties.

The effect of temperature of clarification processes on its efficiency and influence of the "juice-clarifier" contact time on the physical-chemical properties of the finished product were investigated. It was shown that the result of clarification is better at low temperature (4 ºC), and all the used oxides are able to slow down the flow of natural processes of fermentation of raw apple materials. It was found that more than 24 hours contact of juice with clarifiers has a negative influence on the clarification result for all tested samples.

Conclusion. Nano-dispersed oxides of titanium (IV) and silicon (IV) could be effectively utilized to clarify of fresh direct pressing apple juice. Their clarifying ability is higher than bentonite clay and they could be brought in juice without pre-treatment, in the form of powder.

Introduction

According to [1] main substances which cause the turbidity in apple juice could be divided into two groups. The first are substances which settle over time, among them: mold, bacteria, plant cell fragments, protein-tannin complexes. The second – substances which formed colloidal or true solutions: polymeric carbohydrates, proteins, polyphenols (tannins), organic acids, alcohol and other. Because of such composition, clarification of apple juice is the necessary stage of producing.

There are two different processes during juice preparation: clarification and fining [1]. It is well known that the production of apple juice includes both the removal of suspended material and prevention of the development of juice turbidity after bottling. Precipitation of suspended substances before filtration often called clarification. Measures, which are taking to remove soluble materials that have the potential to form after-bottling sediment are called fining [1].

For some fruit juices, a natural clarification process is possible under the prolonged storage. This process is the result of chemical reactions that occur in the juice under the action of natural enzymes [2]. The duration of such self-clarification process is from two weeks to 2-3 months [3]. This method can be successfully applied to grape juice, but not for freshly squeezed apple juice [4].

Modern process of apple juice clarification consists of several stages: adding of clarifiers agent, clarification process, vacuum filtration and final filtration. Most useful clarifiers in technological process are enzymes. Many publications are devoted to the study both of the influence of natural and synthetic enzymes on the process of juices clarification and the mechanism of this process [2,5–7,8]. The principle of enzymatic clarification is based on the destruction of the negatively charged surface layer of protein-carbohydrates complexes and protein-pectin complexes under the action of enzymes [8]. Due to the action of electrostatic attraction forces, floccules are formed and the system is destroyed [1].

A classical well-researched fruit juice clarifier is a bentonite clay [1,9]. The clarification effect of bentonite and other minerals is explained by the combination of three processes: adsorption, coagulation and sedimentation. Bentonite clays (like oxides we study) have a developed surface that is why the adsorption of small proteins and other molecules occur on the clay surface. At the same time, the processes of aggregation of proteins, starches and tannins with bentonite particles in the system take place [1,1,7]. They are caused by the redistribution of electrical charges in the system and the change in charge of coats of protein-carbohydrates complexes. The result of these processes is coagulation. In general case, coagulation is not accompanied by the chemical interaction of the clarifier and the juice components [1].

It should be borne in mind that the properties of bentonite and other adsorbents and their clarification ability depend on place of origin and method of its pre-treatment [10,11]. Such pre-treatment can include pH control, selection of concentration range, temperature conditions, the way of making the suspension in the juice and others. That is why results described in different sources could be slightly different.

An important role is played by the method of bringing of bentonite in the juice: in the form of powder or in suspension. It is believed that the use of the suspension is much more effective [12]. Adsorption capability of bentonites increases with their swelling capability in water [13]. To verify this statement, we introduced all clarifiers into the juice as a suspension and powder.

Our previous work was devoted to the study of the effectiveness of lighting white and red wines using mineral clarifiers [14]. We have shown that mineral nanosized titanium and

silicon oxides are much more effective fining agents for red and white grape wines than bentonite and saponite. However, the process of clarifying apple juice is different from the process of clarifying wine materials and not necessarily clarifiers, which were effective for grape wines, will be effective for apple juice.

Unlike enzymes, the utilization of mineral oxides for clarify juices is practically not described in the literature. In addition to a wide range of works about clarification properties of bentonite clays [12,15], some attention is paid to zeolites [16] and sepiolites [17,18], and utilization of shungite for water treatment [19]. Membrane methods of clarification of fruit and vegetable juices using TiO_2 and Al_2O_3 are described [20,21]. However, this is not enough to assess the prospects of using oxides as clarificators. That is why these studies are a logical continuation of the previous ones [4] in order to evaluate the possibility of using mineral titanium oxides and silicon to clarify apple juice.

The aim was to investigate the prospect of using mineral clarifiers, as they have a number of significant advantages: they are relatively cheap, environmentally safe, easily removed from the finished product, they can be reused after proper cleaning.

Materials and methods

Materials

SiO_2 powder with highly developed surface area (AMD-2) and nanodispersed powders of both SiO_2 and TiO_2 (S_{BET} = 50 m^2/g) were selected as clarifiers. Nanodispersed SiO_2 – product which was obtained by flaming hydrolysis of $SiCl_4$ vapors in an air-aqueous mixture at a temperature of 700 to 1100 °C. The size of the particles is 10-20 nm, the specific surface area S_{BET} = 300 m^2/g. AMD-2 – high-disperse silicon dioxide modified by depolymerizate D-4, specific surface area S_{BET} = 280 m^2/g. For comparison, we used the classic bentonite clarifier, the formula of which is $Al_2[AlSi_3O_9{\times}(OH)](OH)_2{\times}nH_2O$ (S_{BET} = 160 m^2/g).

The juice used for laboratory testing was squeezed from "Glory to the Winners" apples of one crop, steeped for 12 hours at ~ 4 ° C and decanted from the precipitate. The final juice output was 60%.

Sample preparation

All samples were divided into two groups. In the first - the clarifier was added to the juice directly in the form of powder. In the second case, the clarifier was added to the juice in the form of a suspension. For suspensions obtaining, a portion of the powder was stirred in hot (~ 80 ° C) water and left for 12 hours at room temperature. Then it was mixed thoroughly and injected into the juice. The preparation of AMD suspension is not possible because of its high hydrophobicity.

Methods

The optical density was measured with Agilent Cary 60 spectrophotometr at wavelength λ = 400 nm, absorbing layer thickness 3,070 [22]. The comparison solution was water. The content of dry substances was evaluated refractometrically (Atago PAL-1 BLT Digital Brix Refractometer), pH value with device pH-150MI [23].

The titrated acidity (in terms of malic acid) was determined by titration of the sample with 0.1 N alkali solution [24].

Results and discussion

Influence of the clarifier mass and form on juice turbidity

The bentonite utilization for the clarification of juices at the industrial level is minimized now, but the applications of cytosan [25] in combination with ultrafiltration and nanofibrous membranes are widely described in the literature nanofibrous membranes[25,26].

There are several ways to use bentonite clays for juices clarifying. The first is the short-term thermostatation of the juices with a clay suspension at 60° C under the constant stirring conditions. Stirring and increasing of temperature intensify the lighting process [12,27].

The second way is the long staying of the mixture of juice with clarifier. It is believed that the most effective bentonite operates at concentrations of 400-500 g per 1 ton of juice at exposure time 12–24 hours. That is why we chose 0.1–0.5–2.5 g/l (or 0.01–0.05–0.25 g/100 ml of apple juice) for powders that have brought into the juice without pre-treatment and 0.5 g/l (0.05 mg/100 ml juice) when oxides were added as suspension form.

For indication of temperature influence on clarification result all investigation were carried out under the temperatures 4 °C and 20 °C. On the one hand, under the temperature increasing we can suspect the intensification of aggregation and coagulation processes. On the other hand, the juice may deteriorate for a day and become unusable for further processing.

In the first stage of research, the clarifiers were placed in apple juice, kept for 24 hours at a constant temperature, decanted from the precipitate. The optical density of the juices was then measured. The juices were then centrifuged for 5 minutes (1500 min^{-1}) and the optical density was again measured.

Figure 1 illustrates the dependence of the optical density of the juice on the weight of the clarifier (4 °C, before centrifugation). The diagram shows that the best result shows nanodispersed SiO_2 in the form of powder, and the effect is better, the greater the weight of the powder. The efficiency of the illuminators decreases in the row:

Powders *SiO_2> TiO_2> AMD> bentonite*

When we bringing clarifiers in juice in the form of a suspension, we see a similar pattern, but the efficiency of bentonite significantly increases:

Suspension *SiO_2> TiO_2> AMD> bentonite*

In view of the above at 4 °C, the efficiency of clarifiers decreases in the series:

SiO_2 powder & susp > TiO_2 powder & susp > bentonite susp> AMD > bentonite powder

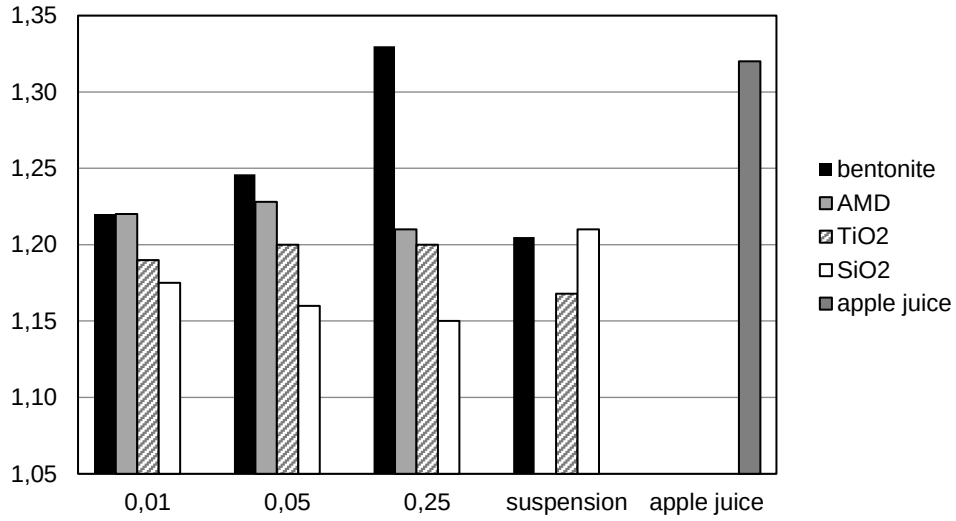

Figure 1. Dependence of the optical density of the juice on the weight of the clarifier (g/100 ml juice) compared to the apple juice without clarifier (4 °C, before centrifugation)

Figure 2 shows the dependence of the optical density of the clarified juices on the weight of the clarifier after centrifugation. It is obvious that centrifugation, as an additional stage of technological clarification of juices, results in a decreasing in their optical density compared to non-centrifuged samples. However, it should be noted that the decrease in optical density for the clarifiyed samples was negligible and did not affect the overall result.

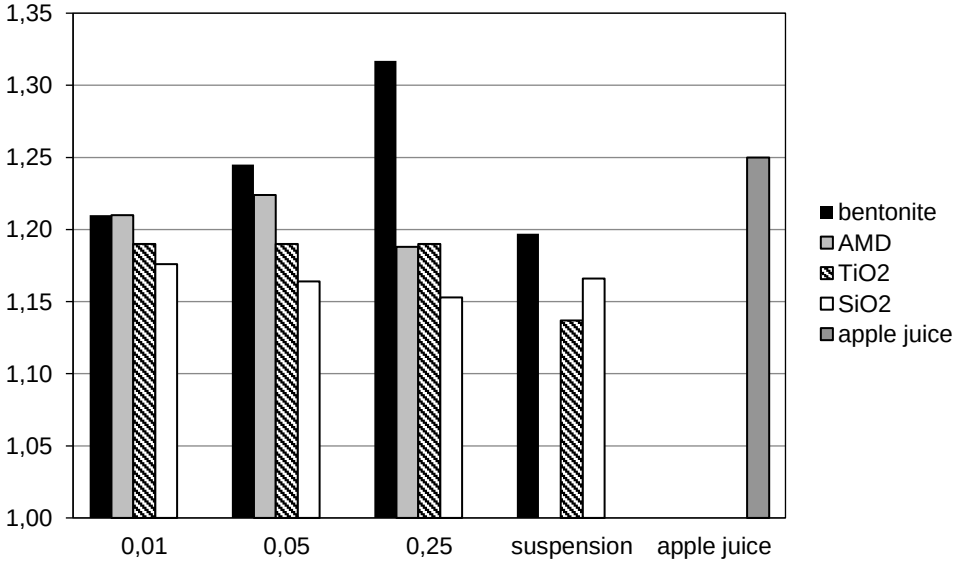

Figure 2. Dependence of the optical density of the juice on the weight of the clarifier (g/100 ml juice) compared to the apple juice without clarifier (4 °C, after centrifugation)

The same experiments were carried out with juices samples under the 20 °C (imitation of production workshop conditions). It is interesting to note that clarification process was not so effective as under higher temperature. The optical density values of all samples were higher than those obtained for lower temperatures (Figure 3).

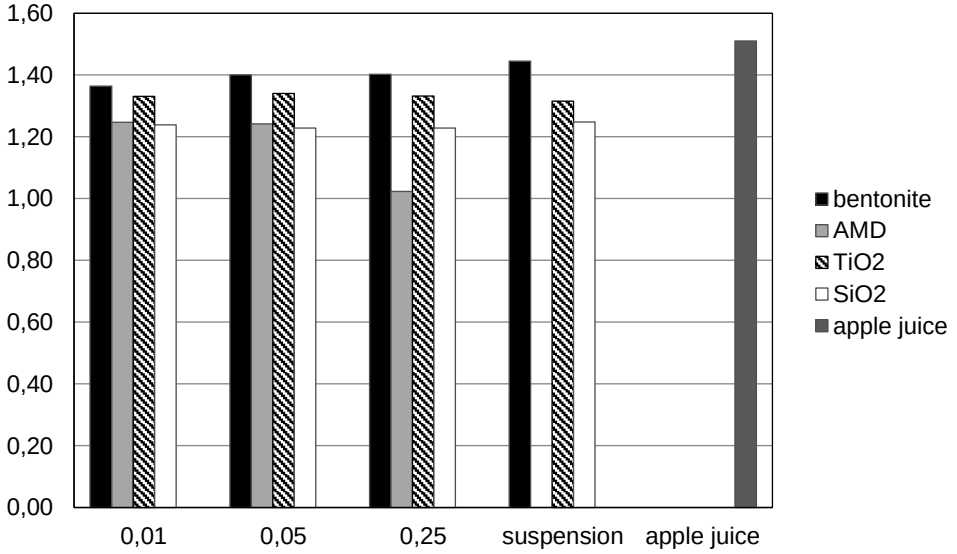

Figure 3. Dependence of the optical density of the juice on the weight of the clarifier (g/100 ml juice) compared to the apple juice without clarifier (20 °C, before centrifugation)

Figure 3 shows that, at 20 °C, there is no significant dependence of the optical density of juices on the clarifier mass, unlike the previous case. For bentonite only, the clarifying efficiency decreases slightly with the increasing of the powder mass.

Talking about the significant difference of values for using clarifiers in the form of powder or suspension is also meaningless. The result of their action is close. After centrifugation, the optical density of juices with and without clarifier additives slightly decreased (Figure 4).

Summarizing the results described above, we can conclude that at 20 ° C the most effective clarifier was hydrophobic AMD (0.25 g sample), the rest of the substances can be placed in a row accordingly to reducing their clarifying efficiency:

$$SiO_2 \text{ powder \& susp} > TiO_2 \text{ powder \& susp} > \text{bentonite powder \& susp}$$

Authors [28] show that for bentonites from different fields, efficiency is directly related to the surface area: the larger is the surface area than clarification process is more effective. On the one hand, difference in clarification ability of the samples may occur due to different adsorption capacity of the substances at different temperatures, on the other hand, titanium and silicon oxides can slow the fermentation processes in the juice.

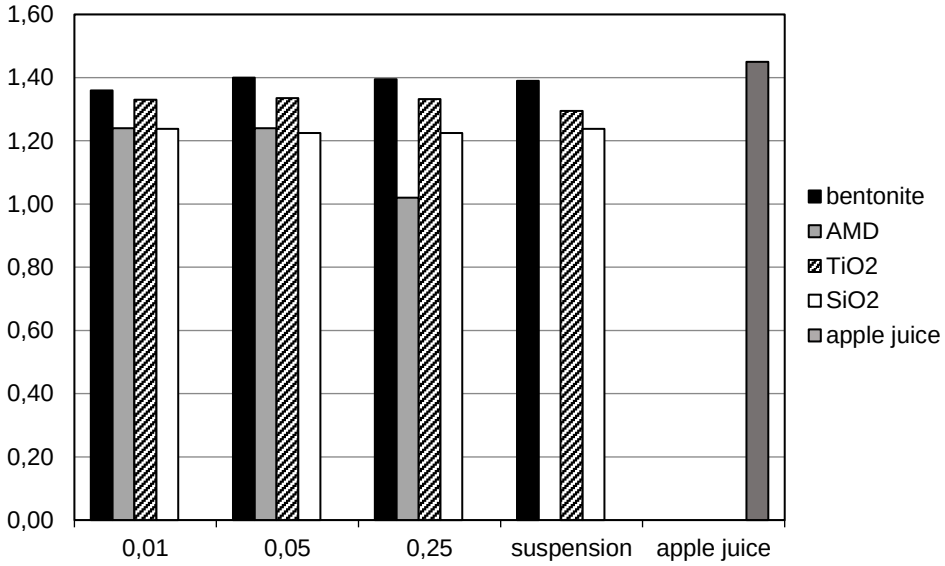

Figure 4. Dependence of the optical density of the juice on the weight of the clarifier (g/100 ml juice) compared to the apple juice without clarifier (20 °C, after centrifugation).

Evaluation of physico-chemical changes in juice-clarifier system with time

For evaluation of physico-chemical properties of (juice+clarifier) system through the time the measurements of optical density, general acidity (in terms of malic acid), pH value and dry substances content were carried out. For these series of experiments the clarifier was added in juice in powder form powder mass was 0.01 g/100 ml of juice).

Optical density

The question "how long does it take to keep the juice mixer together for optimal result" still remains open. It depends on type of juice, pH-value, temperature and clarifier nature. To determine the effect of time of steep, a series of apple juices with mineral clarifiers were prepared. The optical density was measured on the first, second and third days. For this purpose, the samples were decanted from the clarifier and centrifuged immediately before measurements.

Figure 5 shows the optical density clarified juices dependence on contact time juice–clarifier. From the above results it is concluded that clarification process was more successful for 4 °C than for 20 °C. In addition, temperatures of 15-25 °C are considered optimal for fermentation of apple raw materials [15]. Therefore, the experiment was carried out at 4 °C to slow the fermentation process.

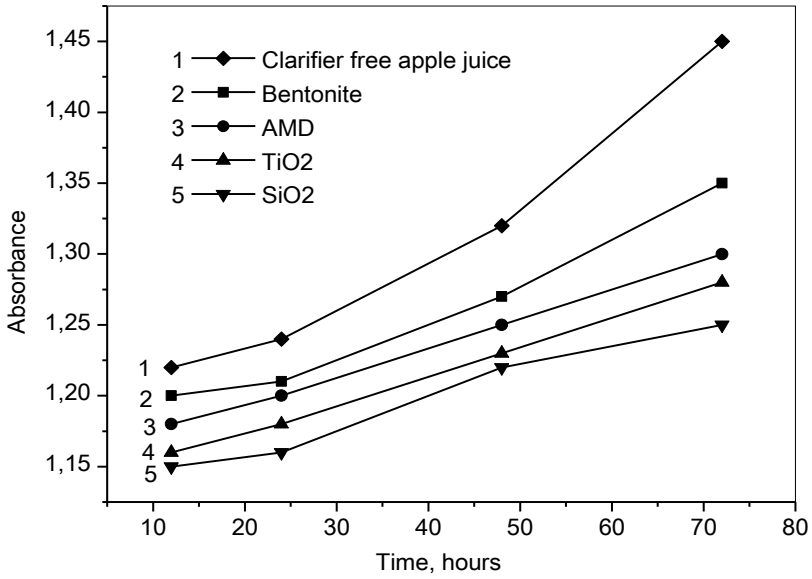

Figure 5. Dependence of optical density of clarified juices on time of standing with clarifier powder. For comparison, the curve 1 is apple juice without clarifiers addition that have undergone the sa me processing stages

From the presented results we can conclude that it is not necessary to storage the juices with the clarifiers for a long time. Although, the results are described by the authors [12] indicate that bentonite should be effective for apple juice clarification at high temperatures (75 ºC) and preserving mixture up to three days. Such effect they explained by the intensification of coagulation processes in juice–clarifier system. At the same time authors authors [29] authors announce that there are three main factors for reaching of optimal condition for fruit juice clarification with bentonite and gelatin: temperature (30–70 ºC), pH (4-6) and short time of contact (40-120 min).

Acidity, pH value and dry substances content

The process of clarification essentially depends on pH value of juice. So, for potato juice it was shown that maximum adsorption of the acid-soluble fraction occurs at pH 5.0. The working conditions recommended for obtaining a protein-free potato juice is acidification to pH 4.5. [30]. For clarification of fruit juices with bentonite–gelatin mixture pH=4–6 was recommended [29].

In our case the pH value correction was not necessary for our samples. Values of pH and general acidity of juices after clarification were almost indistinguishable from the values obtained for pure juice and amounted to 4.00 ± 0.04 and 0.40±0.05 %, respectively. The content of dry substances after clarification was slightly less than for pure juice (Table 1).

Physical-chemical properties of juices after clarification did not change essentially after five days steeping. Values were fixed at 1, 2, 3 and 5 days. Only apple juice without any additions shows a slight increasing of all parameters which could be caused with the flow of

fermentation processes. Similar effects were observed by the authors [14,31] for using bentonite for grape wines clarification.

Table 1

Average values of physicochemical parameters of apple juice with and without clarifiers (4 ºC)

Clarifier	Brix, %	Generat acidity, %	pH
	Days 1, 2, 3 and 5		
Bentonite	12.4±0.1	0.40±0.05	3.99±0.04
AMD	12.3±0.1	0.40±0.05	4.00±0.04
TiO_2	12.2±0.1	0.40±0.05	3.98±0.04
SiO_2	12.3±0.1	0.40±0.05	3.99±0.04
Juice without additions			
Days 1–3	(12.9-13.2) ±0.1	(0.40–0.44) ±0.05	3.97-4.00±0.04
Day 5	13.4±0.1	0.46 ± 0.05	4.02±0.04

General acidity and pH value of oxides-free apple juice increasing slightly with steeping time. It is known that during the fermentation of fruit raw materials the concentration of acids in juice could increase. At the same time partially transformation of malic acid into lactic acid takes place. In addition, the fermentation process may be accompanied by the formation of succinic and other organic acids [32]. According to [33], the general acidity of the juices may slightly decrease in the process of fermentation, or increase slightly. Such changes are determined by the variety of apples and storage conditions. Similar regularities were described for properties of clarified apple juice in 4 weeks storage under 4 ºC [34].

The constancy of physical-chemical properties of juices while they steep with clarifiers indicates on partially or fully cessation of the fermentation processes. This effect may be related both to the observance of the low temperature regime and to the pronounced antibacterial and antifungal action of titanium oxides and silicon [35,36]. For these substances bacteria growth inhibition was observed under the dark condition. Our samples were stored in the refrigerator also under the dark condition.

Conclusions

1. Mineral nano-sized oxides of titanium (IV) and silicon (IV) should be successfully used for apple juice clarification. Of all the substances tested, the classic absorbent – bentonite clay shown the worst performance as a clarifier.
2. It was shown that clarification process was more efficient at low temperature (4 ºC) then at room temperature 20 ºC. By reducing the efficiency of clarification at low temperatures, the test substances can be arranged in the following order:

   SiO_2> TiO_2> AMD > bentonite (4 ºC)

   At 20°C the best clarification effect had *AMD* in concentration 2.5 g/l of juice. The other substances lose their clarification ability in row:

   SiO_2> TiO_2> bentonite (20 ºC)
3. It was confirmed that bentonite possessed much better clarification ability as a suspension form then in powder. On contrary, there is no significant difference for nano-sized SiO_2 and TiO_2. These oxides are equally effective both in suspension and in powder form.

According to our results, the optical density of juices after clarification grows with the time of steeping of mixture. That is why optimal clarification time at 4 ºC was 12 hours.

4. Addition of investigated oxides in apple juice leads to the retardation of fermentation processes in juice. It is interesting to note that clarification ability did not correlate with the antimicrobial activity which generally increased from TiO_2 to SiO_2 [36]. For these substances bacteria growth inhibition was observed under the dark condition. Our samples were stored in the refrigerator also under the dark condition.

References

1. Kilara A., Van Buren J. P. (1989), *Clarification of Apple Juice. Processed Apple Products*, Springer, New York, pp. 83–96.
2. Yamasaki M., Kato A., Chu S.-Y., Akima K. (1967), Pectic Enzymes in the Clarification of Apple Juice, *Agricultural and Biological Chemistry*, 31(5), pp. 552–560.
3. Genovese D.B., Elustondo M.P., Lozano J.E. (1997), Color and Cloud Stabilization in Cloudy Apple Juice by Steam Heating During Crushing, *Journal of Food Science*, 62, pp. 1171–1175.
4. McLellan M.R., Race E.J. (1995), Grape juice processing. In: Ashurst P.R. (eds) *Production and Packaging of Non-Carbonated Fruit Juices and Fruit Beverages*, Springer, Boston.
5. Ceci L., Lozano J. (1998), Determination of enzymatic activities of commercial pectinases for the clarification of apple juice, *Food Chemistry*, 61(1-2), pp. 237–241.
6. Sheu M., Wiley R., Schlimme D. (1987), Solute and Enzyme Recoveries in Apple Juice Clarification using Ultrafiltration, *Journal of Food Science*, 52, pp. 732–736.
7. Oliynyk S., Mel'nyk L., Samchenko I., Tkachuk N., Loginova O., Kisterska L. (2019), Influence of shungite treatment methods on its absorption properties and on water treatment quality for beverages production, *Ukrainian Food Journal*, 8(4), pp. 891–902.
8. Chatterjee S., Chatterjee S., Chatterjee B.P., Arun K. Guha (2004), Clarification of fruit juice with chitosan, *Process Biochemistry*, 39(12), pp 2229–2232.
9. Matko S.V., Mank V.V., Melnyk L.M., Zhestereva N.A (2004), Lighting apple juice with natural adsorbent – paligorskite, *Food and processing industry*, pp. 24–25.
10. Djordjević M., Šereš Z., Došenović T., Šoronja-Simović D., Maravić N., Kukić D., Nikolić I., Djordjević M. (2018), Sugar beet molasses purification by bentonite addition: Analysis of quality enhancement and treatment conditions, *LWT*, 93, pp. 142–149.
11. Melnyk L., Melnyk Z., Kryvorotko V. (2013), Methods of recovering schungite's adsorptive properties after processing red beet juice, *Ukrainian Journal of Food Science*, 1(2), pp. 223–227.
12. Koyuncu H., Kul A.R., Çalımlı A., Yıldız N., Ceylan H. (2007), Adsorption of dark compounds with bentonites in apple juice, *LWT - Food Science and Technology*, 40(3), pp. 489–497.
13. Olsen A. (1987), Low Technology Water Purification by Bentonite Clay and Moringa Oleifera Seed Flocculation as Performed in Sudanese Village: Effect on Schistosoma Mansori Cericariae, *Water Resources*, 21(5), 81–92.
14. Sachko A., Kobasa I., Moysyura O. (2017), Perspectives of utilization of nanodispesive materials based on TiO_2, SiO_2 and SiO_2-TiO_2 for wine fining, *Journal Food and Environment Safety of the Suceava University. Food Engineering*, XVI (4), pp. 216–221.

15. Jalali M., Jahed E., Haddad Khodaparast M.H., Limbo S., Mousavi Khaneghah A. (2014), Evolution of bentonite and gelatin effects on clarification of variety of date fruit Kaluteh juice with response surface methodology, *International Food Research Journal*, 21(5), pp. 1893–1899.
16. Woloshchuk A.G., Kobasa I.M., Bogdanyuk M.P., Petrova G.P. (2013), Natural mineral sorbents in food technology, *Scientific Bulletin of Chernivtsi University, Chemistry*, 658, pp. 141–149.
17. Mirzaaghaei M., Goli S.A.H., Fathi M. (2016), Application of sepiolite in clarification of pomegranate juice: changes on quality characteristics during process, *Int. J. Food Sci. Technol.*, 51, pp. 1666–1673.
18. Mirzaaghaei M., Sayed Amir, Hossein Goli, Milad Fathi (2017), Clarification of apple juice using activated sepiolite as a new fining clay, *Clay Minerals*, 52 (4), pp. 497–508.
19. Melnyk L., Turchun O., Tkachuk N., Kutz A., Melnyk Z. (2014), Water-alcohol adsorbing cleaning out of higher alcohols by shungite, *Ukrainian Journal of Food Science*, 2(2), pp. 312–317.
20. Nasabi M., Labbafi M., Khanmohammadi M. (2017), Optimizing nano TiO_2 assisted decoloration process for industrial date syrup utilizing response surface methodology, *J Food Process Eng.*, 40(5), pp.1–9.
21. Severcan S.S., Uzal N., Kahraman K. (2020), Clarification of pomegranate juice using PSF microfiltration membranes fabricated with nano TiO_2 and Al_2O_3, *J Food Process Preserv*, pp. 1–14.
22. Joslyn Maynard (2014), *Methods in Food Analysis: Applied to Plant Products*, Saint Louis. Elsevier Science.
23. Sadler G.D., Murphy P.A. (2010), *pH and Titratable Acidity. Food Analysis*. Springer, Boston.
24. Ashurst P.R. (2008), *The chemistry and technology of soft drinks and fruit juices*, John Wiley & Sons.
25. Veleirinho B., Lopes-da-Silva J.A. (2009), Application of electrospun poly(ethylene terephthalate) nanofiber mat to apple juice clarification, *Process Biochemistry* , 44(3), pp. 353-356.
26. Jahed E., Khodaparast M. H. H., Mousavi Khaneghah A. (2014), Bentonite, temperature and pH effects on purification indexes of raw sugar beet juice to production of inverted liquid sugar, *Applied Clay Science*, 102, pp. 155–163.
27. Erdogăn B., Demirci Ş., & Akay Y. (1996), Treatment of sugar beet juice with bentonite, sepiolite, diatomite and quartamin to remove color and turbidity, *Applied Clay Science*, 11(1), pp. 55–67.
28. Bilbao A., Irastorza A., Duenas M., Fernandez K. (1997), The effect of temperature on the growth of strains of Kloeckera apiculata and Saccharomyces cerevisiae in apple juice fermentation, *Letters in Applied Microbiology*, 24(1), pp. 37–39.
29. Lindner P., Ben-Gera I., Keren R. (1981), Precipitation of proteins from potato juice with bentonite, *Journal of the Science of Food and Agriculture*, 32(12), pp. 1177–1182.
30. Vinogradov V.A., Zagoruyko V.A., Kulev S.V. (2013), Research of the technological process of complex stabilization of wine materials against colloidal and crystalline opacities, *Viticulture and winemaking*, 43, pp. 83–88.
31. Herrero M., Cuesta I., García L. A., Díaz M. (1999), Changes in Organic Acids During Malolactic Fermentation at Different Temperatures in Yeast-Fermented Apple Juice, *Journal of the Institute of Brewing*, 105(3), pp. 191–196.

32. Tokar A. Yu. (2015), Changing the content of organic acids during fermentation of fruit worts, *Bulletin of the Uman NUS*, 2, pp.39-43.
33. Kobasa I., Vorobets M., Arsenieva L. (2016), Nanosides titanium dioxide as an antibacterial admicxture for the food packaging materials, *Journal Food and Environment Safety of the Suceava University, Food Engineering,* XV(4), pp. 306–311.
34. Cai M., Xie C., Lv Y., Yang K., Sun P. (2020), Changes in physicochemical profiles and quality of apple juice treated by ultrafiltration and during its storage, *Food Sci Nutr*., 8, pp. 2913– 2919.
35. Adams L. K., Lyon D. Y., Alvarez P. J. J. (2006), Comparative eco-toxicity of nanoscale TiO_2, SiO_2, and ZnO water suspensions, *Water Research*, 40(19), pp. 3527–3532.
36. Mu H., Chen Y., Xiao N. (2011), Effects of metal oxide nanoparticles (TiO_2, Al_2O_3, SiO_2 and ZnO) on waste activated sludge anaerobic digestion, *Bioresource Technology*, 102(22), pp. 10305–10311.

Effect of canola oil and natural antioxidant of basil on chemical and sensory properties of fresh cheese

Mihaela Ivanova[1], Olga Teneva[2], Mariya Dushkova[1], Radka Vlaseva[1], Albena Stoyanova[1]

1 – University of Food Technologies, Plovdiv, Bulgaria
2 – Plovdiv university "Paisii Hiledarski", Plovdiv, Bulgaria

Keywords:

Antioxidant
Canola
Oil
Cheese
Milk fat
Polyunsaturated fatty acid

Article history:

Received 23.08.2019
Received in revised form 16.12.2019
Accepted 30.06.2020

Corresponding author:

Mihaela Ivanova
E-mail: mihaela_18bg@abv.bg

DOI: 10.24263/2304-974X-2020-9-2-9

Abstract

Introduction. This research aims at determining the effect of canola oil and natural antioxidant of basil on chemical and sensory properties of fresh cheese.

Materials and methods. A fresh spreadable cheese was prepared by the use of fresh whole milk, canola oil and natural antioxidant of basil. The prepared cheese was analysed on fatty acid profile according to GC method of methyl esters, tocopherol content – according to HPLC method, phytosterol content – according to GC method, health lipid indices – according to empirical calculations complying with the fatty acid profile of the product, sensory evaluation – according to 10-points hedonic scale.

Results and discussion. Canola oil was characterized by a high content of unsaturated fatty acid content above 93 g.100 g^{-1} of the total content and a very good ratio of omega-6/omega-3 – 2/1. The total content of tocopherols in the lipid fraction was comparatively high – 315 mg.kg^{-1}. Canola oil contained significant amount of phytosterols – 0.7 g.100 g^{-1} with individual sterol composition – β-sitosterol (54.7 %) and campesterol (35.3 %) predominated in the sterol fraction.

The cheese with partial replacement of milk fat by canola oil was characterized by a reduced content of saturated fatty acids which have negative effects on the human health – 35.18 g.100 g^{-1} compared to 68.33 g.100 g^{-1} in cheese produced by classical technology containing only milk fat. The product contained a large part of the short-chain fatty acids, typical for milk fat that defines the functionality of the end product. The cheese with added canola oil presented a higher biological value due to atherogenic index of 0.42 compared to 1.60 for cheese produced only of milk fat, thrombogenic index of 0.59 compared to 3.13 for cheese produced only of milk fat and preventive lipid score of 34.89 compared to128.23 for cheese produced only of milk fat.

The fresh cheese with partial replacement of milk fat by canola oil had good sensory properties.

Conclusions. Fresh spreadable cheese with partial replacement of milk fat by canola oil in the ratio (1:1) was characterized by increased healthy characteristics – low levels of atherogenic and prothrombogenic index and preventive lipid score.

Introduction

Vegetable oils were used to enhance fatty acids profile of dairy products [1-4]. Enriching the dairy products with omega fatty acids was made mostly by the inclusion of oil seed and vegetable oil in dairy animal diets [5, 6]. Another possibility was to replace partially or fully the milk fat in dairy products by oils rich in polyunsaturated fatty acids [7, 8]. According to our knowledge, there are insufficient investigations about the enrichment of high fat dairy products with vegetable oils.

Canola oil, in comparison with other vegetable oils, is characterized by the lowest content of saturated fatty acids (less than 10 g.100 g^{-1}), followed by the walnut and flaxseed oil. It is an excellent source of mono- and polyunsaturated fatty acids, wherein the ratio of omega-6/omega-3 is closest to the optimum [9]. Besides valuable fatty acid composition, canola oil is [10, 11]. The current trend for the production of health foods requires on the market the production of canola oil with low content of erucic acid, which is associated with certain diseases of the human [12]. This makes reasonable the addition of canola oil in dairy products.

It is appropriate to supplement natural antioxidant when an addition of vegetable oils is used [13]. Sensory profile and valuable antioxidant properties of basil extract, due to contained aromatic components, are appropriate in combination with canola oil in order to reduce oxidation processes in the oil [14, 15].

The purpose of this work was to investigate the effect of canola oil and natural basil extract on chemical and sensory properties of fresh spreadable cheese.

Materials and methods

Raw materials

Commercially available canola oil (Buldara Ltd., Bulgaria) and fresh natural cream (supplied by United Milk Company AD, Bulgaria) were used.

For the preparation of the emulsions raw cow's milk complying with the requirements of Regulation 853, 2004 from the EU and raw skimmed cow's milk (supplied by United Milk Company AD, Bulgaria) obtained on the day of its adoption were used as dispersible medium.

Other material

Emulsifier – glyceryl monostearate in amount of 0.1 g cm^{-3}, according to data [16] (Cognis with trademark Cutina®, Germany), antioxidant – extract from basil ("Extractum" Ltd., Bulgaria) in the amount of 0.003 cm^3.100 cm^{-3} with the major components in the chemical composition linalool 10,64 g.100 g^{-1}, estragole 46.97 g.100 g^{-1}, methyl eugenol 8.94 g.100 g^{-1}, β-bisabolene 3.06 g.100 g^{-1} [17], characterized by sensory profile, suitable for combination with canola oil.

Starter culture with the following composition: *Lactococcus lactis* subsp. *lactis*, *Lactococcus lactis* subsp. *cremoris*, *Streptococcus thermophilus*, in the amount of 3 cm^3.100 cm^{-3} ("Lactina" Ltd., Bulgaria).

Rennet – pure chymosin with activity 1:15 000, in the amount of 5 cm^3.100 dm^{-3} (Biokom Trendafilov with trademark Daniren®).

Oils and cream were stored at 4-6 °C (Regulation No. 2 of 2017).

Methods

Fatty acid composition and total lipid content analyses. The preparation of methyl esters of fatty acids was in accordance with ISO 5509, 2001. The analysis of methyl esters of the fatty acids was carried out by gas chromatography in accordance with ISO 5508:2000. Fatty acid composition of the obtained cheese was determined after extraction of fat by the method of Schmidt-Bonzynsky-Ratzaloff in accordance with ISO 1735|IDF 5:2004.

Sterols analysis. Unsaponifiables were determined by weight after saponification of the lipid fraction and extraction with hexane in accordance with ISO 18609:2000. Identification was confirmed by comparison of retention times with those of a standard mixture of sterols in accordance with ISO 12228:2014.

Tocopherols analysis. Tocopherols were determined directly in the oil by high performance liquid chromatography (HPLC) by Merck-Hitachi (Merck, Darmstadt, Germany) and the tocopherol content was calculated on the base of tocopherol peak areas in the sample vs. tocopherol peak area of the standard tocopherol solution in accordance with ISO 9936:2016.

Emulsion preparation. It was performed by mixing of the two phases – vegetable oil, cream, milk and emulsifier, stirred with a mixer (Polytron® PT45-80) at speed – 150 s^{-1} during 5 min. The concentrations used were: for emulsifier 0.1 g.100 cm^{-3}, for oil phase 4 cm^3.100 cm^{-3} canola oil with 4 cm^3.100 cm^{-3} cream (1:1). The mixtures were heated to 55-60 °C in order to complete dissolution of the emulsifier [18].

Fresh cheese preparation with addition of vegetable oil. A flowchart for the production of fresh spreadable cheese and addition of vegetable oil was applied [19]. Qualification of milk → Standardization of milk fat to 8 cm^3.100 cm^{-3} → (4 cm^3.100 cm^{-3} canola oil + 4 cm^3.100 cm^{-3} milk fat) and addition of antioxidant 0.003 cm^3.100 cm^{-3} → Heat treatment of milk and addition of emulsifier t = 55-60 °C and glyceryl monostearate (0.1 g.100 cm^{-3}) → Obtaining of emulsion → Pasteurization (88 °C, duration 5 min) → Cooling (25 ºC) → Inoculation (3 cm^3.100 cm^{-3} starter culture) → Pre-biological ripening (an increase in titratable acidity of 0.018 – 0.027 represented as percentage of lactic acid) → Addition of rennet (5 cm^3.100 dm^{-3}) → Coagulation (14-16 h) → Cutting of the gel and curd retention in the whey for 30 min at a temperature of 20-25 °C → Drainage and self-pressing to dry matter approximately 30 g.100g^{-1} → At a temperature of 20-22 °C for 1-2 h → At a temperature of 4-6 °C overnight → Dry salting NaCl (0.5 g.100 g^{-1}) → Homogenization of the curd → Packaging and cooling.

The data for the chemical composition and biological value of cheese produced only with milk fat were taken from our previous study [19].

Health lipid indices. Qualitative indicators of fat atherogenic index (AI) [20]; Preventive lipid score (PLS) [21]; Thrombogenic index (TI) [22].

Sensory analysis. The sensory evaluation of the fresh cheeses was conducted in accordance with the Bulgarian State Standard 15612-83 and ISO 6654:1991. The evaluation criteria were as follows: taste and flavour – 35 points, structure – 25 points, consistence – 20 points, appearance – 10 points, and colour – 10 points (maximum overall score – 100 points). The results were equated to a 10 point evaluation scale in order to be presented in a spider diagram.

Statistical analysis. The Significance of the differences between the average values was evaluated by Least Significant Difference (LSD) test considering $p < 0.05$ as significant [23]. Multiple comparisons were made by LSD method [24]. The results were presented as mean value ± standard deviation (SD) [25].

Results and discussion

Canola oil analyses

The results of performed investigations about the fatty acid composition of canola oil are presented in Table 1.

Table 1

Fatty acid composition of canola oil

Fatty acid		g.100 g^{-1} of total fatty acids
Lauric acid	C12:0	0.06±0.01[a]
Miristic acid	C14:0	ND
Palmitic acid	C16:0	5.07±0.05[b]
Palmitoleic acid	C 16:1	0.28±0.05[c]
Margaric acid	C17:0	0.06±0.01[a]
Stearic acid	C18:0	0.70±0.06[d]
Oleic acid	C18:1	62.39±1.15[e]
Linoleic acid	C18:2	20.06±1.00[f]
α-linolenic acid	C18:3	9.48±0.85[g]
Arachidonic acid	C20:0	0.55±0.15[h]
Eicosenoic acid	C20:1	1.08±0.28[i]
Behenic acid	C22:0	0.27±0.09[j]
Erucic acid	C22:1	ND

[a-j] Means in the same column with different letters show significant differences ($p < 0.05$);
[*] Values are expressed as mean ± Standard deviation (n=3); ND: not detected

The data showed that 13 fatty acids were identified which presented 99.97 g.100 g^{-1} of total fatty acids. The oleic 62.39 g.100 g^{-1} of total fatty acids and linoleic 20.06 g.100 g^{-1} of total fatty acids were prevailing.

Figure 1 presents the fatty acids distribution in canola oil.

The results showed that the canola oil was characterized by a high content of unsaturated fatty acid content above 93 g.100 g^{-1} of the total content and a very good ratio of omega-6/omega-3 – 2/1. The data on fatty acid composition were similar to those obtained by other research teams, for varieties with low erucic acid (C22:1), which emphasizes its healthfulness [12]. Essential fatty acids (C18:2 and C18:3) laid in high amounts on the total content of unsaturated fatty acid content above 30 g.100 g^{-1}. These indicators determined the health characteristics of canola oil and defined it as a vegetable oil with high quality fatty acid profile.

The data showed that canola oil had a very low content of saturated fatty acids, and this indicator was superior to other vegetable oils such as walnut, flaxseed, etc. [26, 27]. The high amount of mono unsaturated fatty acids was similar to that of olive oil and helps the right functioning of various physiological systems in the human body. The amount of omega-3 fatty acids (C18:3), was increased in comparison to other vegetable oils – olive, corn, sunflower and others [19].

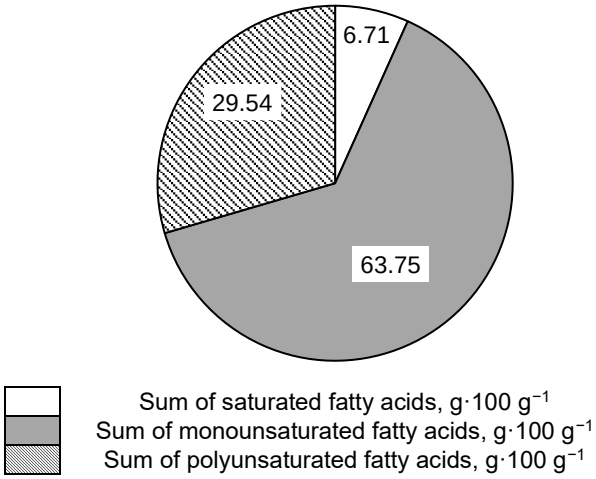

Figure 1. Distribution of the fatty acid groups in canola oil

The tendency of oils to oxidation was determined by the content of polyunsaturated fatty acids. Vegetable oils contained different amounts of natural antioxidants – tocopherols (α, β, γ, δ), which limited the oxidation processes. An important indicator of the healthy nature of canola oil was phytosterol content (brassicasterol, campesterol, β-sitosterol, Δ5-avenasterol, Δ7-avenasterol) [28]. Therefore, the content of tocopherols and phytosterols in canola oil was investigated. The data obtained are presented in Table 2. The data showed that canola oil was characterized by a high content of α and γ-tocopherols, an important indicator of the antioxidant properties of the vegetable oils [29].

The results showed that canola oil was characterized by a high content of phytosterols, which, according to several studies lower the cholesterol and the level of LDL cholesterol in the blood [30]. The total content in the oil was found to be 0.7 g.100 g^{-1}. The individual sterol composition is presented in Table 2. β-Sitosterol (54.7 g.100 g^{-1}) and campesterol (35.3 g.100 g^{-1}) predominated in the sterol fraction.

Tocopherols are a class of organic chemical compounds, many of them have vitamin E activity. The total content of tocopherols in the lipid fraction was comparatively higher – 315 mg.kg^{-1}. The tocopherol composition is presented in Table 2. The γ-tocopherol predominated in the oil, followed by α-tocopherol. The oil with higher content of α and γ-tocopherol proved superior to a number of common food oils [28].

Table 2

Tocopherol and phytosterol content in canola oil

	Total, mg kg^{-1}	**Tocopherols content, % of tocopherol content**				
		α	β	γ	γ-3	δ
Canola oil	315±10	43.5±0.5[a]	1.2 ±0.1[b]	53.6±0.4[c]	1.1±0.1[d]	0.6±0.1[e]
	Total, g 100 g^{-1}	**Phytosterols content, % of phytosterol content**				
		Brassicasterol	Campesterol	β-sitosterol	Δ5 avenasterol	Δ7 avenasterol
	0.7±0.0	9.6±0.2[a]	35.3±0.5[b]	54.7±0.5[c]	0.2±0.1[d]	0.1±0.0[e]

[a-e] Means in the same row with different letters show significant differences ($p < 0.05$);[*] Values are expressed as mean ± Standard deviation (n=3)

Fresh cheese analyses

An important characteristic of the end product is its biological and functional value. Healthiness of cheese with canola oil was determined on the basis of the content of fatty acids and indicators characterizing the wholesomeness of fats, presented in Table 3 and Table 4.

The data showed that the cheese with partial replacement of milk fat by canola oil was characterized by a reduced content of saturated fatty acids which have negative effects on human health – 35.02 g.100 g^{-1} compared to 68.33 g.100 g^{-1} in cheese by classical technology containing only milk fat [19].

The product contained a large part of the short-chain fatty acids, typical for milk fat that defines the functionality of the end product [31, 32].

Figure 2 presents the fatty acids distribution in in cheese with canola oil.

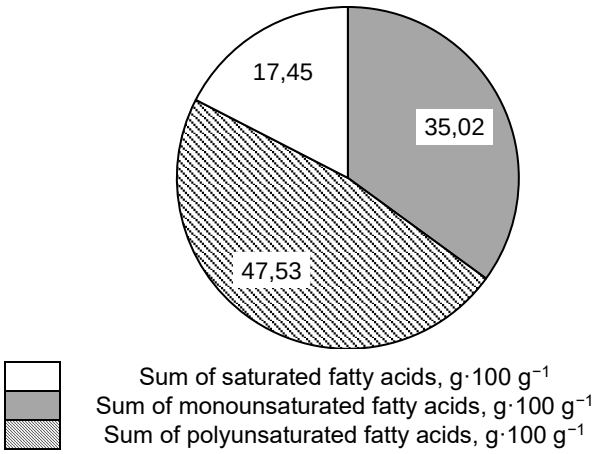

Figure 2. Distribution of the fatty acid groups in cheese with canola oil

The cheese with partial replacement of milk fat by canola oil was characterized by an increased content of unsaturated fatty acids in comparison to cheese, which contains only milk fat [19]. Increased wholesomeness of the end product was determined by the content of oleic acid (C18:1), linolenic acid (C18:3) and linoleic acid (C18:2). Our results were comparable with the reported fatty acid composition studies of dairy products enriched with canola oil [6].

Table 4 presents the evaluation of the biological value of the cheese determined by qualitative indicators of fat values - atherogenic index 0.42 compared to 1.60 for cheese produced only with milk fat, thrombogenic index 0.59 compared to 3.13 for cheese produced only with milk fat and preventive lipid score 34.89 compared to 128.23 for cheese produced only with milk fat [19]. These indicators in the control sample were three to four times higher compared to the cheese with canola oil, which shows higher biological value of the product with vegetable oil. It represents a healthier version of traditional fresh spreadable cheese produced only of milk fat. A similar tendency was observed by other authors [33–35].

Table 3

Fatty acid composition of cheese with canola oil

Fatty acid		g 100.g^{-1} of total fatty acids
Caproic acid	C6:0	0.09 ± 0.00^{a}
Caprilic acid	C8:0	0.96±0.10^{b}
Capric acid	C10:0	1.67±0.15^{c}
Lauric acid	C12:0	5.70±0.85^{d}
Miristic acid	C14:0	0.64±0.15^{e}
Palmitic acid	C16:0	19.18±1.12^{f}
Palmitoleic acid	C16:1	1.16±0.15^{g}
Margaric acid	C17:0	0.37±0.09^{h}
Margarinoleic acid	C17:1	0.20±0.05^{i}
Stearic acid	C18:0	6.41±0.95^{j}
Oleic acid	C18:1	46.17±2.14^{k}
Linoleic acid	C18:2	12.77±1.00^{l}
α-linolenic acid	C18:3	4.68±0.88^{m}

$^{a-m}$ *Means in the same row with different letters show significant differences ($p < 0.05$);*

**Values are expressed as mean ± Standard deviation (n=3)*

Table 4

Health lipid indices of cheese with canola oil

Health lipid indices	g.100 g^{-1} of total fatty acids*
Atherogenic index	0.42
Trombogenic index	0.59
Preventive lipid score	34.89
Total cheese lipid content	20.70

**Values are expressed on the basis of mean fatty acid content*

An important characteristic of the end product is its sensory profile. Figure 3 presents the sensory characteristics of fresh cheese with partial replacement of milk fat by canola oil and antioxidant of basil extract. The sensory profile showed that fresh cheese with partial replacement of milk fat by canola oil had good sensory characteristics. Some variation in colour was established due to the specific sensory profile of canola oil. The values for the indicators of taste and aroma remained relatively high, indicating that canola oil can be successfully used for the partial replacement of milk fat. The overall assessment of sensory indicators was 47.5 of maximum 50 points. Our results complied with the results obtained by other authors [36, 37].

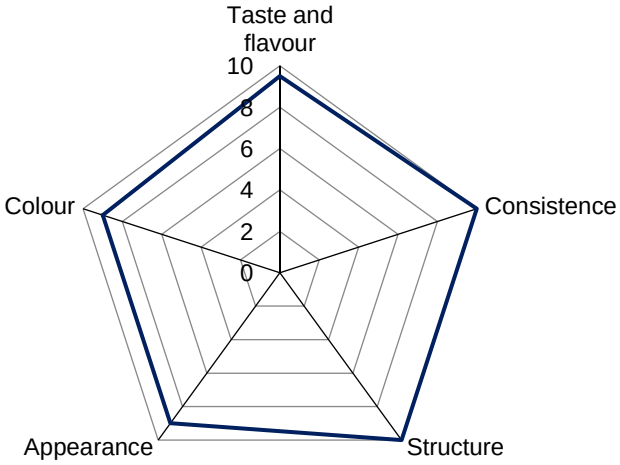

Figure 3. Sensory profile of the cheese enriched with canola oil

Conclusions

The fresh cheese with partial replacement of milk fat by canola oil and the addition of natural antioxidant of basil extract was characterized by improved fatty acid profile, and a significant higher content of essential polyunsaturated fatty acids.

The cheese with partial replacement of milk fat by canola oil was a very good source of tocopherols and phytosterols, which increased its healthy characteristics.

Qualitative indicators of fat – atherogenic and thrombogenic index and preventive lipid score defined the product as a healthy version of the classic fresh high fat spreadable cheese containing only milk fat and reduces the risk of various diseases associated with the consumption of animal fats.

References

1. Ardabilchi Marand M., Amjadi S., Ardabilchi Marand M., Roufegarinejad L., Jafari S.M (2020), Fortification of yogurt with flaxseed powder and evaluation of its fatty acid profile, physicochemical, antioxidant, and sensory properties, *Powder Technology*, 359, pp. 76–84.
2. Bakry A.M., Chen Y., Liang L. (2019), Developing mint yogurt enriched with omega-3 oil: Physicochemical, microbiological, rheological, and sensorial characteristics, *Journal of Food Processing and Preservation*, 43(12), pp. 14287.
3. Goyal A., Sharma V., Sihag M.K., Singh A.K., Arora S., Sabikhi L. (2016), Fortification of dahi (Indian yoghurt) with omega-3 fatty acids using microencapsulated flaxseed oil microcapsules, *Journal of Food Science and Technology*, 53(5), pp. 2422–2433.

4. Ganesan B., Brothersen C., McMahon D.J. (2014), Fortification of Foods with Omega-3 Polyunsaturated Fatty Acids, *Critical Reviews in Food Science and Nutrition*, 54 (1), pp. 98–114.
5. Goiri I. Zubiria I., Benhissi H., Atxaerandio R., Ruiz R., Mandaluniz N., Garcia-Rodriguez A (2019), Use of cold–pressed sunflower cake in the concentrate as a low-input local strategy to modify the milk fatty acid profile of dairy cows, *Animals*, 9(10), pp. 803.
6. Nguyen Q.V., Malau-Aduli B.S., Cavalieri J., Malau-Aduli A.E.O., Nichols P.D. (2019), Enhancing omega-3 long-chain polyunsaturated fatty acid content of dairy-derived foods for human consumption, *Nutrients*, 11(4), pp. 743.
7. Dal Bello B., Torri L., Piochi M., Bertolino M., Zeppa G. (2017), Fresh cheese as a vehicle for polyunsaturated fatty acids integration: effect on physico-chemical, microbiological and sensory characteristics, *International Journal of Food Sciences and Nutrition*, 68(7), pp. 800–810.
8. Soliman T.N., Farrag A.F., Zahran H.A.-H., El–Salam M.E.-H.A. (2019), Preparation and properties nano-encapsulated wheat germ oil and its use in the manufacture of functional labneh cheese, *Pakistan Journal of Biological Sciences*, 22(7), pp. 318–326.
9. Daun J. K., Michael Eskin N.A., Hickling D. (2011), *Canola: Chemistry, Production, Processing, and Utilization*, Elsevier Science, pp. 432.
10. Ghazani S.M., Marangoni A.G. (2016), *Nutrition and food grains in Encyclopedia of Food Grains*, Academic Press.
11. Savva C., Kafatos A. (2016), *Encyclopedia of Food and Health*, Academic Press.
12. Lin L., Allemekinders H., Dansby A., Campbell L., Durance–Tod S., Berger A., Jones P. (2013), Evidence of health benefits of canola oil, *Nutrition Review*, 71(6), pp. 370–385.
13. Taghvaei M., Jafari C. M. (2015), Application and stability of natural antioxidants in edible oils in order to substitute synthetic additives, *Journal of Food Science and Technology*, 52(3), pp. 1272–1282.
14. Juliani H., Simon J. (2002), Antioxidant Activity of Basil. Trends in new crops and new uses, J. Janick and A. Whipkey, ASHS Press, Alexandria, VA.
15. El–Sayed S. M., Youssef A. M. (2019), Potential application of herbs and spices and their effects in functional dairy products, *Heliyon*, 5(6), pp. 01989.
16. Hasenhuettl G., Hartel R. (2008), Food emulsifiers and their applications, Springer, Berlin.
17. Nenov N., Girova V., Iliev I., Stoilova I., Stoyanova A. (2014), Low temperature extraction of essential oil bearing plants by liquefied cases. 20. Basil (*Ocimum basilicum* L.), *Proceedings of International scientific conference Voronej*, 140.
18. Vlaseva R., Ivanova M., Petkova N., Denev P., Stoyanova A., Schreiner, M. (2014), Obtaining stable food emulsions between milk and corn oil, *Bulgarian Journal of Agricultural Science*, 20(5), pp. 1085–1089.
19. Ivanova M. (2016), Obtention de fromage à la composition régulée de la matière grasse, Saarbrucken, Germany: Editions universitaires européennes, (Chapter 3.3.2) (Fr).
20. Ulbritch T., Southgate D. (1991), Coronary heart disease: seven dietary factors, *Lancet*, 338, pp. 985–992.
21. Richard J., Charbonnier A. (1994), Description d'un score lipidique des aliments, *Cahiers de nutrition et de diététique*, 4, pp. 234–240.
22. Senso L., Suarez M., Ruiz–Cara T., Garcia–Gallego M. (2007), On the possible effects of harvesting season and chilled storage on the fatty acid profile of the fillet of farmed gilthead sea bream (*Sparus aurata*), *Food Chemistry*, 101(1), pp. 298–307.
23. Dilchva M., Kinova V. (2008), *Modeling and optimization of technological processes*, UFT, Plovdiv, pp. 14–28.
24. Donchev D., Dilcheva M, Kinova V. (2002), *A Practical Guide to Statistical Data Analysis*, ABT Spectrum, Plovdiv, pp. 110–118.

25. Petrova N., (2002), *Theory of probability and statistics*, HIFFI Academic Publishing House, Plovdiv, pp. 86–97.
26. Jahanban–Esfahlan A., Ostadrahimi A., Tabibiazar M., Amarowicz R. (2019), A Comprehensive Review on the Chemical Constituents and Functional Uses of Walnut (Juglans spp.) Husk, *International Journal of Molecular Science*, 20(16), pp. 3920.
27. Goyal A., Sharma V., Upadhyay N., Gill S., Sihag M. (2014), Flax and flaxseed oil: an ancient medicine & modern functional food, *Journal of Food Science and Technology*, 51(9), pp. 1633–1653.
28. Popov A., Ilinov P. (1986), Chemistry of lipids. Nauka i Iskustvo, Sofia (Bg).
29. Schwartz H., Ollilainen V., Piironen V., Lampi A. (2008), Tocopherol, tocotrienol and plant sterol contents of vegetable oils and industrial fats, *Journal of Food Composition and Analysis*, 21(2), pp. 152–161.
30. Lecerf J., Bard J., Girardet J, Fumeron F., Paillard F., Vergès B. (2014), Phytostérols, phytostanols, et risque cardiovasculaire, *Médecine des Maladies Métaboliques*, 8(5), pp. 483–488.
31. Besten G.D., Eunen K.V., Groen A.K., Venema K., Reijngoud D.J., Bakker B.M. (2013), The role of short-chain fatty acids in the interplay between diet, gut microbiota, and host energy metabolism, *Journal of Lipid Research*, 54(9), pp. 2325–2340.
32. Niccolai E., Baldi S., Ricci F., Russo E., Nannini G., Menicatti M., Poli G., Taddei A., Bartolucci G., Calabrò A.S., Stingo F.C., Amedei A. (2019), Evaluation and comparison of short chain fatty acids composition in gut diseases, *World Journal of Gastroenterology*, 25(36), pp. 5543–5558.
33. Xu J., Zhou X., Deng Q., Huang Q., Yang J., Huang F. (2011), Rapeseed oil fortified with micronutrients reduces atherosclerosis risk factors in rats fed a high–fat diet, *Lipids in Health and Disease*, 10, pp. 96.
34. Abdelhamid A.S., Martin N., Bridges C., Brainard J.S., Wang X., Brown T.J., Hanson S., Jimoh O.F., Ajabnoor S.M., Deane K., Song F., Hooper L. (2018), Polyunsaturated fatty acids for the primary and secondary prevention of cardiovascular disease, *Cochrane Database of Systematic Reviews*, 7, CD012345.
35. Hooper L., Al-Khudairy L., Abdelhamid A.S, Rees K., Brainard J.S, Brown T.J., Ajabnoor S.M., O'Brien A.T., Winstanley L.E., Donaldson D.H., Song F., Deane K. (2018), Omega-6 fats for the primary and secondary prevention of cardiovascular disease, *Cochrane Database of Systematic Reviews*, 11, CD011094.
36. Farmani J., Edalatkhah M., Motamedzadegan A., Mardani M. (2016), Production of set yoghurt analogue through replacement of milk fat with canola and sesame oil, *International Journal of Dairy Technology*, 69(3), pp. 433–440.
37. Dal Bello B., Torri L., Piochi M., Zeppa G. (2015), Healthy yogurt fortified with n-3 fatty acids from vegetable sources, *Journal of Dairy Science*, 98(12), pp. 8375–8385.

Method of pectin esterification determination degree by titrated acidity

Oksana Shulga, Volodymyr Lystopad, Sergii Shulga, Lyudmila Yurchuk

National University of Food Technologies, Kyiv, Ukraine

Keywords:
Pectin
Esterification
Acidity
IR-spectroscopy
NMR-spectrums

Article history:

Received 19.09.2019
Received in revised form 11.12.2019
Accepted 30.06.2020

Corresponding author:

Oksana Shulga
E-mail: shulgaos@ukr.net

DOI: 10.24263/2304-974X-2020-9-2-10

Abstract

Introduction. Studies have been conducted to develop a method for determining the pectin esterification degree in order to limit the use a significant number of costly and hardly available reagents.

Materials and methods. The samples of apple and citric pectin were exhibited at Kyiv market with the different degree of esterification according to accompanying documentation. IR-spectroscopy research was provided on device Nexus-475 Nicolet firm. NMR-spectrums were registered by NMR-spectrometer Mercury, VARIAN firm. Mathematical treatment of the results is done according to mathematical modeling concept.

Results and discussion. In the IR spectrum of low-esterified pectin, this band is low intensity and is in the oscillations region of 1686.71 cm^{-1}. In spectrum of high-ester pectin the intensive line with three maximums at 3400.56 cm^{-1}, 3316.52 cm^{-1}, 3271.70 cm^{-1}, which corresponds to stretching νOH. In IR-spectrums with esterification till 42% the line of free carboxyl group is available, in IR-spectrums of high-esterified pectin there is an intensive line of carboxylate groups (CO^{2-}), and that differs the given spectrums.

The given characteristics of NMR-spectrums show the difference in structure of high- and low-esterified pectin, but it does not give an opportunity to conduct the quantitative determination of esterification degree.

While analyzing the results we can make a conclusion that the degree or hyperbolic models are the best for prognosing.

The difference between chemical method of esterification degree determination and suggested method is 0.6-1.3%.

Conclusions. Determination of the pectin degree esterification is possible by tyranic acidity with subsequent calculation by the regression equation.

Introduction

One the most important nutritional and technological characteristics of pectin is its esterification degree [1]. The determining of this indicator needs the use of essential amount of reagents according to approved methods and time. A task was set up to find an alternative method of determining the degree of pectin esterification, since it is necessary to know the degree of pectin esterification in order to produce marmalade products.

According to the known method by national standard of Ukraine the esterification degree is a correlation of polygalacturonic acid esterified carboxyl groups to their general amount in pectin. This method of determination of pectin esterification degree needs the following reagents: hydrochloric acid, sodium hydroxide, ethyl alcohol rectified, silver nitrate, indicator alizarin, ammonia aqueous solution concentrate, bromothymol blue, cresol red, phenol red.

In literature there are data about the alternative methods of determination of pectin esterification degree such as the suggested method with the use IR-spectroscopy [2, 3, 7], NMR-spectroscopy [8], chromatography [9]. It is developed the improved method of high-performance liquid chromatography (HPLC) for simultaneous determination of pectin degrees of methylation and acetylation [5]. The suggested way includes the saponification in heterogeneous environment with the next separation of methanol, acetic acid and inner standard on C18 column and the quantitative determination with the help of refractometry [6]. But the suggested alternative methods need the use of special expensive equipment: IR- and NMR-spectroscopes and chromatograph [4, 8]. That is why the search of the alternative method which does not need the use of expensive equipment and big amount of reagents on determination of pectin esterification degree remains actual.

The purpose of the study is to develop a method for determining the esterification degree using a minimum number of reagents, which does not require a significant amount of time.

Materials and methods

Materials

Samples of apple and citrus pectin presented with different esterification degrees.

Methods

The total acidity was determined by the titration method of pectin batch solution in the presence of phenolphthalein [16].

The esterification degree was determined method that is based on the titrimetric analysis of free and after saponification esterified carboxyl groups of polygalacturonic acid in pectin batch, which is purified from soluble ballast additives and cations [16].

The presence of a carboxyl group in pectin of different esterification degrees was determined by IR spectroscopy [7]. IR-spectroscopy research was provided on device Nexus-475 Nicolet firm, in pills with KBr.

The chemical shift of the protons that are part of the pectin structural components was recorded using NMR spectra [8]. NMR-spectrums were registered by NMR-spectrometer Mercury, VARIAN firm, 400 MHz in the solution DMSO-d_6.

Processing of research results

Mathematical treatment of the results is done according to mathematical modeling concept [11].

Results and discussion

With the aim to get the complete characteristics of pectin properties with different degree of esterification, except total acidity, IR- and NMR-researches of chosen pectin samples were conducted.

The structure of pectin with different degrees of esterification is characterized by the presence of methylated carboxyl groups (see Figure 1).

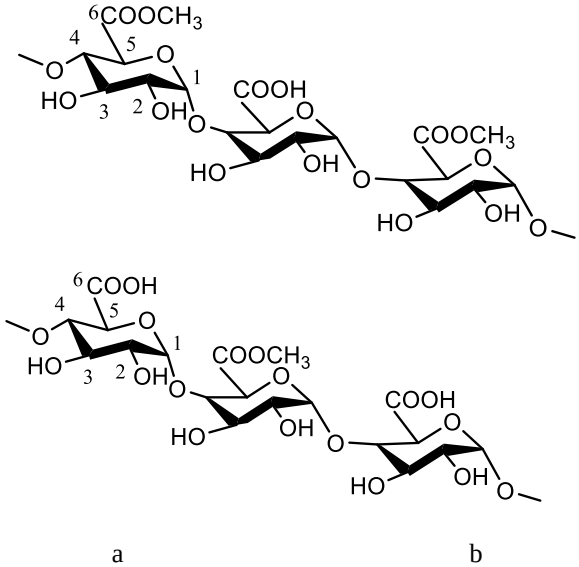

a b

Figure. 1. Pectin structure: a – highly esterified; b – low esterified

The given different pectin structure is confirmed by IR- and NMR-spectrometric researches, which are given further.

IR-spectroscopy research

According to the above given literature data [12], high- and low-esterified pectin have different IR-spectrums.

The IR-spectrums of high-ester (58-62%) and low-ester pectin (27-33%) Figure 2.

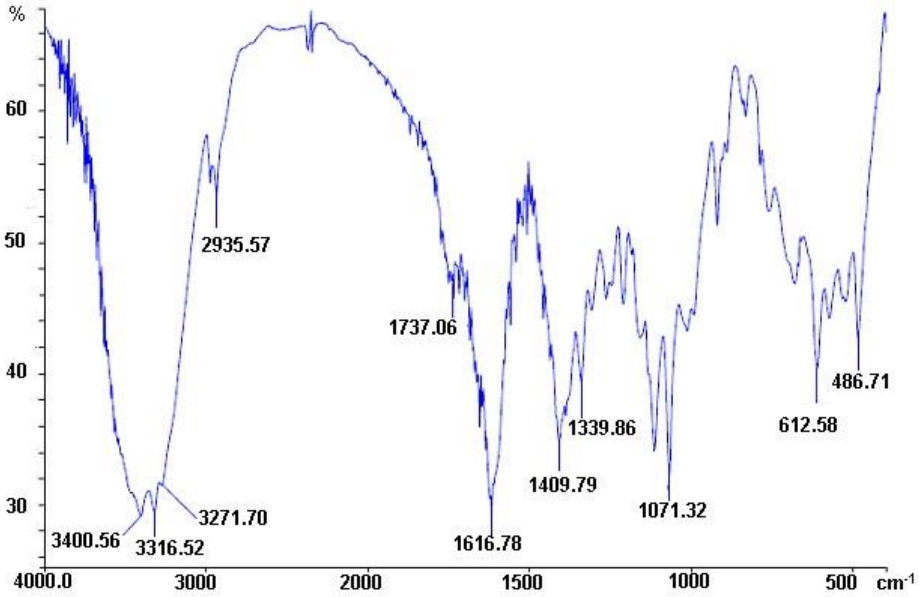

a

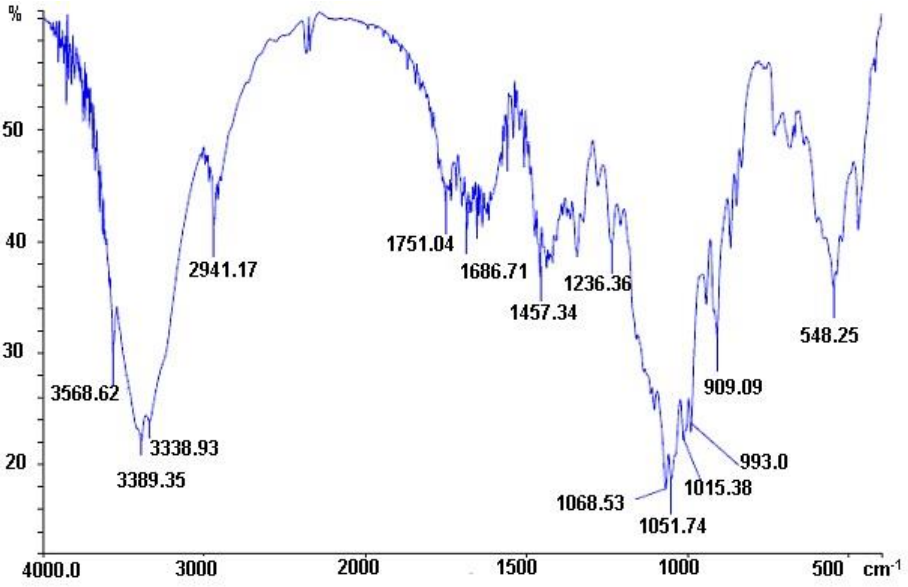

b

Figure 2. IR-spectrums of pectin: a – high-ester; b – low-ester

In spectrum of high-ester pectin the intensive line with three maximums at 3400.56 cm^{-1}, 3316.52 cm^{-1}, 3271.70 cm^{-1} is presented, which corresponds to stretching νOH. In IR-spectrum of low-ester pectin this line has maximum at 3568.62 cm^{-1}, separated from the other two 3389.35 cm^{-1} is located in weaker vibrations region, that shows a greater degree of hydrogen bonds, and confirms a lower degree of esterification. Maximum at 3568.62 cm^{-1} it corresponds to stretching of free carboxyl group, that also confirms low esterification degree.

The line at 2935.57 cm^{-1} of high-ester pectin sample and at 2941.41 cm^{-1} of low-ester sample are due to the presence of asymmetric and symmetric vibrations νC-H, which are located in remainders of galactopyranose rings of pectin.

In both spectrums of low- and high-ester pectin samples lines at 1737.06 cm^{-1} and at 1751.04 cm^{-1} of weak intensity exist, which correspond to vibrations of ester group C=O in composition of high- and low-ester pectin respectively.

In IR-spectrum of high-ester pectin sample the presented line of high intensity at 1616.78 cm^{-1} belongs to latitudinal vibrations of adsorbed related water that is crossed by asymmetric vibrations of carboxylate ion (CO^{2-}). In IR-spectrum of low-ester pectin sample this line is of weak intensity and is located in vibration region at 1686.71 cm^{-1}.

Besides this, IR-spectrums samples with esterification degree 24%, 28-36%, 38%, 36-42%, 65-68%, 66-68% were received. In IR-spectrums with esterification till 42% the line of free carboxyl group is available, in IR-spectrums of high-ester pectin there is an intensive line of carboxylate groups (CO^{2-}), and that differs the given spectrums.

NMR-researches research

NMR-spectrums of high- and low-ester pectin samples shown on Figure 3.

D-galacturonic acid in pectin is in conformational form “chair”. Meanwhile, the hydroxyl groups near Carbon atom 1 and 4 are in axial position, so free rotation around glycoside bond is complicated and pectin acid can be seen as a chain with limited flexibility, that changes the electron density a little around galactopyranose ring protons. The higher density is, the greater influence on inner field is, and therefore in a stronger field the resonance signal of according proton will appear.

The influence of this factor corresponds that the proton, which has more acidic properties (with less density of electronic shell) resonates in weaker field [12].

In general case the position of proton signal depends on electron density at surrounding it atoms, which are determined in such case by inductive and resonance effects, that are transmitted by chemical bonds and anisotropic effect of non-connected atom (interaction “through the space”) [13].

Taking into consideration the above given and literature data [14] in NMR-spectrums of high- and low-ester pectin samples signals are interpreted as shown in Table 1.

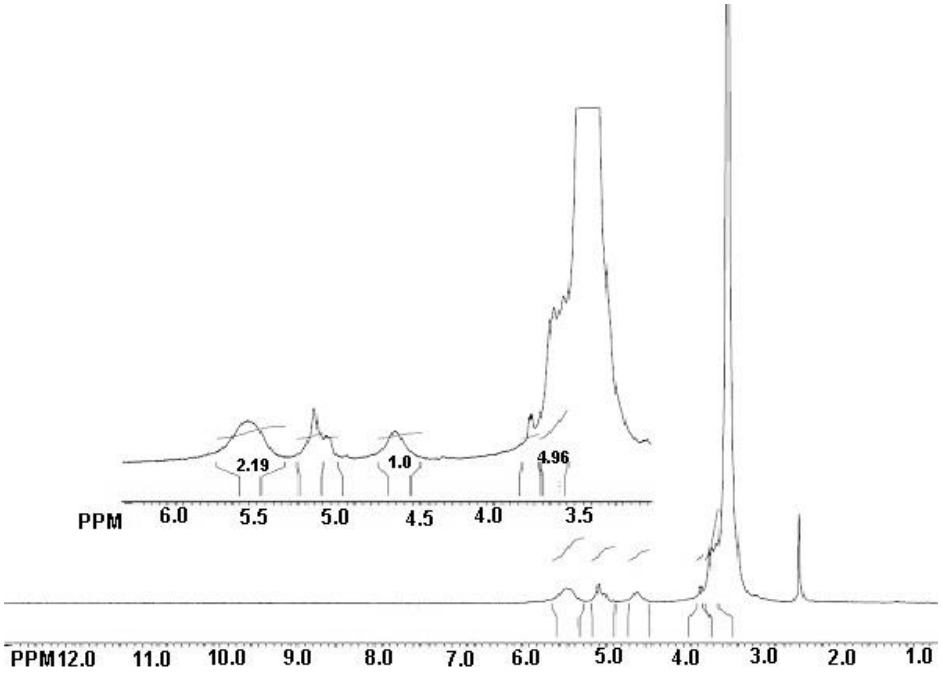

a

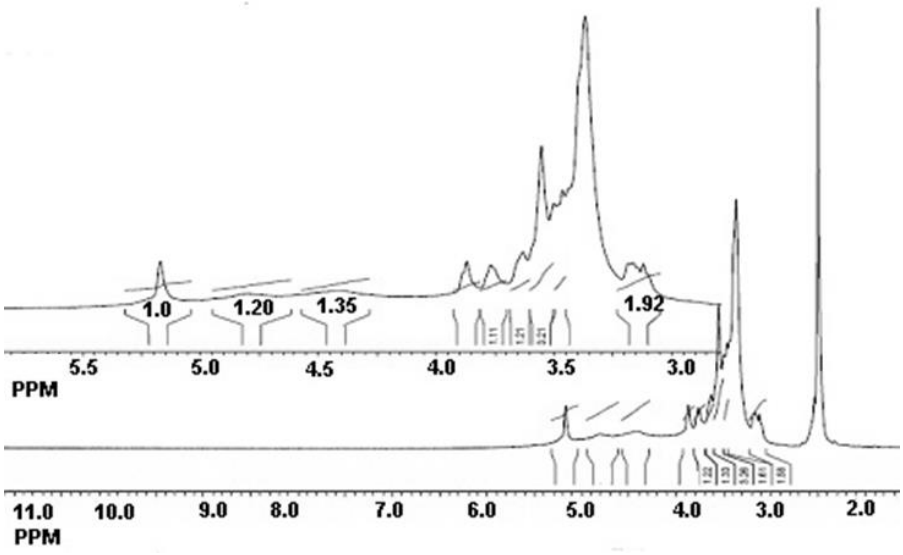

b

Figure 3. NMR-spectrums of pectin: *a* – high-ester; *b* – low-ester

Table 1

Interpretation of NMR-spectrums of high- and low-ester pectin

Proton type	Value of chemical shift ppm	
	High-ester pectin	Low-ester pectin
-OCH_3	3.579	3.567
4-H	3.632	3.639
5-H	3.780*	3.769
3-H		3.870
2-OH	4.605	4.425
1-H	5.102	4.805
3-OH	5.514	5.170
2-H	-	3.184

*signals overlapped one by one

The given characteristics of NMR-spectrums shows the difference in structure of high- and low-ester pectin, but it does not give an opportunity to conduct the quantitative determination of esterification degree.

Total pectin acidity research

Results of research of total acidity determination of pectin samples shown on Figure 4.

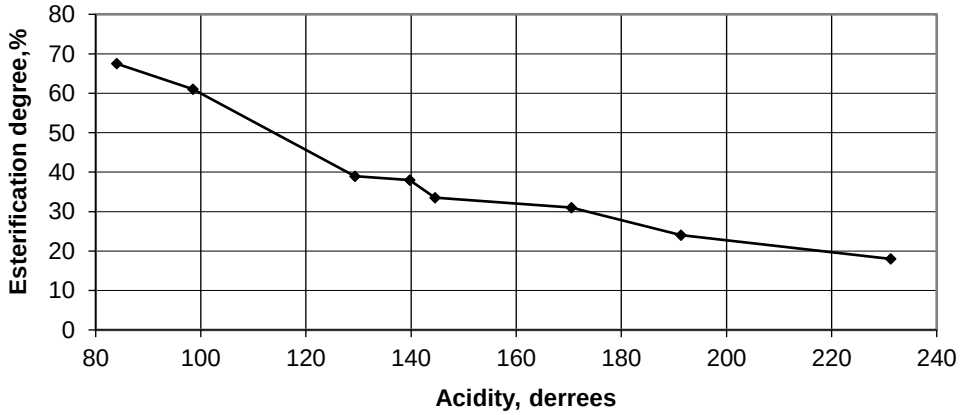

Figure 4. Total acidity change depending on pectin esterification degree

According to the given results (see Figure 4) there is a certain dependence between total acidity and degree of pectin esterification. It gives the base for searching the mathematical model.

Mathematical processing of research results

On the base of the received experimental data the mathematical treatment will be conducted.

According to the dependence graph outlook Y (%) esterification degree from X (degr.) acidity and big tightness of linear connection $\left(r_{yx} \approx -0,96\right)$, we will look through the linear dependence. In order to clarify the best outlook of the resultative factor approximation we will use other kinds of regression equation: hyperbolic, exponential and degree dependence:

$$\hat{y} = a_0 + a_1 x_1 \text{ – linear (1)}$$

$$\hat{y} = a_0 + \frac{a_1}{x}, \text{ – hyperbolic (2)}$$

$$\hat{y} = a_0 e^{a_1 x} \text{ – exponential (3)}$$

$$\hat{y} = a_0 x^{a_1} \text{ – degree (4)}$$

where a_0, a_1 – are unknown regression dependence coefficients.

The unknown model parameters (1-4) (a_0, a_1) we will find by the least squares method. For the formation of methods of receiving the unknown models parameters (1-4) we will consider them as common dependence *y (x)*.

For the model (1) we will use function LINEAR from *Microsoft Excel* (category STATISTICAL), which also contains additional characteristics for the model qualitative analysis.

The model of inverted connection with the help of substitute $t_i = \frac{1}{x_i}$ is reduced to linear $y = a_o + a_1 t$.

To build the exponential model it is necessary to take logarithm of left and right parts (3). We will get $\ln y = \ln a_o + a_1 x$, so as use the function LINEAR for data ($ln\, y_i$; x_i).

For the degree function after taking logarithm as in previous case we will get $\ln y = \ln a_o + a_1 \ln x$ and use function LINEAR for data $\left(lny_i; lnx_i\right)$. The inverted formulae for finding $a_o = e^{\ln a_o}$ based on basic logarithmic identity.

Comparison quantitative and qualitative characteristics of received models and choosing of "the best" for forecast carried out with the help of additional regression statistics.

1. Coefficient (index) of determination R^2, is a part of dispersion, which explains regression (model criterion of adequacy, which is the measure of independent variable x explanatory force x);
2. F – Fisher statistics, univocally gives an answer about model adequacy (an opportunity of use on practice);
3. Sum of squares of remainders (errors) $SSE = \sum_{i=1}^{n}\left(y_i - y_i\right)^2$ (deviation square of real values of independent variable y_i, from calculated y_i);

4. $MAPE = \frac{1}{n}\sum_{i=1}^{n}\frac{\left|y_i - y_i\right|}{y_i}100\%$ – absolute average percent error (indicator of prognosis immutability). This criterion is used while comparing prognosis exactness, because it characterizes the related prognosis exactness.

Meanwhile it is considered that that the definition *MAPE* is less than 10%. It gives high prognosis exactness and the model quality.

These quality criteria are used as additional information while choosing the best model from possible ones.

In calculating the additional models quantities (1-4) we will use formulae with [15].

$SSR = \sum_{i=1}^{n}\left(y_i - \bar{y}\right)^2$ – sum of squares, that explains the regression;

$SST = \sum_{i=1}^{n}\left(y_i - \bar{y}\right)^2$ – total sum of deviation squares;

$R^2 = \frac{SSR}{SST}$.

For the linear model according parameters the egality $SST = SSR + SSE$ is done.

While verifying the model adequacy we will use F-test criterion.

To that end we find the calculated criterion definition

$$F_{\text{estimated}} = \frac{SSR/(m-1)}{SSE/(n-m)} = \frac{R^2/(m-1)}{(1-R^2)/(n-m)},$$

where m – quantity of the unknown parameters in the model $(m = 2)$,

n – quantity of data $(n = 7)$.

For the assigned level of significance (error) α and number of freedom degrees $m-1$ and $n-m$ we find from the statistical tables (or in *Microsoft Excel* function FINV) F_{cr}. If $F_{calc} > F_{cr}$, the model is adequate, otherwise no.

To verify the significance of the received equations coefficients we will use t-test criterion. To that end we will calculate the calculated definitions of the criterion on the formulae $t_{icalc} = |a_i| / \sigma_i$, $i = 0.1$, and will compare it with the table one for 5% level of significance. While using t-test we calculate according to the number of freedom degrees $n-m=5$ and level of significance $\alpha = 0.05$, we will get $t_{cr} \pm 2.57$. The dispersions of models parameters deviations we will calculate on the formulae:

$$\sigma_o^2 = \sigma_\varepsilon^2 \cdot \frac{\sum_{i=1}^{n} x_i^2}{n \cdot \sum_{i=1}^{n}\left(x_i - \bar{x}\right)^2},\ \sigma_1^2 = \frac{\sigma_\varepsilon^2}{\sum_{i=1}^{n}\left(x_i - \bar{x}\right)^2},\ \sigma_\varepsilon^2 = \frac{SSE}{n-m}.$$

All the received results we will put into the Table 2.

Table 2

Results of dispersions calculation of parameters deviations of the suggested models

Model outlook	*Parameters of t-criterion*				
	σ_o	σ_1	t_{calc}	t_{1calc}	t_{cr}
Linear	7.68	0.05	12.78	7.54	±2.57
Inverted	3.51	430.05	3	15.56	±2.57
Exponential	4.68	0.0008	31.48	11.84	±2.57
Degree	0.028	3.947	4553.85	44.81	±2.57

Through the bilateral Student's t-test, it is easy to make sure, using Table 3, that the parameters of all the received models are significant at 5% level.

Table 3

Results of models significance verification at 5% level

Model type	**Equations**	**R^2**	**F-test criterion**	**SSE**	**MAPE,%**
Linear	$\hat{y} = 98 - 0.41x$	0.92	56.85	125.59	11
Hyperbolic	$\hat{y} = -10.55 + \frac{6691.08}{x}$	0.98	242.08	31.44	5
Exponential	$\hat{y} = 147.3 \cdot e^{-0.01x}$	0.98	145.63	46.65	6
Degree	$\hat{y} = 17974.9 \cdot x^{-1.25}$	0.996	242.08	33.20	5

While analyzing the results of Table 3 we can make a conclusion that the degree or hyperbolic models are the best for prognosing.

$$\hat{y} = 17974.9 \cdot x^{-1.25}$$

$$\hat{y} = -10.55 + \frac{6691.08}{x}$$

Let us verify the received models. On condition of the well-known value of pectin titrated acidity 139.7 degr., the degree of esterification is 36.9 and 37.4%, for the first and second models consequently, while by the chemical method it was 38%. On condition of the well-known value of pectin titrated acidity 191.3 degr., the calculated value esterification degree is 29.9% and 24.4%, by the chemical method it was 24.0%.

In this way, the found models are adequate and available for use.

Conclusions

1. High-ester and low-ester pectin characteristics with the help of IR- and NMR-spectroscopy is held, whereas these methods do not give the univocal indication of esterification degree.
2. The pectin titrated acidity determination is held with the mathematical treatment. As a result, two regression equations are received.
3. The difference between chemical method of esterification degree determination and suggested method is 0.6–1.3%.

References

1. Gnanasambandam R., Proctor A. (2000), Determination of pectin degree of esterification by diffuse reflectance Fourier transform infrared spectroscopy. *Food chemistry*, 68(3), pp. 327–332.
2. Chatjigakis A. K., Pappas, C., Proxenia N., Kalantzi O., Rodis, P., & Polissiou M. (1998), FT–IR spectroscopic determination of the degree of esterification of cell wall pectins from stored peaches and correlation to textural changes. *Carbohydrate Polymers*, 37(4), pp. 395–408.
3. Manrique G. D., & Lajolo F. M. (2002), FT–IR spectroscopy as a tool for measuring degree of methyl esterification in pectins isolated from ripening papaya fruit. *Postharvest Biology and Technology*, 25(1), pp. 99–107.
4. Monsoor M. A., Kalapathy U., & Proctor A. (2001), Improved method for determination of pectin degree of esterification by diffuse reflectance Fourier transform infrared spectroscopy. *Journal of Agricultural and Food Chemistry*, 49(6), pp. 2756–2760. DOI: 10.1021/jf0009448
5. Fellah A., Anjukandi P., Waterland M. R., & Williams M. A. (2009), Determining the degree of methylesterification of pectin by ATR/FT–IR: Methodology optimisation and comparison with theoretical calculations. *Carbohydrate polymers*, 78(4), pp. 847–853.
6. Pappas C. S., Malovikova A., Hromadkova Z., Tarantilis P. A., Ebringerova A., & Polissiou M. G. (2004), Determination of the degree of esterification of pectinates with decyl and benzyl ester groups by diffuse reflectance infrared Fourier transform spectroscopy (DRIFTS) and curve–fitting deconvolution method. *Carbohydrate Polymers*, 56(4), pp. 465–469.
7. Barros A. S., Mafra I., Ferreira D., Cardoso S., Reis A., da Silva J. L., & Coimbra M. A. (2002), Determination of the degree of methylesterification of pectic polysaccharides by FT–IR using an outer product PLS1 regression. *Carbohydrate Polymers*, 50(1), pp. 85–94.
8. Grasdalen H., Bakøy, O. E., & Larsen B. (1988), Determination of the degree of esterification and the distribution of methylated and free carboxyl groups in pectins by 1H–NMR spectroscopy. *Carbohydrate Research*, 184, pp. 183–191.
9. Voragen A. G. J., Schols H. A., & Pilnik W. (1986), Determination of the degree of methylation and acetylation of pectins by HPLC. Food hydrocolloids, 1(1): 65–70. DOI: 10.1016/S0268–005X(86)80008–X
10. Levigne S., Thomas M., Ralet M. C., Quemener B., & Thibault J. F. (2002), Determination of the degrees of methylation and acetylation of pectins using a C18 column and internal standards. *Food Hydrocolloids*, 16(6), pp. 547–550.
11. Bondar A. G. (1976), *Planirovanie eksperimenta v himicheskoy tehnologii (osnovnyie polozheniya, primeryi i zadachi)*, Vischa shkola, Kyiv.
12. Mironov V. A., Yankovskiy S.A. (1985), Spektroskopiya v organicheskoy himii. Sbornik zadach. Himiya, Moscow.
13. Braun D., Floyd A., Seynzberi M. (1992), Spektroskopiya organicheskih veschestv. Mir, Moscow.
14. Namazi H., Fathi F., & Dadkhah A. (2011), Hydrophobically modified starch using long–chain fatty acids for preparation of nanosized starch particles. *Scientia Iranica*, 18(3), pp. 439–445.
15. Luk'yanenko I. G., KrasnIkova L. I. (1998), *Ekonometrika*. Znannya, Kyiv.
16. Harris D. C. (2010), *Quantitative chemical analysis*. Macmillan, New York.

Justification of the amino acid composition of sunflower proteins for dietary and functional products

Mykola Oseyko[1], Tetiana Romanovska[1], Vasyl Shevchyk[2]

1 – National University of Food Technologies, Kyiv, Ukraine
2 – "Vasyl Shevchyk's eye microsurgery," Chernihiv, Ukraine

Keywords:

Sunflower
Press cake
Grist
Protein
Amino acid
Functional.

Article history:

Received 21.05.2019
Received in revised form 18.01.2020
Accepted 30.06.2020

Corresponding author:

Mykola Oseyko
E-mail:
nikios@ukr.net

DOI: 10.24263/2304-974X-2020-9-2-11

Abstract

Introduction. The study of samples of sunflower kernel processing was carried out to substantiate the amino acid composition of proteins for dietary and functional products.

Materials and methods. The subject of the study is the samples of press cake, grist, and flour, and their amino acid composition and physicochemical parameters. The amino acid composition of the samples was determined using liquid chromatograph Dionex ICS-3000 with an electrochemical detector. The ratio of hydrophobic and hydrophilic amino acids was studied in the samples.

Results and discussion. It was found that the protein content in flour from sunflower kernels is 22% higher. The content of essential amino acids is 31.1% higher than in the press cake from which the flour was isolated. The increase in protein content in sunflower flour is due to the increase of the fine fraction during fractionation. Along with the increase in total protein content, flour is enriched with essential hydrophobic amino acids, in particular leucine (14.2%), isoleucine (6.7%), methionine (11.2%), as well as replaceable hydrophobic proline (10.5%). Limiting amino acid in flour is lysine (score 78%), the content of other essential amino acids significantly exceeds their content in the ideal protein (score of leucine 153%, isoleucine 143%, methionine 213%, methionine with cystine 258%, phenylalanine and tyrosine 177%). The content of leucine and isoleucine in the classic kinds of sunflower is limited. In sunflower kernel flour, their content is exceeded one and a half times. To balance the obtained sunflower flour by lysine content, it is rational to use its compositions with other lysine-containing types of flour from oilseeds and / or with the use of food microbiological lysine.

Conclusion. Balanced protein-lipid eco-products and drugs on the basis of complex processing of sunflower seeds show functional and technological properties and contribute to disease prevention.

Introduction

Samples of processed sunflower seeds are studied to substantiate the amino acid composition of proteins for dietary and functional products.

Aspects of the protein problem in the world. Protein is crucial in a balanced diet for people of all ages [1, 2]. Protein deficiency in food can affect the health of the population.

According to [3], nine out of ten Indians do not have sufficient protein intake. Most people in the United States and Canada find it almost impossible not to meet their protein needs. (Hamilton et al., 1991).

Dr. Geoff's review [4] presents protein concentrations in food. Energy consumption from the maximum protein requirement for adults is approximately 8% of the estimated average energy requirement. These values represent something similar to the concentration of protein in food. A diet with a protein concentration of about 8% should be adequate for adults (for children, this figure is close to 5%). We consume only a limited number of food products in which at least 8% of calories are attributed to protein. In particular, human milk, which is an ideal food for fast-growing children, is one such product. Oil proteins and modified or processed oil proteins can be included in food to give it nutritional value and functional properties. Vegetable protein processing includes physicochemical and heat treatment, which affects the nutritional value of manufactured products, as well as technical features. Conversely, functional properties \ affect the behavior of the protein during processing and storage. These properties can be changed by chemical and enzymatic treatment [5].

The use of balanced protein-lipid eco-products and drugs in the systemic concept of health (KTIOL® system) contributes to disease prevention, comprehensive recovery and health improvement. It is advisable to use the KTIOL® system for disease prevention and rehabilitation for people of all ages [6, 7].

It is important not only to find available sources of protein-containing food syrups but also to create products that are safe and balanced in the chemical composition of nutrients [8, 9].

An important component of food is a protein with a balanced composition of essential amino acids [10].

Current trends in food technology are the search for new sources of protein and improving the technological processes of processing materials. It is important to study the methods of obtaining protein from the available sources, oilseeds, in particular, striving for the preservation and balance of essential amino acids [11, 12

The problem of obtaining protein is the presence in the raw material of natural substances that adversely affect the quality of the extracted protein, or complicate the processing of raw materials [13].

Of particular interest is the production of dietary and functional foods from sunflower seed kernels [14-17].

Technological aspects of amino acids in proteins. At the same time, the treatment of oilseeds for lipid extraction, including heating, compression and removal, changes the inherent protein, functional and technological properties, as well as affects its digestibility [18-22].

Essential amino acids must be present in proteins, and their balance in a protein determines the biological value of a food product. For cereals, lysine is a restrictive essential amino acid, and for legumes — methionine and cysteine, which contain sulfur. At the same time, limited critical amino acids are thermosensitive and reactive, so that any treatment will affect their content in the resulting product. The oxidation of sulfur-containing amino acids

could also pose a difficulty. Also, hydroperoxides of fatty acids react with amino acids to form sulfoxides. After the interaction of hydroperoxides with methionine, methionine sulfoxide is detected, which has no biological significance. Lysine and methionine are isomerized in alkaline media, and their D-isomers are not biologically valuable. The Maillard reaction involving the same free amino acids, reducing the carbohydrate content when heated, gives a compound consisting of radical reagents such as fructose-L-tryptophan, which reduces the digestibility of free amino acids. The products of the Maillard reaction to toxicity have been studied because it has been found that in animals such substances slow down growth [23].

The difficulty of assessing the native protein is the impossibility of its direct detection. There are methods by which you can indirectly determine the degree of influence of technological processing on the nature of the protein. All of them are based on a comparison of the characteristics of the raw and processed protein. In particular, determining the activity of certain enzymes, protein composition for solubility in water, solutions of salts, acids and alkalis, digestibility of proteins in certain species of animals or birds, and determining the metabolic energy of feed for them [10, 24-26].

Proteins consist of 20 amino acids, eight of which are needed. Amino acids differ in their physical and chemical properties, in particular thermal stability [27, 28], reactivity [22], polarity and hydrophilicity. The hydrophilicity of an amino acid is affected by the presence of radicals and their properties that are not bound by a peptide bond [30].

Proteins are hydrophilic and can absorb up to 200% of water to dry weight. There may be hydrophobic areas, most of which are in the middle of the protein molecule. The hydrophilicity or hydrophobicity of certain parts of the protein is determined by the amino acid radicals that remain after the formation of peptide bonds [30].

Of the eight essential amino acids, only two - lysine and threonine - have hydrophilic properties, and the other six - hydrophobic. In the presence of polar groups, there are amino acids that can carry a positive charge: lysine, arginine and histidine. Tyrosine and cysteine have radicals that can take a negative charge. Asparagine, glutamine, serine and threonine have nonionic polar radicals [31]. Usually, the constituent components determine the properties of the substance. Therefore, it is important to find an experimental correlation between the content of hydrophilic and hydrophobic amino acids in the protein and between the modes of technological processes of protein production [15, 30].

The purpose of our study was to investigate sunflower kernel flour and materials for its production, as well as the ratio of hydrophobic and hydrophilic amino acids in these products.

Materials and methods

The subject of the study is the products from the sunflower seed kernels, including flour, press cake and grist.

Materials

The flour from the sunflower seed kernels was obtained by crushing the kernel, further pressing the material at a temperature of 100-105 C, thus obtaining the press cake [15]. The press cake was used as a raw material for the flour. The press cake was milled and fractionated through a sieve. The fraction of passage through a sieve with apertures 0.3–0.6 mm was selected. The grist was obtained by degreasing the press cake with hexane in a laboratory extraction plant [15, 32]. At the same time, three swabs of sunflower flour were

taken: for preparing the sample for chromatographic analysis, to determine the moisture content, and to determine the residual content of the oil.

Sample preparation for determining the amino acid content. The amino acid composition and physicochemical of processed sunflower seed kernels were studied for flour, press cake and grist.

The sample preparation for determining the amino acid composition was carried out by acid hydrolysis of the sample [7]. The flour was placed in an ampoule tube and added 1:1 by weight 6 n. HCl. The ampoule was sealed and kept at 110 °C for 24 hours. After hydrolysis, the contents of the ampule were filtered, the filtrate was evaporated in a water bath. The dry residue was dissolved in a citrate buffer, filtered again and used for analysis.

Methods

The amino acid composition of the protein in sunflower flour, the press cake and grist was determined chromatographically. The amino acid composition of the prepared samples was determined using a liquid chromatograph Dionex ICS-3000 with an electrochemical detector [7]. The presence of amino acid was determined by the time it was released from the column, having previously calibrated it with pure amino acids. The number of amino acids was determined by the area of the release peak of certain amino acids. The signal from the detector is processed by a computer program that automatically determines the contents of each amino acid in the sample.

In the sunflower flour, the press cake and the grist, the moisture content was determined by an arbitration method [30] by drying to a constant mass at a temperature of 105 °C; residual oil content was measured using the Soxhlet method, and the total protein content measured by the Kjeldahl method.

Study results analysis

The change in amino acid content in sunflower flour was calculated for the content of the respective amino acid in the press cake, that was the source for the flour. The ratio between hydrophobic and hydrophilic amino acids in the studied samples was also calculated.

Results and discussion

Study of amino acid content of the sunflower flour, the press cake and the grist (shrot)

Sunflower flour is a thin homogeneous powder of gray color in appearance with a distinct taste and smell of sunflower kernel [15]. In the sunflower grist from the purified seed, the residual oil content was 14.3 ± 0.4 wt.%, the moisture content of 6.22 ± 0.24 wt.%. The standard deviation of the amino acid content of the flour, the press cake, and the grist was 4.8%.

Tables 1 and 2 show the amino acid composition of sunflower products from the sunflower kernel compared with the literature on the content of amino acids of the press cake and grist sunflower.

Table 1

Amino acid (AA) content of the sunflower flour, the press cake and the grist (shrot), % wt

N	Amino acids (AA)	Flour from the sunflower seed kernels				
		Flour	**Score (account by AA) flour, %**	Increase in AA content in flour,% wt. from the contents of the press cake	**Press cake**	**Grist**
	Essential amino acids:	18,30			13,96	13,87
	hydrophobic	14,63			10,96	10,65
1	Valine (V)	2,61	132		2,15	1,80
2	Isoleucine (I)	2,27	143	6,7	1,78	1,50
3	Leucine (L)	4,26	153	14,1	3,25	3,57
4	Methionine (M)	2,11	213	11,2	1,31	1,59
5	Tryptophan (W)	-			-	-
6	Phenylalanine (F)	3,38	284	12,7	2,47	2,19
	hydrophilic	3,67			3,00	3,22
7	Lysine (K)	1,71	78		1,52	1,52
8	Threonine (T)	1,96	124		1,48	1,70
	Non-essential amino acids:	21,40			18,57	18,49
	hydrophobic	8,56			6,80	6,89
9	Alanine (A)	2,54			2,04	2,08
10	Glycine (G)	2,90			2,42	1,93
11	Proline (P)	2,96		10,5	2,21	2,77
12	Cystine (C)	0,16			0,13	0,11
	hydrophilic	12,84			11,77	11,60
13	Arginine (R)	5,50			5,93	5,41
14	Aspartic acid (D)	0,95			0,78	0,89
15	Histidine (H)	1,13			0,87	0,75
16	Glutamic acid (E)	1,86			1,52	1,81
17	Serine (E)	2,56		9,0	1,92	1,92
18	Tyrosine (Y)	0,84			0,75	0,82
	Total number of	39,70		22,0	32,53	32,36

During the processing of sunflower seeds, the prepared material is subjected to wet heat treatment, so it is possible to break covalent bonds and proteins [15]. Chemical interactions with other substances are possible between amino acids and proteins [13]. As a result, they lose their properties and undergo chemical transformations. Therefore, the content of amino acids in the grist decreases compared to the cake, and this trend is maintained for all amino acids.

The preparation of flour from the press cake requires grinding at the micro-level, and probably the peptide and covalent bonds in the protein molecules are preserved. This is confirmed by the fact [15] that the amount of protein in flour increases and the bonds between other components (cellulose, minerals, lignin) are destroyed faster than in protein molecules, which allows us to obtain a fraction enriched in protein. Logically, the enrichment of the product with protein is due to an increase in the content of amino acids in sunflower flour obtained from the cake.

Comparative analysis of amino acid content of sunflower flour, the press cake and the grist

Experimental studies (Table 2) confirm the increase in the content of amino acids in sunflower flour compared to the press cake, which was the raw material for the production of flour.

It was found that sunflower kernel flour has a higher total protein content and a higher content of essential amino acids than in the cake from which it was obtained. In the flour from the purified kernel found a limited content of the amino acid lysine (78%), the content of other essential amino acids significantly exceeds their content in the ideal protein (leucine 153%, isoleucine 143%, methionine 213%, methionine in the amount of cystine 158%, phenylalanine 284% phenylalanine in the amount of tyrosine 177%). The content of leucine and isoleucine in the sunflower of classical processing is limited [25], in sunflower flour from the purified kernel their content exceeds one and a half times. Improving the composition of sunflower flour is provided by the introduction of food additives that have a higher content of amino acids, which is limited to flour [26].

The protein content of cake and meal is lower than the protein content of the flour, which is due to the enrichment of the protein fraction of fine particles during fractionation. Along with the increase in total protein content, the fine fraction is enriched with essential hydrophobic amino acids, in particular, leucine, isoleucine, and methionine. Also, the content of the substituted amino acids alanine, glycine, proline, which are hydrophobic, and the hydrophilic amino acids serine and histidine increases.

Content of hydrophobic and hydrophilic amino acids and their ratio in sunflower products

The calculated ratio of hydrophobic and hydrophilic amino acids in sunflower products from the purified kernel is given in Table 3.

Sunflower cake and meal are obtained by heat treatment in the presence of hydrophobic reagents. Fractionation of crushed cake particles promotes the concentration of protein in sunflower flour and increases the content of hydrophobic amino acids.

As a result of fractionation, the content of hydrophobic amino acids and the content of total protein in sunflower flour increased in comparison with cake and meal.

The ratio of hydrophobic amino acids to hydrophilic amino acids showed that the content of hydrophobic amino acids increases, and the number of hydrophilic amino acids decreases. This indicates that free radicals, which are not involved in the formation of the peptide bond in the protein, are better able to resist the processing during oil production and the production of sunflower flour than the hydrophilic amino acids (Table 3).

Table 2

Comparative analysis of amino acid (AA) content of sunflower flour, the press cake and the grist (shrot), % wt

N	Amino acids (AA)	Sunflower press cake [22]	Sunflower press cake [20]	Sunflower grist [14]	Sunflower grist [21]	Sunflower grist [21]
	Essential amino acids:	8,60	7,03			
	hydrophobic					
1	Valine (V)	1,32	1,23	3,83	1,96	2,00
2	Isoleucine (I)	2,73	2,44	3,26	1,26	1,64
3	Leucine (L)			7,40	2,28	2,54
4	Methionine (M)	0,71	0,51	2,38□	0,93	0,91
5	Tryptophan (W)	-	-	1,22	-	-
6	Phenylalanine (F)	1,41	0,92	8,17□□	1,75	1,84
	hydrophilic					
7	Lysine (K)	1,09	0,86	3,75	1,34	1,43
8	Threonine (T)	1,34	1,07	4,85	-	-
	Non-essential amino acids:	13,43	12,63			
	hydrophobic					
9	Alanine (A)	1,35	1,25		-	-
10	Glycine (G)	1,81	1,48		-	-
11	Proline (P)	1,45	1,54		-	-
12	Cystine (C)	-	-		-	-
	hydrophilic					
13	Arginine (R)	1,91	1,83		3,23	3,14
14	Aspartic acid (D)	-	-		-	-
15	Histidine (H)	0,89	0,59		0,85	1,01
16	Glutamic acid (E)	3,93	4,22		-	-
17	Serine (E)	1,31	1,11		-	-
18	Tyrosine (Y)	0,78	0,61		-	-
	The total number of	22,03	19,66	34,86	13,60	14,51

□ - Methionine + Cystine, □□ - Phenylalanine + Tyrosine

Table 3

Content of hydrophobic and hydrophilic amino acids and their ratio in sunflower products

Indicator	Products from sunflower kernel			Sunflower press cake [15]	Sunflower press cake [13]
	Flour	Press cake	Grist (shrot)		
Content of essential amino acids (EA)	18.30	13.96	13.87	8.60	7.03
hydrophobic	14.63	10.96	10.65	6.17	5.10
hydrophilic	3.67	3.00	3.22	2.43	1.93
The ratio of hydrophobic to hydrophilic EA	3.99	3.65	3.31	2.54	2.64
The content of substitutable amino acids (SA)	21.40	18.57	18.49	13.43	12.63
hydrophobic	8.40	6.67	6.78	4.61	4.27
hydrophilic	13.00	11.90	11.71	8.82	8.36
Ratio of hydrophobic to hydrophilic	0.65	0.56	0.58	0.52	0.51
Total content of hydrophobic amino acids	23,03	17,63	17,42	10,78	9,37
Total content of hydrophilic amino acids	16,67	14,90	14,93	11,25	10,29
The ratio of hydrophobic to hydrophilic	1,38	1,18	1,17	0,96	0,91

This property of proteins to retain functional hydrophobic properties during the technological processing of press cake, flour, and grist allows us to use these products as raw bio materials for the production of dietary and functional protein-containing and protein-lipid products and to improve their quality.

Conclusion

1. The balanced amino acid composition of sunflower flour is substantiated.
2. An increase in the content of hydrophobic amino acids improves the technological properties of flour. It is advisable to use sunflower kernel as a formulation component for the development and introduction of dietary and functional products with improved consumer properties, as well as for expanding the range of food products and improving their quality.
3. Balanced protein-lipid eco-products and drugs on the basis of complex processing of sunflower seeds show functional and technological properties and contribute to disease prevention.

References

1. Carpenter K.J. (1994), Protein and energy: a study of changing ideas in nutrition, *Cambridge University Press*, Cambridge
2. Webb G.P. (2012), *Nutrition: maintaining and improving health. 4th edition*, Taylor and Francis, Oxford
3. Times of India (2015), *Nine out of ten Indians lack proper protein intake*, Avialable at: http://timesofindia.indiatimes.com/city/nagpur/Nine-out-of-10-Indians-lack-proper-protein-intake/articleshow/47534086.cms.
4. Dr Geoff (2016) *The Protein Gap – one of the biggest errors in nutritional science. Overview*, Avialable at: https://drgeoffnutrition.wordpress.com/2016/12/07/the-protein-gap-one-of-the-biggest-errors-in-nutritional-science/ Dr. Geoff / December 7, 2016
5. Andre´s Mourea, J. Sineirob, Herminia Domı´ngueza, Juan Carlos Parajo´a (2006), *Functionality of oilseed protein products: A review*, Avialable at: https://www.academia.edu/20956984/Functionality_of_oilseed_protein_products_A_review.
6. Mykola Oseyko, Vasyl Shevchyk, Olena Pokryshko (2019), Antimicrobial and antifungal activity of model drugs on the basis of food plant extracts in the systemic concept of health, *Ukrainian Journal of Food Science*, 7(1), pp. 70–82 DOI: 10.24263/2310-1008-2019-7-1-9.
7. Mykola Oseyko, Nataliia Sova, Maryna Lutsenko, Viktoriia Kalyna (2019), Chemical aspects of the composition of industrial hemp seed products // *Ukrainian Food Journal*, 8(3), pp. 544–559, DOI: 10.24263/2304- 974X-2019-8-3-11.
8. Oseyko M., Romanovska T., Shevchyk V. (2017), Funktsionalnyy Produkt v kontseptsiyi endoekolohiyi zdorovya (Functional products in endoecology health concepts), *Scientific Works of NUFT*, 23(3), pp. 192–203.
9. Tutel'yan V.A., Vyalkov A.I., Razumov A.N., Mixajlov V.I., Moskalenko K.A., Odinec A.G., Sbezhneva V.G., Sergeev V.N. (2010), *Nauchnye osnovy zdorovogo pitaniya*, Moscow.
10. Gonzalez-Perez S., Vereijken J.M. (2007), Sunflower proteins: an overview of their physicochemical, structural, and functional properties, *J. Sci. Food Agric*., 87(12), pp. 2173–2191.
11. Salgado P.R., Molina Ortiz S.E., Petruccelli S. et al. (2011), Sunflower protein concentrates and isolates prepared from oil cakes have high water solubility and antioxidant capacity, *J. Am. Oil Chem. Soc*., 88(3), pp. 351–360.
12. Shirokoryadova O.V., Minakova A.D., Shherbakov V.G., Logunova O.V. (2008), Bioximicheskie osobennosti belkovykh fraktsiy iz semyan podsolnechnika, *Izvestiya vuzov. Pishhevaya tekhnologiya*, 1, pp. 23-24.
13. Nosenko T. (2017), Comparison of biological value and technological properties of oilseed proteins, *Ukrainian Food Journal*, 6(2), pp. 226–238.
14. Labeyko M.A., Lytvynenko O.A., Fedyakina Z.P., Petik P.F. (2012), Otrymannya bilkovoho produktu z nasinnya sonyashnyku vitchyznyanoyi selektsiyi, *Visnyk Nats. tekhn. un-tu "KhPI"*, 39, pp. 117-124, Available at: http:// archive.kpi.kharkov.ua/files/18128/
15. Oseiko N.I. (2006), *Tekhnolohiia roslynnykh olii*, Varta, Kyiv.

16. Kamsulina N.V., Skurikhina L.A., Hubal L.M. Doslidzhennia funktsionalno-tekhnolohichnykh vlastyvostei bilkiv iz nasinnia soniashnyku, *Prohresyvni tekhnika ta tekhnolohii kharchovykh vyrobnytstv restorannoho hospodarstva i torhivli: zb. nauk. pr.*, 2(22), pp. 50-61, Available at: http://elib.hduht.edu.ua/jspui/handle/123456789/589
17. Fadeev L.V. (2013), *Podsolnechnik Ukrainy – sehodnia i zavtra*, Spetsemm, Kyiv.
18. Sitohy M.Z., Badr E.H., Perifanova-Nemska M., Khadjiskf T.S. (1993), Characterization of enzymatically extracted sunflower seed oil as well as the protein residues, *Grasas y Aceites*, 44(6), pp. 345–347.
19. Villanueva A., Vioque J., Sanchez-Vioque R., Clemente A., Bautista J., Millan F. (1999), Production of an extensive sunflower protein hydrolysate by sequential hydrolysis with endo- and exo-proteases, *Grasas y Aceites*, 50(6), p. 472–476.
20. Nikolaev S.I., Dikusarov V.G., Randelin D.A. i dr. (2016), Sravnitelnyy analiz khimicheskogo sostava produktov pererabotki semyan maslichnykh kultur, *Nauchnyj zhurnal KubGAU*, 118(04), available at: http://ej.kubagro.ru/2016/04/pdf/106.pdf
21. Nikolaev S.I., Karapetyan A.K., Kornilova E.V. i dr. (2015), Sravnitelnyy analiz aminokislotnogo sostava kormov, *Nauchnyj zhurnal KubGAU*, 107(03), Available at: http://ej.kubagro.ru/2015/03/pdf/110.pdf
22. Nikolaev S.I., Karapetyan A.K., Chekhranova S.V. i dr. (2016), Sravnitelnyy analiz khimicheskogo sostava produktov pererabotki semyan maslichnykh kultur, *Nauchnyj zhurnal KubGAU*, 118(04), Available at: http://ej.kubagro.ru /2016/04/pdf/83.pdf
23. Flaumenbaum B.L., Tanchev S.S., Grishin M.A. (1986), *Osnovy konservirovaniya pischevyikh produktov*, Moscow.
24. Ivanova P., Chalova V., Koleva L., Pishtiyski I. (2013), Amino acid composition and solubility of proteins isolated from sunflower meal produced in Bulgaria, *International Food Research Journal*, 20(6), pp. 2995–3000.
25. Gonzalez-Vega J.C., Stein H.H. (2015), Amino acid digestibility in canola, cottonseed, and sunflower products fed to finishing pigs, *J. Anim. Sci*., 20, pp. 4391–4400.
26. Nenova N., Drumeva M. (2012), Investigation on protein content and amino acid composition in the kernels of some sunflower lines, *Helia*, 35(56), pp. 41–46.
27. González-Pérez S., Vereijken J.M., Merck K.B. et al. (2004), Conformational states of sunflower (Heliantus annuus) Heliantinin: effect of heat and pH, *J. Agric. Food Chem*., 52(22), pp. 6770-6778.
28. Molina M.I., Petruccelli S., Anon M.C. (2004), Effect of pH and ionic strength modifications on thermal denaturation of the 11S globulin of sunflower (Helianthus annuus), *J. Agric. Food Chem*., 52(19), pp. 6023–6029.
29. Nicolson S., Human H. (2013), Chemical composition of the `low quality' pollen of sunflower (Helianthus annuus, Asteraceae), *Apidologie, Springer Verlag*, 44(2), p.144-152.
30. Romanovska T.I. (2006), *Fizyko-khimichni aspekty kharchovykh tekhnolohiy*, Naukova dumka, Kyiv.
31. Hans-Dieter Jakubke, Hans Jeschkeit (1982). *Aminosäuren, Peptide, Proteine*, Akademie-Verlag, Berlin.
32. Cristina Popovici (2013), Soxhlet extraction and characterisation of natural compounds from walnut (Juglans regia L.) by-products, *Ukrainian food journal*, 2(3), pp. 328–336
33. Oseyko M. (1987), Bilkovo-lipidni dobavky, *Zerno i khlib*, 4, p. 31.

Antioxidant capacity of alcoholic beverages based on infusions from non-traditional spicy-aromatic vegetable raw materials

Oleg Kuzmin[1], Volodymyr Kucherenko[2], Iryna Sylka[1], Volodymyr Isaienko[3], Yuliia Furmanova[1], Olena Pavliuchenko[1], Viacheslav Hubenia[1]

1 – National University of Food Technologies, Kyiv, Ukraine
2 – Ukrainian Corporation for Viticulture and Wine Industry "Ukrvinprom"
3 – National Aviation University, Kyiv, Ukraine

Keywords:

Spicy-aromatic
Antioxidant
Redox
Infusion
Alcohol

Article history:

Received 01.08.2019
Received in revised form 23.12.2019
Accepted 30.06.2020

Corresponding author:

Oleg Kuzmin
E-mail: kuzmin_ovl@ukr.net

DOI:
10.24263/2304-974X-2020-9-2-12

Abstract

Introduction. The aim of the study is to determine the antioxidant capacity of aqueous-alcoholic infusions using non-traditional spicy-aromatic raw materials in the technology of alcoholic beverages.

Materials and methods. Antioxidant ability of infusions of spicy-aromatic plants: *Perilla frutescens*; *Elsholtzia stauntonii Benth*; *Artemisia abrotanum*; *Monarda didyma*; *Agastache foeniculum*; *Satureja hortensis*; *Ruta graveolens*; *Nepeta transcaucasica Grossch* was determined by redoxmetry and pH-metry; sensory evaluation – by expert method; the results of mathematical and statistical processing – by the method of linear Pearson correlation.

Results and discussion. The minimum theoretical value of redox potential (*RP*) for plant aqueous-alcoholic infusions was obtained, which has a value from 228.0 mV (*Satureja hortensis*) to 260.4 mV (*Agastache foeniculum*). The actual measured *RP* of infusions was established – from 117 mV (*Elsholtzia stauntonii Benth*) to 134 mV (*Nepeta transcaucasica Grossch*). The hydrogen index for aqueous-alcoholic infusions from spicy-aromatic raw materials has a value of 6.66 units pH (*Agastache foeniculum*) to 7.20 units *pH* (*Satureja hortensis*). Aqueous-alcoholic infusions from vegetable raw materials and a volume fraction of ethanol of 40% have the value of recovery energy (*RE*) in the range from 100.0 mV (*Nepeta transcaucasica Grossch*) to 138.2 mV (*Ruta graveolens*).

Aqueous-alcoholic infusions from spicy-aromatic raw materials have values of sensory evaluation (*S.e.*) from 9.50 to 9.69 points. The highest value of *S.e.* 9.69 points is characteristic of *Nepeta transcaucasica Grossch*: color – light brown; taste – mint; aroma – soft, pleasant, sweet.

Conclusion. It is proposed for the technology of alcoholic beverages the use of aqueous-alcoholic infusions from *Ruta Gravelens* and *Nepeta transcaucasica Grossch*, which received increased antioxidant characteristics *RE* 138.2 mV and *RE* 100.0 mV, respectively, and positive *S.e.* 9.57 and *S.e.* 9.69 points on a 10-point scale.

Introduction

One of the important directions of food industry development is improvement of taste, aroma of food, preservation (or addition) of nutritional value of the final product (Dubovkina I. et al., 2019; Kuzmin et al., 2016; Kuzmin et al., 2017) [1–3].

Currently, the use of vegetable raw materials in the technology of alcoholic beverages is very relevant (Andreou et al., 2018; Chandrasekara, Shahidi, 2018; Iannitti, Palmieri, 2009; Halliwell, Gutteridge, 1990; Kawa-Rygielska et al., 2019; Fotakis et al., 2016 [4-9], especially when used in restaurant business. Herbal beverages commonly consumed worldwide contain different chemical substances that display a broad spectrum of biological activities (Kamdem et al., 2013; Frolova et al., 2019; Gerolis et al., 2017; Imark et al., 2000; Pyrzynska, Sentkowska, 2019; Wong et al., 2020; Sentkowska, Pyrzynska, 2018; Siddiqui et al., 2018; Steenkamp et al., 2004) [10–18]. They have gained growing interest among scientists and consumers due to their antioxidant properties (Breiter et al., 2011; Dube et al., 2017 [19, 20]. The ability of plant phenolics to act as free radical scavengers has led to increased interest in their ability to act as antioxidants (Keating et al., 2014; Oh et al., 2013; Herrera et al., 2018; Humia et al., 2020) [21–24]. Antioxidants are able to reduce the output of oxidation products: hydroperoxides, alcohols, aldehydes, ketones, fatty acids.

Beverages are rich sources of natural bioactive compounds such as carotenoids, phenolic acids, flavonoids, coumarins, alkaloids, polyacetylenes, saponins and terpenoids, among others (Ruiz-Ruiz et al., 2020; Naithani et al., 2006) [25, 26]. Of particular interest in the production of alcoholic beverages is a spicy-aromatic raw material that exhibits antioxidant and tonic properties (Vergun et al., 2018; Vergun et al., 2019; Kurylo et al., 2018) [27–29]. At present, the antioxidant characteristics of all prescription components, food additives, biologically active substances and their combinations have not been sufficiently studied (Buglass et al., 2012; Grunert et al., 2018; Gullón et al., 2018; Gulua et al., 2018; Joubert, Beer, 2012) [30–34].

RP is an important indicator of the biological activity of solutions (Kuzmin O. et al., 2016; Merwe et al., 2017) [2, 35]. It characterizes the deviation from the ionic balance of free electrons in a liquid medium. Changing the concentration of free electrons leads to a change in its electron charge and, accordingly, the *RP*. If the *RP* is positive, it indicates the oxidizing ability of the solution, negative indicates recovery ability. The value of *RP* allows to estimate the energy of processes, that is, characterizes the activity of ions in redox reactions (Bahir, 1999; Priluckij, 1997) [36, 37]. Therefore, in order for the human body to optimally use in the exchange processes aqueous-alcoholic mixtures and food, the *RP* values must correspond to the *RP* values of the internal environment of the organism, or have more negative values (Bahir, 1999) [36].

But among all the useful properties, the main thing will be to change the redox reactions (Priluckij, 1997) [37]. Redox reactions affect the ratio of energy to support homeostasis – relativity of dynamic constancy of composition and properties of internal environment and stability of basic physiological functions of an organism. This ensures the vital activity of any organism. The magnitude of this rate depends on the ratio and concentration of oxidized and reduced substances in the body, including substances coming from food and beverages, so one of the main factors in the regulation of redox reactions is the redox potential (Kuzmin O. et al., 2016; Bahir, 1999; Priluckij, 1997) [2, 36, 37].

These circumstances determine the relevance of this work, which is to develop aqueous-alcoholic infusions of vegetable raw materials in the technology of alcoholic cocktails for restaurants. Creating alcoholic cocktails with reduced toxicity through the introduction of spicy-aromatic infusions with antioxidant properties, allows restaurant establishments to create new products, which favorably differentiates them from competitors, creating a favorable image of

the institution, which cares for the protection of consumers.

The *purpose* of the work is to develop the scientific bases of antioxidant activity of aqueous-alcoholic infusions from vegetable raw materials and to identify the most promising plants as sources of natural antioxidants in the creation of alcoholic beverages.

It is necessary to solve the following *problems*:

- To substantiate the prospect of using aqueous-alcoholic infusions from vegetable raw materials in the production of alcoholic beverages;
- To establish the value of the restorative capacity of aqueous-alcoholic infusions from vegetable raw materials;
- To develop statistics on the frequency of values in a certain range of the data obtained during sensory evaluation and physicochemical values;
- To carry out mathematical and statistical analysis of indicators of aqueous-alcoholic infusions and establish internal correlation;
- Identify the most promising sources of natural antioxidants for use in alcoholic beverage technology.

Materials and methods

Materials

The study used plant raw materials that are allowed to be used in the production of alcoholic beverages. In the *M.M. Gryshko National Botanic Garden of NAS of Ukraine* was created new cultures of spicy-aromatic plants, which became the subject of these studies (Rakhmetov, 2011) [38].

In the Figure 1 shows a photo of vegetable raw materials: *Perilla frutescens; Elsholtzia stauntonii Benth; Artemisia abrotanum; Monarda didyma; Agastache foeniculum; Satureja hortensis; Ruta graveolens; Nepeta transcaucasica Grossch.* For preparation of extracts used the following basic raw materials: ethanol rectified, water, cardboard filtering.

The extracts should meet the requirements on sensory evaluation (Table 1). The extracts must meet the requirements by physicochemical parameters (Table 2).

Table 1

Sensory evaluation of extract

Indicator	Characteristic
Appearance	Transparent without sediment and foreign impurities fluid, acceptable opalescence that disappears after filtration
Color, taste, aroma	The inherent vegetable raw materials from which they are made, without the foreign taste and odor

Table 2

Physicochemical parameters of extract

Parameter	Norm
Ethyl alcohol by volume, %	20.0–90.0
Mass fraction of essential oil, %	0.0–15.0
Mass concentration of the total extract, g/100 cm^3	0.1–20.0

Figure 1. Photo of vegetable raw materials:
a – *Perilla frutescens*; b – *Elsholtzia stauntonii Benth*; c – *Artemisia abrotanum*; d – *Monarda didyma*; e – *Agastache foeniculum*; f – *Satureja hortensis*; g – *Ruta graveolens*; h – *Nepeta transcaucasica Grossch*

Aqueous-alcoholic infusion – semi-finished product, which is prepared by extraction of raw materials in aqueous-alcoholic solution with a strength of 40 %. The static method of extraction is called maceration. The tested aromatic raw material (dry) was infused in a aqueous-alcoholic mixture in this work.

Description of research procedure

The first stage – the preparation of infusions. Plant raw materials were minced into a size of 3x3 mm (Figure 2), suspensions of 4 g were placed into the glass bottles, were filled by 100 ml of alcohol solvent with volume fraction of rectified ethyl alcohol 40 %. The resulting infusions were cooled to 20 °C for 7 days, stirring periodically.

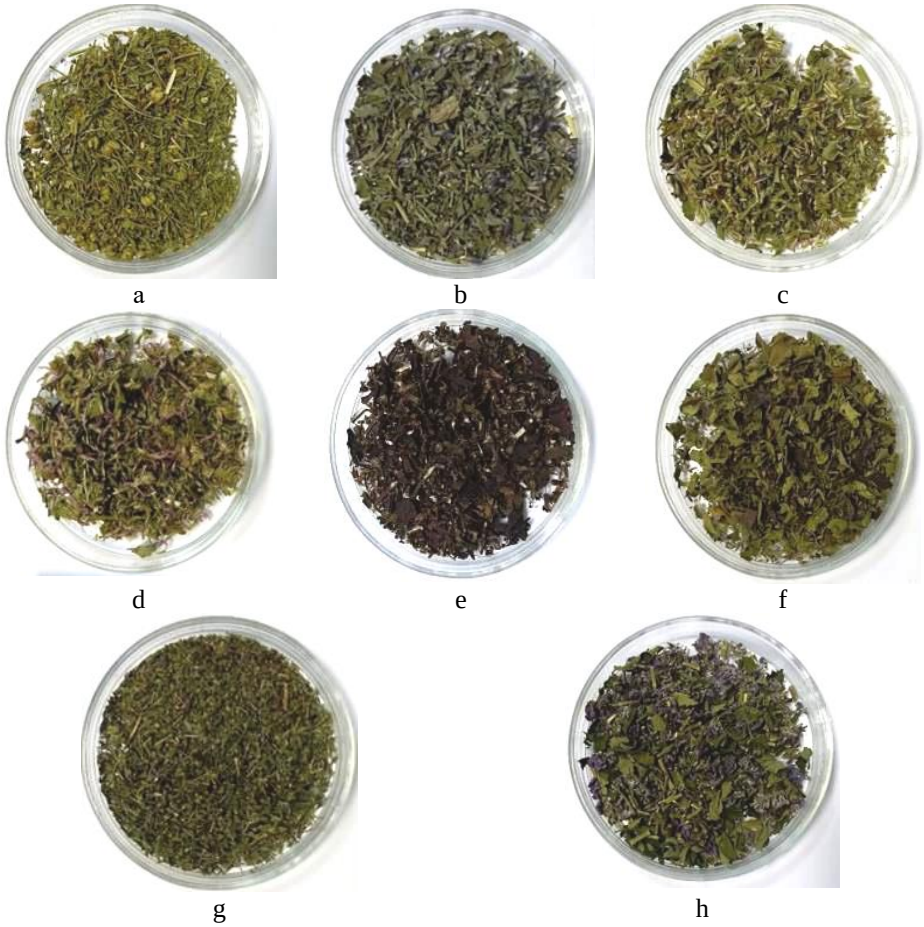

Figure 2. Photo of Samples of crushed plant raw materials:
a – *Perilla frutescens*; b – *Elsholtzia stauntonii Benth*; c – *Artemisia abrotanum*; d – *Monarda didyma*; e – *Agastache foeniculum*; f – *Satureja hortensis*; g – *Ruta graveolens*; h – *Nepeta transcaucasica Grossch*.

Next, the infusions were filtered and studies were performed to determine the indicators of active acidity, which was measured on a *pH* meter in the mode of *pH* measurement with a combined glass electrode. The *RP* was measured in the potential measurement mode with a combined redoxmetric platinum electrode.

Description of methods

Expert method of sensory evaluation. The expert method of determination of values of indexes of quality is based on the account of opinions of group highly skilled specialists-experts. (The expert of − it a specialist on the certain type of object which owns the increased sensitiveness to properties of this object) (Kuzmin et al., 2016; Kuzmin et al., 2017) [2, 3].

Methods for determining antioxidant capacity. To evaluate the antioxidant properties of the obtained aqueous-alcoholic plant infusions, the *method* (Priluckij, 1997) [37], based on the difference of *RP* in inactivated inorganic solutions and complex biochemical media. The main criteria of this method were its clarity, simplicity, specificity, reproducibility of results and efficiency. A number of researchers also emphasize that method allows to determine the total antioxidant activity of liquid products, including in total in a complex mixture, and multifunctional antioxidants (Kuzmin et al., 2016) [2].

Formula (1) holds for inactivated inorganic solutions in equilibrium. This formula links the active acidity of the *pH* and the *RP* (Priluckij, 1997) [37]:

$$Eh_{min}=660–60\cdot pH, \text{ mV} \quad (1)$$

where Eh_{min} – the minimum theoretically expected value of the *RP*;
pH – active acidity of the test solution.

Acquired *RP* values were compared with actual measurements of Eh_{act} solution. The change of the *RP* toward the recovery energy (*RE*) was determined by the formula:

$$RE = Eh_{min}–Eh_{act}, \text{ mV} \quad (2)$$

where *RE* – the shift of *RP* to the side of recovered meanings (resilence);
Eh_{min} – minimal theoretically expected meaning of *RP*;
Eh_{act} – actual measured *RP*.

Mathematical and statistical methods. Pearson correlation coefficient measures the strength of the linear association between variables. Each variable should be continuous, random sample and approximately normally distributed. There are many rules of thumb on how to interpret a correlation coefficient, but all of them are domain specific. For example, here is correlation coefficient (Table 3) interpretation for behavioral sciences offered by Hinkle et al., 2003 [39].

Table 3

Correlation coefficient interpretation

Absolute value of coefficient (*r*)	Strength of correlation
0.90–1.00	Very high
0.70–0.90	High
0.50–0.70	Moderate
0.30–0.50	Low
0.00–0.30	Little, if any

The correlation coefficient can take a range of values from +1 to -1. Positive correlation coefficient means that if one variable gets bigger, the other variable also gets bigger, so they tend to move in the same direction. Negative correlation coefficient means that the variables tend to move in the opposite directions: If one variable increases, the other variable decreases, and vice-versa. When correlation coefficient is close to zero two variables have no linear relationship (Hinkle et al., 2003; Shendrik et al., 2019) [39, 40].

Results and discussions

Sensory evaluation

The results of sensory evaluation (Kuzmin et al., 2017) [3] of the obtained infusions on the extractant are presented in the Table 4 and Figures 3.

Table 4

Sensory evaluation (*S.e.*) of extracts

Plant raw materials	Color	Aroma	Test	S.e., points
1. Perilla frutescens	Light amber	Floral	Sour-bitter, tart, unpleasant	9.50
2. Elsholtzia stauntonii Benth	Light brown	Grassy, floral	Sour-bitter	9.64
3. Artemisia abrotanum	Thatched	Grassy	Bitter, with a long, bitter aftertaste	9.51
4. Monarda didyma	Thatched	Fragrant, floral	Sour-bitter, unpleasant, with a bitter aftertaste	9.52
5. Agastache foeniculum	Light amber	Bright ethereal, herbal, fragrant	Bitter, tart	9.65
6. Satureja hortensis	Light brown	Spicy, fragrant, herbal	Moderately hot, irritable, with a sweet taste	9.67
7. Ruta graveolens	Thatched	Fragrant, grassy, floral	Bitter, tart	9.57
8. Nepeta transcaucasica Grossch	Light brown	Mint	Soft, pleasant, sweet	9.69
9. Extractant – aqueous-alcoholic mixture	Transparent	Alcoholly	Abrupt	9.57

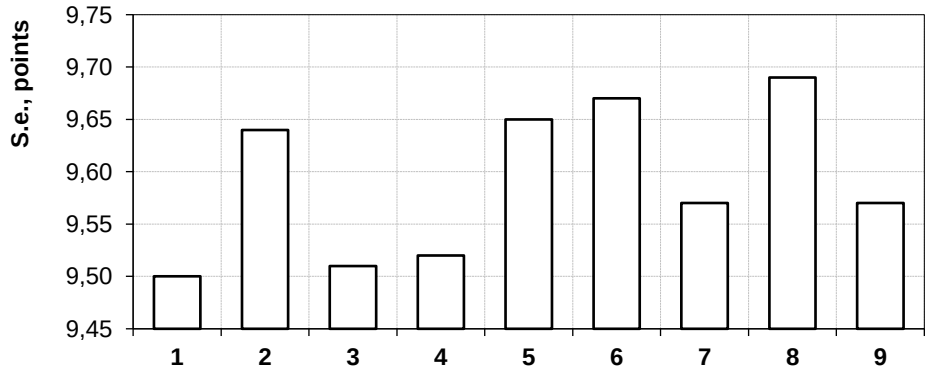

Figure 3. Sensory evaluation indicators of extracts on the extractant:
1 – Perilla frutescens; 2 – Elsholtzia stauntonii Benth; 3 – Artemisia abrotanum;
4 – Monarda didyma; 5 – Agastache foeniculum; 6 – Satureja hortensis;
7 – Ruta graveolens; 8 – Nepeta transcaucasica Grossch; 9 – aqueous-alcoholic mixture

Antioxidant capacity

Physicochemical studies, namely determination of the *pH* level and *RP* (Prévost, Brillet-Viel, 2014; Nicoli et al., 2004) [41, 42], were performed according to the method (Priluckij, 1997) [37] and calculations given above (Kuzmin et al., 2016) [2]. As a result of extraction received infusions (Andreou et al., 2018; Chandrasekara, Shahidi, 2018; Iannitti, Palmieri, 2009; Halliwell, Gutteridge, 1990; Kawa-Rygielska et al., 2019) [4-8], physicochemical indicators (Breiter et al., 2011; Dube et al., 2017 [19, 20] of which are presented in the Table 5.

Table 5

Quality indicators of extracts on extractant

Plant raw materials	***t*, °C**	***pH***	Eh_{min}**, mV**	Eh_{act}**, mV**	***RE*, mV**
1. Perilla frutescens	18	7.07	235.8	123	112.8
2. Elsholtzia stauntonii Benth	17	7.04	237.6	117	120.6
3. Artemisia abrotanum	16	7.18	229.2	118	111.2
4. Monarda didyma	17	6.79	252.6	132	120.6
5. Agastache foeniculum	17	6.66	260.4	132	128.4
6. Satureja hortensis	17	7.20	228.0	125	103.0
7. Ruta graveolens	16	6.73	256.2	118	138.2
8. Nepeta transcaucasica Grossch	19	7.10	234.0	134	100.0
9. Aqueous-alcoholic mixture	*18*	*7.96*	*182.4*	*180*	*2.4*
min	**16**	**6.66**	**228.0**	**117**	**100.0**
max	**19**	**7.20**	**260.4**	**134**	**138.2**

where: *t* – temperature of infusion; *pH* – active acidity of the test solution; Eh_{min} – minimal theoretically expected meaning of *RP*; Eh_{act} – actual measured *RP*; *RE* – recovery energy

Figures 4–7 show graphically the change in the physicochemical indicators of the quality of extracts of spicy-aromatic raw materials on the extractant.

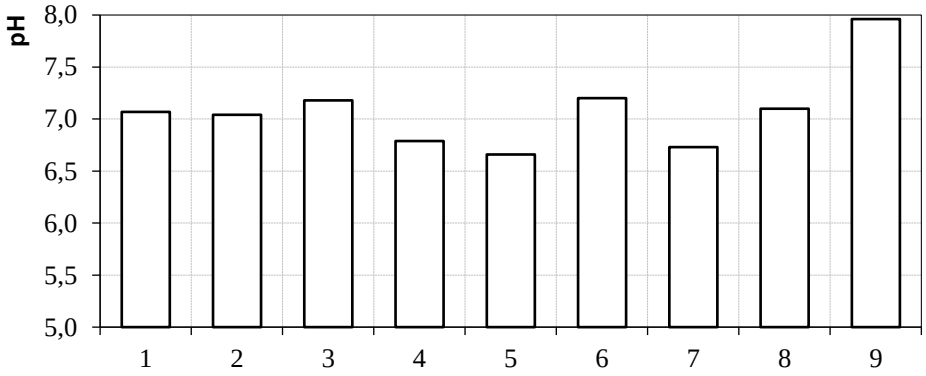

Figure 4. Hydrogen index (pH) of infusions of the investigated raw material:
1 – Perilla frutescens; 2 – Elsholtzia stauntonii Benth; 3 – Artemisia abrotanum; 4 – Monarda didyma; 5 – Agastache foeniculum; 6 – Satureja hortensis; 7 – Ruta graveolens; 8 – Nepeta transcaucasica Grossch; 9 – Aqueous-alcoholic mixture

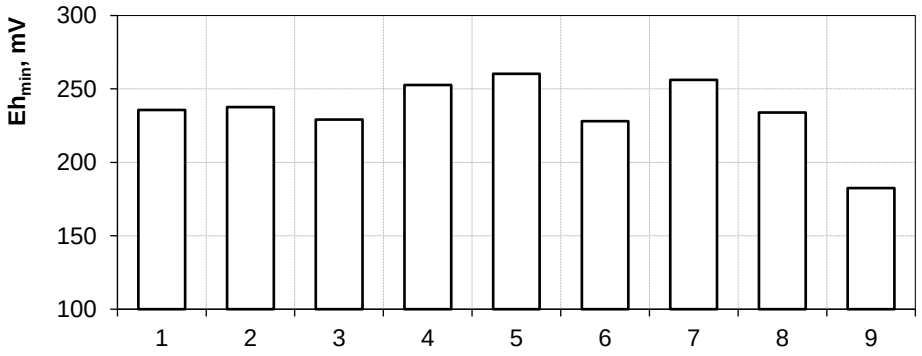

Figure 5. The minimum theoretical value of RP (Eh$_{min}$) of infusions of the investigated raw material

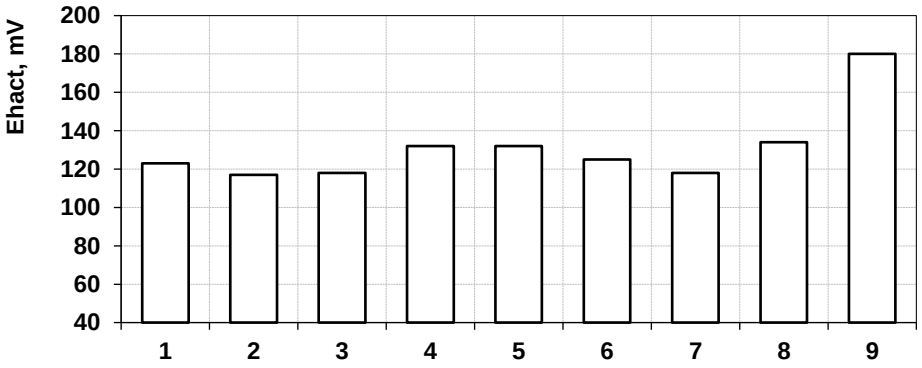

Figure 6. The actual measured RP of infusions (Eh$_{act}$) of infusions of the investigated raw material

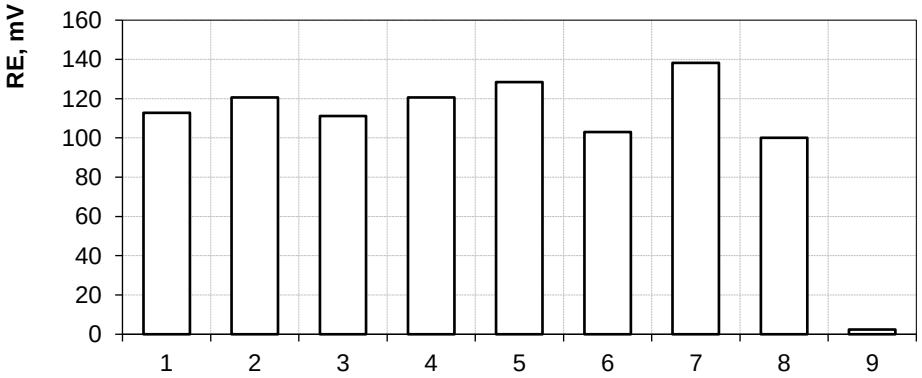

Figure 7. Recovery energy (RE) of infusions of the investigated raw material

For Figures 5–6: 1 – Perilla frutescens; 2 – Elsholtzia stauntonii Benth; 3 – Artemisia abrotanum; 4 – Monarda didyma; 5 – Agastache foeniculum; 6 – Satureja hortensis; 7 – Ruta graveolens; 8 – Nepeta transcaucasica Grossch; 9 – Aqueous-alcoholic mixture

The minimum theoretical value of *RP* (Eh_{min}) for plant aqueous-alcoholic infusions (Priluckij, 1997) [37] was obtained, which has a value from 228.0 mV (*Satureja hortensis*) to 260.4 mV (*Agastache foeniculum*). The actual measured *RP* of infusions (Eh_{act}) was established – from 117 mV (*Elsholtzia stauntonii Benth*) to 134 mV (*Nepeta transcaucasica Grossch*). The hydrogen index for aqueous-alcoholic infusions from spicy-aromatic raw materials has a value of 6.66 units *pH* (*Agastache foeniculum*) to 7.20 units *pH* (*Satureja hortensis*).

Aqueous-alcoholic infusions from vegetable raw materials and a volume fraction of ethanol of 40% have the value of regenerative capacity (recovery energy – *RE*) in the range from *RE* 100.0 mV (*Nepeta transcaucasica Grossch*) to *RE* 138.2 mV (*Ruta graveolens*). For the restaurant business in the manufacture of alcoholic beverages are promising aqueous-alcoholic infusions of *Ruta Gravelens* and *Nepeta transcaucasica Grossch*, which received increased antioxidant characteristics *RE* 138.2 mV and *RE* 100.0 mV, respectively, and positive sensory evaluation (*S.e.*) 9.57 and *S.e.* 9.69 points.

The prescription composition of alcoholic beverages may include aqueous-alcoholic infusions with a mass fraction of extractives – up to 60 g/100 cm^3 (liqueur).

Determination of Pearson's linear correlation

According to the physicochemical and sensory evaluation, mathematical and statistical analysis (Hinkle et al., 2003; Shendrik et al., 2019) [39, 40] was performed in the Pearson correlation matrix (Table 6).

Table 6

Marked correlations (*r*) are significant at *p*<0,05; *N*=9

	t	***pH***	***Eh$_{min}$***	***Eh$_{act}$***	***RE***	***S.e.***
t	1,00	0,40	-0,40	0,48	-0,46	0,30
pH	0,39	1,00	**-1,00**	**0,76**	**-0,95**	-0,06
Eh$_{min}$	-0,39	**-1,00**	1,00	**-0,76**	**0,95**	0,06
Eh$_{act}$	0,48	**0,80**	**-0,80**	1,00	**-0,93**	0,01
RE	-0,46	**-0,90**	**0,90**	**-0,93**	1,00	0,03
S.e.	0,30	-0,10	0,10	0,01	0,03	1,00

where: *t* – temperature of infusion; *pH* – active acidity of the test solution; *Eh$_{min}$* – minimal theoretically expected meaning of *RP*; *Eh$_{act}$* – actual measured *RP*; *RE* – recovery energy; S.e. – sensory evaluation

According to the obtained matrix 6*6, it was found that of the 6 indicators (*t*, *pH*, *Eh$_{min}$*, *E$_{hact}$*, *RE*, *S.e.*), only 4 indicators are statistically significant. As a result of research it was found that physicochemical parameters (*t*, *pH*, *Eh$_{min}$*, *Eh$_{act}$*, *RE*) are statistically insignificant for sensory evaluation (*S.e.*), because the correlation coefficient is very weak (*r*=0.0–0.3). Also, a weak (*r*=0.3–0.5) and very weak (*r*=0.0–0.3) relationship is observed between temperature (*t*) and other physicochemical and sensory evaluation. The range of values with very high correlation (*r*=0.9–1.0) includes the following indicators: *pH*, *Eh$_{min}$*, *E$_{hact}$*, *RE*.

Figure 8 shows the graphical dependence of *pH* on *Eh$_{min}$*. It was found that the *pH* is in the range of 6.66–7.96, and *Eh$_{min}$* 182.4–260.4 mV. According to the obtained equation, at a *pH* value of 7.00 *Eh$_{min}$* is 240 mV. When the *pH* value changes by 1 (*pH* 8.00), the *Eh$_{min}$* decreases by 60 mV (*Eh$_{min}$* 180 mV). That is, the relationship between *Eh$_{min}$* and *pH* is very high, because *r*=-1, because it is inversely correlated, which leads to an increase in *pH* to a

decrease in the level of Eh_{min}. Based on the research, it was found that the addition to the aqueous-alcoholic system with a weakly alkaline environment of vegetable spicy-aromatic raw materials, which leads to acidification and reduction of the *pH* level in the neutral environment (*pH* 6.66–7.20).

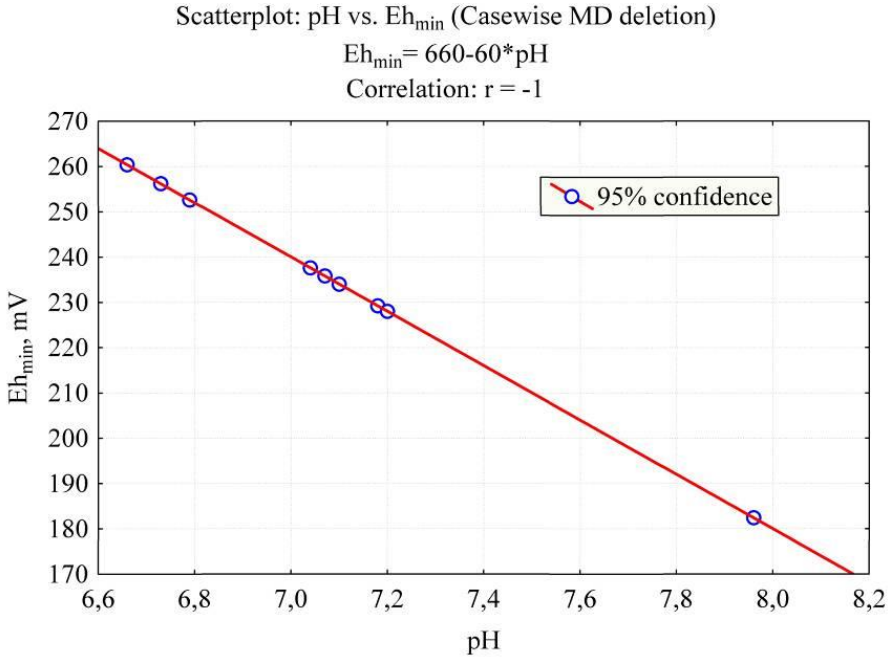

Figure 8. Dependence of *pH* level on the *RP* (Eh_{min})

Figures 9–13 show the graphical dependence of the *pH* level, Eh_{act}, Eh_{min}, *RE*.

It was found that Eh_{act} is in the range from 117 to 180 mV, and the *pH* is 6.66–7.96. At the value of Eh_{act} 120 mV, the *pH* level is 6.8. If you increase the *pH* to by one to 7.8 then the value of Eh_{act} will be 159 mV, i.e. Eh_{act} will increase by 39 mV. This is due to the fact that there is a very strong interdependence between the variables Eh_{act} and *pH* (r=0.8). As the *pH* value increases, the Eh_{act} index increases.

It was found that *RE* is in the range from 2.4 to 138.2 mV, and the *pH* is 6.66–7.96. When the value of *RE* 132 mV, the *pH* level is 6.8. If you increase the *pH* by one to 7.8, the value of *RE* will be 32 mV. Increasing the *pH* per unit from 6.8 to 7.8 leads to a decrease in *RE* by 100 mV. This is due to the fact that there is a very strong interdependence between the variables *RE* and *pH* (r=-0.9). As the *pH* value increases, the *RE* decreases.

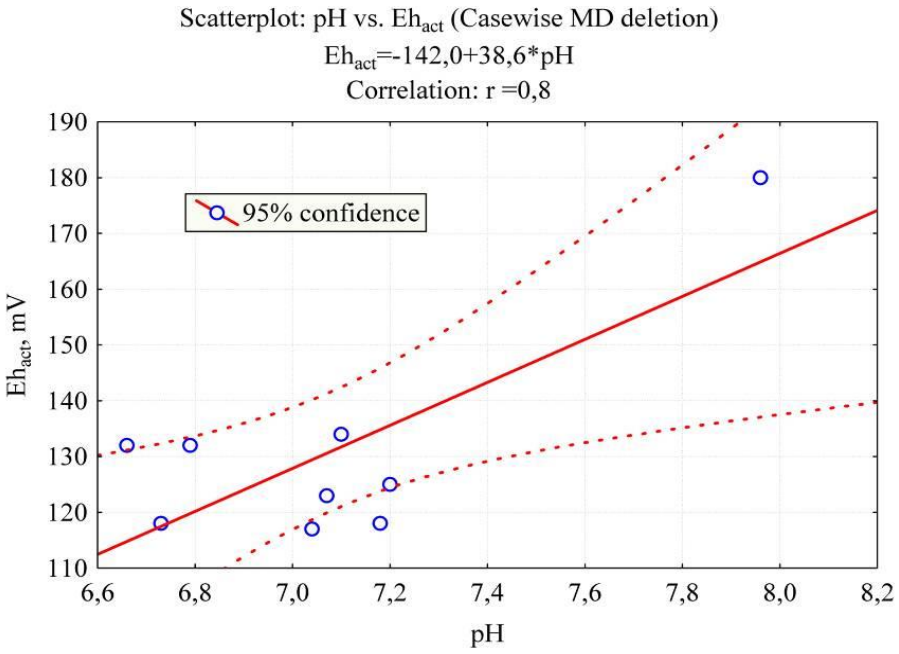

Figure 9. Dependence of *pH* level on the *RP* (*Eh$_{act}$*)

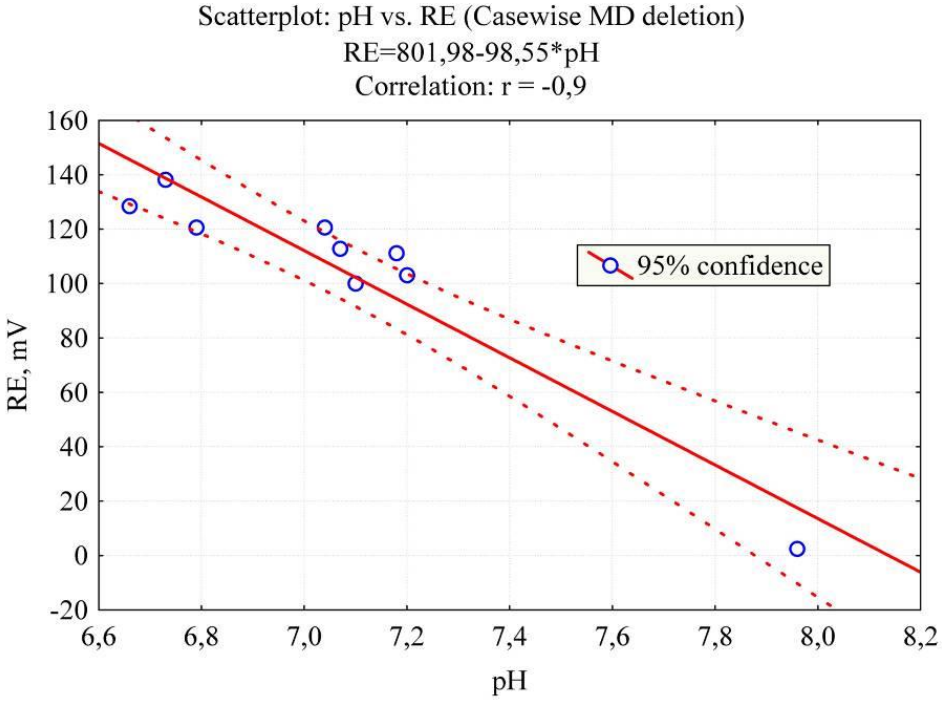

Figure 10. Dependence of *pH* level on reduction energy (*RE*)

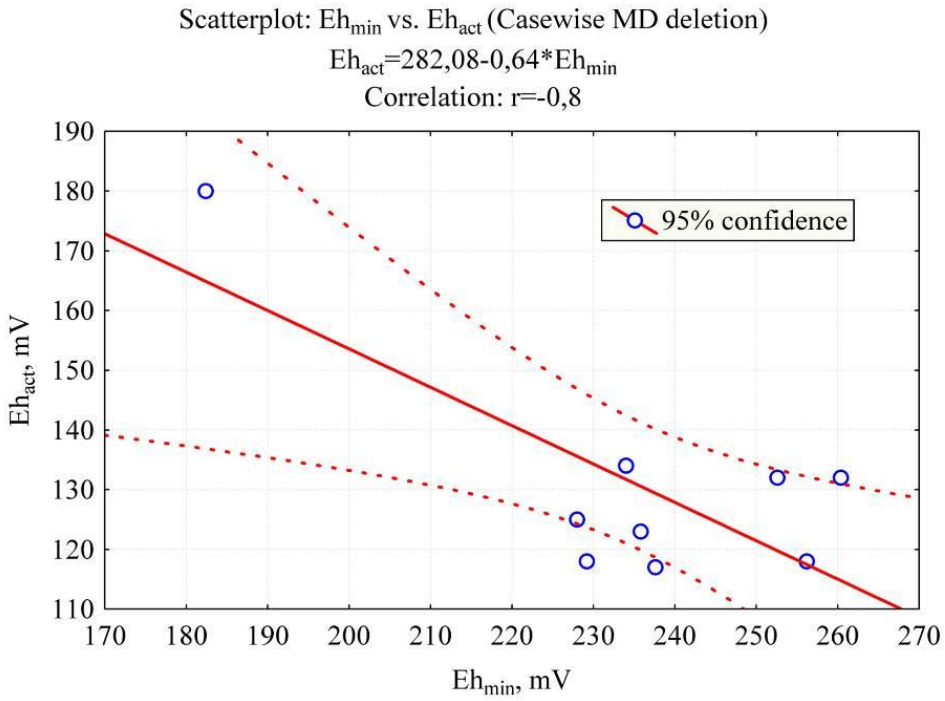

Figure 11. Dependence of *RP* (*Eh_{min}*) on *RP* (*Eh_{act}*)

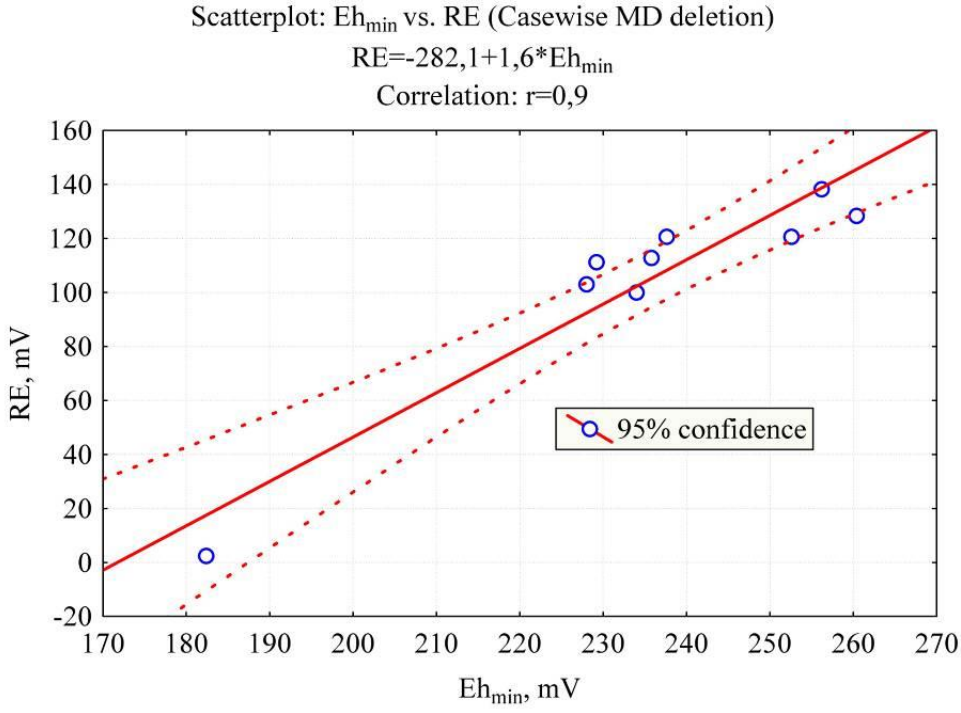

Figure 12. Dependence of *RP* (*Eh_{min}*) on reduction energy (*RE*)

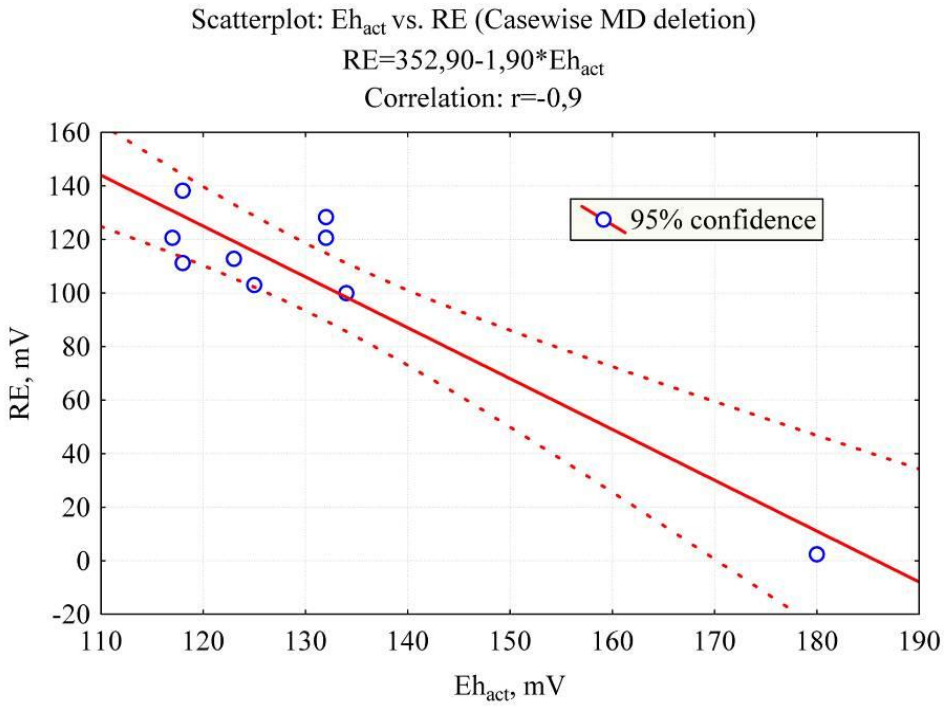

Figure 13. Dependence of *RP* (*Eh$_{act}$*) on reduction energy (*RE*)

The general graph of the three most correlation-significant physicochemical parameters is shown in Figure 14. In volumetric form, it is seen that some points (*Eh$_{act}$*, *RE*, *Eh$_{min}$*) are as close as possible to the surface, i.e. there is a very strong correlation between them. The farther the points are from the surface, the weaker the relationship.

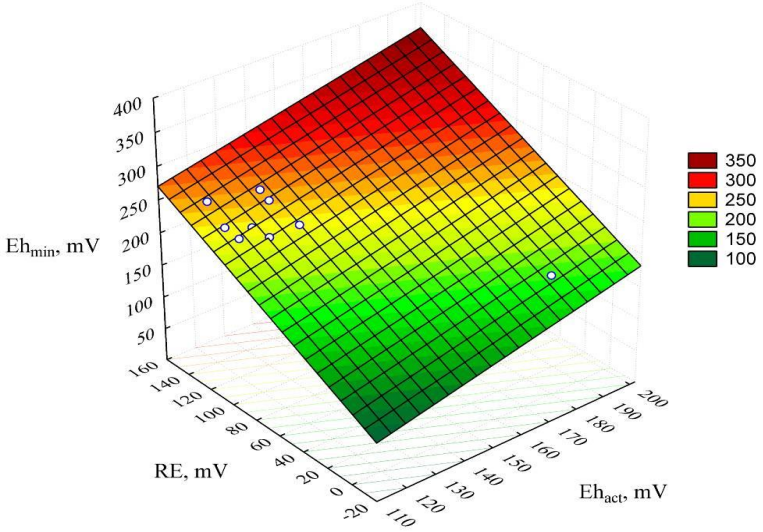

Figure 14. Response surface of *RP* (*Eh$_{act}$*) from reduction energy (*RE*) and *RP* (*Eh$_{min}$*)

Figures 15-19 show graphs with histograms that show the frequency of variable values in individual intervals. The histogram visually represents the distribution of a continuous numerical variable, which measures the frequency of occurrence of similar values in the data set. The x-axis shows the numerical values, which are divided into ranges. Each range corresponds to a column of the histogram; the width of the column corresponds to the value of the interval, and the height is the number of elements in the data set, the values of which fall into this interval.

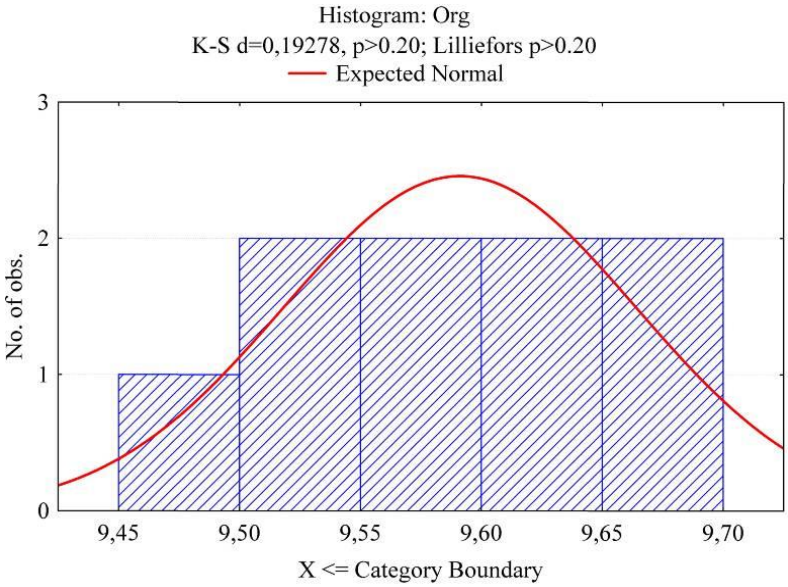

Figure 15. Histogram of the distribution of sensory evaluation (S.e.)

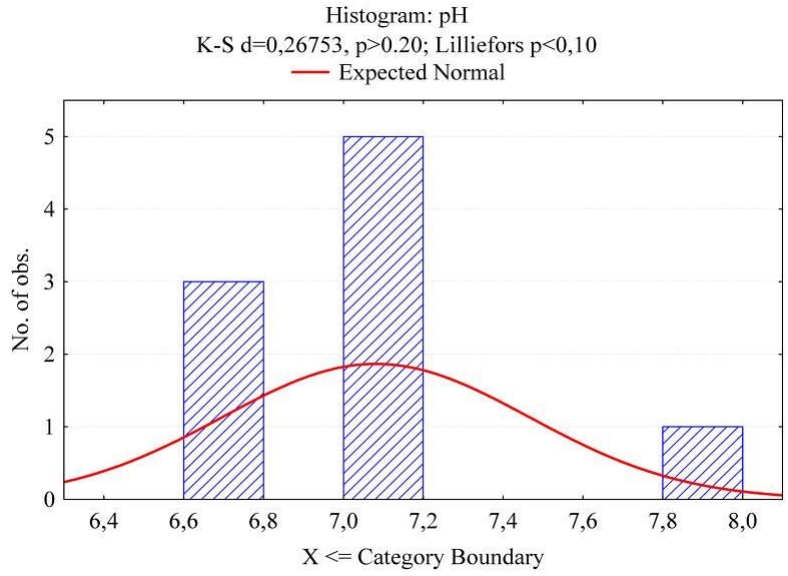

Figure 16. Histogram of the distribution of *pH* values

The histogram of the distribution of sensory evaluation is shown in Figure 15. Numerical values are divided into ranges with an interval of 0.5, starting from 9.45 to 9.70 points. Only 5 ranges and the same number of columns. The maximum frequency is typical for 4 ranges in the range 9.50–9.70 points – 8 values of the variable. The lowest frequency has the range 9.45–9.50 points, which got 1 value of the variable.

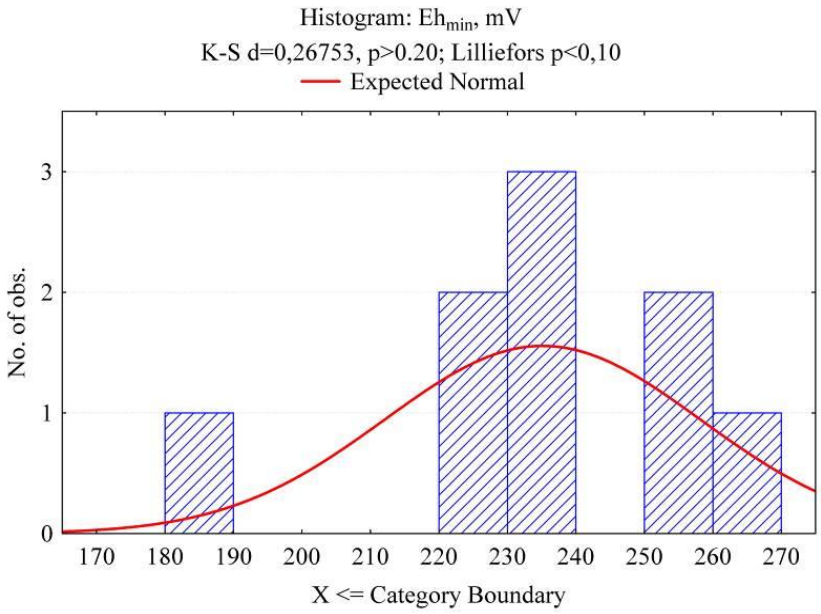

Figure 17. Histogram of the distribution of values of the level of *RP* (*Eh_{min}*)

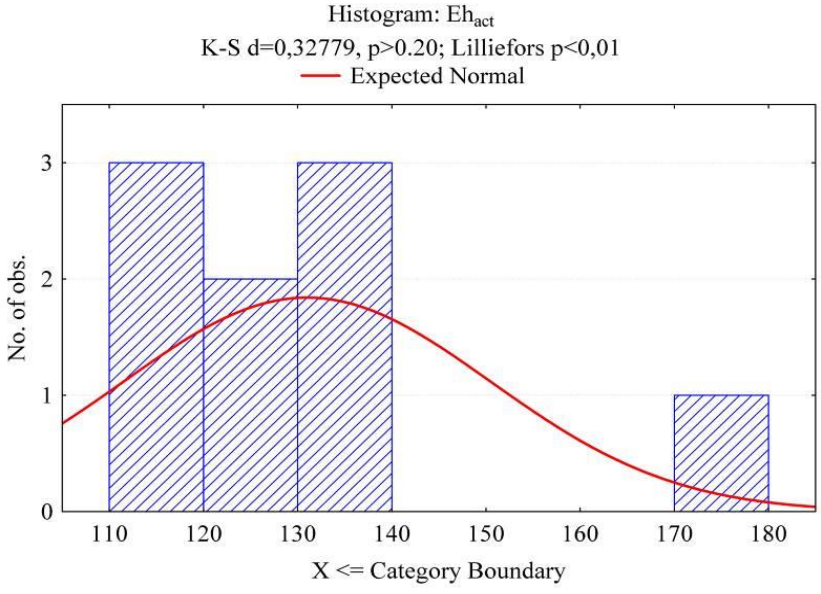

Figure 18. Histogram of the distribution of values of the level of *RP* (*Eh_{act}*)

Figure 16 shows the distribution of pH values, the range of which is divided into 3 columns. It is established that 9 data elements lie in the range of *pH* values 6.6–8.0. The highest frequency 5 is the range of *pH* values 7.0–7.2, 3 – in the range of *pH* values 6.6–6.8, and only 1 – in the range 7.8–8.0, which is the lowest frequency.

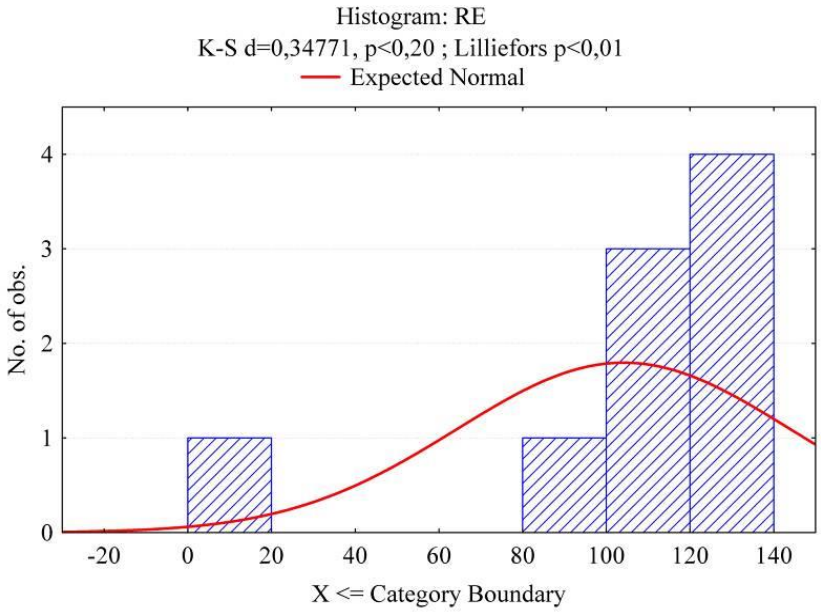

Figure 19. Histogram of the distribution of recovery energy values (*RE*)

Figure 17 shows the histogram of *RP* (Eh_{min}). The x-axis is divided into 5 ranges ranging from 180 to 270 mV. According to the values of the elements in the data set, only 5 columns. The maximum frequency is typical for the range 230–240 mV, which includes 3 elements. The lowest frequency is characteristic for the ranges 180–190 mV, 260–270 mV, which includes 1 element.

The value of the histogram (Eh_{act}) (Figure 18) is divided into 4 ranges, starting with 110 and ending with 180 mV. The maximum repetition rate is typical for the range 110–120 mV and 130–140 mV, each includes 3 values. The lowest frequency of the ranges is 170–180 mV, which includes 1 element.

Figure 19 shows a histogram of *RE*, which includes 4 ranges starting from 0 to 140 mV. The maximum frequency, which consists of 4 elements, belongs to the range 120–140 mV, and the lowest 0–20 mV and 80–100 mV, which include 1 element.

Histograms allow you to develop statistics on the frequency of values in a certain range. They are a generalized view of the data obtained during sensory evaluation and physicochemical values (Shendrik et al., 2019) [40].

Based on mathematical and statistical analysis, it was found that physicochemical parameters (*pH*, Eh_{min}, Eh_{act}, *RE*) are statistically insignificant for sensory evaluation (*S.e.*) and infusion temperature (*t*). The range of values with very high correlation (r=0.9–1.0) includes the following indicators: *pH*, Eh_{min}, Eh_{act}, *RE*.

Development of recipes of alcoholic beverages

On the basis of the obtained results, it was established that the maximum values of *RP* have extracts of *Ruta graveolens* and *Nepeta transcaucasica Grossch*. These extracts were used in the preparation of cocktails, the recipes of which are presented in Table 7-8.

Table 7

Composition of the cocktail «Mint mulled wine»

Ingredients	Content, %
Red wine	62.65
Extract of *Nepeta transcaucasica Grossch*	25.0
Sugar	12.0
Nutmeg, cloves, cinnamon, allspice	0.35

Table 8

Composition of the cocktail «Pomegranate grog»

Ingredients	Content, %
Extract of *Ruta graveolens*	27.0
Ginger	0.5
Grenadine	8.5
Lemon fresh	14.0
Black tea	50.0

The data obtained are correlated with the basic scientific concepts which are displayed in the works (Kamdem et al., 2013; Frolova et al., 2019; Gerolis et al., 2017; Imark et al., 2000; Pyrzynska, Sentkowska, 2019; Wong et al., 2020; Sentkowska, Pyrzynska, 2018; Siddiqui et al., 2018; Steenkamp et al., 2004; Ruiz-Ruiz et al., 2020; Naithani et al., 2006; Buglass et al., 2012; Grunert et al., 2018; Gullón et al., 2018; Gulua et al., 2018; Joubert, Beer, 2012; Silka et al., 2016; Naumenko et al., 2015; Frolova, Korablova, 2016) [10–18, 25, 26, 30–34, 43–45], regarding the processes of extracting of plant materials.

Improvement of the technology of alcoholic beverages (Andreou et al., 2018; Chandrasekara, Shahidi, 2018; Iannitti, Palmieri, 2009; Halliwell, Gutteridge, 1990; Kawa-Rygielska et al., 2019; Fotakis et al., 2016; Vergun et al., 2018; Vergun et al., 2019; Kurylo et al., 2018) [4–9, 27–29] is due to the addition of spicy-aromatic aqueous-alcoholic infusions. It allows to increase the antioxidant properties of the product (Breiter et al., 2011; Dube et al., 2017; Keating et al., 2014; Oh et al., 2013; Herrera et al., 2018; Humia et al., 2020; Vergun et al., 2018; Vergun et al., 2019; Kurylo et al., 2018) [19–24, 27–29], will help to increase the immunity of the human body, improve the metabolism, positively affect the cardiovascular system, in addition it increases the consumer properties and will allow to reduce the cost of the finished product.

Conclusions

1. It is established that one of the promising ways of forming consumer properties and expanding the range of alcoholic products is the use of new types of spicy-aromatic plants, which include biologically active substances. Such substances improve the sensory evaluation of beverages, contribute to the promotion of human health (antioxidant effects, enhancing redox reactions).
2. Experimental studies show that all aqueous-alcoholic infusions of aromatic origin contain antioxidant systems. It was found that the recovery value of all the tested extracts is positive and ranges from 100.0 to 138.2 mV.
3. Histograms allow you to develop statistics on the frequency of values in a certain range. They are a generalized view of the data obtained during sensory evaluation and physicochemical values.
4. Based on mathematical and statistical analysis, it was found that the infusion temperature (*t*) has a statistically insignificant effect on physicochemical parameters (*pH*, Eh_{min}, Eh_{act}, *RE*), which have a statistically insignificant effect on sensory evaluation (*S.e.*). The range of values with very high correlation (r=0.9–1.0) includes the following indicators: *pH*, Eh_{min}, Eh_{act}, *RE*.
5. Improvement of the technology of alcoholic cocktails by adding spicy-aromatic aqueous-alcoholic infusions allows to increase the redox properties of the product, increases consumer properties and reduces the cost of the finished product.

References

1. Dubovkina I., Davydenko B., Rikhter V. (2019), Modelling of the hydrodynamic conditions throughout liquid system treatment by alternating impulses of pressure, *Ukrainian Food Journal*, 8(2), pp. 343–354.
2. Kuzmin O., Kovalchuk Y., Velychko V., Romanchenko N. (2016), Improvement technologies of aqueous-alcoholic infusions for the production of syrups, *Ukrainian Journal of Food Science*, 4(2). pp. 258–275.
3. Kuzmin O., Levkun K., Riznyk A. (2017), Qualimetric assessment of diets, *Ukrainian Food Journal*, 6(1), pp. 46–60.
4. Andreou V., Strati I.F., Fotakis C., Liouni M., Sinanoglou V.J. (2018), Herbal distillates: A new era of grape marc distillates with enriched antioxidant profile, *Food Chemistry*, 253, pp. 171–178.
5. Chandrasekara A., Shahidi F. (2018), Herbal beverages: Bioactive compounds and their role in disease risk reduction – A review, *Journal of Traditional and Complementary Medicine*, 8(4), pp. 451–458.
6. Iannitti T., Palmieri B. (2009), Antioxidant therapy effectiveness: an up to date, *European Review for Medical and Pharmacological Sciences*, 13, pp. 245–278.
7. Halliwell B., Gutteridge J.M.C. (1990), The antioxidants of human extracellular fluids, *Archives of Biochemistry and Biophysics*, 280, pp. 1–8.
8. Kawa-Rygielska J., Adamenko K., Kucharska A.Z., Szatkowska K. (2019), Fruit and herbal meads – Chemical composition and antioxidant properties, *Food Chemistry*, 283, pp. 19–27.
9. Fotakis C., Tsigrimani D., Tsiaka T., Lantzouraki D.Z., Zoumpoulakis P. (2016), Metabolic and antioxidant profiles of herbal infusions and decoctions, *Food Chemistry*, 211, pp. 963–971.

10. Kamdem J.P., Olalekan E.O., Hassan W., Kade I.J., Rocha J.B.T. (2013), Trichilia catigua (Catuaba) bark extract exerts neuroprotection against oxidative stress induced by different neurotoxic agents in rat hippocampal slices, *Industrial Crops and Products*, 50, pp. 625–632.
11. Frolova N., Ukrainets A., Sylka I., Nemirich A., Kuzmin O. (2019), Separation of terpenes from lemon essential oil by selective fractionation under a vacuum, *Eastern-European Journal of Enterprise Technologies*, 2/11(98), pp. 32–36.
12. Gerolis L.G.L., Lameiras F.S., Krambrock K., Neves M.J. (2017), Effect of gamma radiation on antioxidant capacity of green tea, yerba mate, and chamomile tea as evaluated by different methods, *Radiation Physics and Chemistry*, 130, pp. 177–185.
13. Imark C., Kneubühl M., Bodmer S. (2000), Occurrence and activity of natural antioxidants in herbal spirits, *Innovative Food Science & Emerging Technologies*, 1 (4), pp. 239–243.
14. Pyrzynska K., Sentkowska A. (2019), Herbal Beverages as a Source of Antioxidant Phenolics, *Natural Beverages*, 5, pp. 125–142.
15. Wong F.C., Xiao J., Wang S., Ee K.Y., Chai T.T. (2020), Advances on the antioxidant peptides from edible plant sources, *Trends in Food Science & Technology*, 99, pp. 44–57.
16. Sentkowska A., Pyrzynska K. (2018), Investigation of antioxidant interaction between Green tea polyphenols and acetaminophen using isobolographic analysis, *Journal of Pharmaceutical and Biomedical Analysis*, 15910, pp. 393–397.
17. Siddiqui N.A., Al-Yousef H.M., Alhowiriny T.A., Alam P., Abdallah R.H. (2018), Concurrent analysis of bioactive triterpenes oleanolic acid and β-amyrin in antioxidant active fractions of Hibiscus calyphyllus, Hibiscus deflersii and Hibiscus micranthus grown in Saudi Arabia by applying validated HPTLC method, *Saudi Pharmaceutical Journal*, 26, pp. 266–273.
18. Steenkamp V., Fernandes A.C., Rensburg C.E.J., Jäger A.K. (2004), Antioxidant scavenging potential of South African export herbal teas, *South African Journal of Botany*, 70(4), pp. 660-663.
19. Breiter T., Laue C. Kressel G., Gröll S., Hahn A. (2011), Bioavailability and antioxidant potential of rooibos flavonoids in humans following the consumption of different rooibos formulations, *Food Chemistry*, 128(215), pp. 338–347.
20. Dube P., Meyer S., Marnewick J.L. (2017), Antimicrobial and antioxidant activities of different solvent extracts from fermented and green honeybush (Cyclopia intermedia) plant material, *South African Journal of Botany*, 110, pp. 184–193.
21. Keating L., Hayes J., Moane S., Lehane M., Furey A. The effect of simulated gastro-intestinal conditions on the antioxidant activity of herbal preparations made from native Irish hawthorn. *Journal of Herbal Medicine*. 4(3). 2014. pp. 127–133.
22. Oh J., Jo H., Cho A.R., Kim S.J., Han J. (2013), Antioxidant and antimicrobial activities of various leafy herbal teas, *Food Control*, 31(2), pp. 403–409.
23. Herrera T., Aguilera Y., Rebollo-Hernanz M., Bravo E., Martín-Cabrejas M.A. (2018), Teas and herbal infusions as sources of melatonin and other bioactive non-nutrient components, *LWT*, 89, pp. 65–73.
24. Humia B.V., Santos K.S., Schneider J.K., Leal I.L., Padilha F.F. (2020), Physicochemical and sensory profile of Beauregard sweet potato beer, *Food Chemistry*, 312.
25. Ruiz-Ruiz J.C., Aldana G.C.E, Cruz A.I.C., Segura-Campos M.R. (2020), Antioxidant Activity of Polyphenols Extracted From Hop Used in Craft Beer, *Biotechnological Progress and Beverage Consumption*, 9, pp. 283–310.
26. Naithani V., Nair S., Kakkar P. (2006), Decline in antioxidant capacity of Indian herbal teas during storage and its relation to phenolic content, *Food Research International*, 39(2), pp. 176–181.
27. Vergun O., Kačaniova M., Rakhmetov D., Shymanska O., Bondarchuk O., Brindza J., Ivanišová E. (2018), Antioxidant and antimicrobial activity of Bunias orientalis L. and

Scorzonera hispanica L. ethanol extracts, Agrobiodiversity for Improving Nutrition, Health and Life Quality, 2, pp. 29–38.
28. Vergun O., Svydenko L., Grygorieva O., Shymanska O., Rakhmetov D., Brindza J., Ivanišová E. (2019), Antioxidant capacity of plant raw material of Scutellaria baicalensis Georgi, Potravinarstvo Slovak Journal of Food Science, 13(1), pp. 614–621.
29. Kurylo V.L., Rakhmetov D.B., Kulyk M.I. (2018), Biological features and potential of yield of energy crops of the thin-skinned family in the conditions of Ukraine, *Bulletin of Poltava State Agrarian Academy*, 1, pp. 11-17.
30. Buglass A.J., Caven-Quantrill D.J. (2012), Applications of natural ingredients in alcoholic drinks, *Natural Food Additives, Ingredients and Flavourings*, 16, pp. 358–416.
31. Grunert K.G., Hieke S., Juhl H.J. (2018), Consumer wants and use of ingredient and nutrition information for alcoholic drinks: A cross-cultural study in six EU countries, *Food Quality and Preference*, 63, pp. 107–118.
32. Gullón B., Eibes G., Moreira M.T., Herrera R., Gullón P. (2018), Yerba mate waste: A sustainable resource of antioxidant compounds, *Industrial Crops and Products*, 113, pp. 398–405.
33. Gulua L., Nikolaishvili L., Jgenti M., Turmanidze T., Dzneladze G. (2018), Polyphenol content, anti-lipase and antioxidant activity of teas made in Georgia, *Annals of Agrarian Science*, 16 (3), pp. 357–361.
34. Joubert E., Beer D. (2012), Phenolic content and antioxidant activity of rooibos food ingredient extracts, *Journal of Food Composition and Analysis*, 27(1). pp. 45–51.
35. Merwe J.D., Beer D., Swanevelder S., Joubert E., Gelderblom W.C.A. (2017), Dietary exposure to honeybush (Cyclopia) polyphenol-enriched extracts altered redox status and expression of oxidative stress and antioxidant defense-related genes in rat liver, *South African Journal of Botany*, 110, pp. 230–239.
36. Bahir V.M. (1999), *Sovremennye tehnicheskie jelektrohimicheskie sistemy dlja obezzarazhivanija, ochistki i aktivirovanija vody*, VNIIIMT.
37. Priluckij V.I. (1997), *Okislitel'no-vosstanovitel'nyj potencial dlja harakteristiki protivokislitel'noj aktivnosti razlichnyh napitkov i vitaminnyh komponentov*, Jelektrohim. aktivacija v medicine, sel. hozjajstve, prom-sti: I Mezhdunar. Simpozium.
38. Rakhmetov D.B. (2011), *Teoretychni ta prykladni aspekty introduktsiyi roslyn v Ukrayini*, Kiev: Ahrar Media Crup.
39. Hinkle D.E., Wiersma W., Jurs S.G. (2003), *Applied statistics for the behavioral sciences*, Boston, Mass: Houghton Mifflin.
40. Shendrik T., Levandovskyi L., Kuts A., Prybylskyi V., Karputina M. (2019), Correlation between the quality indicators of activated coal in vodka technology, *Ukrainian Journal of Food Science*, 7(1), pp. 33–48.
41. Prévost H., Brillet-Viel A. (2014), Ecology of bacteria and fungi in foods, Influence of Redox Potential, *Encyclopedia of Food Microbiology (Second Edition)*, pp. 595–601.
42. Nicoli M.C., Toniolo R., Anese M. (2004), Relationship between redox potential and chain-breaking activity of model systems and foods, *Food Chemistry*, 88(1), pp. 79–83.
43. Silka I., Frolova N., Huts V. (2016), Kinetic model of the quality change of modern foodstuffs, *Food Science and Technology*, 10(1), pp. 11–15.
44. Naumenko K., Petrusha O., Frolova N., Fedorenko O. (2015), Quality assessment of extracts from unconventional plant raw materials, *Eastern-European Journal of Enterprise Technologies*, 4(10), pp. 49–54.
45. Frolova N., Korablova O. (2016), Scientific basis of use of fruits coriandrum sativum L. in food technologies, *Potravinarstvo Slovak Journal of Food Sciences*, 10(1), pp. 469–474.

Influence of alpha acids hop homologues of bitter and aromatic varieties on beer quality

Lidia Protsenko[1], Serhii Ryzhuk[1], Mykola Liashenko[1], Oleksandr Shevchenko[2], Svitlana Litvynchuk[2], Liliia Yanse[3], Henrikh Milosta[4]

1 – Polissya Institute of Agriculture of NAAS of Ukraine, Zhytomyr, Ukraine
2 – National University of Food Technologies, Kyiv, Ukraine
3 – National Academy of Agrarian Sciences of Ukraine, Kyiv, Ukraine
4 – Educational institution "Grodno State Agrarian University", Grodno, Belarus

Keywords:

Hop
Alpha-acids
Cohumulone
Wort
Beer

Article history:

Received 08.08.2019
Received in revised form 20.12.2019
Accepted 30.06.2020

Corresponding author:

Svitlana Litvynchuk
E-mail: Litvynchuk@nuft.edu.ua

DOI:
10.24263/2304-974X-2020-9-2-13

Abstract

Introduction. The aim of the study was to study the bitter substances of hops to establish the dependence of the bitterness of the wort and the quality of beer hops on the quantitative and qualitative composition of alpha-acids hop homologues, in particular, on the content of cohumulone in alpha-acids.

Materials and methods. Aromatic and bitter hops with different content of cohumulone in the composition of alpha-acids and beer made from it were studied. High-performance liquid chromatography was used to determine the amount and composition of hop bitter substances and products of their transformation in the brewing process as well as spectrophotometric methods of quality control of the bitterness of hopped wort and finished beer.

Results and discussion. It is noted that alpha-acids of the studied varieties contain a wide range of cohumulone content: from 19.6% in hops of Alta variety to 43.8% in hops of Ruslan variety. Establishing the relationship between the quantity and quality of bitter substances of hops and the bitterness and quality of hopped wort and beer show that with increasing mass fraction of cohumulone in the composition of alpha-acids of aromatic hops by 1% with a ratio of beta-acids to alpha-acids of 1.11–1.34 the value of bitterness of the wort hopped by them increases from 0.69% for Gaidamats'kyi variety to 1.05% for Slovyanka variety. In bitter hops, the ratio of beta-acids to alpha-acids is much lower and is 0.51–0.74. Analysis of the relationship between the growth of cohumulone and the change in the bitterness of the wort hopped with bitter varieties shows that with increasing the share of cohumulone in the alpha-acids of bitter hops by 1% the bitterness of hop wort increases from 0.19% for Ruslan to 0.38% for the variety Promin'. Between the bitterness of the wort and the amount of cohumulone with hops when using both bitter and aromatic varieties, there is a strong relationship as evidenced by the correlation coefficient which is for bitter varieties $r = 0.90 \pm 0.10$, for aromatic $r = 0.98 \pm 0.20$. In the formation of the bitterness of the wort, hopped with aromatic varieties from the ratio of beta-acids to alpha-acids is more than one, the role of beta-acid compounds is much higher compared to bitter varieties.

Conclusions. When used for hop wort of bitter type hops with different composition of alpha-acids, their use is more effective in varieties with a high content of cohumulone.

Introduction

Previous research [1, 3–7] show that high-quality beer with a characteristic bitter taste and aroma can be obtained only with the use of hops and products of its processing of certain breeding varieties. This is due to the peculiarities of their biochemical composition, and above all, with the quantitative content and qualitative composition of bitter substances, polyphenolic compounds and essential oil of hops aromatic and bitter varieties [2, 8–10]. Different ratio of components of these compounds affects taste and aromatic properties of beer [11, 15].

Bitter substances, polyphenols and aromatic essential oils of hops take part in the formation of taste and aromatic properties of beer [1–3, 8–15]. The specific qualities of beer are most affected by isomers of the original bitter substances of hops, which are contained in cones in small quantities, and are formed during the boiling of wort with hops [1–3, 7]. Iso-alpha-acids are quantitatively the most important fraction of hops in beer. They give a typical bitter taste, and depending on the desired bitterness and type of beer, their concentration ranges from 10 to 100 mg/l [16]. Iso-alpha-acids are more soluble in beer wort and more bitter than alpha-acids and form 90–95% of the total bitterness of beer [1, 7]. In addition to the isomerization reaction, iso-alpha-acids undergo both oxidative and non-oxidative transformations. As a result, both the intensity and the quality of the bitterness of beer are negatively affected [16]. Trans-iso-alpha-acids in beer are significantly less stable than their counterparts. At the same time, a sharp, lingering bitter taste develops and an aroma defect is formed, which occurs during the aging of beer [16]. The formation of volatile substances from iso-alpha-acids after beer aging is explained by the process of cyclization of trans-iso-alpha-acids into tri- and tetracyclic decomposition products. These non-volatile breakdown products of trans-iso-alpha-acids have only recently been identified [16].

According to the results of research, in the formation of the bitterness of beer [1, 3, 7, 16] in the hop the main importance are alpha-acids, which consist of humulone, cohumulone, adhumulone, prehumulone and posthumulone. Insoluble alpha-acids are converted at high temperatures by hopping the wort into soluble iso-alpha-acids (isohumulone, isocohumulone, isoadhumulone), giving the beer a bitter taste [3, 8, 16]. Moreover, depending on the length of the side chains of the acyl residue in the second carbon atom of the hexadiene ring changes the solubility of alpha-acid homologues, and the rule is the longer the side chain, the lower the solubility. Therefore the solubility of cohumulone is much higher than that of humulone and adhumulone [1, 3, 7, 16]. When studying the bitterness and iso-alpha-acid content of some brands of Brazilian and North American beer [17] it was found that the isoadhumulone fraction was a fraction of lower concentration in all samples, and most samples showed a higher concentration of isohumulone. The range of isohumulone ranged from 3.0 to 17.0 mg/l.

Not all alpha-acids have a positive effect on the quality of bitterness in beer. It is known [1, 3, 7, 16, 17] that isohumulone, isocohumulone and isoadhumulone have approximately the same degree of bitterness. However, when the wort is boiled with hops, the isomerization of alpha-acid homologues proceeds with different formation of isocomponents. Of great importance is the quantitative ratio of homologues of alpha-acids. Czech hops (Zaaz variety) are characterized by a high content of humulone and adhumulone (up to 80%), while in German and American high-resin varieties such as Hercules, Tomahawk is dominated by cohumulone (up to 50%).

Cohumulone is converted to the isomer better than other components of alpha-acids. But this faction is attributed a negative role in the formation of the bitterness of beer [18]. However, although in Czech varieties the composition of alpha-acids is dominated by

humulone, the bitterness of Czech beer is represented mainly by isohumulone. In the processing of hops varieties with a predominant content of cohumulone, beer contains mainly isocohumulone, and the quality of bitterness according to M. Kusche and others. much worse [19-20]. It is possible that the qualitative difference in the composition of the original alpha-acids is also the reason for the known difference in the quality of beer, which is very significant. But the question remains whether varieties of hops with a high content of cohumulone create more bitterness in beer. It follows from the above that the selection of varieties with the optimal composition of bitter substances for beer with excellent and high quality bitterness is a topical issue for brewers of the American Association [18], European brewers [19] and Ukrainian beer producers [21].

As can be seen from the analysis of literature sources the composition of bitter substances of hops of European and American varieties and the influence of their homologues on the quality of beer bitterness are well studied. Instead, there have been almost no similar studies with Ukrainian hop varieties. In this regard to ensure stable and high-quality bitterness of beer it is important to investigate the effect of certain components of alpha-acids of Ukrainian hops on the qualitative and quantitative indicators of the drink.

The aim of the work was to study the bitter substances of hops, to establish the dependence of the bitterness of the wort and the quality of beer hops on the quantity and quality of homologues of alpha-acids of Ukrainian and European varieties, in particular the content of cohumulone in alpha-acids.

Materials and methods

The cones of pressed hops of Ukrainian and European selection of typical representatives of the aromatic group of varieties were used for research: Slovyanka, Nationalnyi, Zaaz, Gaidamats'kyi and bitter: Alta, Magnum, Northern Brewer, Promin', Ksanta, Ruslan and beer made from them.

Methods of research of bitter substances of hops. Bitter substances of hops from cones were extracted with an organic solvent – methanol [22]. The ratio between the mass of hop cones and the extractant was 1:10. The amount of alpha and beta-acids and the content of cohumulone in the composition of alpha-acids were determined by the international method of EMU 7.7 using liquid chromatography HPLC [23]. Chromatography was performed using a liquid chromatograph Ultimate 3000 with a UV detector at a temperature of 35 °C [1]. Used a column measuring 100 x 2.1 mm which was filled with sorbent Pinacle DV C18 3 μm [1]. A solution of methanol, water and acetonitrile in the ratio 38:24:38 was used as the mobile phase [24].

The international standard ICF-3 was used to quantify the components of bitter substances [23].

Methods for the presentation of wort and beer. Beer from the studied hop samples was produced at the mini-breweries of the Department of Hop and Beer Biochemistry of the Polissya Institute of Agriculture of the National Academy of Agrarian Sciences of Ukraine with a yield of 100 liters, which fully simulates the conditions of real enterprises on a scale of 1: 100, compact and allows to achieve research goals [2].

Rationing of hops in mini-brewery was performed on the content of alpha-acids in them. The wort was prepared from 100% barley malt. The hopping was performed at the rate of 60 mg of bitter substances per 1 liter of wort. After complete set the wort was boiled for 30

minutes. Then in the wort in each variant of the experiment was made hops of the presented varieties in two steps: 85% at the beginning of hopping, 15% – 15 minutes before the end of hopping. The total boiling time of hop wort was 90 minutes [21].

The bitterness of the wort formed during its boiling with hops, as a result of extraction and isomerization of bitter substances of hops, was determined on a spectrophotometer according to the method of EMU 8.8 (International method of IM) [23]. The method is based on measuring the optical density of the isooctane extract obtained by extracting bitter substances from acidified beer wort or beer with isooctane (2,2,4-trimethylpentane), on a spectrophotometer at a wavelength of 275 nm against isooctane [23]. The value of the rate, the number of turns in the units of the international scale for the value of the terms of the EBC were estimated on the basis of the optical index of the weight, as in the international units of the unit – EBC [23].

The beer quality was evaluated organoleptically at the tasting, hardened tasting committee of the designated Institute, for the 25-point integrated assessment [21].

Results and discussion

Bitter substances of hops of aromatic and bitter varieties

Complex biochemical studies of hops of different breeding varieties made it possible to establish that hops of aromatic and bitter varieties have different biochemical composition, and hence different brewing value.

The most important among bitter substances are alpha-acids, which in the process of isomerization during hop hopping are converted into iso-alpha-acids, the main compounds of beer bitterness. When the wort is hopped with freshly harvested hops almost 90% of the bitterness of beer is formed as a result of isomerization of alpha-acids into iso-alpha-acids, as a result of which the hexadiene ring of alpha-acids is converted into pentadiene iso-alpha-acids, giving beer a bitter taste [3, 7, 8, 16]. The amount of alpha-acids is the main pricing factor in the evaluation of hops and hop products.

The biochemical characteristics of bitter substances of the studied varieties of the bitter group of hops are given in Table 1. From the data of table 1 it is seen that in the hops of the studied varieties the content of alpha-acids ranges from 9.5 to 11.2%. Most alpha-acids were found in Magnum hops – 11.2%.

Table 1

Characteristics of bitter substances of hops of bitter group varieties

№	Variety of hop	Contents alpha-acids,%	Cohumulone in the composition alpha-acids,%	Contents beta-acids,%	The ratio of beta/alpha-acids
1	Alta (Ukraine)	10.3	19.6	3.8	0.53
2	Magnum (Germany)	11.2	23.1	5.3	0.51
3	Northern Brewer (Great Britain)	9.5	27.8	3.9	0.52
4	Promin' (Ukraine)	9.6	29.6	4.1	0.53
5	Ksanta (Ukraine)	9.9	34.7	6.0	0.74
6	Ruslan (Ukraine)	9.7	43.8	5.7	0.73

The content of beta-acids in the studied varieties is from 3.8% in hops of the Alta variety to 6.0%, respectively, in the Ksanta variety. Beta-acids are not bitter in taste but in the process of oxidation, compounds are formed that have a pleasant bitterness. One of their main properties is a high antiseptic effect which is important to increase the biological stability of beer during storage [8–15]. The coefficient of aromaticity between the content of beta- and alpha-acids for this group of varieties is from 0.51 to 0.74 which is less than one.

Not all alpha-acids have a positive effect on the quality of bitterness in beer. Cohumulone is converted to the isomer better than other components of alpha-acids, so the solubility of cohumulone is much higher than humulone and adhumulone [1, 3, 7, 16]. But this faction is attributed a negative role in the formation of the bitterness of beer [18].

The analysis of table 1 shows that the selected varieties of bitter hops have a slight deviation of alpha-acids and the ratio of beta-acids to alpha-acids is less than one, instead have a wide range of cohumulone content: from 19.6% in cones of Alta up to 44.1% in the Ruslan variety, which will allow to investigate its influence on the quality of beer.

Bitter substances of typical representatives of aromatic varieties of hops were also studied (Table 2).

Table 2

Characteristics of bitter substances of aromatic varieties of hops

№	Variety of hop	Contents alpha-acids,%	Cohumulone in the composition alpha-acids,%	Contents beta-acids,%	Ratio of beta/alpha-acids
1	Nationalnyi (Ukraine)	5.1	20.1	5.7	1.11
2	Slovyanka (Ukraine)	5.5	22.1	7.4	1.34
3	Zaaz (Czech Republic)	5.3	25.3	6,8	1.28
4	Gaidamats'kyi (Ukraine)	4.2	29.6	5.3	1.27

In the samples of hops of the studied varieties, the content of alpha-acids ranges from 4.2 to 5.5% which is much less compared to bitter varieties. A characteristic feature of cone hops of aromatic varieties, in contrast to bitter, is a high positive coefficient of aromaticity between the content of beta and alpha-acids, ranging from 1.11 to 1.34. Among the studied varieties, hop cones of Slovyanka and Zaaz varieties are characterized by the highest indicator of aromaticity.

From the analysis of table 2 shows that the selected varieties of hops of aromatic type have a ratio of beta-acids to alpha-acids greater than one. The content of cohumulone in the composition of alpha-acids ranges from 20.1% in the cones of the Nationalnyi variety to 29.6% in the Gaidamats'kyi variety which will allow to investigate its effect on the quality of beer.

Influence of cohumulone bitter and aromatic varieties of hops on the quality of the wort

Experimental beer samples were made with the studied hop varieties. The amount of alpha-acids and cohumulone up to 1 liter of wort was calculated.

Since the hop was carried out with bitter hops at the rate of 60 mg of bitter substances per 1 liter of wort, the same amount of alpha-acids is added to the wort – about 60 mg/l but different amount of cohumulone: from 11.8 mg/l with Alta hops to 26.3 mg/l with the Ruslan variety. In this case, the value of the bitterness of the hopped wort also varies from 33.2 units EBC (variety Alta) up to 41.3 units EBC when using Ksanta hops which is shown in Figure 1.

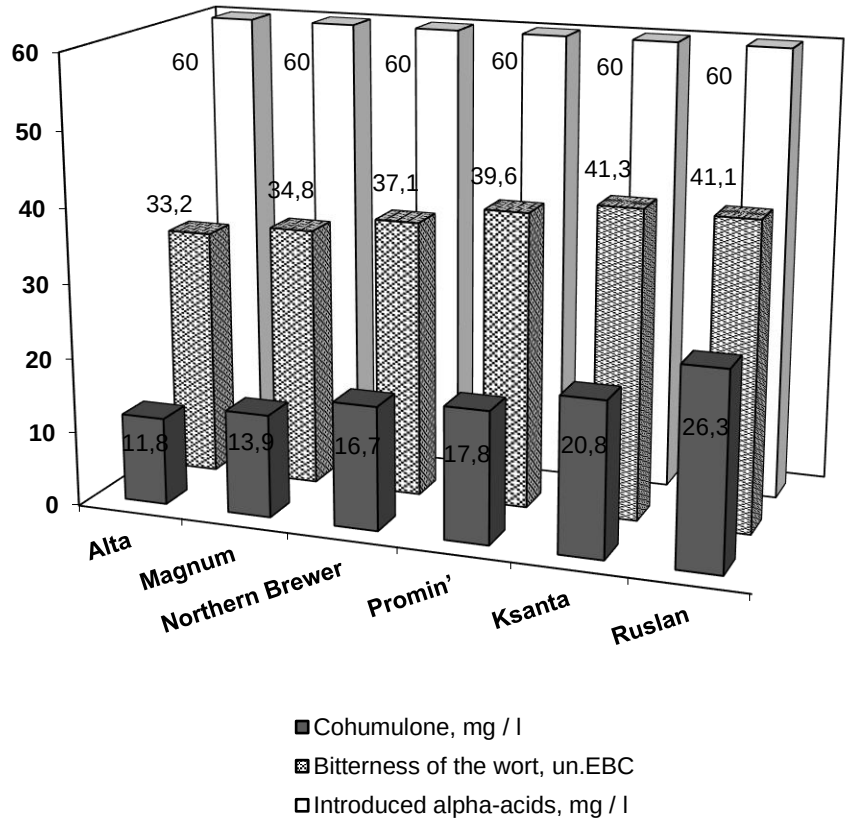

Figure 1. The amount of bitter substances introduced into the wort and identified in it when using bitter hops

From the analysis (Figure 1) we see that with hops of the Ksanta variety in the wort is introduced 76.3% more cohumulone with alpha-acids compared to hops of the Alta variety which has the lowest content of cohumulone in the composition of alpha acids. At the same time the value of the bitterness of the hopped wort increased by 24.3% compared to the use of the Alta variety. That is with an increase in the mass fraction of cohumulone in the alpha-

acids of Ksanta hops by 1% the value of the bitterness of the hopped wort increases by 0.32%. When the wort is hopped with Ruslan hops with a much higher content of cohumulone in the composition of alpha-acids, the value of the bitterness of the wort practically does not change. But if in Ruslan hops the amount of cohumulone in the composition of alpha-acids was 123.4% more compared to Alta hops, the value of the bitterness of the wort hopped by this hop increased only by 23.7% compared to Alta. With an increase in the mass fraction of cohumulone in the composition of alpha-acids of the Ruslan variety by 1% the value of the bitterness of the hopped wort increases by only 0.19%. After analyzing the relationship between the growth of cohumulone in the composition of alpha-acids and the change in the value of the bitterness of the hops watered by these varieties, it follows that with increasing the share of cohumulone in the composition of alpha-acids of bitter hops by 1% the bitterness of hop wort increases from 0.19 for the Ruslan variety up to 0.38% for the Promin' variety. For other studied varieties of bitter type this figure is in the range of 0.27–0.32. The obtained research data explain why when normalizing hops according to the content of alpha-acids with different content of cohumulone they do not always get stably normalized bitterness of beer because with increasing the share of cohumulone in alpha-acids increases the bitterness of the wort which is consistent with other scientists [16, 19–20].

In Figure 2 shows the correlation field between the bitterness of the wort (axis y) and the amount of cohumulone (axis x) introduced when using bitter hops, the regression equation and the coefficient of determination R^2 constructed a trend line which is also shown in this figure.

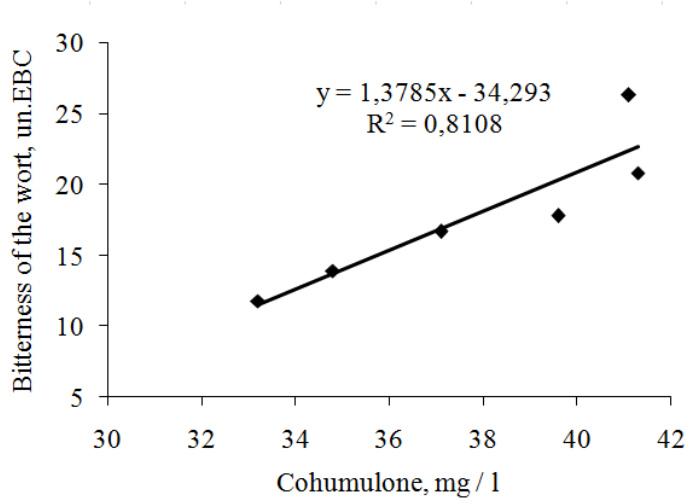

Figure 2. Coreliness of deposits between the must of wort and the amount of wort introduced by cohumulon with hops of rich varieties

The occurrence of the wort and the wort must have been added to the cohumulone with the hops in the case of vicarious vigorous varieties of currencies that are correlated: y = 1.3785x – 34.293. Among the signs of speeding straight ahead. The coefficient of correlation (r = 0.90 ± 0.10) shows that there is less wort and more wort introduced to the cohumulone with hops in case of strong vigorous varieties. Some determinants R^2 = 0.8108 per case, 81.08% of the amount of wort added is due to the amount of wort added to the hop and the 18.82% was found to be unavailable.

Studies have shown that when used for hop wort bitter type hops with different alpha-acid composition more effective use in varieties with high content of cohumulone which is consistent with the results of studies by other scientists [16, 19–20].

Influence of cohumulone of aromatic varieties of hops on wort quality

The correlation between the content of cohumulone in the composition of alpha-acids of aromatic varieties and the bitterness of hop wort was investigated in the manufacture of beer samples with aromatic samples of hops.

In the obtained samples of wort, the amount of beta-acids and cohumulone up to 1 liter of wort and the value of the bitterness of the wort were determined which is shown in Figure 3.

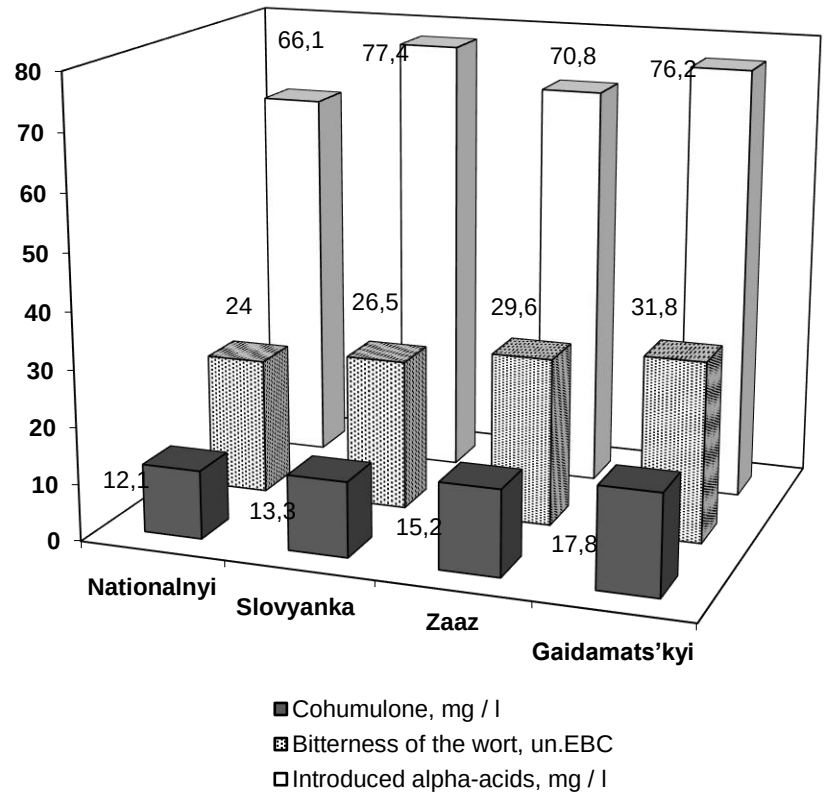

Figure 3. The amount of bitter substances introduced into the wort and determined in it when using aromatic varieties of hops

When the same amount of alpha-acids (about 60 mg/l) is added to the wort different amounts of cohumulone are added to the wort: from 12.1 mg/l with hops of the Nationalnyi variety to 17.8 mg/l with the Gaidamats'kyi variety. The magnitude of the bitterness of the hopped wort also varies from 24.0 units EBC up to 31.8 units EBC. But if in the hops of the

Gaidamats'kyi variety the amount of cohumulone in the composition of alpha-acids was 47.2% more compared to the hops of the Nationalnyi variety which has the lowest content of cohumulone, the value of bitterness of the hop wort hop increased by 32.5% compared to the Nationalnyi, i.e. with an increase in the mass fraction of cohumulone in the alpha-acids of hops of the Gaidamats'kyi variety by 1%, the value of the bitterness of the hopped wort increases by 0.69%. When using hops of the Slavyanka variety 13.3 mg/l of cohumulone is added to the wort with alpha-acids which is 9.9% more than the hops of the Nationalnyi variety and the value of the bitterness of the hop wort increased by 10.4% compared to Nationalnyi. For hops of this variety with an increase in the mass fraction of cohumulone in the composition of alpha-acids by 1% the value of the bitterness of the wort hopped by it increases by 1.05%.

In Figure 4 shows the correlation field between the bitterness of the wort and the amount of cohumulone introduced using hops of aromatic varieties.

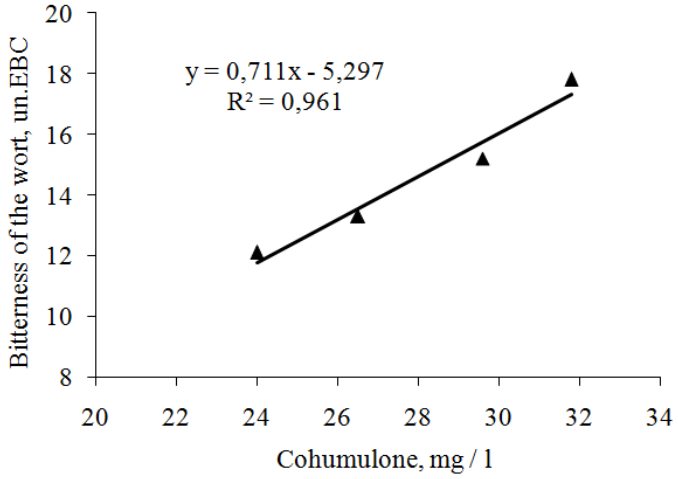

Figure 4. Correlation between the bitterness of the wort and the amount of cohumulone with hops of aromatic varieties

Given the use of aromatic hops, this dependence is expressed by the correlation equation: y = 0,711x – 5,297. There is a direct connection between the signs. There is a strong correlation between two factors: the bitterness of the wort (axis y) and the amount of cohumulone (axis x) added to hops of aromatic varieties, as evidenced by the correlation coefficient (r = 0.98 ± 0.20). The total variation in the bitterness of the wort (96.10%) is due to changes in the amount of cohumulone and the remaining 3.90% is other factors that were not taken into account in this case.

We found that with an increase in the mass fraction of cohumulone in the composition of alpha-acids of aromatic hops by 1% at a ratio of beta-acids to alpha-acids of 1.11-1.34, the value of the bitterness of the wort hopped by them increases from 0.69% for hops Gaidamats'kyi variety up to 1.05% for hops of the Slovyanka variety while for bitter hops in which the ratio of beta-acids to alpha-acids is 0.51–0.74, this figure was much lower and amounted to only 0.19–0.38%. Thus it was found that in the formation of the bitterness of the wort hopped with aromatic varieties of hops from the ratio of beta-acids to alpha-acids is more than one, the role of beta-acid compounds is much higher compared to bitter varieties.

Influence of cohumulone of aromatic hops on beer quality

The established dependences remain and at research of ready beer which characteristic is resulted in Table 3.

Table 3

Content of bitter substances and polyphenolic compounds in beer samples

№	Variety of hops from which beer is made	Magnitude of the bitterness of beer, units EBC	Total polyphenols, mg/dm^3
1	Nationalnyi	19.3	172.0
2	Slovyanka	22.6	183.4
3	Zaaz	24.8	180.0
4	Gaidamats'kyi	26.1	218.0

Sensory evaluation of experimental samples of beer and its biochemical characteristics showed that all samples differed significantly in taste, bitterness and aroma (Table 4).

Table 4

Technological evaluation of the studied varieties of hops

Options	Name of quality indicators							
					Taste			
	Transparency	Color	Foaming	Aroma	Completeness	Hop bitterness	Overall score	Rating
Nationalnyi	3	3	5	3.6	4.1	4.3	23.0	perfectly
Slovyanka	3	3	5	3.9	4.3	4.6	23.8	perfectly
Zaaz	3	3	5	3.9	4.2	4.6	23.7	perfectly
Gaidamats'kyi	3	3	5	3.5	3.9	3.9	22.3	perfectly

Slovyanka and Zaaz obtained the best beer in the case of hop worting with finely aromatic hop varieties. The beer had a pleasant taste, fresh hop of polyphenolic compounds, which are rich in hop of this aroma and a gentle, residual bitterness. Excellent quality was also beer using the aromatic variety of hops Nationalnyi. The fourth sample of beer had good taste, but was inferior in aroma and hop bitterness to other samples. The members of the commission noted a slightly rough astringent bitterness, characteristic of the excessive amount variety.

The members of the tasting commission also noted that in the first sample of beer, in which the lowest amount of cohumulone and beta-acids was added with Nationalnyi hops, the value of beer bitterness was the lowest. With an increase in the content of cohumulone in the composition of alpha-acids from 20.1% in hops of the Nationalnyi variety to 29.6% in

the variety Gaidamats'kyi and with an increase in the amount of cohumulone with these varieties of hops from 12.1 to 17.8 mg to 1 liter of wort, increases the amount of bitterness of beer both spectrophotometric and sensory which is consistent with the data of other scientists [3, 8] who also note that ways to create new varieties of hops are intended to maintain the level of cohumulone formation not more than 25% of total alpha-acids in aromatic hops and 35% in bitter hops [3, 8]. Thus different representatives of the bitter substances of hops have different bitterness both in total intensity and in individual flavors. Taking into account the maximum qualities of all components of the group of bitter substances allows you to rationally use the most expensive raw materials, creating new beers.

Conclusions

1. The quality and magnitude of the bitterness of beer depends on the varietal characteristics of hops, i.e., the quantity and quality of homologues of alpha-acids and beta fractions.
2. When used for hop wort hop with a slight deviation of the ratio of beta-acids to alpha-acids and different composition of alpha-acids, their use is more effective in varieties with a high content of cohumulone.
3. More intense coarse bitterness in beer is created by cohumulone, so the methods of creating new varieties of hops are intended to maintain the level of cohumulone formation of not more than 25% of the total alpha-acids content in aromatic hops and 35% in bitter hops.
4. Establishing the relationship between the quantity and quality of bitter substances of hops and the bitterness and quality of hopped wort and beer which show that with increasing mass fraction of cohumulone in the composition of alpha-acids of aromatic hops by 1% at a ratio of beta-acids to alpha-acids 1.11–1.34, the value of the bitterness of the wort hopped by them increases from 0.69% for hops of the Gaidamats'kyi variety to 1.05% for hops of the Slavyanka variety, while for bitter hops in which the ratio of beta-acids to alpha-acids 0.51–0.74, this figure was much lower and was only 0.19-0.38%.
5. The role of beta-acid compounds in the formation of the bitterness of the wort, hopped with aromatic varieties of hops with a ratio of beta-acids to alpha-acids greater than one is much higher compared to bitter varieties.

References

1. Lyashenko N.I. (2002), *Hops and hop products biochemistry*, Polissja, Zhitomir.
2. Protsenko Lidiya, Litvynchuk Svitlana (2015), Competitiveness of Ukrainian pellet hops production, *Ukrainian Journal of Food Science*, 3(1), pp. 51–59.
3. Podeszwa Tomasz, Harasym Joanna (2016), New methods of hopping (dryhopping) and their impact on sensory properties of beer, *Acta Innovations*, 21, pp. 79–86.
4. Lyashenko N.I., Mykhajlov M.G. (2010), Curative potential of hop and beer, *Agropromyslove vyrobnytstvo Polissja*: *Zbirnyk naukovykh prats'*, 3, pp. 50−54.
5. Narziß L. (2005), *Abriß der Bierbrauerei.* 7th ed., Wiley-VCH: Weinheim, pp. 163–170.
6. Biendl M., Pinzl C. (2007), *Arzneipflanze Hopfen. Deutsches Hopfenmuseum Wolnzach*, Wolnzach.

7. Ting Patrick, Ryder David (2017), The Bitter, Twisted Truth of the Hop: 50 Years of Hop Chemistry, *Journal of the American Society of Brewing Chemists*, 75(3), pp. 161–180. DOI: 10.1094/ASBCJ-2017-3638-01.
8. Baranowski K. (2016), Chmielowe akcenty smakowo-zapachowe w piwie? No problem, ale …, *Przemysł Fermentacyjny i Owocowo – Warzywny*, 11 pp. 10.
9. Skomra U. (2016), *Chmiel zwyczajny (Humulus lupulus L.) Gatunek o szerokim spektrum aktywności biologicznej,* Instytut Uprawy Nawożenia i Gleboznawstwa (IUNG), Available at: http://pw.ihar.edu.pl/assets/Uploads/1.2-Koryciny-Skomra-kolekcja-chmielu-referat.pdf (dostęp 18.12.2016).
10. Oberholster A., Titus B, (2016), Review: Impact of Dry Hopping on Beer Flavor Stability, *Ann Food Process Preserv*, 1(1), pp. 1004.
11. Hieronymus S. (2012), *For the Love of Hops: The Practical Guide to Aroma, Bitterness and the Culture of Hops*, Boulder, Brewers Publications, a division of the Brewers Association, Colorado.
12. Drexler G. (2016), *Dry Hopping*, Barth-Haas Hops Academy, Blumenau Available at: http://www.cervecon.com.br/Palestras/Georg_Drexler.PDF (access 18.12.2016).
13. Forster A., Gahr A., (2013), On the fate of certain hop substances during dry hopping, *BrewingScience,* 66(7-8), pp. 93-103.
14. Schnaitter M., Kell A., Kollmannsberger H., Schüll F., Gastl M., Becker T. (2016), Scale-up of Dry Hopping Trials: Importance of Scale for Aroma and Taste Perceptions, *Chem Ing Tech*, 88(12) pp. 1955–1965.
15. Forster A., Gahr A., Van Opstaele F. (2014), On the transfer rate of geraniol with dry hopping, *BrewingScience*, 67(3-4), pp. 60–62.
16. Jessika De Clippeleer, Guido Aerts (2014), Beer's bitter compounds – A detailed review on iso-a-acids: Current knowledge of the mechanisms for their formation and degradation, *Brewing Science*, 67(11), pp.167–182.
17. Paulo Alves da Silva, Fernanda Carolina de Faria (2008), Bitterness Unit and iso-alfa-acids contents of some brands of Brazilian and North American beers, *Ciência e Tecnologia de Alimentos*, 28(4), pp. 902–906.
18. Shellhammer T. (2004), Bitter quality of beer as affected by isocohumulone levels, *Proceedings of the World Brewing Congress,* San Diego.
19. Kusche M., Stettner G., Stephan A., Mitter W., Kaltner D. (2007), Influence of the new high alpha hop variety Herkules on beer quality, *Proceedings of the European Brewery Convention Congress,* Venice.
20. Malowicki M. G., Shellhammer T. H. (2006), Factors affecting hop bitter acid isomerization kinetics in a model wort boiling system, *J. Am. Soc. Brew. Chem.,* 64, pp. 29–32.
21. Protsenko Lidia, Rudyk Ruslan, Hryniuk Tetiana, Vlasenko Aliona, Protsenko Alona, Litvynchuk Svitlana, Ovadenko Olena (2018) Beer enrichment with biologically active hop compounds, *Ukrainian food journal*, 7(1), pp. 65–78, DOI: 10.24263/2304-974X-2018-7-1-7.
22. Biendl M., Virant M., Varjú P. (2004), Determination of iso-alpha-acids, alpha- and beta-acids in isomerised hop pellets by HPLC, *J. Inst. Brew.,* 110, pp. 242–243.
23. Ahalitika – EBC (1987), *European Brebery Convention, Fourth edition***.**
24. Jaskula B., Goiris K., De Rouck G., Aerts G., De Cooman L. (2007), Enhanced quantitative extraction and HPLC determination of hop and beer bitter acids, *J. Inst. Brew.,* 113, pp. 381–390.

Improving the process of kneading yeast dough with cam working elements

Vitalii Rachok[1], Volodymyr Telychkun[1], Stanka Damyanova[2], Yuliia Telychkun[1]

1 – National University of Food Technologies, Kyiv, Ukraine
2 – "Angel Kanchev" University of Ruse, Razgrad Branch, Razgrad, Bulgaria

Keywords:

Dough
Kneading
Cam
Modeling

Article history:

Received 25.07.2019
Received in revised form 01.12.2019
Accepted 30.06.2020

Corresponding author:

Vitalii Rachok
E-mail: RachokV3478@gmail.com

DOI: 10.24263/2304-974X-2020-9-2-14

Abstract

Introduction. It was conducted a study of the process of kneading wheat yeast dough with cam working. The aim is to determine the rational configuration of structural elements for continuous kneading of dough at different levels of frequency of the working elements rotation and the distance between them.

Materials and methods. It was investigated the kneading of wheat yeast dough by cam working elements. Mathematical modeling was performed using the Flow Vision software package based on the simulation of three-dimensional motion of liquids and gases in technical structures, as well as for the visualization of flow curves by computer graphics. Physical modeling was performed via experimental setup with cam kneading elements. The distance between the cams is 2–4–6–8–10 mm, the rotation speed is 20–100 rpm.

Results and discussion. As the rotational speed of the working elements increases from 20 to 100 rpm, the mixing speed increases from 0.1 to 0.6 m/s, the distance between the cams does not affect the mixing in the specified range. The maximum values of pressure reach 16560 Pa for the distance between the cam working elements 2 mm and a speed of 100 rpm, the minimum 555 Pa for the distance between the cam working elements 10 mm and a speed of 20 rpm. In the mixing chamber, the highest-pressure values are formed in the contact zone of the cam working elements with the wall of the mixing chamber and in the contact zone of the two cams. The dependence of the viscosity in the mixing chamber on the speed of rotation of the working element is of a power nature and with increasing speed from 20 to 100 rpm decreases from 1600 to 320 Pa·s. Parts of the mixing chamber in which viscosity values in the range from 320 to 960 Pa·s are achieved are considered to be the most effective during mixing. Reducing the viscosity of the dough involves reducing energy costs during kneading.

Conclusions. To increase the carrying capacity of the cam working elements, improve mixing and reduce heat consumption, it is rational to use cam working elements with a variable pitch and a variable position of the cams at $\alpha = 45°$ or a combined cam working element using a screw auger at the beginning of the working element.

Introduction

The development of a continuous-action dough-mixing machine is accompanied by the choice of a rational configuration of the working element. Rationalization is realized by analyzing the various configurations of the working element and its effect on the kneading process. Imitation modeling aims to calculate the values of certain characteristics of a process that develop over time, by reproducing the flow of this process on a computer via its mathematical model [1–2].

During projecting of the process of dough mixing, there is a range of issues related to the type of working elements is supposed to be chosen. On the basis of theoretical searches and obtained experimental results, after comparative analysis of working elements, it was decided to simulate the process of kneading yeast wheat dough using cam working elements [3].

Obtaining information about the process of mixing at any point in the mixing tank using simulation modeling and the results of a physical experiment allow to project an effective working element in a high-tech continuous mixing machine [4].

Dough kneading is a complex process that involves creating a homogeneous capillary-porous mass of flour, water, yeast, salt, and other components. The formation of dough during kneading occurs as a result of a number of processes, of which the most important are: physico-mechanical, colloidal and biochemical processes. All these processes occur simultaneously, mutually affecting each other and depend on the duration of kneading, temperature and the amount and quality of raw materials used during kneading the dough [5–6].

The yeast dough is considered as a complex colloidal system, which consists of several continuous and periodic phases. Solids and liquids (gluten and water) in the dough are continuous phases, starch grains and gas formed during fermentation of the dough is a periodic phase. As a result, the physical properties of the dough are characterized by the parameters of solids, liquids, gases, and indices that are caused by the interaction of these phases. This process is carried out by mechanical processing of the dough, and based on the swelling of the starch and protein complex with the formation of elastic-elastic-viscous homogeneous mass containing active-acting microorganisms and ferments [7–8].

The research methodology is based on the information technologies of designing of processes of elastic-viscous-plastic deformation of thixotropic dispersed materials using modern computer technologies [9–10].

Based on the literature analysis, the task for mathematical modeling of the kneading process of the yeast dough with using cam working elements of the selected geometric shape was formed. The speed was in the range from 20 to 100 rpm and the distance between the structural elements for kneading from 2 to 10 mm.

The aim is to determine the rational configuration of cam structural elements for continuous kneading of dough at different levels of frequency of the working elements rotation and the distance between them.

Materials and methods

The object of the study is the process of kneading of yeast dough [20].

The dough is considered as a complex colloidal system consisting of several continuous and periodic phases [19]. Solid and liquid (gluten and water) in the dough are continuous phases, starch grains and gas formed during the fermentation of the dough – the periodic phase. As a result, the physical properties of the dough are characterized by the parameters of solids, liquids and gases and the indicators arising from the interaction of these phases.

This process takes place during machining, and consists in the swelling of starch and protein complex with the formation of elastically elastic viscous homogeneous mass containing active microorganisms and enzymes. The aim of kneading yeast dough is to obtain a homogeneous mass with certain structural and mechanical properties [19].

Theoretical basis of the modeling problem

To determine the exercise of calculating the motion of liquids, it is necessary to formulate and solve a system of differential equations: energy, continuity, motion, change of density and rheological properties. Equation data for non-compressible liquids but cannot adequately describe the process of movement of the yeast dough are used in the literature, as several researchers prove that the dough is compressed due to the significant content of the gas phase [3–4].

The one-dimensional equations (Saint-Venant), which expresses the principle of mass conservation, for cases of steady motion and non-compressible fluid:

$$\frac{\partial vx}{\partial x}+\frac{\partial vy}{\partial y}+\frac{\partial vt}{\partial z}=0\ , \tag{1}$$

where, vx, vy, vz – velocity components, m/s.

The equation of motion of a continuous, non-compressible environment is a system of equations and has the form:

$$\begin{cases}\rho\left(\frac{\partial vx}{dt}+\frac{vx\partial vx}{\partial x}+\frac{vy\partial vx}{\partial y}+\frac{vz\partial vx}{\partial z}\right)=-\frac{\partial\rho}{\partial x}+\left(\frac{\partial\sigma x}{\partial x}+\frac{\partial\tau yx}{\partial y}+\frac{\partial\tau zx}{\partial z}\right)+\rho gx\\ \rho\left(\frac{\partial vy}{dt}+\frac{vx\partial vy}{\partial x}+\frac{vy\partial vy}{\partial y}+\frac{vz\partial vy}{\partial z}\right)=-\frac{\partial\rho}{\partial y}+\left(\frac{\partial\tau xy}{\partial x}+\frac{\partial\sigma y}{\partial y}+\frac{\partial\tau zy}{\partial z}\right)+\rho gy\\ \rho\left(\frac{\partial vz}{dt}+\frac{vx\partial vz}{\partial x}+\frac{vy\partial vz}{\partial y}+\frac{vz\partial vz}{\partial z}\right)=-\frac{\partial\rho}{\partial z}+\left(\frac{\partial\tau xz}{\partial x}+\frac{\partial\tau yz}{\partial y}+\frac{\partial\sigma z}{\partial z}\right)+\rho gx\end{cases} \tag{2}$$

where, ρ is the density, kg/m^3; t – time, s; p – pressure, Pa; g is the acceleration of free fall, m/s^2.

Energy equations for non-compressible liquids:

$$\rho c\left(\frac{\partial T}{\partial t}+\frac{vj\partial T}{\partial xj}\right)=\left(\frac{\partial\tau}{2xj}\right)\left(\frac{\lambda T}{\partial xj}\right)+\frac{\tau_i j\partial v_i}{\partial xj}\ , \tag{3}$$

where, c is the specific heat, J/kg; λ – coefficient of thermal conductivity, W/m;

T – temperature, K.

$\tau_i j\partial vi/\partial xj=F$ – the intensity of the kinetic energy transition into thermal, to the unit of volume. In the Cartesian coordinate system, F is equal to:

$$F=\frac{\tau x\partial vx}{\partial x}+\frac{\tau y\partial vy}{\partial y}+\frac{\tau z\partial vz}{\partial z}+\tau zy(\frac{\partial vx}{\partial y}+\frac{\partial vy}{\partial x}+vyz\left(\frac{\partial vy}{\partial z}+\frac{\partial vz}{\partial y}\right)+\tau zx(\frac{\partial vz}{\partial x}+\frac{\partial vx}{\partial z}) \tag{4}$$

The material density equation describes its dependence on temperature, pressure, humidity, and other factors. In logarithmic coordinates, the dependence of τ on j for many non-Newtonian materials becomes linear for the most part, thus explaining the widespread use of the Ostwald equation:

$$\tau=k\gamma^n, \tag{5}$$

where, τ – the shear stress, Pa; k- the coefficient of consistency; γ – the shear rate, s^{-1}; n – the fluidity index.

For processes occurring in mixers, it is quite difficult to determine the criteria that includes the velocity of the particles of solution V. It is often used a conditional velocity equal to the velocity at the outside diameter of the working element of the mixer u. The traditional definition of the Reynolds (Re) criterion for flow in pipes is as follows:

$$\mathrm{Re} = \frac{V_{av} \cdot d_0 \cdot \rho}{\eta}, \quad (6)$$

where, V_{av} – average speed, m/s; ρ – density, kg/m^3; d_0 – the inside diameter, m;

η – the coefficient of the structured viscosity of the non-Newtonian fluid, Pa·s.

For the case of movement of the blend in the mixer is conditionally taken [5, 7]:

$$V_{av} = \omega \cdot R, \quad (7)$$

where, ω is the angular velocity, rad/s; R – the outer radius of the working element, m.

$$Re = \frac{\omega \cdot R^2 \cdot \rho}{\eta}. \quad (8)$$

The Reynolds criterion calculated by this method is not universal, which determines the nature of the flow of the blend in the mixer, since the nature of the flow also depends on the design of the chamber and the working elements of the mixer, which are not shown in the last formula. This drawback does not make it possible to use the resulting criterion universally to analyze many food processes occurring in mixers, so it is necessary to develop separate formulas for each type of mixer to determine the power consumed for mixing. The Froude criterion (Fr) is the ratio of the inertia forces of the mixable mixture to the gravitational forces. For mixers it can be written as following:

$$Fr = \frac{\omega^2 \cdot R}{g}, \quad (9)$$

where, ω is the angular velocity of rotation of the working element of the mixer, rad/s;

R – the outer radius of the working element, m; g – the acceleration of free fall, m/s^2.

This criteria takes into account the effect of the vorticity formed on the back of the working element during movement in the yeast dough.

Generalization of the results of the study of the power consumed for mixing non-Newtonian fluids is associated with some difficulties, since the viscosity of such fluids depends on the hydrodynamic regime in the mixer [4], and, accordingly, the angular speed of rotation of the working element and its configuration. The rheological properties must also be taken into account. This can be done using the dimensionless Hedstrom criterion [5]:

$$He = \frac{\tau_0 \cdot R^2 \cdot \rho}{\eta^2}, \quad (10)$$

where, R is the outer radius of the working element, m; ρ – the density of the mixture, kg/m^3.

The basic definition of the Eulerian criteria in the general case is as follows [6–7]:

$$Eu = \frac{\Delta\rho}{\rho \cdot V^2} \quad (11)$$

where, Δp – pressure drop, Pa; V is the speed of movement of the mixture, m/s.

The Eulerian criteria is the ratio of the forces that cause the movement of the mixture to the forces of dynamic pressure. For processes occurring in mixers, the pressure drop Δp and velocity V should be replaced by the power consumed for mixing. We obtain the modified Euler criterion or the power criterion K_N:

$$K_N = \frac{N}{\rho \cdot n^2 \cdot R^5}. \quad (12)$$

Thus, taking account mentioned above, the basic criteria equation is describing the motion of a viscous-plastic stirring medium will be as follows:

$$\frac{N}{\rho \cdot n^2 \cdot R^5} = f\left(\frac{\omega \cdot R^2 \cdot \rho}{\eta}, \frac{\omega^2 \cdot R}{g}, \frac{\tau_0 \cdot R^2 \cdot \rho}{\eta^2}\right), \quad (13)$$

also, the obtained equation can be written in the form of a step monomial:

$$K_N = C \cdot Re^m \cdot Fr^n \cdot He^z, \quad (14)$$

where, C is the coefficient; m, n, s are the exponents.

When kneading wheat yeast dough, the role of gravity is quite small, so the value of gravity is neglected. In general, the criteria equation of the mixing power can be written as:

$$K_N = C \cdot Re^m \cdot He^z. \quad (15)$$

Therefore, the considered mathematical models of the movement of wheat yeast dough allow to simulate the process of kneading wheat yeast dough and can be used for simulation in the software complex Flow Vision.

Mathematical modeling the process of kneading the yeast dough

Modeling of the yeast dough kneading process was performed via the Flow Vision software package, which is designed to model the three-dimensional motion of liquids and gases in technical and natural objects, as well as to visualize flow curves by computer graphics.

To simulate the process of kneading the yeast dough by the cam working elements, the software program "Flow Vision" was selected, which is designed to simulate the three-dimensional motion of liquids and gases in technical and natural objects, as well as to visualize curves of currents by computer graphics.

To simulate the process of kneading the wheat yeast dough, an incompressible fluid model was chosen, which describes the flow of a viscous fluid at small and large (turbulent) Reynolds numbers, followed by its visualization [7]. In the model it was used following equations:

Navier-Stokes equation:

$$\frac{\partial \mathrm{V}}{\partial \mathrm{t}} + \nabla(\mathrm{V} \cdot \mathrm{V}) = \frac{\partial \mathrm{P}}{\rho} + \frac{1}{\rho}\nabla((\mu + \mu_t)\big(\nabla V + (\nabla)^T\big)) + (1 - \frac{\rho_{hyd}}{\rho})g; \quad (16)$$

Flow continuity equation:

$$\nabla V = 0, \quad (17)$$

where, V is the velocity vector m/s, P is the pressure Pa, μ_t is the turbulent viscosity Pa·s, ρ_{hyd} is the hydrostatic density of kg/m^3, g is the vector of gravity m/s^2.

"The incompressible fluid" simulation model is based on the use of k-ε of the first-level turbulence model [8], which requires to get the formula for turbulent viscosity μC

Equation for turbulent viscosity:

$$\mu\mathrm{C} =_{\mu} \rho\frac{\mathrm{k}^2}{\varepsilon}; \quad (18)$$

turbulent energy equation k is also included in the model

$$\frac{(\rho k)}{\partial t} + \nabla(\rho V k) = \partial\nabla\left(\left(\mu + \frac{\mu_t}{\sigma_k}\right)\nabla k\right) + \mu_t G - \rho\varepsilon; \quad (19)$$

Turbulent energy dissipation rate equation:

$$\frac{\partial(\rho\varepsilon)}{\partial \mathrm{t}} + \nabla(\rho \mathrm{V}\varepsilon) = \nabla\left(\left(\mu + \frac{\mu_\mathrm{t}}{\sigma_\varepsilon}\right)\nabla\varepsilon\right) + \tilde{\mathrm{N}}_1\frac{\varepsilon}{\mathrm{k}}\mu_\mathrm{t}\mathrm{G} - \mathrm{C}_2\rho\frac{\varepsilon^2}{\mathrm{k}}; \quad (20)$$

marked by G expression:

$$G = D_{ij}\frac{\partial V_i}{\partial x_j}; \quad (21)$$

$$\mathrm{D_{ij}} = \mathrm{S_{ij}} - \frac{2}{3}(\nabla \cdot \mathrm{V} + \frac{\rho\mathrm{k}}{\mu_\mathrm{t}})\delta_{\mathrm{ij}}; \quad (22)$$

$$S_{ij} = \frac{\partial v_i}{\partial x_j} + \frac{\partial v_j}{\partial x_i}\ ; \qquad (23)$$

Parameter values are:

$$\sigma_k = 1;\ \sigma_z = 1{,}3;\ C_\mu = 0{,}09;\ C_1 = 1{,}44;\ C_2 = 1{,}92.$$

To load the geometry of the working elements, we use the filter "Element Movement in the Geometry Template", in which we enter the mass of the kneading element, the matrix of inertia, the angular velocity and the primary location. The next step in the simulation is to establish the boundary conditions of the problem, as shown in Figure 1.

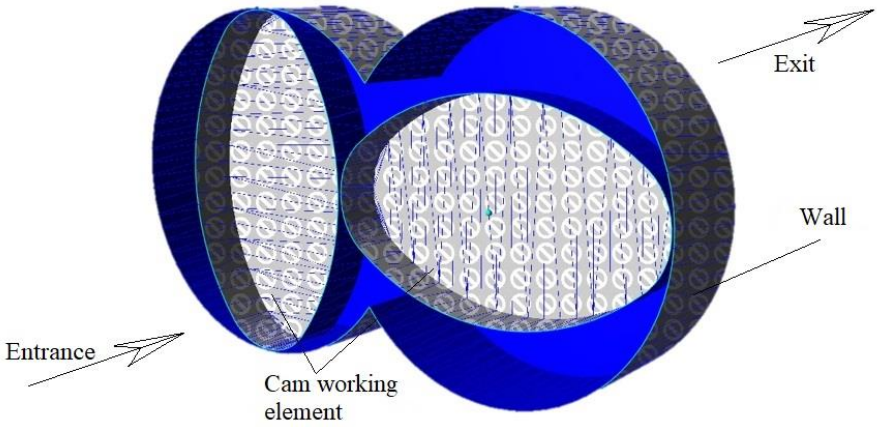

Figure 1. Boundary conditions for simulation modeling

At the "Input" border, we set the "Normal Speed" boundary condition; on the border "Cam working element" we establish the "Logarithmic law"; at the Exit boundary we set the Free Exit boundary condition.

The next step of entering the input parameters is to build a grid in the calculation area, which is used to select a uniform grid along the guides x, y, z.

To obtain reliable results, it is necessary to enter the parameters of numerical calculation, which determine the program step by time and take into account the action of gravity.

Several methods were used to visualize the obtained results in the Flow Vision software package: visualization of scalar fields, individual numerical values, velocity vector fields.

Physical modeling of kneading the yeast dough

To compare the results of physical and mathematical modeling, we have developed a kneading machine (Figure 2) that allows us to investigate the process of kneading wheat yeast dough and changing rheological properties, to perform a comparative analysis of different structures of working elements, and based on research to develop effective working elements for kneading yeast dough.

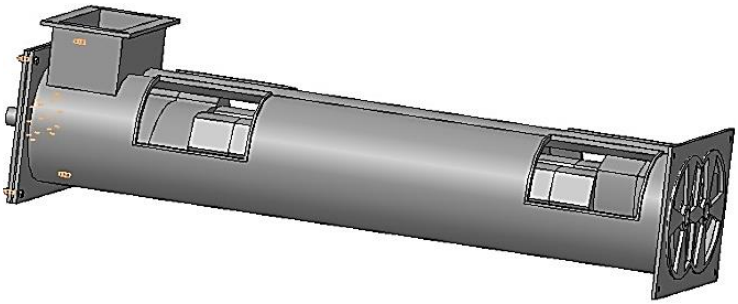

Figure 2. Experimental kneading machines

The procedure for performing physical modeling:

1. Preparation of raw materials and installation, installation of devices.

Yeast dough for the study, prepared for 300 grams of flour, according to the following recipe:

Wheat flour, premium grade 300 g;

Baking yeast, granulated 3 g;

Food salt 4,5 g;

Drinking water 175 ml.

Yeast dough, with a humidity 43%, was prepared in a steamless way from high-grade flour. The duration of fermentation is 30 minutes at a temperature of 33 °C.

2. Pre-mixing the prescription components for 10 s.
3. Loading pre-mixed components into the receiving hopper of the working chamber.
4. Kneading yeast dough and recording data.
5. Determine the mass and humidity of the yeast dough.
6. Determination of structural and mechanical properties of the dough.
7. Determination of the porosity of the finished product.

After the research based on the received data, we build graphics with the dependences of kneading of yeast dough.

Results and discussion

Mathematical modeling of kneading the yeast dough

We conducted studies on the effect of the distance between the cams and the speed of rotation of the working element on the kneading process of yeast dough. The distance between the cam working elements was changed from 2 mm to 10 mm (2–4–6–8–10 mm), the rotation speed was changed in the range from 20 rpm to 100 rpm (20–40–60–80–100 rpm). Simulation modeling of the kneading process was performed in the Flow Vision software package. The simulation results were obtained in the form of graphical images with a color scale of distribution of variables with numerical values (Figures 3, 5, 7).

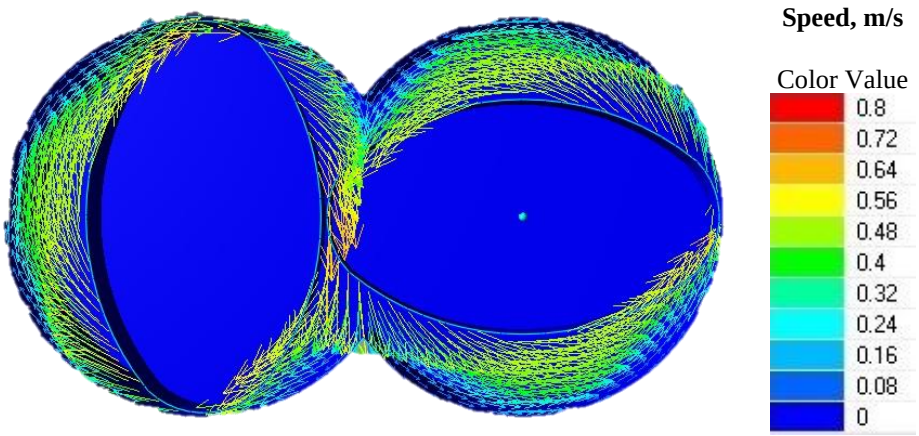

Figure 3. Visualization of the speed of movement of the dough in the mixing chamber during simulation parametric modeling of the cam working elements in the software complex Flow Vision.

This result is explained by the fact that the cam working elements rotate in the opposite rotation, forcing and accelerating the speed of mixing of the components of the yeast dough [11– 12].

Based on the results, after parametric modeling of the kneading process by the cam working elements, a linear dependence of the speed of movement of the dough in the working chamber was obtained (Figure 4).

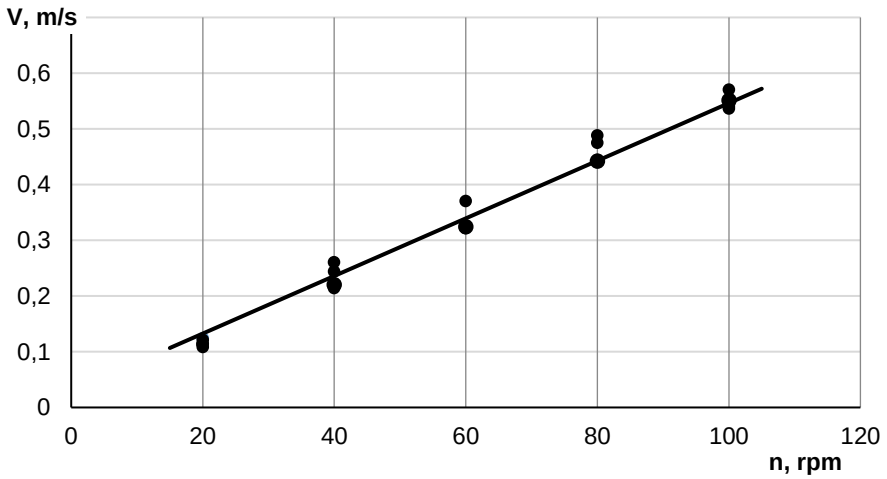

Figure 4. Variation of mixing speed, depending on the distance between the cams and the speed of rotation of the working element

It has been investigated that with increasing the speed of the working element, the speed of movement of the dough in the mixing chamber increases, under these conditions of the

mixing process the distance between the cam working elements does not affect the speed of mixing.

This result is explained by the fact that the rotational speed of the working element directly affects the mixing speed of the prescription components of the yeast dough, which mix faster with increasing rotational speed despite the distance between the cam working elements in the specified range [11–14].

The change in the mixing speed [V = m/s], depending on the distance between the cams and the speed of rotation of the working element, is determined by the mathematical formula:

$$V = 0{,}005n + 0{,}03\ , \tag{24}$$

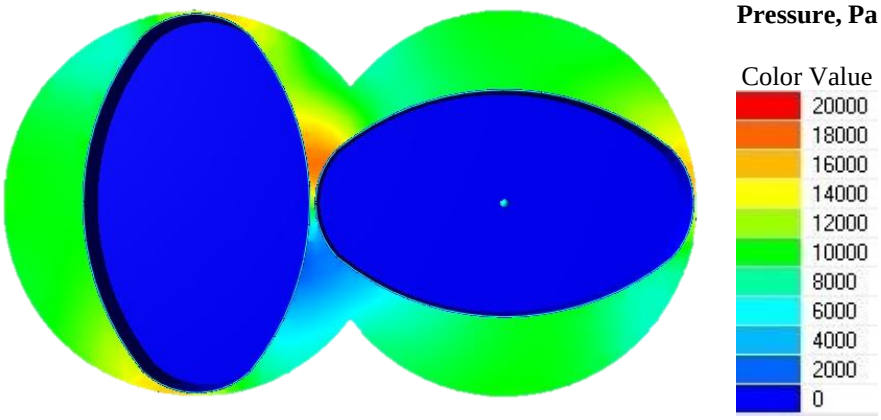

Figure 5. Visualization of pressure in the mixing chamber during simulation of parametric modeling of cam working elements in the software complex Flow Vision.

The simulation data on the change in pressure in the mixing chamber were analyzed (Figure 5), which made it possible to obtain the dependence of the pressure on the rotation speed of the working element and the different distance between the cams (Figure 6). It was found that with increasing the speed of the working element, the pressure in the mixing chamber increases. The pressure in the chamber is also affected by the distance between the cam working elements, the smaller the distance, the greater the pressure in the chamber. The maximum pressure values are 16560 PA at a distance between cam working elements of 2 mm and a rotational speed of 100 rpm, a minimum of 555 PA at a distance between cam working elements of 10 mm and a rotation frequency 20 rpm.

In the mixing chamber, the highest pressure values are formed in the contact zone of the cam working elements with the wall of the mixing chamber and in the contact zone of the two cams (Figure 5)

This result is explained by the fact that the cam working elements rotate to meet each other, the highest pressure is observed in the area of engagement of the cam working elements and in the area of contact with the wall of the housing [14–16].

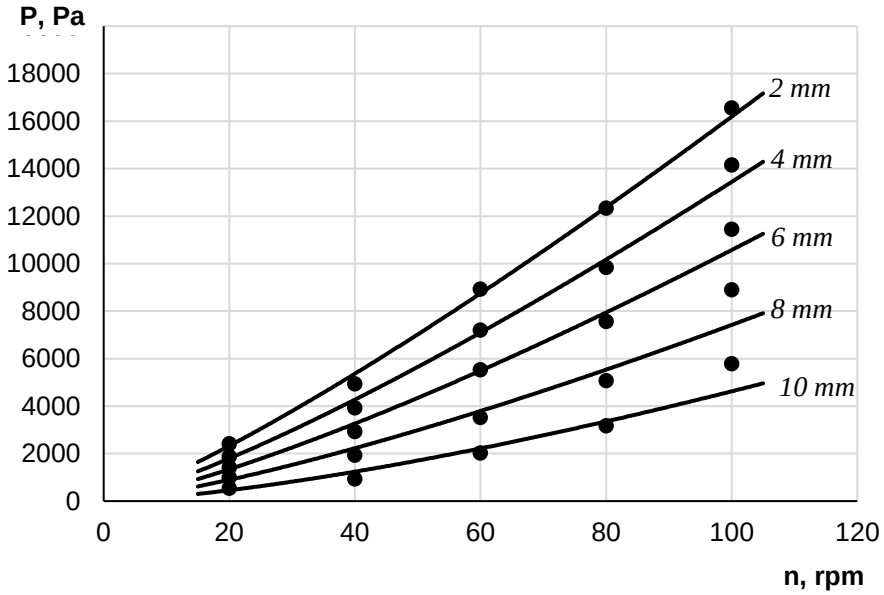

Figure 6. Changing the pressure in the mixing chamber, depending on the distance between the cams and the speed of rotation of the working element.

The change in pressure [P = PA] in the mixing chamber, depending on the distance between the cams and the speed of rotation of the working element is of a power character and is described by the formula:

$$P = (73 - 6{,}9\mathrm{S})n^{0{,}03S + 1{,}14}, \quad (25)$$

where, S is the distance between the cam working elements, mm; *n* is the speed of rotation of the working element, rpm.

We obtained the viscosity distribution of the kneading chamber at different rotational speeds and working element distances. The simulation results confirmed the pseudoplastic nature of the test, which is explained by the variable numerical viscosity data of the dough in the kneading chamber (Figure 7). Based on the obtained results, a graph of viscosity change in the mixing chamber was constructed, depending on the distance between the cams and the rotation speed of the working element (Figure 8).

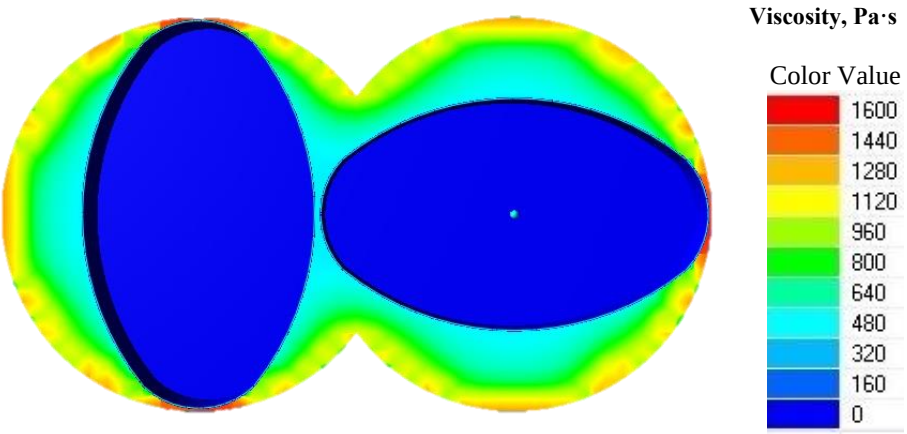

Figure 7. Visualization of the change in viscosity in the mixing chamber during simulation parametric modeling of the cam working elements in the software program Flow Vision

The parts of the kneading chamber that achieve the lowest viscosity are considered to be most effective during mixing. Increasing the rotation speed of the working element leads to an increase in the speed of movement of the dough in the work chamber, which in turn leads to a decrease in the viscosity of the dough and a decrease in energy costs during the kneading process.

This result is explained by the fact that with increasing speed of the working elements decreases the viscosity of the yeast dough, and the change in viscosity is affected by the distance between the cam working elements in the process of kneading the dough [15–17].

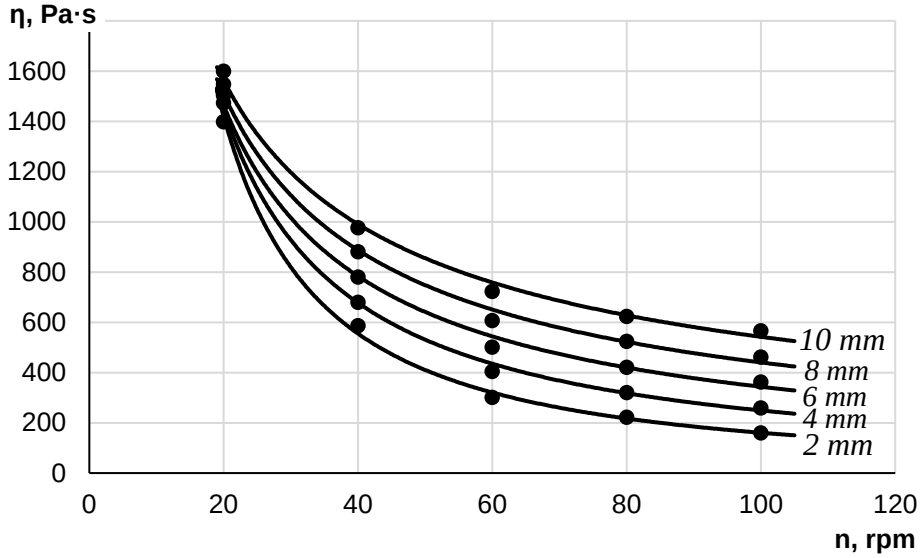

Figure 8. Viscosity change in the kneading chamber, depending on the distance between the cams and the rotation speed of the working element

It has been investigated that with increasing rotation speed, the viscosity of the dough [η = Pa · s] decreases in the kneading chamber. The decrease in viscosity is also affected by the reduction of the distance between the cam working elements, as the distance between the cams during the kneading process will decrease the viscosity of the dough.

The mathematically obtained dependence is described as:

$$\eta = (201431 \cdot S^{-1,4}) n^{0,09S - 1,4}, \quad (26)$$

where, S is the distance between the cam working elements, mm; n is the speed of rotation of the working element, rpm.

Physical modeling of kneading the yeast dough

Simulation parametric model of the yeast dough kneading process allowed us to study in detail the processes occurring in the dough mixing chamber, the dependence of the flow motion on the design and configuration of the cam working elements, and the rotational speed.

The results of simulation parametric modeling were tested on a physical model (Figure 9).

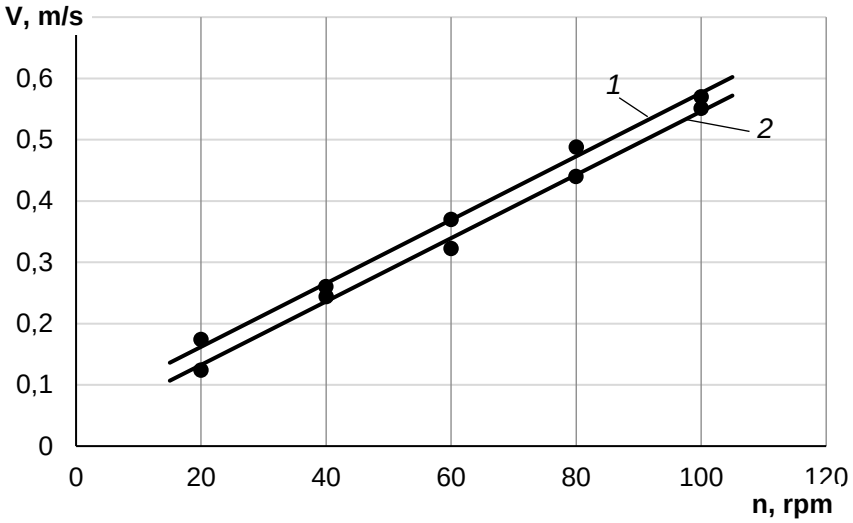

Figure 9. Comparison of the results of physical and simulation modeling of change of speed [V, m/s] in the mixing chamber at different speed of the cam working element (1 – physical; 2 – simulation)

Comparing the results of physical and simulation modeling of the yeast dough kneading process with the camshafts, and carrying out the mathematical processing of the obtained results, the error is less than 5%, the mathematical model corresponds to adequacy.

On the basis of simulation modeling and experimental studies, the design of the working element for kneading yeast dough in a continuous kneading machine is proposed.

It is rational to use the gap between the cams and the wall of the mixing chamber for cam working elements, this will help during production to compensate for production tolerances and irregularities, compensate for uneven heat distribution and reduce the excessive pressure on the semi-finished product.

Rational parameters of the cam working elements

To increase the carrying capacity of the cam working elements, improve the mixing and reduce the cost of heat (increase the temperature of the dough), rational use of the cam working elements with a variable pitch and a variable position of the cams at $\alpha = 45°$ (Figure 10) or combined cam working element with the use of turns auger (Figure 11) at the beginning of the working element. It is rational to use the selected cam working element profile ($\alpha = 45°$), so that the location of the cam can be changed on the shaft of the working element depending on the needs of the process. Changing the cam pitch also affects the intensity of the kneading process and the duration of the kneading steps.

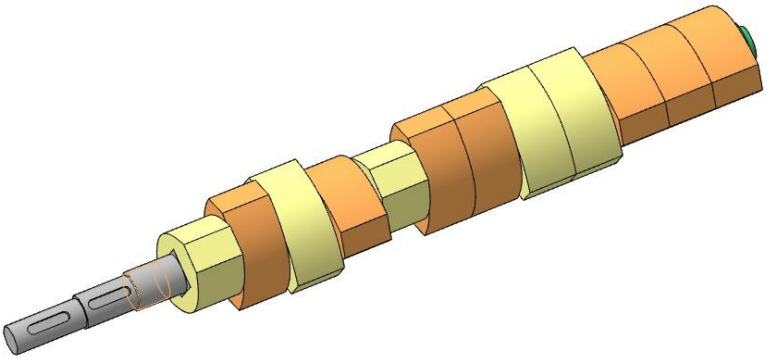

Figure 10. Cam working element with variable pitch

It is possible to rationalize the process of kneading the dough and reduce the time it takes to stand and ferment due to the intensive mechanical processing of the dough by the working cams, and as a result of obtaining the qualitative characteristics of the bakery products.

It is advisable to knead yeast dough using cam working elements. In the first kneading stage, to ensure the mixing of components and to improve the transport properties, it is advisable to use a cam working element with a pitch of 18 mm and a distance between the cams of 2 mm, the number of doubly located cam 5 pairs with an angle $\alpha = 45°$ or a screw working element (Figure 11) with a pitch of 18 mm is paired with 4 turns of the screw auger on the shaft.

In the second kneading stage, it is advisable to use 2 doubly arranged cam elements with 36 mm increments and 8 mm cam spacings, under these conditions the working volume in the mixing chamber will increase and the mixing chamber pressure will decrease. It is advisable to carry out the plasticization step with a pairwise cam working element with a pitch of 54 mm and a distance between the cams of 4 mm under these conditions, the outlet stabilizes the viscosity of the product.

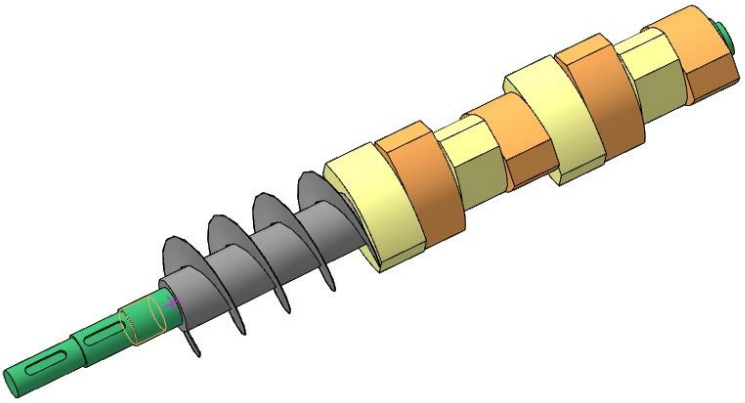

Figure 11. Combined (cam-screw) working element

In the case of positioning at the beginning of the shaft of the screw element, for the second and third stages on the rest of the shaft, it is advisable to place the cam working element in 18 mm increments and the distance between the cams for 5–8 pairs of cams 2 mm for proper mixing, under these conditions, the pressure is increased, thereby reducing the viscosity and, consequently, the load on the engine, which saves electricity, then 9–12 pairs of cams with the distance 4 mm to plasticize the dough.

Conclusions

The simulated parametric model of the kneading process by cam working elements has been developed that allows to perform design calculations effectively in case rational structural and technological parameters selection. The use of the presented scientific and methodological developments will greatly speed up and economically save the process of creating reliable technological equipment for kneading yeast dough.

Changes in the shear stresses of the yeast dough in the mixing chamber, in the area of engagement of the working elements and close to the contact with the walls of the mixing chamber are studied. The dissipation distribution in the kneading chamber and the temperature change during the kneading process were investigated. At a rotation speed of the working element of 60 rpm, the temperature of the yeast dough rises to 5° C, which is acceptable during kneading of the dough.

Mixing speed, dough viscosity, and mixing chamber pressure were investigated. With increasing rotation speed of the working element, the speed of mixing the dough in the mixing chamber increases. Increasing the rotational speed from 20 rpm to 100 rpm increases the pressure in the kneading chamber and reduces the viscosity of the yeast dough.

Based on the simulation modeling of the yeast dough kneading process, effective working elements for kneading yeast dough in a continuous kneading machine are proposed.

References

1. Šćepanović P., Goudoulas Th.B., Germann N. (2018), Numerical investigation of microstructural damage during kneading of wheat dough, *Food Structure,* 223, pp. 8–16.
2. Cappelli A., Guerrini L., Cini E., Parenti A. (2019), Improving whole wheat dough tenacity and extensibility: A new kneading process, *Journal of Cereal Science,* 180, pp. 109–118.
3. Packkia-Doss P.P., Chevallier S., Pare A., Le-Bail A. (2019), Effect of supplementation of wheat bran on dough aeration and final bread volume, *Journal of Food Engineering*, 252, pp. 28–35.
4. Hackenberga S., Vogelb C., Scherfb K.A., Jeklea M., Beckera T. (2019), Impact of altered starch functionality on wheat dough microstructure and its elongation behavior, *Food Chemistry*, 290, pp. 64–71.
5. Tozattia P., Hopkinsa E.J., Briggsb C., Huclb P., Nickerson M. (2019), Effect of chemical oxidizers and enzymatic treatments on the rheology of dough prepared from five different wheat cultivars, *Journal of Cereal Science,* 90, pp. 24–35.
6. Lamrinia B., Della G., Treleac T., Perrotc N., Trystram G. (2012), A new method for dynamic modelling of bread dough kneading based on artificial neural network, *Food Control,* 600, pp. 512–524.
7. Lia1 H., Thompsona M., O'Donnellb K. (2014), Understanding wet granulation in the kneading block of twin screw extruders, *Chemical Engineering Science,* 113, pp. 11–21
8. Schittnyab A., Ogawac H., Huwylera J., Puchkova M. (2018), A combined mathematical model linking the formation of amorphous solid dispersions with hot-melt–extrusion process parameters, *European Journal of Pharmaceutics and Biopharmaceutics,* 250, pp. 127–145
9. Sadot M., Cheio J. Le–Bail A. (2017), Impact on dough aeration of pressure change during mixing, Journal of Food Engineering, 195, pp. 150–157
10. Li H., Thompson M., O'Donnell K. (2014), Understanding wet granulation in the kneading of twin screw extruders, *Chemical Engineering Science,* 133, pp. 11–21
11. Oestersötebiera F., Traphönera P. (2016), Design and implementation of intelligent control software for a dough kneader, *Procedia Technology,* 26, pp. 473–482
12. Bucheabcde S., Davidouabc F., Vertée J. (2014), Influence of oxygen content of kneading atmosphere on oxygen uptake and relaxation index of bread dough with various additives, *Journal of Cereal Science,* 60, pp. 282–288
13. Hackenberg S., Jekl M. (2018), Mechanical wheat flour modification and its effect on protein network structure and dough rheology, *Food Chemistry,* 248, pp. 296–303
14. Guy B., Ioan D., Trelea C., (2012), A new method for dynamic modelling of bread dough kneading based on artificial neural network, *Food Control,* 26, pp. 512–524
15. Ruiz T., Delalonde M., Bataille B. (2005), Texturing unsaturated granular media submitted to compaction and kneading processes, *Powder Technology*, 154, pp. 43–53
16. Asaithambiabc N., Fontainebcd J., Lancelotbc E. (2020), Evaluation of bread dough aeration during kneading by an air–jet impulse system, *Journal of Food Engineering,* 278, pp. 109–121
17. Cappelli A., Guerrini L., Cini E. (2019), Improving whole wheat dough tenacity and extensibility: A new kneading process, *Journal of Cereal Science*, 90, pp. 102–122
18. Morgensternb O. Campanellacf1 N. Larsenb (2000), Rheological Properties of Dough During Mechanical Dough Development, *Journal of Cereal Science*, pp. 293–306
19. Vitalii Rachok, Volodymyr Telychkun, Yevgenii Shtefan, Yuliya Telychkun, Stanka Damyanova (2018), Modeling of the process of kneading the yeast dough by cam operating elements, *Ukrainian Food Journal*, 8(2), pp. 355–367.
20. Rachok V.V., Hudzenko V.V., Telychkun Yu.S., Telychkun V.I. (2018), Formuvannia struktury pshenychnoho tista v protsesi zamishuvannia, *Naukovi pratsi Natsionalnoho Universytetu kharchovykh tekhnolhii*, 24(2), pp. 155–162

Influence of gas-dynamic parameters of the heat carrier on the efficiency of drying peas in rotary dryers with a fluidized bed

Roman Yakobchuk, Sviatoslav Lementar

National University of Food Technologies, Kyiv, Ukraine

Keywords:

Drying
Peas
Rotory
Dryer
Fluidization

Article history:

Received 02.09.2019
Received in revised form 27.01.2020
Accepted 30.06.2020

Corresponding author:

Roman Yakobchuk
E-mail: yakroman@ukr.net

DOI: 10.24263/2304-974X-2020-9-2-15

Abstract

Introduction. The aim of the research is determination the influence of gas-dynamic parameters of heat carrier movement in the chamber of a rotary drying unit with a fluidized bed on the efficiency of the peas drying process.

Materials and methods. The research was carried out on an experimental drying unit with a conical element installed in the drying chamber, and with the help of 3D models of drying units. The simulation of the heat carrier movement was performed using CFD methods, followed by verification in a pilot plant.

Results and discussion. It is established that the heat carrier speed in the drying chamber without a conical element is in the recommended limits (1.8–2 m/s) only in the range from 0 to 0.7 m in the height of the chamber. The zone from 0.7 to 1.2 m is used less efficiently, because the velocity of the heat carrier is in the range of 1.65–1.8 m/s. The reason for this is that when the heat carrier passes through the wet product, its temperature decreases, it leads to decreasing of heat carrier volume. This causes the destruction of the constant mode of heat carrier and consequently reducing of the intensity of drying of the product.

In the drying unit with a conical element, the stabilization of the heat carrier speed is achieved within the recommended (1.8–2 m/s) limits along the entire height of the drying zone, which provides a constant height of the fluidized bed of product in the drying chamber. This creates the conditions for a higher intensity of drying the material and improves the quality of the dried product, because it does not stay for a long time in the high temperature zone.

It is found out that with heat carrier speed increasing over 2 m/s there is a decrease in the efficiency of its potential. Thus at an initial speed of 2 m/s and an initial temperature of 100 °C, its final temperature is about 55 °C, which coincides with drying regulations for installations of this type. While increasing speed up to 2.2 and 2.4 m/s there is final temperature increasing of the heat carrier up to 58 and 60 °C and as a result it reduces the efficiency of this installation.

Conclusions. This research allows to determine the influence of the installation of a conical element in the drying chamber on the speed of the of heat carrier and its pressure in the drying zone, as well as the influence of the speed of the drying agent on its temperature in this zone.

Introduction

There are various methods of green peas drying, including drying in a fluidized bed, which has proved its effectiveness as it provides equal distribution of the heat carrier inside the layer of material and high intensity of its drying [1]. One of the most efficient drying units of this type is a rotor dryer which provides equal distribution of the drying agent in the cross section of the drying chamber and its intensive interaction with the product [2]. However it is difficult to ensure a constant height of the fluidized bed, which reduces its efficiency in this kind of dryer [2].

It is necessary to research the gas-dynamic parameters of the heat carrier in the drying chamber to solve this problem and provide recommendations for improving the design of the drying unit. It should take into account not only the highest acceptable temperature of the product, but also the rate of its achievement, i.e. the heating rate, as well as the duration of the product at this temperature [3, 4]. In addition, the interaction of the heat carrier and the product is substantiated by design features of the drying unit [5].

In order to reduce the cost of experimental dryers and expand the range of research [6, 7], the feasibility of using CFD methods to model the process of drying products in a fluidized bed is substantiated. According to this approach, it is important to choose an appropriate calculation model and the reliability of the input data [8, 9]. Taking into account the peculiarity of the research process, the authors [10] argue that while modelling it is also very important to analyze the sensitivity of the model's responses to changes in parameters in the main components of the equations to identify possible weaknesses in model prediction. For this reason in this research [10, 11] the influence of the following parameters was analyzed: total volumetric heat transfer coefficient, heat loss coefficient, drying rate, specific heat of solid and specific heat of dry air on the forecasting model studied in this research [12]. These data can be used to describe the functional dependencies of the input parameters that are embedded in the calculation model. It is also important to be able to scale research results. The authors of [11] proposed a method for scaling the results of studies of fluidized bed dryers using the volume coefficient of heat transfer.

The research results of [13, 14, 15] authors mentioned above and other ones showed high reproducibility in real research facilities and in the operation of industrial equipment, but they were carried out on equipment that is structurally different from those which are considered in this article.

Therefore, the aim of the research is to determine the gas-dynamic parameters of the heat carrier movement during peas drying in the chamber of a rotary drying unit with a fluidized bed [2].

Materials and methods

The process of drying peas was researched. Preparation of research samples was carried out according to the methodology [13].

For modeling, 3D-models of rotary-type drying units with a fluidized bed without a conical element [2] and with a conical element were used (Figure 1). Inside the drying chamber with a conical element there is a perforated lattice with a sector cutout, where the drive shaft with a conical element with welded blades is placed (Figure 2). The design of the basic drying chamber [2] is different as there is no conical element. The geometrical parameters of the model are shown in Figure 3.

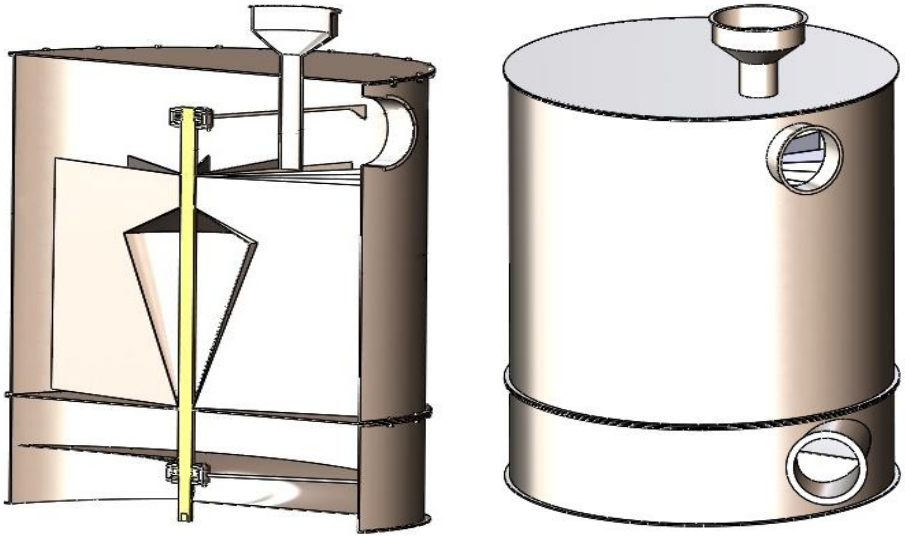

Figure 1. Improved drying chamber of rotary dryer with a fluidized bed

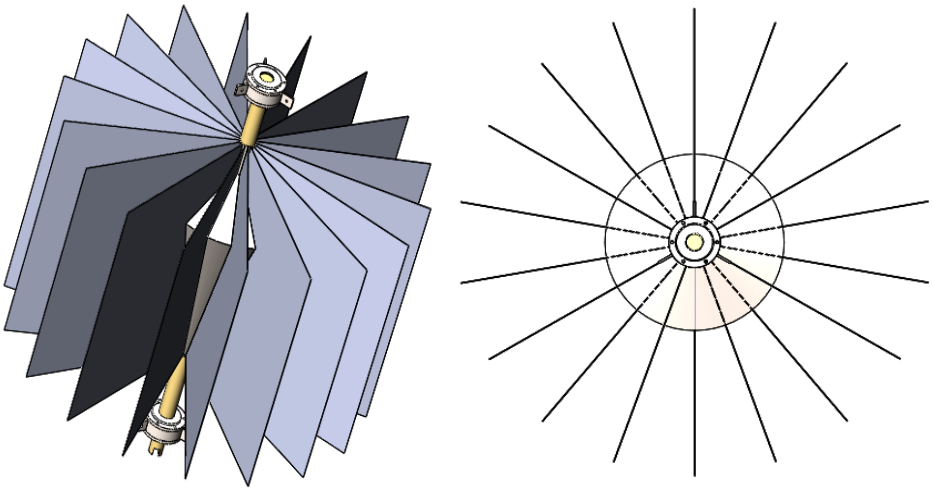

Figure 2. Model of the drive shaft with a conical element and blades

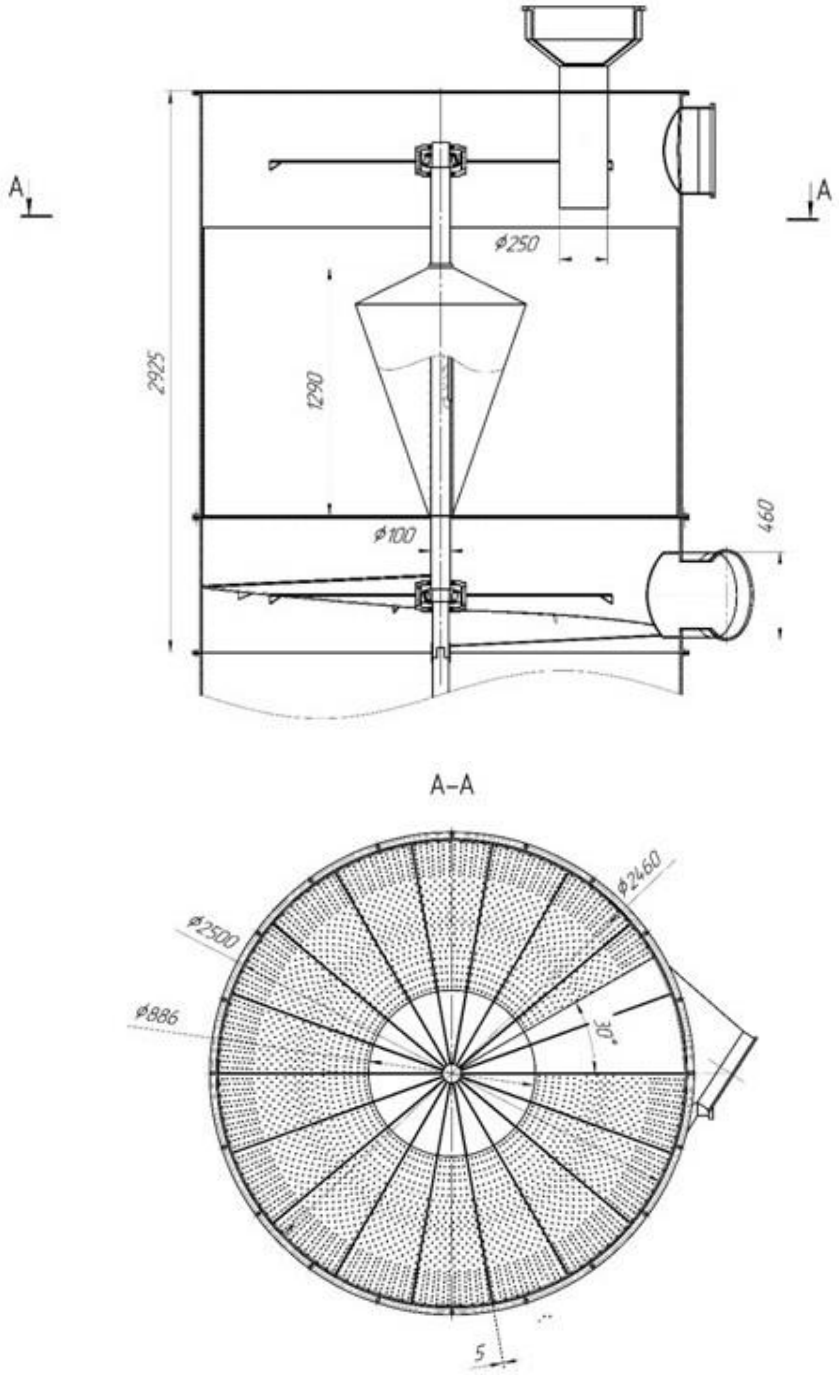

Figure 3. Geometric parameters of the model

Modeling of drying agent flows was performed using the methods of Computational Fluid Dynamics (CFD), according to the method [16]. 3D models created in CAD Autodesk Inventor.

The following input parameters are entered into the model:

- initial temperature of the drying agent – 100 °C;
- final drying agent temperature – 55 °C;
- initial temperature of the material – 18 °C;
- final temperature of the material – 40 °C;
- initial humidity of material – 25%;
- final moisture content of the material – 14%;
- initial relative humidity – 63%;
- final relative humidity – 80%;
- air velocity at the entrance to the material layer – 2 m/s;
- the average particle diameter of the material is 5 mm.

The expected result of modeling the drying agent flows is finding the characteristic features of the gas-dynamic pattern in the drying chamber of this drying unit, to identify areas of intense vortex formation and separation in order to determine the rational parameters of the drying process.

Description of the experimental dryer

The simulation results were checked on an experimental plant (Figure 4).

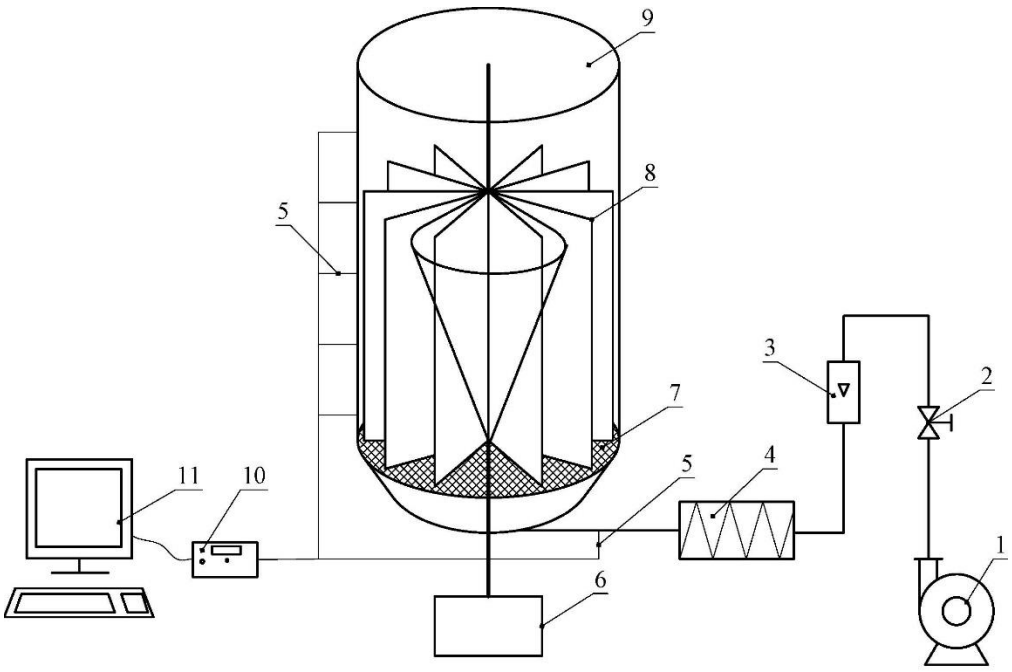

Figure 4. The scheme of the experimental plant for the drying peas research:
1 – blower; 2 – control valve; 3 – flow meter; 4 – heater; 5 – thermocouples;
6 – drive rotor of the device; 7 – gas distribution grille; 8 – rotor of the drying chamber;
9 – drying chamber; 10 – data logger; 11 – PC

The input parameters of the heat carrier and product for experimental research were the same as for modeling.

The air is supplied by a blower 1 through the control valve 2 and the flow meter 3 to the heater 4, where it is heated to 100 °C and enters the drying chamber 9 through the gas distribution grid 7. The product is filled into the drying chamber 9 between the rotor blades 8. The temperature at the inlet and along the drying chamber is measured by thermocouples 5. The signals from the thermocouples are sent to the data logger 10 connected to the PC.

Results and discussion

As a result of researches graphs of distribution of speed, pressure and temperature of the heat carrier in the drying chamber are received.

According to [14], the minimum required heat carrier supply rate to create a stable fluidization regime when drying peas with an initial humidity of 23–25% is 1.8–2 m/s. It is discovered (Figure 5) that the velocity of the heat carrier in the drying chamber of the base unit [2] is according to the recommended limits only in the range from 0 to 0.7 m in the height of the chamber. The zone from 0.7 to 1.2 m is used less efficiently, because the velocity of the heat carrier is in the range of 1.65–1.8 m/s. The reason for this is that when the heat carrier passes through the wet product, its temperature decreases, which leads to a decrease in the volume of the heat carrier [18]. This causes the destruction of the constant mode of fluidization and, consequently, reduce the intensity of drying of the product. For a product with a higher initial humidity, this effect will be even much greater, as the minimum rate of fluidization increases linearly with the moisture content of the product [14].

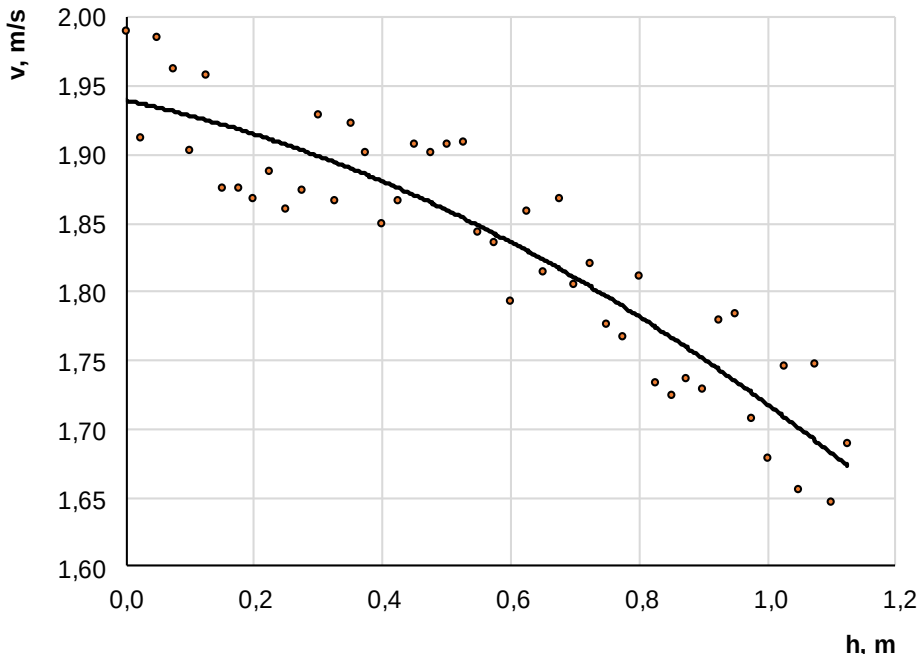

Figure 5. Change of heat carrier velocity on the height of the drying chamber

Investigating the change in heat carrier temperature along the height of the drying chamber depending on its initial speed (Figure 6), we found that when it grows above 2 m/s there is a decrease in the efficiency of the drying agent potential. Thus, at the initial velocity of the heat carrier of 2 m/s and the initial temperature of 100 °C, its final temperature is about 55 °C, which corresponds to the accepted drying regulations for installations of this type. With increasing speed to 2.2 and 2.4 m/s, there is an increase in the final temperature of the heat carrier to 58 and 60 °C. This is because the heat carrier does not have time to give the required amount of heat to the product at high speeds.

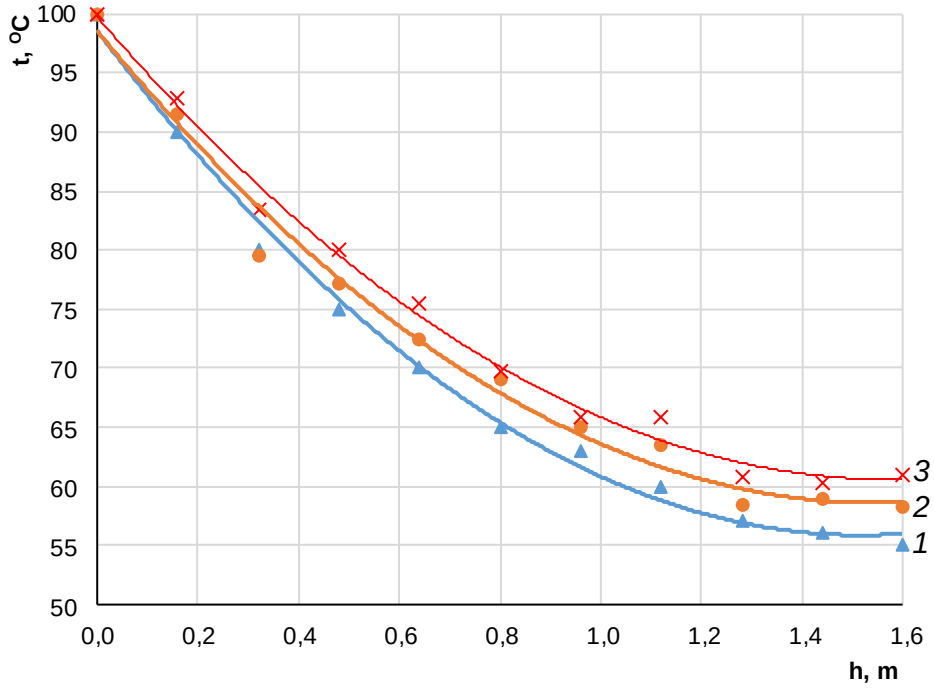

Figure 6. Change of heat carrier temperature on height of the drying chamber depending on its initial speed: 1 – 2m/s; 2 – 2.2 m/s; 3 – 2.4 m/s.

Therefore, it is impossible to ensure a constant fluidization mode by increasing the inlet velocity of the heat carrier without reducing the efficiency of the drying unit. To ensure a uniform fluidization rate along the height of the chamber, a conical element with an expanded base at the top is installed, which gradually reduces the cross section of the drying chamber (Figure 1, 2, 3).

The positive effect of installing a conical element is as follows. As it was mentioned before, lowering the heat carrier temperature leads to a decrease in its volume. However, reducing the cross-sectional area where the heat carrier passes in the dryer with a conical element stabilizes its speed. As a result, the velocity of the heat carrier remains constant throughout the height of the fluidized bed, which creates conditions for higher drying intensity of the material and improves the quality of the dried product, because it cannot stay too long in the high temperature zone [18].

In addition, to detect the effect of the installation of a conical element on the pressure of the heat carrier flow, the change of this pressure along the height of the chamber was investigated. It is seen (Figure 7) that in the chamber of the basic dryer (without a conical element) there are fluctuations of this parameter in the range from 3350 to 3720 Pa. There is a slight decrease of average pressure from 3565 to 3550 Pa from the beginning to the end of the zone of intensive drying.

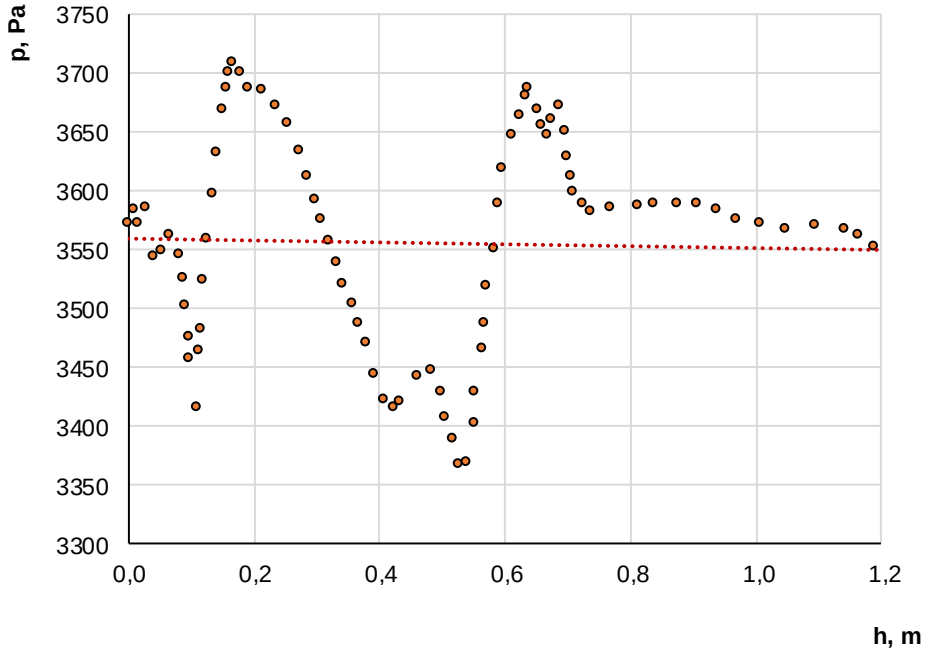

Figure 7. Change of drying agent pressure on the height of the drying chamber

For a more detailed picture of the pressure distribution of the heat carrier flows over the volume of the chamber, the results of research in the form of vector pressure fields are given (Figure 8).

The following results of similar researches are shown, but for a dryer with a conical element.

It is shown on the Figure 9. that in this kind of drying chamber the velocity of the heat carrier is according to the recommended (1.8–2 m/s) limits along the entire height of the drying zone, which confirms the correct choice of design and geometric parameters of the conical element (Figure 3).

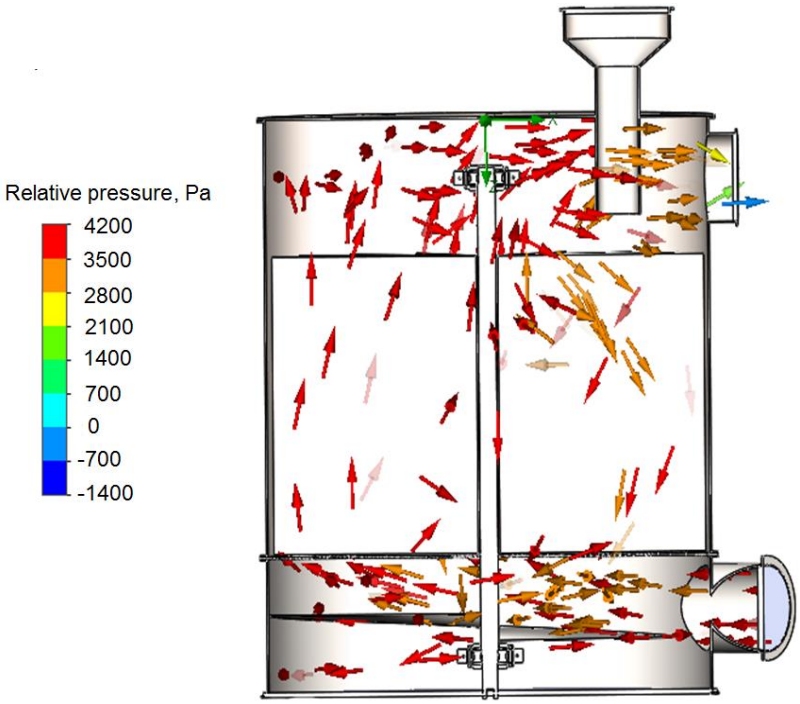

Figure 8. Vector pressure fields of the drying agent in the drying chamber

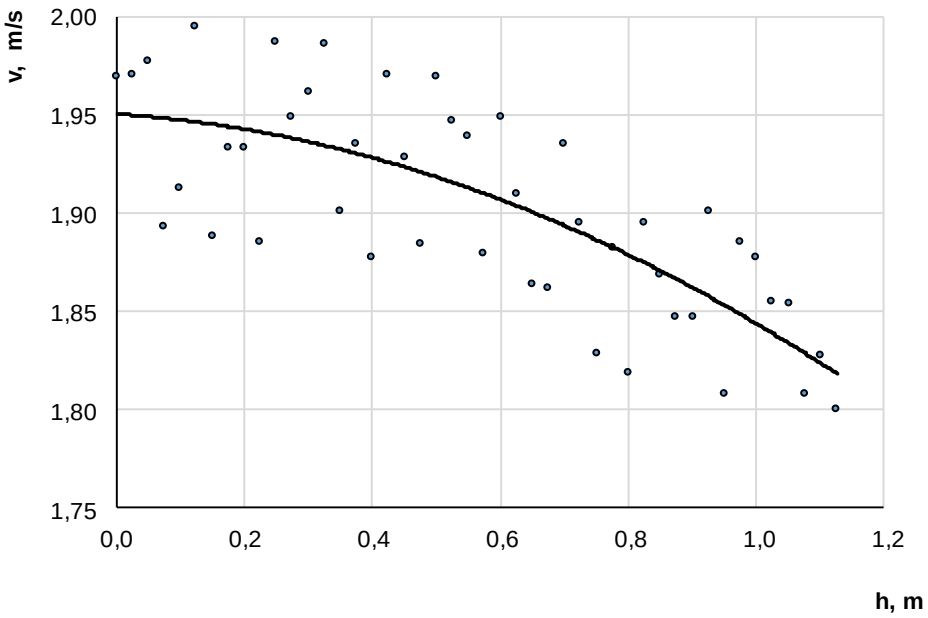

Figure 9. Change of the heat carrier speed on height of the drying chamber with a conic element

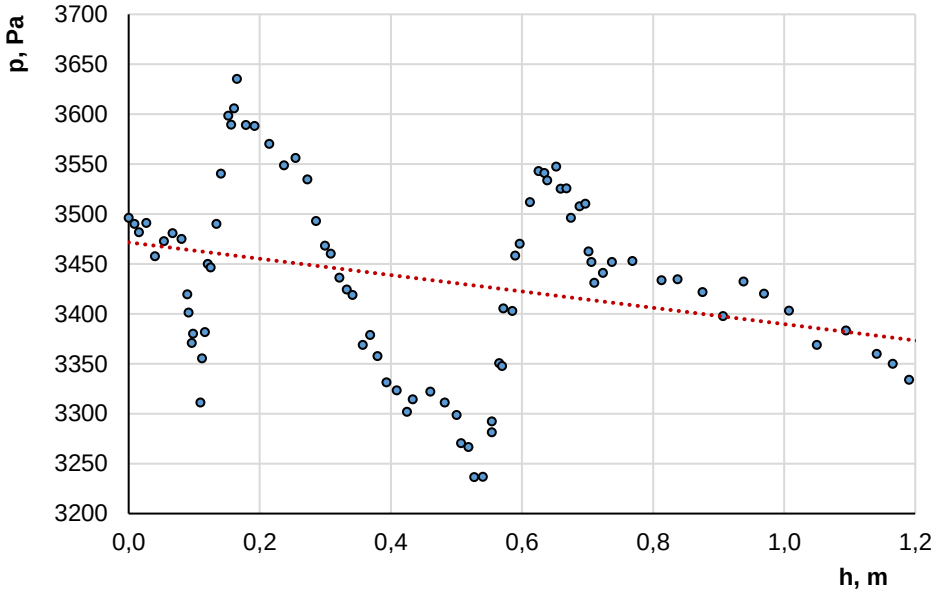

Figure 10. Change of the heat carrier pressure on height of the drying chamber with a conic element

In the chamber of the dryer with a conical element (Figure 10), the nature of the pressure change has changed slightly and there is a more pronounced decrease compared to the basic dryer. Pressure fluctuations are in the range from 3240 to 3630 Pa. There is a slight decrease in the average pressure from 3475 to 3380 Pa from the beginning to the end of the drying zone. These changes are fully consistent with the laws of gas dynamics, because the speed of the heat carrier in the dryer with a conical element is slightly higher than in the basic one.

The results of research on the experimental plant confirm the data obtained by simulation.

From Figure 11, it is seen that the nature of the temperature change corresponds to the data obtained by simulation in the corresponding range of heights of the drying chamber. The error varies between 3-4%. The nature of the change in the gas-dynamic parameters of the heat carrier is confirmed in researches [14, 17].

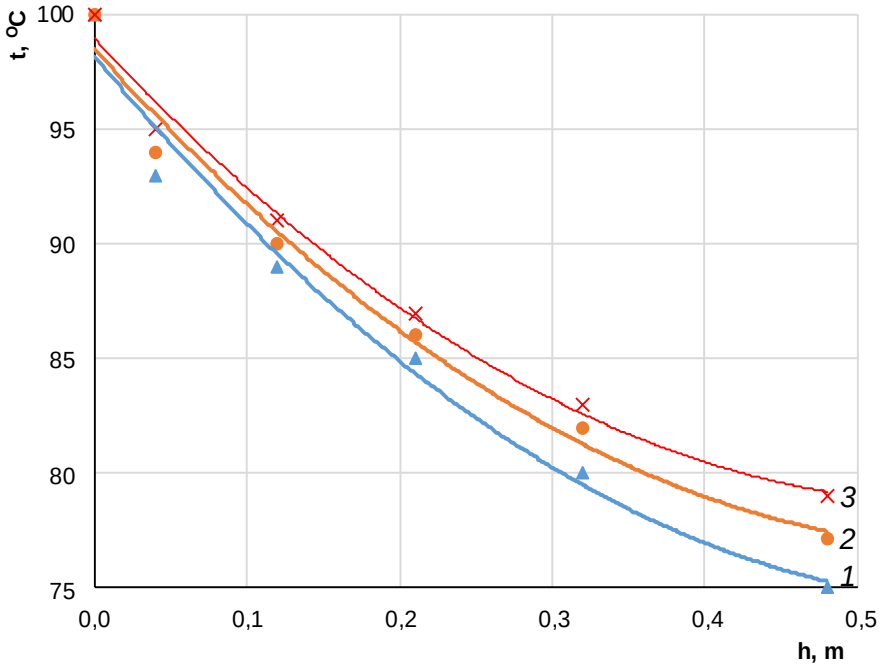

Figure 11. Change of the heat carrier temperature on the height of the drying chamber of the experimental plant depending on its initial speed: 1 – 2 m/s; 2 – 2.2 m/s; 3 – 2.4 m/s

Conclusions

1. It is found out that the speed of the heat carrier in the drying chamber of the dryer without a conical element is in the recommended range (1.8–2 m/s) only in the range from 0 to 0.7 m in the height of the chamber. The zone from 0.7 to 1.2 m is used less efficiently, because the velocity of the heat carrier is in the range of 1.65–1.8 m/s.
2. In the dryer with a conical element, the stabilization of the heat carrier velocity is achieved within the recommended (1.8–2 m/s) limits along the entire height of the drying zone, which provides a constant height of the fluidized bed of product in the drying chamber. This creates the conditions for a higher intensity of drying the material and improves the quality of the dried product, because it does not stay for a long time in the high temperature zone.
3. It is discovered that when speed of the heat carrier increases over 2 m/s efficiency decrease of use of its potential is observed. Thus, at an initial velocity of 2 m/s and an initial temperature of 100 °C, its final temperature is about 55 °C, which corresponds to the adopted drying regulations for installations of this type. With increasing speed to 2.2 and 2.4 m/s there is an increase in the final temperature of the heat carrier to 58 and 60 °C what consequently reduces the efficiency of this dryer.

References

1. Hatamipour M.S., Mowla D. (2007), Correlations for shrinkage, density and diffusivity for drying of maize and green peas in a fluidized bed with energy carrier, *Journal of Food Engineering*, 59(2-3), pp. 221–227.
2. Yakobchuk R. (2014), The influence of design parameters of rotary dryer on sunflower seeds drying, *Ukrainian Food Journal*, 3(3), pp. 437–445.
3. Scaar H., Franke G., Weigler F., Delele M.A., Tsotsas E., Mellmann J. (2016), Experimental and numerical study of the airflow distribution during mixed-flow grain drying, *Drying Technology*, 34(5), pp. 595–607.
4. Fabian Weigler, Jochen Mellmann (2014), Investigation of grain mass flow in a mixed flow dryer, *Particuology*, 12, pp. 33–39.
5. Mykhailyk V., Lementar S., Yakobchuk R., Skrynnyk Y., Semenko R. (2016), Wheat grain drying kinetics in a thin layer, *Ukrainian Journal of Food Science*, 4(2), pp. 316–326.
6. Guo B., Langrish T.A.G., Fletcher D.F. (2003), Simulation of gas flow instability in a spray dryer, Trans IChemE, Part A, *Chem Eng Res Des*, 81, pp. 631–175.
7. Harvie D. J. E., Langrish T.A.G., Fletcher D.F. (2001), Numerical simulations of gas flow patterns within a tall-from spray dryer, Trans IChemE, Part A, *Chem Eng Res De*s,79, pp. 235–248.
8. Kota K., Langrish T. (2007), Prediction of Deposition Patterns in a Pilot-Scale Spray Dryer Using CFD Simulations, *Chem. Prod. and Proc. Modeling*, 2(3), pp. 26–35.
9. Silva, M. G., Lira, T. S., Arruda, E. B., Murata, V. V., & Barrozo, M. A. S.. (2012). Modelling of fertilizer drying in a rotary dryer: parametric sensitivity analysis, *Brazilian Journal of Chemical Engineerin*g, 29(2), pp. 359–369.
10. Poós T., Szabó V. (2017), Application of mathematical models using volumetric transfer coefficients in fluidized bed dryers, *Energy Procedia*, 112, pp.374–381.
11. Arruda, E. B. (2008), *Comparison of the performance of the roto-fluidized dryer and conventional rotary dryer. PhD. Thesis*, Uberlândia-Brazil, Federal University of Uberlândia.
12. Ghalavand Y., Hatamipour M.S. & Rahimi A. (2011), Kinetics Study of Green Peas Drying in a Spouted Bed in the Presence of a Heat Carrier, *Drying Technology: An International Journal*, 29, pp. 1648–1655.
13. Zhanyong Li, Jingsheng Ye, Hongtai Wang, Ruifang Wang (2006), Drying characteristics of green peas in fluidized beds, *Transactions TSTU*, 12(3A), pp. 668–675.
14. Liu Y., Peng J., Kansha Y., Ishizuka M., Tsutsumi A., Jia D., Bi X.T., Lim C.J., Sokhansanj S., Novel fluidized bed dryer for biomass drying, *Fuel Processing Technology*, 122, pp. 170–175.
15. Lementar S., Ponomarenko V., Lulka D., Dubivko A. (2015), Modeling of the air supply system in spray dryer, *Ukrainian Food Journal*, 2(1), pp. 77–87.
16. Kaur, H. & Bawa, Amarinder. (2002). Studies on fluidized bed drying of peas, *Journal of Food Science and Technology – Mysore*, 39, pp. 272–275.
17. Siddique A.B. and Wright D. (2003), Effects of Different Drying Time and Temperature on Moisture Percentage and Seed Quality (Viability and Vigour) of Pea Seeds (Pisum sativum L.), *Asian Journal of Plant Sciences*, 2, pp. 978–982.

Analysis of the grain market in Ukraine in the context of land reform

Tetiana Rybachuk-Iarova, Iryna Tiukha

National University of Food Technologies, Kyiv, Ukraine

Keywords:

Grain
Production
Export
Ukraine
Reform

Article history:

Received 22.10.2019
Received in revised form 15.02.2020
Accepted 30.06.2020

Corresponding author:

Iryna Tiukha
E-mail: tykhaiv@outlook.com

DOI:
10.24263/2304-974X-2020-9-2-16

Abstract

Introduction. The aim of this research is to identify the main disproportions in the development of the grain market in Ukraine in the implementation of land reform.

Materials and methods. The Ukrainian grain market is researched in the context of land reform. The compliance of the implemented transformations with the international dimensions and the concept of market regulation is monitored. A logical-abstract method was used to group national and international analytical results.

Results and discussion. In 2018, the production of grain crops in Ukraine was the highest within the period from 1991 to 2018. In general, the positive dynamics of growth in grain crop production is observed since 2003. The growth of grain crops production was achieved by increasing the crop production area and increased yields. The main cereals are wheat, corn, sunflower, barley, soybeans and rapeseed. The profitability of wheat in Ukraine corresponds to the level of major producer countries, and averages 26.8%

Sunflower production volumes during the period from 2011 to 2019 demonstrate positive dynamics of growth. The highest yield was in 2016, 2018 and in 2019. The highest indicators of soybean production were recorded in 2016 and 2018, which is associated with significant yields. Since 2016, there has been a gradual positive dynamics of rapeseed production.

According to the national balance of supply and demand for grains and legumes, it should be noted that Ukraine consumes not more than 30–40 centners of grain crops and oilseeds out of 92 million tons of harvested products. Therefore, further increasing of production is only possible by means of increasing exports of Ukrainian grain to the world market that, in spite of tough requirements applied by it to quality and safety of Ukrainian grain, is characterized by a rapidly growing demand. The volume of foreign currency earnings from exports of grain crops by Ukraine within the period from 2011to 2019 has a positive upward trend, except for 2013 and 2015

There are 32,214 economic entities in the field of grain growing, of which 71.3% are farms. At the same time, their share in the areas from which the harvest is harvested is only 15.8%, which indicates a low level of land concentration in farms.

The main risks of opening the land market for legal entities is massive buying of land by large agricultural holdings and fall of investment attractiveness of Ukraine. Financial risks will increase for small farmers due to the lack of the credit history and unavailability of financial instruments for the purchase of land.

Conclusions. The introduction of the land market requires the improvement of state regulation and mechanisms for the support of production, strengthening of exports capacity, formation of the adequate infrastructure of the grain market, etc.

Introduction

The state of the country's grain market is an important indicator of the quality of economic reforms carried out in the country, the implementation of agri-food policy. As an object of state regulation, the grain market needs to identify its nature, mission, functions, role in the macroeconomic system of the country [1,12,19].

Efficiency of developing the crop production industry influences welfare of population, ensures national food security and country's export capabilities [20]. The grain is the basis of all agricultural production that determines the volume of supply and the cost of food staples, forms a considerable part of the agricultural producers' income, determines the status and trends of development of rural areas, and generates foreign exchange earnings of the state [12,17].

Market transformations of strategically important commodity markets, in particular, grain, are reflected in the works of many domestic and foreign scientists [1,7,14,18,19]. At the same time, the issues of grain production, foreign trade and internal distribution in the conditions of land market opening remain insufficiently covered and require further research [10,11,19].

The above-mentioned conditioned consideration and critical analysis of the following tasks: the balance of supply and demand of grain in Ukraine in 2014/15 - 2018/19 marketing years [5,6]; the factors influencing the state of the grain market in Ukraine, in particular the dynamics of areas sown with cereals and legumes [6,9,10], the volume and structure of grain production [6,9]; the structure of land depending on the type of owner [10]; the risks and opportunities of land reform for grain producers in Ukraine [11].

The purpose of the study is to identify problems in the functioning of the grain market of Ukraine in the implementation of land reform.

Materials and methods

Materials

The object of study is the grain market of Ukraine.

Subjects of research are: the crop production area planted with grain crops and grain legumes, the grain yield, the volume of grain crop production, the production of wheat, corn, sunflower, rape seeds and soybeans, the volume of foreign currency earnings from exports of grain crops by Ukraine, the countries leading in exporting wheat, the leading exporters of corn (Kernel, COFCO Agri Ukraine, ADM Trading Ukraine, Nibulon, Suntrad) and also risks and opportunities of land reform in Ukraine.

Methods

The methodology of the study included statistical analysis, grouping, systematization of indicators of grain market development. The logic of presentation of the material follows the structure of the national grain market. The logic of the study is subordinated to the task of analyzing the constituent parts of the national grain market.

It was used used official materials of the State Statistics Committee of Ukraine about the harvesting of grain crops: harvested areas [6], production [6,9], yielding capacity [6,20]; indicators of grain supply and demand in Ukraine [6,14,15,16,18,20], volume of grain exports [4–6; 12,13].

In addition, we used research and analytical studies of domestic and foreign organizations of the countries that lead in exports of wheat and maize [1,7,12–14;18], and results of the rating evaluation of the leading exporters of grain [8–10].

Results and discussion

Grain production is a sector, products of which always was, is and will be one of the most important sources of wealth of any state. In the global agriculture, grain crops constantly dominated, and even today grain remains the most important and strategic agricultural product [9].

Grain is used by human beings in the form of bread, cereals, pasta, confectionery, etc. These products are distinguished by high nutritional and taste qualities, contain enough protein, carbohydrates, vitamins, amino acids, and minerals. Products of grain growing industry are raw materials for the processing industry. Alcohol, starch and other products can be obtained as the result of grain processing, pulp, paper, etc. can be produced as a result of straw processing. Grain is the main and indispensable forage in animal husbandry. It has a much higher nutritional value as compared with other types of feed, is characterized by a high content of forage units, digestible protein, macro- and micronutrients. By-products of grain growing — straw and chaff — and grain by-products are also used as forage.

The total demand for grain in the country is determined by the amount of grain consumed for nutrition, processing, forage, seeds, exports, and creation of state reserves. The largest share in this volume is occupied by grain that is consumed by human beings and animals as food/feed. In Ukraine, 52–57 % of the total volume of produced grain crops are used as forage for livestock and poultry, 15–17 % — as food, 8–10 % — as seeds, 3–4% are processed and up to 6–8 % are lost during storage and post-harvesting [9].

It is quite natural, climatic conditions are favorable for cultivation of almost all the well-known grains and legumes. As of 1 January 2020, 68.7 % of Ukraine — almost 41.5 million hectares — are agriculturally used areas. In particular, 32.5 million hectares are arable lands. 1.7 million hectares out of 10.4 million hectares of agriculturally used areas owned by the state were transferred to united municipalities, while 1.6 million hectares are rented, 1.4 million hectares are reserve lands, 1.3 million hectares remain in constant use, 700 thousand hectares are located at the occupied territory. Within the period from 2013 to 2019, 630 thousand hectares were transferred to private ownership. And it is surprising that almost 30 % — 3.1 million hectares are marked as the “statistical error”.

Balance of grain crops supply and demand in Ukraine

In marketing year 2018/19, grain crop production in Ukraine was by 7.9 million tons higher than in marketing year 2017/18 and reached almost 70 million tons. Production of corn increased the most. Along with the growth of the gross production, volume of exports in the 2018/19 MY was at the level of 47.5 million tons that exceeds last year's level by 6.5 million tons. Forage consumption of grain crops increased by 11 % or by 1.2 million tons again mainly due to corn [6].

The balance of grain crops supply and demand in Ukraine in marketing years 2014/15–2018/19 is shown in Table 1.

Table 1

Balance of grain crops supply and demand in Ukraine in marketing years 2014/15 to 2018/19 MP, thousand tons

Indicator	Years				
	2014/15	**2015/16**	**2016/17**	**2017/18**	**2018/19**
Initial reserves	6831	8981	6044	6454	6305
Harvesting areas, ha	14,627	14,641	14,337	14,560	14,782
Crop capacity, kg/centner	4.4	4.1	4.6	4.3	4.7
Production	63,859	60,126	66,088	61,917	69,800
Imports	197	211	223	279	237
Aggregate supply	*70,888*	*69,318*	*72,355*	*68,649*	*76,342*
Exports	35,179	39,924	45,212	40,956	47,472
Forage consumption	14,933	12,728	10,226	10,610	11,671
Food processing	6208	5835	5685	5578	5392
Industrial consumption	1294	1057	1258	1577	1142
Seeds	2236	2325	2217	2221	2266
Losses	2056	1405	1303	1403	1756
Domestic distribution	*61,906*	*63,273*	*65,901*	*62,344*	*69,789*
Final stocks	8981	6044	6454	6305	6554

Source: [6]

As Table 1 shows, the overall supply of grain crops during marketing years 2014/15–2018/19 tended to increase from 70,888 thousand tons in the 2014/15 MY to 76,342 thousand tons in 2018/19 MY.

It should be noted that, with a slight increase in production areas, there was the growth in grain yield in 2014/15 MY from 4.4 kg/ha to 4.7 kg/ha in 2018/19 MY.

Crop production area planted with grain crops and grain legumes

The dynamics of the areas planted with grain crops and grain legumes within the period from 1991 to 2018 is shown in Figure 1.

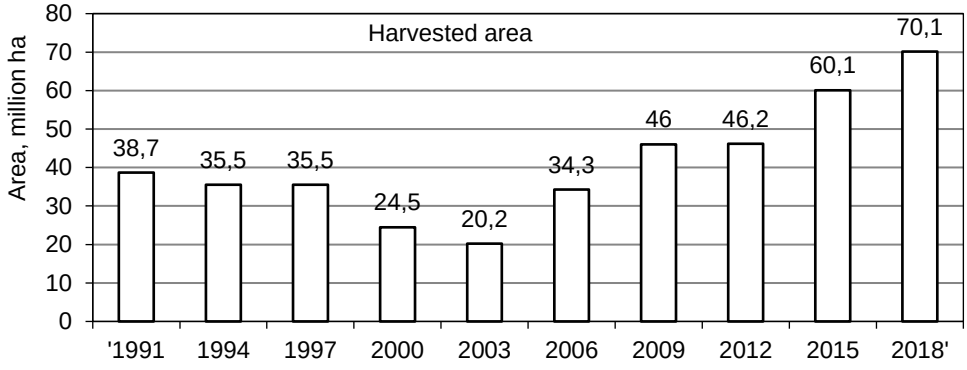

Figure 1. Dynamics of the area planted with grain crops and grain legumes within the period from 1991 to 2018, million ha [6].

Thus, the crop production area planted with grain crops and grain legumes remained almost unchanged over the period from 1991 to 2018.

Volume of grain crop production

The figure illustrates the volume of grain crop production within the period from 1991 to 2018.

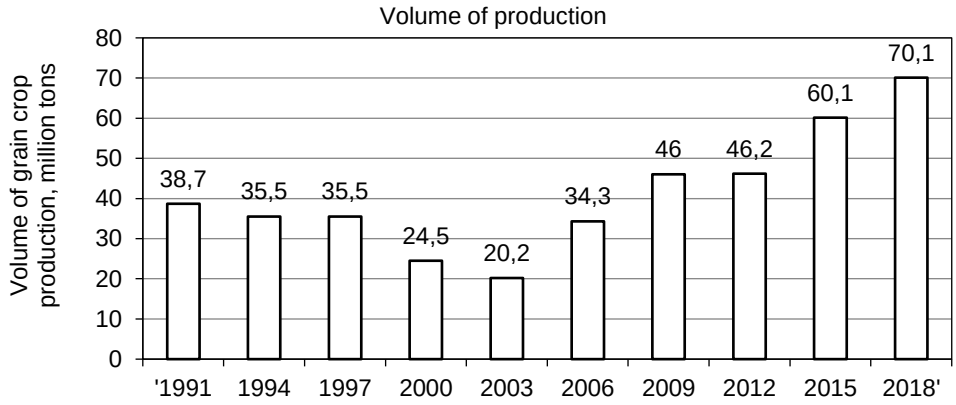

Figure 2. Volume of grain crop production within the period from 1991 to 2018 in Ukraine, million tons [6]

As Figure 2 shows, In 2018, the production of grain crops in Ukraine was the highest within the period from 1991 to 2018. In general, the positive dynamics of growth in grain crop production is observed since 2003. Thus, in 2003, Ukraine produced grain in the amount of 20.2 million tons, in 2018 — 70.1 million tons that is by 24,7 % more than in 2003 and by 81.14 % more than in 1991. The growth of grain crops production was achieved by increasing the crop production area and increased yields [5].

Production of wheat, corn, sunflower, rape seeds and soybeans

The main grain crops and grain legumes with the highest share in the total production are wheat, corn, sunflower, barley, soybeans, and rape.

The volume of basic grain crops harvested within the period from 2011 to 2019 is shown in Figure 3–4.

The Figure 3 shows that the largest volume of production within the period from 2011 to 2019 was wheat. While in 2011 the volume of production was 18.38 million tons, in 2019, its value has increased by 1.6 times. The cost of wheat production shows the tendency to growth. Over the past 5 years, the cost of wheat has almost doubled. The profitability of wheat in Ukraine corresponds to the major countries producing this culture and is in average equal to 26.8 %.

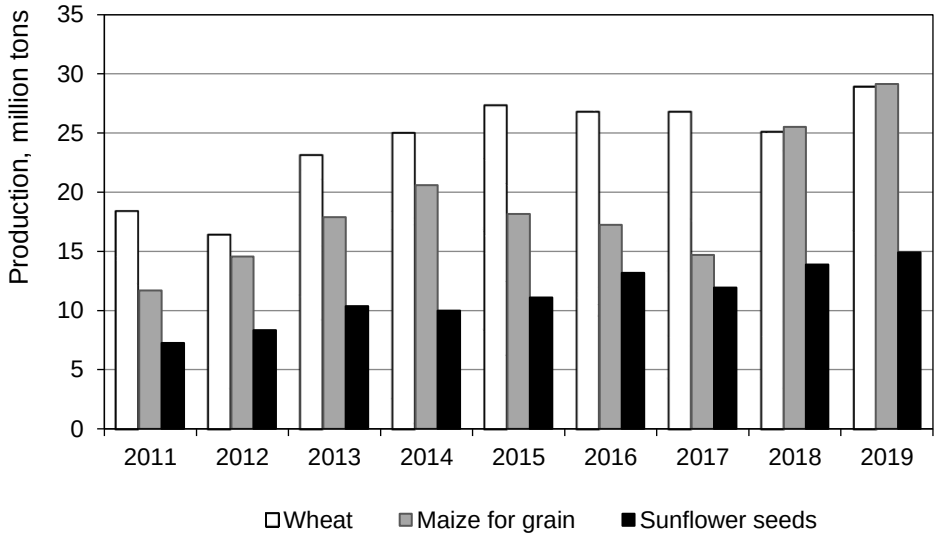

Figure 3. Production of wheat, corn, sunflower within the period from 2011 to 2019, million tons [6]

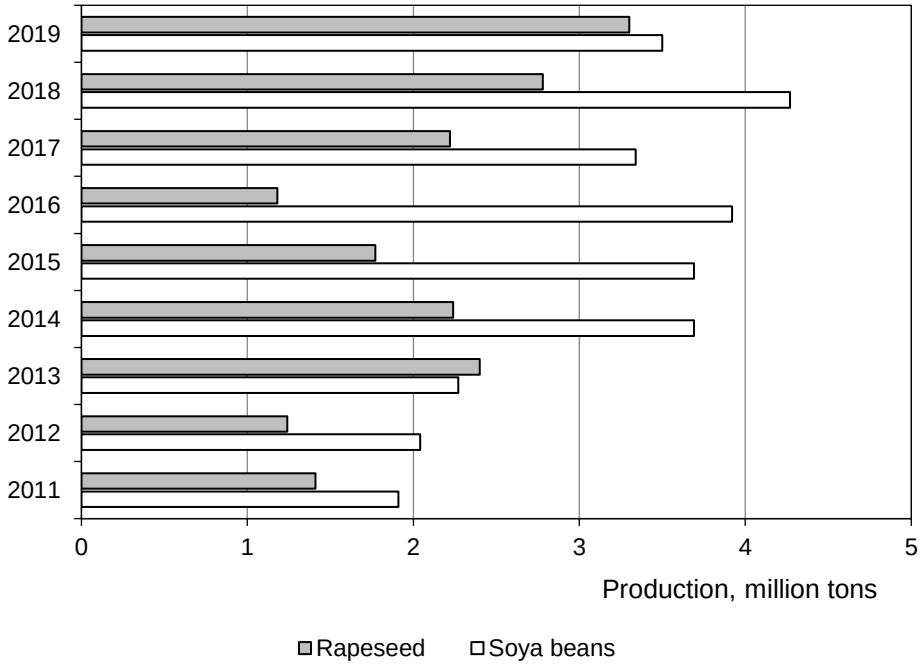

Figure 4. Production of rape seeds and soybeans within the period from 2011 to 2019, million tons [6]

Considerable positive dynamics inherent to volume of corn production within the period from 2018 to 2019 While, within the period from 2011 to 2017, the largest amount of corn production was observed in 2014, corn production in 2018 increased by 1.2 up times to 25.52 million tons as compared with this level and by 1.4 times to 29.16 million tons in 2019 due to its high yield, i. e. the amount of corn harvested per area unit. The highest corn yield indexes until 2019 were recorded in 2018, when the corn yield was 76 centners per hectare that is by 10.14 % more than in 2011 and indicates the growing efficiency of corn growing [4].

Sunflower production volumes during the period from 2011 to 2019 demonstrate positive dynamics of growth. The highest yield was in 2016. (13.19 million tons), 2018 (13.88 million tons) and in 2019 (14.92 million tons).

Within the period from 2011 to 2019, soybean production had a positive trend. The highest indexes were recorded in 2016. (105% increase relative to 2011) and in 2018 (123.6% increase relative to 2011) that is associated with a significant volume of harvested crops. Thus, the soybean yield in 2018 was 26.4 centners per 1 ha, and in 2016 — 23.6 centners per 1 ha, and in 2019 — 23.2 centners per 1 ha.

The yield of rapeseed (winter rape and colza (spring rape)) in 2018 was 27 centners per 1 ha, and in 2016 — 26.2 centners per 1 ha, and in 2019 — 25.9 centners per 1 ha. Despite the fact that the rape yield in 2016 was the highest, volumes of its production during the researched period were the lowest (1.18 million tons). It is year of 2016, since which a gradual positive trend of its production is observed that indicates an extensive way of production intensification.

According to the national balance of supply and demand for grains and legumes, it should be noted that Ukraine consumes not more than 30–40 centners of grain crops and oilseeds out of 92 million tons of harvested products.

Despite the steady growth of grain production, Ukraine still has the potential for increasing the yield of grain crops. Thus, the average yield of grain crops in the USA is 82 centners per 1 ha, in China and Brazil — 52–56 centners per 1 ha, while in Ukraine in 2019 it was 48.2 centners per 1 ha.

Further growth in production of grain crops will lead to the increased deficit in storage facilities in Ukraine, the size of which is only approximately 40 million tons. Thus, 70 % of the existing elevators are morally and physically obsolete. In most of them, grain is stored in bulk on the floor — under such conditions, it is very difficult to ensure quality and safety of grain. At such facilities, there are no effective transport equipment that would allow performing fast unloading and dispatch of certain types of grain.

Therefore, further increasing of production is only possible by means of increasing exports of Ukrainian grain to the world market that, in spite of tough requirements applied by it to quality and safety of Ukrainian grain, is characterized by a rapidly growing demand.

Volume of foreign currency earnings from exports of grain crops by Ukraine

Ukraine exports grain to 190 countries. The largest buyers of Ukrainian grain in 2019 was Africa, Asia, and Europe. Egypt remains the leader in the ranking of the largest importers (with a share of 14.1 %) for several years running. Significant shares in Ukrainian exports of grain crops accounted to China (9.6 %), Spain (7.5 %), Turkey (7.4 %), the Netherlands (6.8 %), Indonesia (5.1 %), Bangladesh (3.9 %), Israel (3.4 %), Tunisia (3.1%), and Italy (3.1%). In aggregate, these 10 countries generate 64 % of total revenues from exports of this group. The traditionally high demand for Ukrainian grain by the European Union is still preserved — 23.9 % in the structure of export supplies [3,6].

The total value of exports of grain crops by Ukraine within the period from 2011 to 2019 is shown in Figure 5.

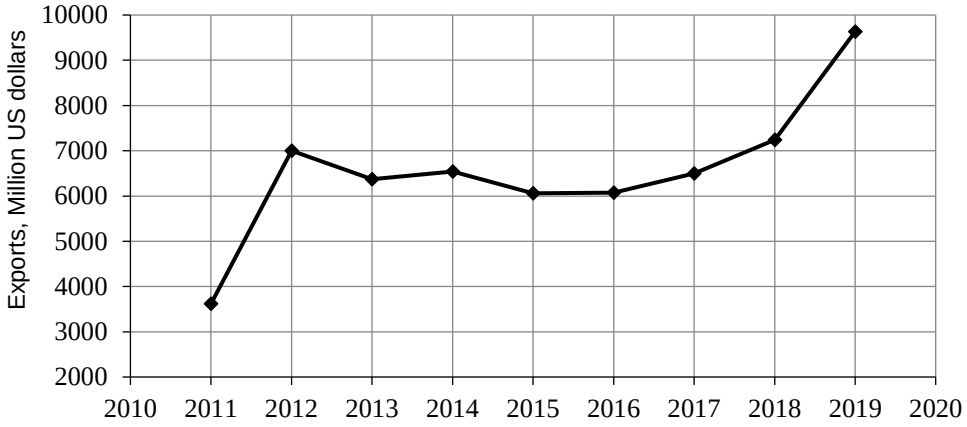

Figure 5. Exports of grain crops by Ukraine within the period from 2011 to 2019, million US dollars [6]

Thus, the volume of foreign currency earnings from exports of grain crops by Ukraine within the period from 2011to 2019 has a positive upward trend, except for 2013 and 2015 Significant rates of growth in foreign currency earnings from the export of grain crops was observed in 2012 (193.5 %) and in 2019 (133.1 %) along with a more noticeable increase of the share of grain crops in total exports of the country (Figure 6).

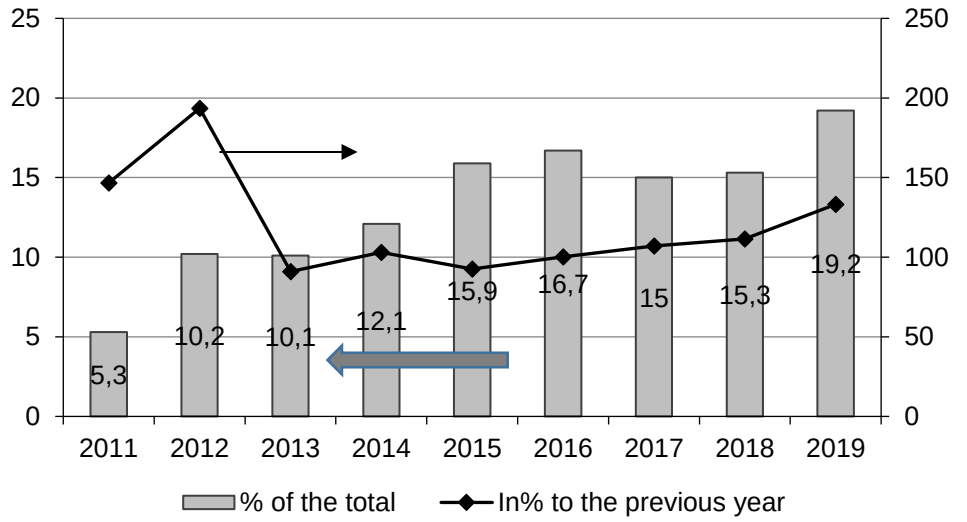

Figure 6. Share of Ukrainian exports of grain crops in the total exports and rates of growth of foreign currency earnings within the period from 2011 to 2019, % [6]

According to results of the 2018/2019 marketing year, Ukraine exported 50.4 million tons of grain crops, grain legumes and flour — by 10.5 million tons more than last marketing year (MP) .

Since the 2019–2020 marketing year, exports of Ukrainian wheat to EU countries increased by more than six times as compared to the same period — from 29.7 thousand tons to 188.8 thousand tons. This allowed Ukraine to become the main supplier of soft wheat to the EU with a share of 42 % in total imports.

Countries leading in exporting wheat

Table 2 shows the top 10 countries-exporters of wheat.

Table 2

Countries leading in exporting wheat in 2018 [2]

Number in the ranking	Country	Exports, billion US dollars	Share in world exports, %
1	Russia	8.4	20.51
2	Canada	5.7	13.87
3	United States of America	5.5	13.27
4	France	4.1	10.04
5	Australia	3.1	7.54
6	Ukraine	3.0	7.31
7	Argentina	2.4	5.88
8	Romania	1.2	2.98
9	Germany	1.2	2.84
10	Kazakhstan	0.97	2.35

In the ranking of the 10 largest world exporters of wheat, Ukraine ranks sixth with exports for an amount of 3 billion US dollars. and a share in world exports of 7.31 %.

Ukraine is the third largest exporter of corn after the USA and Brazil. In the 2018-2019 marketing year, 21.4 million tons of corn were exported. The largest amount of it — 11.8 million tons were purchased by European countries. Asia ranks second (6.1 million tons), countries of North Africa rank third (3.5 million tons) [3,4].

Ukrainian corn is purchased in large quantities by 12 countries that already account for 90 % of exports or 18.9 million tons. Ukraine exports the largest amount of corn to the Netherlands (3.2 million tons), Spain (3.1 million tons), China (2.9 million tons), Egypt (2.4 million tons), Italy (1.8 million tons) and Iran (1.2 million tons). Germany, Turkey, Israel, Portugal, Belgium and Libya belong to twelve countries that are the major importers of Ukrainian corn [2-5].

Leading exporter of corn

The largest exporter of corn in 2018 are shown in the Table 3.

Table 3

Leading exporter of corn in 2018 [4]

Number in the ranking	Exporter	Exports, million tons	Share in national exports of corn, %
1	Kernel	2.8	13.5
2	COFCO Agri Ukraine	2.3	11
3	ADM Trading Ukraine	2.1	10
4	NIBULON	1.6	8
5	Suntrade (the major subsidiary of Bunge)	1.5	7.3

The ten corn exporters also includes JSC "State Food and Grain Corporation of Ukraine", "Glencore Agriculture", "Ahroprosperis", "Louis Dreyfus Company Ukraine" and Black Sea Commodities, a relatively young trader on the Ukrainian market with the registered office in UAE [4].

Risks and opportunities of land reform in Ukraine

Studies have shown that, as of 1 January 2018, there are 32,214 entities engaged in growing the grain crops. 71.3 % of them are farms (22,977). In this case, the area, at which their share gathers in the crops, is only 15.8 % that indicates that insignificant concentrations of land in farms. In addition, farms occupy 17.0 % of the gross production of grain (8736 thousand tons).

The main reason for the low rate of productivity of farms is the low level of yield that is less than 15–20 % as compared with that of large manufacturers operating in the industry. The reason is poor logistics, limited access of small producers to advanced technology, lack of working capital that would provide an opportunity to purchase new plant selection varieties and appropriate means to protect them and increase yields (fertilizers, growth stimulants, etc.). However, the share of industrial enterprises with a land bank of more than 10 thousand hectares increased almost twice: from 14.2 % in 2010 to 24.8 % in 2016 [6]. This trend is due, firstly, to the process of consolidation of farms, including the increased levels of agricultural technology and culture cultivation ensured by increased scale. Secondly, large companies more often prefer to grow corn that, in spite of higher costs of production, has a higher yield than other crops.

The cancellation of the moratorium on sale of land brings new risks and opportunities for producers of grain crops. Thus, among the main risks of opening the land market for legal entities is massive buying of land by large agricultural holdings and fall of investment attractiveness of Ukraine. Financial risks will increase for small farmers due to the lack of the credit history and unavailability of financial instruments for the purchase of land.

The increase in prices for land after introduction of the land market will lead to an increase in rental rates that will affects both small farmers and agricultural holdings.

In addition, a long extensive development led to reduction of land banks that requires the increased efficiency in production of grain crops on smaller areas.

A positive consequence of opening the market land to those farmers who will purchase land, on which they work: they will be able to use these lands as mortgage when taking loans in the bank [2].

Conclusions

Modern agriculture is the most dynamic sector of the national economy that is being developing actively. Ukrainian agrarian market feeds not only Ukraine with its 40 million population, but also 190 countries, and the tendency to increased production is still preserved. Our country has a huge potential for growth in production, and there is a rapidly growing demand in the world markets.

In 2019, the agricultural sector generated approximately 12–13 % of Ukrainian GDP. The share of agricultural products in the total exports of Ukraine for this period was 39.8 % or a record-breaking value for Ukraine of 18.8 billion US dollars. This means the receipt of foreign exchange earnings by Ukraine, stability of the hryvnia. Moreover, today, approximately three million people work for the agricultural complex. That is, if the goal of the reform lied specifically in development of the industry, then the question arises: Why do we need the land reform with such expected results? If the purpose of the reform is to attract investment, then there are barriers to development of financial and banking system of Ukraine. In this case, the farmer has to get access to credits, and hence mechanisms allowing to make loans cheaper are necessary for development of agricultural production.

References

1. (2009), *Norman Borlaug: Wheat breeder who averted famine with a "Green Revolution"*, Available at: https://blogs.scientificamerican.com/news-blog/norman-borlaug-wheat-breeder-who-av-2009-09-14.
2. (2019), *U reitynhu 10 naibilshykh svitovykh eksporteriv pshenytsi Ukraina – shosta*, Available at: https://dzi.gov.ua/press-centre/news/u-rejtyngu-10-najbilshyh-svitovyh-eks/porteriv-pshenytsi-ukrayina-shosta/
3. (2019), *Ukraina u 2019 rotsi stala holovnym eksporterom pshenytsi do Yevropeiskoho soiuzu*, Available at: https://www.5.ua/ekonomika/ukraina-holovnyi-eksporter-pshenytsi-do-yevropeiskoho-soiuzu-u-2019-rotsi-198579.html.
4. (2019), *Ukraina voshla v trojku mirovyh jeksporterov kukuruzy*, Available at: https://biz.liga.net/uaexport/prodovolstvie/novosti/ukraina-voshla-v-troyku-mirovyh-eksporterov-kukuruzy.
5. (2019), *Ukraina vstanovyla novyi rekord z eksportu zernovykh*, Available at: https://www.epravda.com.ua/news/2019/11/4/653295/
6. (2020), *Derzhavnyi komitet statystyky Ukrainy*, Available at: http://www.ukrstat.gov.ua.
7. (2020), *Izrailskie uchenye raskryli tajny genoma pervoj pshenicy na Zemle*, Available at: https://mfa.gov.il/MFARUS/InnovativeIsrael/Bi%D0%BEtech/Pages/Israeli-scientists-map-Emmer-wheat-genome.aspx.
8. (2020), *O mirovyh zernovyh zapasah i drugih instrumentah resheniya problemy nestabilnosti zernovyh rynkov*, Available at: http://www.fao.org/3/a-i3338r.pdf
9. (2020), *Rynok zerna ta produktiv pererobky*, Available at: http://www.proagro.com.ua/periodical/grain/20580.html.

10. (2020), *Wheat: Science and Trade (World Agriculture Series) 1st Edition by Brett F. Carver*, Available at: https://www.amazon.com/Wheat-Science-Trade-World-Agriculture/dp/0813820243.
11. (2020), *Zemelna reforma: potribni zapobizhnyky*, Available at: https://m.day.kyiv.ua/uk/article/ekonomika/zemelna-reforma-potribni-zapobizhnyky.
12. Francisco Ceballos, Manuel A. Hernandez, Nicholas Minot, Miguel Robles (2017), Grain Price and Volatility Transmission from International to Domestic Markets in Developing Countries, World Development, 94, pp. 305–320.
13. Henry An, Feng Qiu, Yanan Zheng (2016), How do export controls affect price transmission and volatility spillovers in the Ukrainian wheat and flour markets?, *Food Policy*, pp. 142–150.
14. Hridin O. (2018), Suchasnyi stan ta tendentsii rozvytku sfer vyrobnytstva, pererobky ta realizatsii zerna: ukrainskyi ta zahalnosvitovyi kontekst, *Skhidna Yevropa: ekonomika, biznes ta upravlinnia*, 3 (14), pp. 60–68.
15. Kozak O., Hryshchenko O. (2016), Rozvytok zernovoi haluzi Ukrainy na suchasnomu etapi, *Ekonomika APK*, 1, pp. 38-47.
16. Lebid V., Pryshchepa K. (2013), Suchasnyi stan rynku zerna Ukrainy, problemy ta perspektyvy rozvytku, *Ekonomichnyi visnyk Donbasu*, 1, pp. 131–135.
17. Materynska O. (2017), Stratehichni zasady innovatsiinoho rozvytku vyrobnytstva zerna silskohospodarskymy pidpryiemstvamy, *Ekonomika. Finansy. Menedzhment: aktualni pytannia nauky i praktyky*, 5, pp. 26–34.
18. Patrick T. (2008), Cultivation of the Higher Self: William Smith Clark and Agricultural Education, *Historical Journal of Massachusetts: journal. – Westfield State College*, l, pp. 36-41.
19. Shpaar D., Beme K. (2004), Reforma Obshej agrarnoj politiki v Evrosoyuze i ee posledstviya dlya FRG, *APK: ekonomika, upravlenie*, 7, pp. 67–76.
20. Shpykuliak O., Materynska O., Mazur H. (2014), Efektyvnist vyrobnytstva zerna silskohospodarskymy pidpryiemstvamy: teoretyko-metodolohichnyi aspekt. *Ekonomika APK*, 12, pp. 42–49.
21. Zakharchenko O. (2014), Suchasnyi stan ta otsinka rozvytku rynku zerna v Ukraini, *Visnyk Sumskoho natsionalnoho ahrarnoho universytetu*, 8, pp. 54–58.

Анотації

Харчові технології

Вплив ефірної олії шавлії (Salvia sclarea L.) на паперові пакувальні матеріали

Іліана Костова[1], Веска Лашева[2], Хафізе Фідан[3],
Даріна Георгієва[1], Станка Дамянова[1], Албена Стоянова[3]
1 – Русенський університет, філія в м. Разград, Болгарія
2 – Університет хімічної технології та металургії, Софія, Болгарія
3 – Університет харчових технологій, Пловдів, Болгарія

Вступ. Мета досліджень – визначити вплив ефірної олії шавлії (Salvia sclarea L.) на паперові пакувальні матеріали.

Матеріали і методи. Досліджувалися пакувальні матеріали вивчені на основі паперу, покритого ефірною олією шавлії. Хімічний склад ефірної олії шавлії визначався хроматографічно. Антимікробну дію ефірної олії визначали проти грампозитивних, грамнегативних бактерій, дріжджів і грибів методом дифузії агару.

Результати і обговорення. Хімічний склад ефірної олії шавлії показав переважну кількість оксигенованих монотерпенів (83,43%), далі монотерпенових вуглеводнів (7,86%) та сесквітерпенових вуглеводнів (5,16%). Основними компонентами ефірної олії шавлії були ліналілацетат, β-ліналоол, α-терпінеол, лімонен та геранілацетат, які визначали антимікробну дію олії.

Ефірна олія виявляла фунгіцидну дію проти плісняви та дріжджів. Її високі антимікробні властивості можливо пов'язані з високим вмістом ліналілацетату (40,31%) та β-ліналоолу (22,72%).

Наші результати показали високу фунгіцидну ефективність для трьох типів пакувальних матеріалів. Пригнічувальна дія проти *C. albicans* протягом досліджуваного періоду зберігання становила близько 100%. Було виявлено високу ефективність переробленого паперу проти A. brasiliensis (99,2% – 81,9%). Визначено, що бактерицидний ефект випробуваних пакувальних матеріалів був нижчим до грамнегативних бактерій *S. abony.*

Висновок. Ефірна олія шавлії може бути використана як протимікробний засіб у харчових технологіях завдяки своїм антимікробним властивостям з метою поліпшення якості продуктів та продовження терміну їх зберігання.

Ключові слова: *упаковка, папір, шавлія, ефірна олія, антитимікробний*.

Механізм водозв'язування та водоутримання наночастинками харчової добавки на основі подвійного оксиду дво- і тривалентного заліза

Ірина Цихановська[1], Вікторія Євлаш[2], Ольга Благій[1]
1 – Українська інженерно-педагогічна академія, Харків, Україна,
2 – Харківський державний університет харчування та торгівлі, Харків, Україна

Вступ. Обґрунтовано механізм водозв'язувальної та водоутримувальної здатності харчової добавки на основі подвійного оксиду дво- і тривалентного заліза «Магнетофуд» (Fe_3O_4).

Матеріали і методи. Модельні системи на основі наночастинок добавки «Магнетофуд» (Fe_3O_4) та води, крохмалю, яєчного білка, жиру, лінолевої кислоти, житньо-пшеничного борошна. Водоутримувальну здатність (ВУЗ) досліджували енергодисперсійною рентгенівською (EDX) та ІЧ-Фур'є спектроскопією (FTIR), методом Шоха, індикаторним методом (ІМ), диференційно-термічним аналізом (ДТА), визначенням водопоглинання на приладі Догадкіна, набухання($см^3/г$), ефективної в'язкості на ротаційному віскозиметрі «Реотест-2».

Результати і обговорення. Вивчено механізм взаємодії наночастинок харчової добавки на основі подвійного оксиду дво- і тривалентного заліза «Магнетофуд» (ХДМ) шляхом самоорганізації наночастинок добавки (НЧ Fe_3O_4) в електростатичні комплекси з білками, полісахаридами та жирами за типом «кластерів», «клатратів», «кавітатів». Установлено, що в харчових системах, які містять білки, полісахариди, воду, ВУЗ коригується завдяки «кластерофільності» ХДМ та здатності НЧ Fe_3O_4 до поляризації, електростатичної координації, утворення акваасоціатів.

Виявлене зсунення максимуму поглинання зв'язку Fe-O у високочастотну область на (57±2) $см^{-1}$ порівняно з дослідним зразком чистої ХДМ свідчить про хімічну взаємодію катіонів феруму ХДМ з молекулами високомолекулярних сполук (крохмалю, яєчного білка, жиру).

Визначено хімічний склад модельних систем високомолекулярних сполук з ХДМ: для частинок чистої ХДМ – Fe 75,5%; O 24,5%; для частинок добавки, покритих яєчним білком – Fe 44,7%; O 26, 9%; C 21,4%; N 5,9%; S 1,1%; для частинок добавки, покритих крохмалем, – Fe 41,7%; O 35,7%; C 22,6%; для частинок добавки, покритих лінолевою кислотою, – Fe 45,6%; O 34, 7%; C 19,7%; для частинок добавки, покритих соняшникової олією,– Fe 39,7%; O 36,7%; C 23,67%.

Встановлено співвідношення зв'язаної та вільної вологи в сольватованій ХДМ: кількість зв'язаної води: фізико-хімічної 68,9–69,4%, фізико-механічної 21,5–22,3% і вільної 8,8–9,1%.

Висновки. Вперше запропоновано моделі взаємодії НЧ Fe_3O_4 з водою, білками, жирами, вуглеводами для обґрунтування механізму водоутримання наночастинками харчової добавки на основі подвійного оксиду дво-і тривалентного заліза.

Ключові слова: *водоутримання, оксид заліза, кластерофільність.*

Вплив деяких нетрадиційних інгредієнтів на виробництво чорного пива

Маріус Ціокан, Адріана Дабіжа, Георгіна Габріела Кодіна
Університет «Штефан чел Маре», Сучава, Румунія

Вступ. Мета цього дослідження – обгрунтувати використання нетрадиційних інгредієнтів, таких як борошно жолудя, борошно топінамбура та меляси, у технології напою, подібного до чорного пива.

Матеріали і методи. Чорне пиво отримували за звичайним методом на пивоварному заводі. У рецепті виготовлення солод коричневого кольору замінено борошном із жолудя, топінамбуру і мелясою з 50% сахарозою в наступних варіантах: варіант 1 – 0,5:1,5:1; варіант 2 – 1:1:1; варіант 3 – 1:1,5:0,5; варіант 4 – 1,25:1,25:0,5. Вміст екстракту, вміст алкоголю для зразків чорного пива були проаналізовані за допомогою пристрою Антона Паара.

Результати і обговорення. Вміст CO_2, висота піни, стабільність піни, загальна кислотність пива для всіх аналізованих зразків знаходяться в допустимих межах для

чорного пива. Сенсорні характеристики оцінених зразків чорного пива, а саме зовнішній вигляд, колір, запах, смак, виділення газу та стабільність піни, свідчить про те, що варіант 1 чорного пива отримав найнижчу оцінку, тоді як варіант 4 отримав найвищий. Результати сенсорного аналізу були несподіваними, отримане пиво без клейковини отримало дуже високу оцінку, учасники форуму віддають перевагу їм над чорними пивними кормами, виготовленими з традиційних інгредієнтів. Чорне пиво, отримане у всіх чотирьох експериментальних версіях – це пиво з концентрацією алкоголю, яка коливалася між 7,06% та 8,16%, з високим ступенем кінцевого бродіння, яке становило від 73,26% для варіанту 2 та 85,85% для варіанту 4. Результати, отримані для пива з нетрадиційної сировини (борошно жолудя, топінамбура і патоки), були порівнянні з комерційним чорним пивом, яке виступало контрольним зразком. Найкращий результат щодо рівня кінцевої ферментації (85,85%) був отриманий для варіанту 4, і був вищим, ніж для комерційного пива (80,20%). Також варіант 4 найкраще оцінили з органолептичної точки зору. Цей варіант пропонується для отримання чорного пива в промислових масштабах, оскільки він має хороші фізико-хімічні властивості, порівнянні з чорним пивом на ринку.

Висновок. Чорне пиво, отримане на основі інноваційного рецепту виготовлення, мало добрі органолептичні характеристики, свіжо смажений кавовий аромат, фруктовий смак і гіркоту.

Ключові слова: *чорне пиво, жолудь, топінамбур, меляса.*

Вплив пшеничних харчових волокон на процес формування структури сироватко-вершкових сирів

Олена Грек[1], Кіра Овсієнко[1], Алла Тимчук[1], Олена Онопрійчук[1], Аміт Кумар[2]
1 – Національний університет харчових технологій, Київ, Україна
2 – Інтегральний університет, Лакнау, Індія

Вступ. Проведені дослідження впливу пшеничних харчових волокон з метою раціоналізації процесу структуроутворення сироватко-вершкових сирів.

Матеріали і методи. Сировиною для отримання сироватко-вершкового сиру була підсирна молочна сироватка, вершки та Вітацель WF400. Технологічні властивості харчових волокон визначали за кількістю утриманого жиру й адсорбованої води в процесі настоювання і центрифугування суспензії. Також визначали граничне напруження зсуву та активність води в модельних зразках сироватко-вершкових сирів, оптимальну кількість внесення Вітацель WF400, температуру і тривалість перемішування підзгущеної молочної сироватки.

Результати і обговорення. Уточнено технологічні властивості Вітацель WF400. Так, вологоутримувальна здатність у підсирній молочній сироватці та жиротримувальна у вершках з м.ч.ж. 33 склали 104,2±1,0 та 82,0±0,5 відповідно. Із збільшенням кількості внесення Вітацель WF400 (від 1,0 до 4,0) та підвищенням температури структуроутворення (від 62 до 74ºС) показник граничного напруження зсуву зростає з 350±1,1 Па до 430±1,3 Па, а тривалість перемішування скорочується з 90 до 70 хв. Підвищення температури до 68ºС, збільшення кількості Вітацель WF400 до 2,5 та скорочення тривалості перемішування до 70 хв призводить до зменшення кількість дисперсійного середовища, тому відбувається зневоднення коагуляційної структури зразків сироватко-вершкових сирів. Модельні зразки досліджуваних продуктів з різною кількістю Вітацель WF400 (від 2% до 3%), якщо порівняти з

контрольним зразком, характеризуються зниженням показника активності води. Для контрольного зразка a_w становить 0,898.

Після досягнення вмісту сухих речовин 66 і відповідного зниження вмісту рідкої фази показник граничного напруження зсуву сягає 427 Па. Зразки сироватково-вершкових сирів набувають консистенції пластичних паст, в яких відновлення структури можливе лише за умови дії навантаження, що спричиняє пластичну деформацію, яка діє на всій площі поверхні розподілу фаз.

При подальшому підвищенні температури до 74ºС і тривалості перемішування до 70 хв відбувається подальше ущільнення структури – зменшується товщина прошарків рідкого середовища, тиксотропія і пластичність зникають.

Висновки. Обґрунтовано оптимальні значення кількості Вітацель WF400 на рівні 2,5±0,5, температури – 68±1ºС і тривалості перемішування під час структуроутворення – 70±2 хв. Сироватково-вершкові сири з додаванням раціональних кількостей харчових волокон характеризуються зниженням значень активності води від 0,885 до 0,823.

Ключові слова: *волокна, сир, сироватка, вершки, Вітацель, активність води, реологія.*

Часо-температурна індикаційна плівка на основі альгінату і екстракту червоного буряка (Beta vulgaris L.): характеристика *in vitro*

Ерса Текін, Ісіл Баракту Маці, Хасан Тюре
Університет Орду, Орду, Туреччина

Вступ. Визначено характеристики біорозкладного часо-температурної індикаційної (TTI) плівки шляхом включення екстракту червоного буряка (*Beta vulgaris* L.), який багатий беталаїновими пігментами, у плівку із суміші альгінату (A) / полівінілового спирту (PVA).

Матеріали і методи. Суміші альгінату-PVA (APVA) готували шляхом змішування 1% розчинів PVA та 3% A при різних співвідношеннях A: PVA (2:3, 1:1, 3:2). Плівки TTI були отримані додаванням аскорбінової кислоти та екстракту червоного буряка до сумішей APVA та регулювання pH шляхом додавання NaOH. Плівки виготовлялися методом лиття. Характеристики чистої A, чистих PVA, APVA і TTI отримали за допомогою Фур'є-спектроскопії (FT-IR), термогравіметричного аналізу (TGA) та сканувальної електронної мікроскопії (SEM). Механічні властивості плівок були встановлені за допомогою тестів на напруження/деформацію. Кольорові параметри CIE L*a*b* TTI-плівки були отримані протягом семи днів зберігання за температури 4, 25, 40 та 60 ° C.

Результати і обговорення. Підвищення концентрації A забезпечувало збільшення модуля пружності, міцності на розрив і подовження при розриві (%) плівок APVA і TTI. Плівка TTI (3:2) мала кращу гнучкість у порівнянні з A, APVA, TTI (1:1) та TTI (2:3). Співвідношення A до PVA у змішаних плівках не суттєво впливає на термограми TGA. Більш висока частка плівки TTI зменшила поділ фаз, що спостерігається на зображеннях SEM. Інтенсивність O-H смуги розтягування явно зростала в плівках TTI порівняно з іншими плівками. Плівка, що зберігається при 4 °C, не змінювалась протягом 7 днів, тоді як колір TTI, що зберігався при більш високих температурах, поступово змінювався під час зберігання залежно від температури зберігання. Зміни параметрів b* та значень кута відтінку були більш вираженими; і зазвичай b* та

значення кута відтінку зразків, що зберігаються за температури вище 4 °С, значно збільшуються на початку першого дня.

Висновок. Розроблена ТТІ плівка завдяки зміні кольору дає можливість контролювати зміну якості продуктів, які неправильно зберігаються, і, як правило, мають бути замороженими.

Ключові слова: *ТТІ, плівка, індикатор , червоний буряк, альгінат*

Ефективність освітлення яблучного соку з використанням нанорозмірних мінеральних оксидів

Анастасія Сачко, Ігор Кобаса, Олеся Мойсюра, Марія Воробець
Чернівецький національний університет імені Юрія Федьковича, Чернівці, Україна

Вступ. Досліджено ефективність освітлення яблучного соку прямого віджиму за допомогою суспензії та порошків нанодисперсних діоксидів титану та силіцію, модифікованого оксиду силіцію (АМД). Для порівняння обрано високодисперсну бентонітову глину.

Матеріали і методи. Сік, який використовували для лабораторних досліджень, був відтиснутий з яблук сорту «Слава переможцям». Аеросил – порошок діоксиду силіцію (АМД-2, площа питомої поверхні 280 $м^2/г$) та нанодисперсні порошки оксидів силіцію (IV) (площа питомої поверхні 300 $м^2/г$) та титану (IV) (площа питомої поверхні 50 $м^2/г$) були обрані як освітлювачі. Для порівняння використали бентонітову глину (площа питомої поверхні 160 $м^2/г$). Оптичну густину вимірювали спектрофотометрично, сухий залишок оцінювали рефрактометрично,-величину pH і титровану кислотність визначали за загальновідомими методиками.

Результати і обговорення. Доведено перспективність використання мінеральних оксидів SiO_2 та TiO_2 для освітлення яблучного соку. Встановлено, що найефективнішим освітлювачем є порошок і суспензія аеросилу. Оптимальна маса 2,5 г на 1 л соку, час витримки не більше 1 доби. Форма внесення (у вигляді порошку чи суспензії) не має суттєвого впливу на результат освітлення.

Найменшою освітлювальною здатністю володіє бентоніт. Підтверджено, що використання суспензії бентоніту підвищує ефективність освітлення. Збільшення наважки бентоніту від 0,1 до 2,5 г/л соку погіршує оптичні властивості отриманого соку.

Досліджено вплив температури, при якій проводилося освітлення, на ефективність дії освітлювачів і вплив часу витримування соку з освітлювачем на фізико-хімічні властивості готового продукту. Доведено, що результат освітлення є кращим при низьких температурах (4ºС), а всі використані освітлювачі здатні пригальмовувати перебіг природних процесів бродіння сировини. Встановлено, що витримування соку з освітлювачем більше 1 доби негативно впливає на результат освітлення для всіх досліджуваних зразків.

Висновки. Нанодисперсні оксиди титану та силіцію можуть бути успішно використані для освітлення свіжовідтиснутого яблучного соку. Їхня освітлювальна здатність є вищою, ніж у бентонітової глини, тож вони можуть додаватися в сік без попередньої підготовки у формі порошку.

Ключові слова: *освітлення, яблучний сік, діоксид титану, діоксид силіцію, бентоніт.*

Вплив рапсової олії та природного антиоксиданту базиліка на хімічні та органолептичні властивості свіжого сиру

Міхаела Іванова[1], Ольга Танєва[2], Марія Душкова[1],
Радка Власева[1], Албена Стоянова[1]
1 – Університет харчових технологій, Пловдів, Болгарія
2 – Пловдівський університет "Паїсій Хілдарський", Пловдів, Болгарія

Вступ. Мета досліджень – визначити вплив рапсової олії і природного антиоксиданту базиліка на хімічні та органолептичні властивості свіжого сиру.

Матеріали і методи. Свіжий розсипчастий сир був виготовлений зі свіжого незбитого молока, рапсової олії та природного антиоксиданту базиліка. Підготовлений сир аналізували на профіль жирних кислот за методом GC метилових ефірів, вміст токоферолу – за методом HPLC, вміст фітостеролу – за методом GC, сенсорне оцінювання – за 10-бальною гедонічною шкалою.

Результати і обговорення. Рапсова олія характеризувалася високим вмістом ненасичених жирних кислот вище 93 г на 100 г від загального вмісту і добрим співвідношенням омега-6/омега-3 – 2/1. Загальний вміст токоферолів у ліпідній фракції був порівняно високим – 315 мг на kg. Канолова олія містила значну кількість фітостеролів – 0,7 г на 100 г з індивідуальним стерольним складом – у фракції стеролу переважали β-ситостерол (54,7%) і кампестерол (35,3%).

Сир з частковою заміною молочного жиру рапсовою олією характеризувався зниженим вмістом насичених жирних кислот, які негативно впливають на здоров'я людини – 35,18 г на 100 г порівняно з 68,33 г на 100 г у сирі, виробленому за класичною технологією, що містить тільки молочний жир. Продукт містив велику частину коротколанцюгових жирних кислот, характерних для молочного жиру, що визначає функціональність кінцевого продукту. Сир з додаванням рапсової олії виявив більшу біологічну цінність завдяки атерогенному індексу 0,42 порівняно з 1,60 для сиру, виробленому лише з молочного жиру, тромбогенному індексі 0,59 порівняно з 3,13 для сиру, виробленому лише з молочного жиру, та профілактичному ліпідному показнику 34,89 порівняно з 128.23 для сиру, виробленого лише з молочного жиру.

Висновок. Свіжий сир з частковою заміною молочного жиру рапсовою олією у співвідношенні (1:1) характеризувався низьким рівнем атерогенного та протромбогенного показників і профілактичним показником ліпідів.

Ключові слова: *антиоксидант, рапсова олія, сир, молочний жир.*

Метод визначення ступеня етерифікації пектину за титрованою кислотністю

Оксана Шульга, Володимир Листопад, Сергій Шульга, Людмила Юрчук
Національний університет харчових технологій, Київ, Україна

Вступ. Проведені дослідження методу з визначення ступеня етерифікації пектину з метою обмеження використання значної кількості вартісних і складнодоступних реактивів.

Матеріали і методи. Зразки пектину яблучного та цитрусового мають різний ступінь етерифікації. Наявність карбоксильної групи в пектині різного ступеня етерифікації визначено за допомогою ІЧ-спектроскопії. Хімічний зсув протонів, які

входять до структурних складових пектину, зареєстровано за допомогою ЯМР-спектрів.

Результати і обговорення. В ІЧ-спектрі зразка високоетерифікованого пектину наявна смуга сильної інтенсивності при 1616,78 $см^{-1}$ належить деформаційним коливанням адсорбційно-зв'язаної води, що перекривається асиметричною вібрацією карбоксилатного іона (CO_2^-). В ІЧ-спектрі зразка низькоетерифікованого пектину ця смуга слабкої інтенсивності і знаходиться в області коливань 1686,71 $см^{-1}$. У спектрі високоетерифікованого пектину наявна інтенсивні смуга з трьома максимумами при 3400,56 $см^{-1}$ 3316,52 і 3271,70 $см^{-1}$, яка відповідає валентним коливанням νOH. В ІЧ-спектрах з етерифікацією до 42% наявна смуга вільної карбоксильної групи, а в ІЧ-спектрах високоетерифікованих пектинів наявна інтенсивна смуга карбоксилатних груп (CO_2^-), чим і різняться наведені спектри.

Наведена характеристика ЯМР-спектрів показує відмінності у будові високо- та низькоетерифікованого пектину, проте не надає можливості проводити кількісне визначення ступеня етерифікації.

Відповідно до отриманих результатів спостерігається залежність між загальною кислотністю та ступенем етерифікації пектину, яка може бути представлена степеневою або гіперболічною моделлю. Найкращими для прогнозування є степенева або гіперболічна моделі.

Похибка між хімічним методом визначення ступеня етерифікації та запропонованим методом становить 0,6–1,3%.

Висновки. Визначення ступеня етерифікації пектину можливе за титрованою кислотністю з подальшим розрахунком за рівнянням регресії.

Ключові слова: *пектин, етерифікація, кислотність, ІЧ-спектроскопія, ЯМР-спектри.*

Обґрунтування амінокислотного складу соняшникових білків для дієтичних і функціональних продуктів

Микола Осейко[1], Тетяна Романовська[1], Василь Шевчик[2]
1 − Національний університет харчових технологій, Київ, Україна
2 – «Мікрохірургія очей Василя Шевчика», Чернігів, Україна

Вступ. Проведено дослідження зразків переробки насіння соняшнику з метою обґрунтування амінокислотного складу білків для дієтичних і функціональних продуктів.

Матеріали і методи. Досліджуються зразки макухи, макухи знежиреної (шрот), борошна, отриманого з очищеного ядра соняшнику, амінокислотний склад і фізико-хімічні показники продуктів очищеної фракції ядра соняшнику, борошна, макухи, жирної макухи. Амінокислотний склад зразків визначали на рідинному хроматографії Dionex ICS-3000 з електрохімічним детектором. У зразках досліджено співвідношення гідрофобних і гідрофільних амінокислот.

Результати і обговорення. Встановлено, що борошно з соняшникового ядра на 22,0% має більший вміст щодо загального білка. Вміст незамінних амінокислот на 31,1% більше ніж у макусі, з якої вони виділені. Збільшення вмісту білка в соняшниковому борошні пояснюється збагаченням дрібної фракції під час фракціонування. Поряд із збільшенням загального вмісту білка борошно збагачується незамінними гідрофобними амінокислотами, зокрема лейцином (14,2%), ізолейцином

(6,7%), метіоніном (11,2%), а також заміним гідрофобним проліном (10,5%). Обмеженою амінокислотою у борошні є лізин (скор 78%), вміст інших незамінних амінокислот значно перевищує їхній вміст в ідеальному білку (скор лейцину – 153%, ізолейцину – 143%, метіоніну – 213%, метіоніну разом з цистином – 258%, фенілаланіну разом з тирозином – 177%). Вміст лейцину та ізолейцину в соняшнику класичних сортів обмежений. У борошні із соняшникового ядра їхній вміст перевищено в півтора раза.

Для збалансованості отриманого соняшникового борошна за вмістом лізину раціональним є використання його композицій з іншими лізиновмісними видами борошна з насіння олійних культур і/або з використанням харчового мікробіологічного лізину.

Висновок. Використання збалансованих білково-ліпідних екопродуктів і препаратів на основі комплексної переробки насіння соняшнику покращує функціональні-технологічні властивості та сприяє профілактиці захворювань.

Ключові слова: *соняшник, продукт, білок, амінокислота, здоров'я.*

Антиоксидантна здатність алкогольних напоїв на основі настоїв з нетрадиційної пряно-ароматичної рослинної сировини

Олег Кузьмін[1], Володимир Кучеренко[2], Ірина Силка[1], Володимир Ісаєнко[3], Юлія Фурманова[1], Олена Павлюченко[1], В'ячеслав Губеня[1]

1 – Національний університет харчових технологій, Київ, Україна

2 – Українська корпорація по виноградарству і виноробній промисловості «Укрвинпром»

3 – Національний авіаційний університет, Київ, Україна

Вступ. Метою дослідження є визначення антиоксидантної здатності водно-спиртових настоїв з використанням нетрадиційної пряно-ароматичної сировини у технології алкогольних напоїв.

Матеріали і методи. Антиоксидантну здатність настоїв з пряно-ароматичних рослин: *Perilla frutescens; Elsholtzia stauntonii Benth; Artemisia abrotanum; Monarda didyma; Agastache foeniculum; Satureja hortensis; Ruta graveolens; Nepeta transcaucasica Grossch* визначали за методом редоксметрії та *pH*-метрії; сенсорні показники – за експертним методом; результати математико-статистичної обробки – за методом лінійної кореляції Пірсона.

Результати. Отримано мінімальне теоретичне значення окисно-відновного потенціалу для рослинних водно-спиртових настоїв, яке змінюється від 228.0 мВ (*Satureja hortensis*) до 260.4 мВ (*Agastache foeniculum*).

Встановлено фактичний виміряний окисно-відновний потенціал настоїв – від 117.0 мВ (*Elsholtzia stauntonii Benth*) до 134.0 мВ (*Nepeta transcaucasica Grossch*).

Водневий показник для водно-спиртових настоїв з пряно-ароматичної сировини має значення від 6.66 од. *pH* (*Agastache foeniculum*) до 7.20 од. *pH* (*Satureja hortensis*).

Водно-спиртові настої з рослинної сировини та об'ємною часткою етанолу 40% мають величину енергії відновлення (*EB*) в межах від 100.0 мВ (*Nepeta transcaucasica Grossch*) до 138.2 мВ (*Ruta graveolens*).

Водно-спиртові настої з пряно-ароматичної сировини мають значення сенсорних показників (*S.e.*) від 9.50 до 9.69 балів. Найбільше значення *S.e.* – 9,69 балів характерне для *Nepeta transcaucasica Grossch*: колір – світло-коричневий; смак – м'ятний; аромат – м'який, приємний, солодкуватий.

Висновки. Запропоновано для технології алкогольних напоїв застосування водно-спиртових настоїв з *Ruta graveolens* та *Nepeta transcaucasica Grossch*, які отримали підвищені антиоксидантні характеристики *ЕВ* – 138.2 мВ та *ЕВ* – 100.0 мВ відповідно, та позитивні сенсорні показники *S.e.* – 9.57 та *S.e.* – 9.69 балів за 10-бальною шкалою.

Ключові слова: *пряно-ароматичний, антиоксидант, окисно-відновний потенціал, настій, алкоголь.*

Вплив гомологів альфа-кислот хмелю гірких та ароматичних сортів на якість пива

Лідія Проценко[1], Сергій Рижук[1], Микола Ляшенко[1], Олександр Шевченко[2], Світлана Літвинчук[2], Лілія Янсе[3], Генріх Мілоста[4]

1 – Інститут сільського господарства Полісся НААН України, Житомир, Україна
2 – Національний університет харчових технологій, Київ, Україна
3 – Національна академія аграрних наук України, Київ, Україна
4 – Заклад освіти «Гродненський державний аграрний університет», Гродно, Республіка Білорусь

Вступ. Досліджено гіркі речовини хмелю, встановлено залежності величини гіркоти сусла і якості охмеління пива від кількісного і якісного складу гомологів альфа-кислот хмелю, зокрема від вмісту когумулону у складі альфа-кислот.

Матеріали і методи. Досліджувався хміль ароматичних і гірких сортів з різним вмістом когумулону у складі альфа-кислот та пиво, виготовлене з нього. Використано високоефективну рідинну хроматографію для визначення кількості та складу гірких речовин хмелю і продуктів їх перетворення в процесі пивоваріння, а також спектрофотометричні методи контролю якості гіркоти охмеленого сусла та готового пива.

Результати і обговорення. При дослідженні гірких речовин ароматичних і гірких сортів хмелю встановлено відмінності у їхньому біохімічному складі за абсолютним значенням таких показників, як масова частка альфа-кислот, бета-кислот і показника вмісту когумулону в складі альфа-кислот. Відмічено, що альфа-кислоти досліджуваних сортів мають у своєму складі широкий діапазон показника вмісту когумулону: від 19,6% у хмелі сорту Альта до 43,8% у хмелі сорту Руслан. Встановлені залежності між кількістю і якісним складом гірких речовин хмелю і гіркотою та якістю охмеленого сусла і пива показують, що із збільшенням масової частки когумулону в складі альфа-кислот хмелю ароматичних сортів на 1%, при співвідношенні бета-кислот до альфа-кислот 1,11–1,34 величина гіркоти охмеленого ними сусла збільшується від 0,69% для хмелю сорту Гайдамацький до 1,05% для хмелю сорту Слов'янка. У хмелі гірких сортів співвідношення бета-кислот до альфа-кислот є значно нижчим і становить 0,51–0,74. Аналіз співвідношення між зростанням когумулону та зміною величини гіркоти сусла, охмеленого гіркими сортами, свідчить, що із зростанням частки когумулону в складі альфа-кислот хмелю гіркого типу на 1%, величина гіркоти охмеленого ним сусла збільшується від 0,19% для сорту Руслан до 0,38% для сорту Промінь. Між гіркотою сусла та кількістю внесеного когумулону з хмелем при використанні як гірких, так і ароматичних сортів існує сильний зв'язок, про що свідчить коефіцієнт кореляції, який становить для гірких сортів r = 0,90±0,10, для ароматичних r = 0,98±0,20. В утворенні гіркоти сусла,

охмеленого ароматичними сортами із співвідношення бета-кислот до альфа-кислот більше одиниці, роль сполук бета-кислот значно вища порівняно з гіркими сортами.

Висновки. При застосуванні для охмелiння сусла хмелю гіркого типу з різним складом альфа-кислот більш ефективне використання для сортів з високим вмістом когумулону.

Ключові слова: *хміль, альфа-кислоти, когумулон, сусло, пиво.*

Процеси і обладнання

Математичне моделювання процесу замішування дріжджового тіста кулачковими робочими елементами

Віталій Рачок[1], Володимир Теличкун[1], Станка Дамянова[2], Юлія Теличкун[1]

1 – *Національний університет харчових технологій, Київ, Україна*

2 – Русенський університет «Ангел Канчев», філія в м. Разград, Болгарія

Вступ. Проведено дослідження процесу замішування пшеничного дріжджового тіста кулачковими робочими елементами з метою визначення раціональної конфігурації конструктивних елементів для безперервного замішування тіста за різної частоти обертання робочих елементів і відстані між ними.

Матеріали і методи. Досліджується замішування пшеничного дріжджового тіста кулачковими робочими елементами. Математичне моделювання проведено з використанням програмного пакета Flow Vision що базується на моделюванні тривимірного руху рідин і газів у технічних конструктивних об'єктах, а також для візуалізації кривих течій методами комп'ютерної графіки. Фізичне моделювання проведено на експериментальній установці з кулачковими місильними елементами. Відстань між кулачками становила 2, 4, 6, 8 і 10 мм, швидкість обертання – 20–100 об/хв.

Результати і обговорення. За збільшенням частоти обертання робочих елементів від 20 до 100 об/хв збільшується швидкість перемішування від від 0,1 до 0,6 м/с, відстань між кулачками на перемішування у вказаному діапазоні не впливає. Встановлено, що чим менша відстань між кулачковими елементами, тим більший тиск у камері замішування. Максимальні значення тиску сягають 16560 Па за відстані між кулачковими робочими елементами 2 мм та частоти обертання 100 об/хв, мінімальні 555 Па за відстані між кулачковими робочими органами 10 мм та частоти обертання 20 об/хв. У камері замішування найбільші показники тиску утворюються в зоні контакту кулачкових робочих елементів зі стінкою камери замішування та в зоні контакту двох кулачків. Залежність в'язкості в камері замішування від швидкості обертання робочого елемента має степеневий характер та зі збільшенням частоти обертання від 20 до 100 об/хв зменшується від 1600 до 320 Па·с. Частини камери замішування, в яких досягаються показники в'язкості в межах від 320 до 960 Па·с, вважаються найбільш ефективними під час перемішування. Зменшення в'язкості тіста передбачає зниження енергетичних затрат в процесі замішування.

Висновки. Для підвищення транспортуючої здатності кулачкових робочих органів, покращення змішування і зменшення витрат теплоти раціонально використовувати кулачкові робочі органи зі змінним кроком і змінним положенням кулачків на α=45° або комбінований кулачковий робочий орган з використанням витків шнека на початку робочого органу.

Ключові слова: *замішування, тісто, кулачок.*

Вплив газодинамічних параметрів теплоносія на ефективність сушіння гороху в ротаційних сушарках з псевдозрідженим шаром

Роман Якобчук, Святослав Лементар
Національний університет харчових технологій, Київ, Україна

Вступ. Метою досліджень є визначення впливу газодинамічних параметрів руху теплоносія в камері ротаційної сушильної установки з псевдозрідженим шаром на ефективність процесу сушіння гороху.

Матеріали і методи. Досліджень проводилися на експериментальній сушильній установці з встановленим у сушильній камері конічним елементом та за допомогою 3D-моделей сушильних установок. Моделювання руху теплоносія проводилося з використанням методів CFD з подальшою перевіркою на експериментальній установці.

Результати і обговорення. Встановлено, що швидкість теплоносія в сушильній камері установки без конічного елемента знаходиться в рекомендованих межах (1,8–2 м/с) лише в діапазоні від 0 до 0,7 м по висоті камери. Зона від 0,7 до 1,2 м використовується менш ефективно, оскільки в ній швидкість теплоносія знаходиться в межах 1,65–1,8 м/с. Причиною цього є те, що при проходженні теплоносія через вологий продукт його температура зменшується, що приводить до зменшення об'єму теплоносія. Це викликає руйнування сталого режиму псевдозрідження і, як наслідок, зниження інтенсивності висушування продукту.

У сушильній установці з конічним елементом досягається стабілізація швидкості теплоносія в рекомендованих (1,8–2 м/с) межах по всій висоті зони сушіння, що забезпечує сталу висоту псевдозрідженого шару продукту в камері сушіння. Це створює умови для більш високої інтенсивності висушування матеріалу і сприяє підвищенню якості висушеного продукту, оскільки він не знаходиться занадто довго в зоні високих температур.

Встановлено, що при зростанні швидкості теплоносія понад 2 м/с спостерігається зменшення ефективності використання його потенціалу. Так, при початковій швидкості теплоносія 2 м/с і початковій температурі 100 °С його кінцева температура складає близько 55°С, що відповідає прийнятому регламенту сушіння для установок даного типу. При підвищенні швидкості до 2,2 і 2,4 м/с спостерігається збільшення кінцевої температури теплоносія до 58 і 60 °С відповідно, що знижує ефективність роботи установки.

Висновки. Дослідження дають змогу визначити вплив встановлення конічного елемента в сушильній камері на швидкість теплоносія та його тиск у зоні сушіння, а також вплив швидкості теплоносія на його температуру в цій зоні.

Ключові слова: *сушарка, ротор, теплоносій, псевдозрідження.*

Економіка

Аналіз ринку зерна в Україні в умовах впровадження земельної реформи

Тетяна Рибачук-Ярова, Ірина Тюха
Національний університет харчових технологій, Київ, Україна

Вступ. Метою дослідження є виявлення основних диспропорцій розвитку ринку зерна в Україні в умовах впровадження земельної реформи.

Матеріали і методи. Досліджується український ринок зерна в контексті земельної реформи. Контролюється відповідність здійснених перетворень міжнародним вимірам і концепції регулювання ринку. Для групування національних і міжнародних аналітичних результатів використовувався логічно-абстрактний метод.

Результати і обговорення. У 2018 р. обсяги виробництва зернових в Україні були найвищими протягом 1991-2018 років. Позитивна динаміка спостерігається з 2003 року. Зростання досягнуто шляхом збільшення засівних площ під зернові та завдяки зростанню урожайності. Основними зерновими є пшениця, кукурудза, соняшник, ячмінь, соя та ріпак. Рентабельність пшениці в Україні відповідає рівню основних країн-виробників і в середньому становить 26,8%.

Обсяги виробництва соняшнику протягом 2011–2019 рр. демонструють позитивну динаміку до зростання. Найвищі обсяги виробництва були у 2016 р., 2018 р. та у 2019 році. Найвищі показники виробництва сої фіксувалися у 2016 р. та у 2018 р., що пов'язано зі значною врожайністю. З 2016 р. спостерігається поступова позитивна динаміка виробництва ріпаку.

Відповідно до національного балансу попиту і пропозиції зернових та зернобобових, слід відзначити, що в Україні споживається не більше 30-40 млн тонн зернових та олійних культур з 92 млн тонн зібраних. Тож подальше нарощування виробництва можливе тільки за рахунок збільшення експорту українських зернових на світовий ринок, який характеризується динамічно зростаючим попитом.

У галузі вирощування зернових культур налічується 32 214 суб'єктів господарювання, з них 71,3% – фермерські господарства. При цьому за площами, з яких збирається врожай, їхня частка становить лише 15,8%, що свідчить про низький рівень концентрації земель у фермерських господарств.

Серед основних ризиків відкриття ринку землі для юридичних осіб є її масове скуповування великими агрохолдингами та падіння інвестиційної привабливості України. Для дрібних фермерів зростуть фінансові ризики через відсутність кредитної історії та недоступність фінансових інструментів на купівлю землі.

Висновки. Запровадження ринку землі вимагає удосконалення державного регулювання та механізмів підтримки виробництва, нарощення експортного потенціалу, формування належної інфраструктури зернового ринку тощо.

Ключові слова: *зерно, виробництво, експорт, Україна, реформа.*

Instructions for authors

Dear colleagues!

The Editorial Board of scientific periodical
"**Ukrainian Food Journal**"
invites you for publication of your research results.

Requirements to all texts:
Language – English.
Recommended size of the article – 15–20 pages.
Font – Times New Roman, font size – 14, line intervals – 1, margins on both sides – 2 cm.

The structure of the article:

1. The title of the article
2. Authors (full name and surname)
3. Institution, where the work has been performed.
4. Abstract (2/3 of a page). The structure of the abstract should correspond to the structure of the article (Introduction, Materials and methods, Results and discussion, Conclusion).
5. Keywords.
6. The main body of the article should contain the following parts:
   - Introduction
   - Materials and methods
   - Results and discussion
   - Conclusion
   - References

   If you need you can add another parts and/or divide them into subparts.
7. The information about the author (Name, surname, scientific degree, place of work, email and contact phone number).

All figures should be made in graphic editor, the font size 14.

The background of the graphs and charts should be only in white color. The color of the figure elements (lines, grid, text) – in black color.

Figures and EXCEL format files with graphs additionally should be submitted in separate files.

Photos are not recommended to be used as graphical materials.

Website of Ukrainian Food Journal: http://ufj.ho.ua

Email for all submissions and other inquiries: ufj_nuft@meta.ua

Шановні колеги!

Редакційна колегія наукового періодичного видання «**Ukrainian Food Journal**» запрошує Вас до публікації результатів наукових досліджень.

Вимоги до оформлення статей

Мова статей – англійська.

Мінімальний обсяг статті – **10 сторінок** формату А4 (без врахування анотацій і списку літератури)**.**

Для всіх елементів статті шрифт – **Times New Roman**, кегль – **14**, інтервал – 1.

Всі поля сторінки – по 2 см.

Структура статті:

1**.** УДК**.**
2. **Назва статті.**
3. Автори статті (ім’я та прізвище повністю, приклад: Денис Озерянко).
4. *Установа, в якій виконана робота*.
5. Анотація. **Обов’язкова** структура анотації:
   - Вступ (2–3 рядки).
   - Матеріали та методи (до 5 рядків)
   - Результати та обговорення (пів сторінки).
   - Висновки (2–3 рядки).
6. Ключові слова (3–5 слів, але не словосполучень).

Пункти 2–6 виконати англійською і українською мовами.

7. Основний текст статті. Має включати такі обов’язкові розділи:
   - Вступ
   - Матеріали та методи
   - Результати та обговорення
   - Висновки
   - Література.

За необхідності можна додавати інші розділи та розбивати їх на підрозділи.

8. Авторська довідка (Прізвище, ім’я та по батькові, вчений ступінь та звання, місце роботи, електронна адреса або телефон).
9. Контактні дані автора, до якого за необхідності буде звертатись редакція журналу.

Рисунки виконуються якісно. Скановані рисунки не приймаються. Розмір тексту на рисунках повинен бути **співрозмірним** (!) тексту статті. **Фотографії можна використовувати лише за їх значної наукової цінності.**

Фон графіків, діаграм – лише білий. Колір елементів рисунку (лінії, сітка, текст) – чорний (не сірий).

Рисунки та графіки EXCEL з графіками додатково подаються в окремих файлах.

Скорочені назви фізичних величин в тексті та на графіках позначаються латинськими літерами відповідно до системи СІ.

В списку літератури повинні переважати англомовні статті та монографії, які опубліковані після 2010 року.

Правила оформлення списку літератури

В Ukrainian Food Journalвзято за основу загальноприйняте в світі спрощене оформлення списку літератури згідно стандарту Garvard. Всі елементи посилання розділяються **лише комами**.

1. Посилання на статтю:

Автори А.А. (рік видання), Назва статті, Назва журналу (курсивом), Том (номер), сторінки.

Ініціали пишуться після прізвища.

Всі елементи посилання розділяються комами.

1. Приклад:
   Popovici C., Gitin L., Alexe P. (2013), Characterization of walnut (Juglans regia L.) green husk extract obtained by supercritical carbon dioxide fluid extraction, *Journal of Food and Packaging Science, Technique and Technologies,* 2(2), pp. 104–108.

2. Посилання на книгу:

Автори (рік), Назва книги (курсивом), Видавництво, Місто.

Ініціали пишуться після прізвища.

Всі елементи посилання розділяються комами.

Приклад:

2. Wen-Ching Yang (2003), *Handbook of fluidization and fluid-particle systems*, Marcel Dekker, New York.

Посилання на електронний ресурс:

Виконується аналогічно посиланню на книгу або статтю. Після оформлення даних про публікацію пишуться слова ***Available at:*** та вказується електронна адреса.

Приклади:

1. (2013), *Svitovi naukovometrychni bazy*, available at: http://www1.nas.gov.ua/publications/q_a /Pages/scopus.aspx
2. Cheung T. (2011), *World's 50 most delicious drinks [Text],* Available at: http://travel.cnn.com/explorations/drink/worlds–50-most-delicious-drinks–883542

Список літератури оформлюється лише латиницею. Елементи списку українською та російською мовою потрібно транслітерувати. Для транслітерації з українською мови використовується паспортний стандарт, а з російської – стандарт МВД (в цих стандартах використовуються символи лише англійського алфавіту, без хвостиків, апострофів та ін).

Зручні сайти для транслітерації:

З української мови – http://translit.kh.ua/#lat/passport

З російської мови – http://ru.translit.net/?account=mvd

Додаткова інформація та приклад оформлення статті – на сайті

http://ufj.ho.ua

Стаття надсилається за електронною адресою: ufj_nuft@meta.ua

УДК 663/664

Ukrainian Food Journal публікує оригінальні наукові статті, короткі повідомлення, оглядові статті, новини та огляди літератури.

Тематика публікацій в Ukrainian Food Journal:

Харчова інженерія
Харчова хімія
Мікробіологія
Фізичні властивості харчових продуктів
Якість та безпека харчових продуктів
Процеси та обладнання
Нанотехнології
Економіка та управління
Автоматизація процесів
Упаковка для харчових продуктів

Періодичність виходу журналу 4 номери на рік.

Результати досліджень, представлені в журналі, повинні бути новими, мати чіткий зв'язок з харчовою наукою і представляти інтерес для міжнародного наукового співтовариства.

Ukrainian Food Journal індексується наукометричними базами:
Index Copernicus (2012)
EBSCO (2013)
Google Scholar (2013)
UlrichsWeb (2013)
Global Impact Factor (2014)
Online Library of University of Southern Denmark (2014)
CABI full text (2014)
Directory of Research Journals Indexing (DRJI) (2014)
Universal Impact Factor (2014)
Directory of Open Access scholarly Resources (ROAD) (2014)
European Reference Index for the Humanities and the Social Sciences (ERIH PLUS) (2014)
Directory of Open Access Journals (DOAJ) (2015)
InfoBase Index (2015)
Chemical Abstracts Service Source Index (CASSI) (2016)
Emerging Sourses Citaton Index (2018)

Рецензія рукопису статті. Матеріали, представлені для публікування в «Ukrainian Food Journal», проходять «Подвійне сліпе рецензування» двома вченими, призначеними редакційною колегією: один є членом редколегії і один незалежний учений.

Авторське право. Автори статей гарантують, що робота не є порушенням будь-яких авторських прав, та відшкодовують видавцю порушення даної гарантії. Опубліковані матеріали є правовою власністю видавця «**Ukrainian Food Journal**», якщо не узгоджено інше.

Політика академічної етики. Редакція «Ukrainian Food Journal» користується правилами академічної етики, викладених в роботі Miguel Roig (2003, 2006) "Avoiding plagiarism, self-plagiarism, and other questionable writing practices. A guide to ethical writing". Редакція пропонує авторам статей і рецензентам прямо слідувати цьому керівництву, щоб уникнути помилок у науковій літературі.

Інструкції для авторів та інша корисна інформація розміщені на сайті
http://ufj.ho.ua

Редакційна колегія

Наукове видання

Ukrainian Food Journal

Volume 9, Issue 2
2020

Том 9, № 2
2020

Підп. до друку 30.06.2020 р. Формат 70x100/16.
Обл.-вид. арк. 15.21. Ум. друк. арк. 15.34.
Гарнітура Times New Roman. Друк офсетний.
Наклад 100 прим. Вид. № 14н/20.

НУХТ. 01601 Київ–33, вул. Володимирська, 68

Свідоцтво про державну реєстрацію
друкованого засобу масової інформації
КВ 18964–7754Р
видане 26 березня 2012 року.